

CZECH UNIVERSITY OF LIFE SCIENCES PRAGUE

Faculty of Tropical AgriSciences



Czech University of Life Sciences Prague

**Faculty of Tropical
AgriSciences**

**Char derivation from date palm biomass and
microalgae; characterization, thermal and
economic analysis**

Ph.D. Thesis

Prague 2019

Author: Mr. Ali Akhtar

Supervisor: Assoc. Prof. Vladimír Krepl, CSc.

Co-Supervisor: Assoc. Prof. Tatiana Ivanova, Ph.D.

© Copyright 2019 Ali Akhtar

Declaration

I hereby declare that I have done this thesis entitled “Char derivation from date palm biomass and microalgae; characterization, thermal and economic analysis” independently, all texts in this thesis are original, and all the sources have been quoted and acknowledged by means of complete references and according to Citation rules of the FTA.

In Prague 29-05-2019

.....

Ali Akhtar

Acknowledgement

My work at the Czech University of Life Sciences Prague was the most wonderful experience due to diligent, kind and respectful teachers and professors who guided me through every thick and thin. All the people around me were not only considerate of my needs but went above and beyond to make my experience magnificent which could not be attained anywhere else. I would like to pay special thanks to Assoc. Prof. Vladimír Krepl who supported me at every stage and was helpful with his technical advice. His guidance and supervision were invaluable and provided me with all the tools required to accomplish the goal of this dissertation. Moreover, I also would like to thank Assoc. Prof. Tatiana Ivanova who was not only helpful in my day-to-day experiments but also personally helped me on several occasions and encouraged me to present at the conference and writing articles.

I further would like to special thanks to Dr. Ivo Jiríček of University of Chemistry and Technology Prague. His collaboration and guidance were invincible for this dissertation, and his support cannot be explained in words. I also would like to take this opportunity to thank other staff members of the Department of Sustainable Technologies and University of Chemistry and Technology Prague who helped directly or indirectly to guide me towards this dissertation. This work was partially completed at Crop Research Institute Prague, and their support and availability of equipment are highly appreciated.

My colleagues Sayfullo Akhmedov, Libuše Valešová, and Kristina Rušarová were patient with my working schedule and were supportive in every way possible. Finally, I would like to thank my family who was supportive throughout my academic career and stood beside me in every walk of life. I cannot thank enough how grateful I am with your presence and your love and care means a lot to me.

Abstract

Waste-derived products are considered to address the question of sustainability in a variety of projects and applications. These products provide a consistent source of raw materials as well as cope with the waste handling dilemma. Waste derived carbon is one of these products which not only has gained serious consideration from an environmental point of view but also proven to be useful in soil amendment, wastewater treatment and production of nano-materials. This study provided a thorough approach to the production of optimised carbon materials from date palm biomass and wastewater derived microalgae. Their individual and co-pyrolysis behaviour with product performance in energy application including combustion and pyrolysis presented thoroughly.

Slow pyrolysis of the date palm branches (DB) and wastewater derived microalgae (WMA) was conducted in the temperature range (HTT) of 400-600 °C. Mass yield decreased; whereas, ash content increased with the increase in HTT. Algae biochar (AB) char showed higher mass yield and ash content and reduced heating values as compared to DB samples. DB chars, however, showed higher stability than AB chars. Combustion of both types of the char samples found to degrade through a two-stage devolatilization process whereas char pyrolysis showed one stage devolatilization. DB samples at 400 and 500 °C and, AB samples at 500 and 600 °C showed lower activation energy during combustion than their feedstock.

Similarly, co-pyrolysis of date palm branches and wastewater derived microalgae was conducted between 400-600 °C for multi-stage pyrolysis. Char aromaticity increased, and mass yield decreased substantially with the increase in treatment temperature in both single stage pyrolysis and two stage pyrolysis from 40% to 30% by weight. Nitrogen concentration was decreased with the increase in temperature, which determines its transformation to the gas phase. Combustion of the feedstock and the char samples produced at 400 °C and 500 °C showed two-stage degradation. The optimum treatment temperature for two-stage pyrolysis to gain the lowest activation energy is found to be 500 °C during combustion, moderate heating values and lowest price. The economic analysis showed a decrease in price with the increase in treatment temperature for two stage pyrolysed biochar due to a decrease in energy content. It can be concluded that co-pyrolysed char from multi-stage pyrolysis process contains the superior properties and complements each other. The obtained product may be useful for potential applications in multiple areas such as energy and adsorption than individual pyrolysis of each of the concerned feedstock which has certain limitations.

Keywords: biomass; kinetic modelling; combustion; pyrolysis.

Table of Contents

Chapter 1	1
Background	1
Chapter 2	3
Literature review	3
2.1 Introduction	4
2.2 Combustion	5
2.2.1 Biomass components	5
2.2.2 CO₂ emissions	7
2.2.2.1 CO₂ remediation through chemical looping combustion (CLC)	7
2.2.2.2 Co-combustion with other fuels	10
2.2.3 NO_x emissions	11
2.2.3.1 NO_x treatment	11
2.2.3.2 Catalytic remediation	12
2.2.3.3 Post-combustion treatment	12
2.2.4 Biomass ashes	15
2.2.4.1 Slagging and fouling	15
2.2.4.2 Factors affecting the slagging and fouling	18
2.2.4.3 Biomass ash applications	20
2.3 Pyrolysis	20
2.3.1 Slow pyrolysis	21
2.3.1.1 Activation and applications of char	22
2.3.2 Fast pyrolysis	24
2.3.2.1 Bio-oil upgradation	25
2.3.2.1.1 Catalytic cracking	25
2.3.2.1.2 Catalytic steam reforming	26
2.3.2.1.3 Catalytic hydrodeoxygenation	27
2.3.2.1.4 Catalytic hydrocracking	28
2.3.2.2 Cellulose, hemicellulose and lignin degradation during pyrolysis 28	
2.4 Gasification	33
2.4.1 Advances in syngas treatment	35
2.4.2 Advances in syngas applications	38
2.4.3 Supercritical water gasification (SWG)	41
2.5 Conclusive remarks	45

2.6	References	46
	Aim of the thesis.....	60
	Hypothesis.....	60
	Research objectives	60
	Thesis outline.....	61
	Chapter 3	62
	Characterisation of waste from date palm branches.....	62
3.1	Introduction	63
3.2	Materials and Methods	64
3.2.1	Biomass collection and processing	64
3.2.2	Moisture content	65
3.2.3	Proximate analysis	65
3.2.4	Ultimate analysis	65
3.2.5	Heating values	65
3.2.6	Error analysis	65
3.2.7	Exergy	66
3.2.8	X-ray fluorescence (XRF) spectrometry	66
3.2.9	Inductively coupled plasma mass spectrometry (ICP-MS) analysis	68
3.2.10	X-ray diffraction (XRD) analysis	68
3.2.11	Thermogravimetric (TGA) analysis	69
3.2.12	Attenuated total reflection fourier transform infrared (ATR-FTIR) spectroscopy	69
3.3	Results and Discussion	69
3.3.1	Moisture content	69
3.3.2	Proximate analysis	70
3.3.3	Ultimate analysis	71
3.3.4	X-ray fluorescence spectrometry	72
3.3.5	ICP-MS analysis	73
3.3.6	Heating values and Exergy	76
3.3.7	Error analysis	77
3.3.8	FTIR analysis	79
3.3.9	XRD analysis	79
3.3.10	TGA analysis	80
3.4	Conclusive remarks	83

3.5	References	84
Chapter 4	89
Slow pyrolysis of date palm and high rate algal pond biomass	89
4.1	Introduction	90
4.2	Experimental section	93
4.2.1	Biomass feedstock	93
4.2.2	Char preparation	93
4.2.3	Char characterisation	93
4.2.4	Kinetics modelling	94
4.2.5	Economic analysis	95
4.3	Results and Discussion	95
4.3.1	Char characteristics.....	95
4.3.2	Ultimate analysis	96
4.3.3	Van Krevelen diagram	97
4.3.4	Statistical analysis	97
4.3.5	Fourier transform infrared spectroscopy	98
4.3.6	X-ray photoelectron spectroscopy	101
4.3.7	TGA-DSC analysis.....	103
4.3.7.1	Combustion	103
4.3.7.2	Pyrolysis.....	107
4.3.8	Economic analysis	107
4.4	Conclusive remarks.....	111
4.5	References.....	112
Chapter 5	118
Combined multi-stage pyrolysis of date palm biomass and microalgae	118
5.1	Introduction	119
5.2	Materials and Methods.....	121
5.2.1	Pyrolysis experiment	121
5.2.2	Char characterisation	122
5.2.3	Energy economics.....	123
5.3	Results and Discussion.....	123
5.3.1	Char characteristics.....	123
5.3.2	Atomic ratios and Van Krevelen diagram	125

5.3.3	Fourier transform infrared spectroscopy	126
5.3.4	X-ray photoelectron spectroscopy	129
5.3.5	TGA-DSC analysis.....	130
5.3.5.1	Combustion.....	130
5.3.5.2	Pyrolysis.....	136
5.3.6	Energy economics.....	137
5.4	Conclusive remarks.....	139
5.5	References.....	140
Chapter 6.....		145
Comprehensive summary.....		145
Appendices		148
Journal publications		157
Conference presentation		157

List of Figures

<i>Figure 2-1 Biomass processing technologies and respective products obtained through each of the technologies</i>	5
<i>Figure 2-2 Chemical structure of cellulose, hemicellulose and structural units [149] found in lignin (SW = soft wood, HW = hard wood). (With permission from Royal Society of Chemistry)</i>	6
<i>Figure 2-3 Major factors affecting the CO₂ capture and oxygen demand in chemical looping combustion. (Adapted from reference [140] with permission from Elsevier)</i>	8
<i>Figure 2-4 Three types of electrostatic precipitators (b) with fluidized boilers classifying the fly ash according to its composition. (Reprinted from reference [150] with permission from Elsevier)</i>	13
<i>Figure 2-5 Schematic diagram of moving bed absorber. (Reprinted from reference [141] with permission from Elsevier)</i>	14
<i>Figure 2-6 Elements contributing towards ash production in biomass during combustion. (Reprinted from reference [151] with permission from Elsevier) (db = dry basis)</i>	16
<i>Figure 2-7 Transport pathway of potassium, chlorine and sulphur from biomass to fine particles during combustion of biomass. (Reprinted from reference [142] with permission from Elsevier)</i>	16
<i>Figure 2-8 Classification of ash produced from biomass combustion according to its chemical composition. (Reprinted from reference [46] with permission from Elsevier)</i>	17
<i>Figure 2-9 Slagging mechanism due to alkali during combustion of biomass. (Reprinted from reference [59] with permission from Elsevier)</i>	19
<i>Figure 2-10 Categorization of char according to the feedstock type. (Reprinted from reference [74] with permission from Elsevier)</i>	22
<i>Figure 2-11 Bio-oil upgrading process in a nutshell. (Adapted from reference [96] with permission from Elsevier)</i>	24
<i>Figure 2-12 Bio-oil and kitchen waste oil upgradation pathway over HZSM-5 catalyst. (Reprinted from reference [94] with permission from Elsevier)</i>	26
<i>Figure 2-13 Hemicellulose degradation under pyrolysis into bio-oil, gas and char. (Reprinted from reference [152])</i>	29
<i>Figure 2-14 Pyrolysis of cellulose to volatiles. Four possible pathways from Glycosidic cleavage to the formation of (1) formic acid, CO₂ and 2,5 dihydroxy-3-pentanal (2) formaldehyde and 2,3 hydroxy-4-pentanal (3) glyoxal and 3-(vinyloxy)-2-oxiranol (4) formaldehyde, carbon monoxide and 4-hydroxy-2-butenal (5) malondialdehyde and a radical intermediate. (Adapted from reference [153] with permission from Royal Society of Chemistry)</i>	31

<i>Figure 2-15 Pyrolysis mechanism explained for β-O-4 type lignin model compound. (Reprinted from reference [154] with permission from Royal Society of Chemistry).....</i>	<i>32</i>
<i>Figure 2-16 Catalytic and non-catalytic process for lignin conversion during fast pyrolysis. (Reprinted from reference [155] with permission from Elsevier).....</i>	<i>32</i>
<i>Figure 2-17 Biomass gasifiers traditionally used with their pros and cons. (Adapted from reference [156] with permission from Elsevier).....</i>	<i>34</i>
<i>Figure 2-18 Moving granular bed filter for syngas cleaning. (Reprinted from reference[120] with permission from Elsevier).....</i>	<i>35</i>
<i>Figure 2-19 Gasification mechanism of toluene as a model tar compound in dielectric barrier discharge plasma reactor (a) energetic electrons and excited Ar (b) OH radicals. (Reprinted from reference [128] with permission from Elsevier).....</i>	<i>37</i>
<i>Figure 2-20 Energy distribution during the syngas production in a micro gas turbine. (Adapted from reference [131] with permission from Elsevier).....</i>	<i>40</i>
<i>Figure 2-21 Schematic diagram of the hybrid gasification and fermentation system. (Adapted from reference [141] with permission from Elsevier).....</i>	<i>42</i>
<i>Figure 2-22 Biomass gasification under supercritical conditions. Catalysts A, B, C, and D represents (Ni, Ru, Rh, Pt, Pd, Ni/Al₂O₃, Ni/C, Ru/Al₂O₃, Ru/TiO₂), (Ni, Ru, Pt and activated carbon), (Ni, Rh, Ru, Pt and activated carbon) and (Ni, Ru, NaOH, KOH) respectively. (Reprinted from reference [143] with permission from Elsevier).....</i>	<i>43</i>
<i>Figure 2-23 Supercritical water gasification of glucose at 400 °C. (Reprinted from reference [157] with permission from Elsevier).....</i>	<i>44</i>
<i>Figure 3-1 Moisture content changing pattern with time (months) in L, SB, MB and LB.....</i>	<i>70</i>
<i>Figure 3-2 Proximate analysis of date palm branches on dry basis.....</i>	<i>71</i>
<i>Figure 3-3 Inorganic elements in biomass by XRF analysis in percentage.....</i>	<i>75</i>
<i>Figure 3-4 ICP-MS analysis of biomass for inorganic elements in percentage.....</i>	<i>75</i>
<i>Figure 3-5 Heating values and exergy values of biomass samples.....</i>	<i>76</i>
<i>Figure 3-6 Trend of Exs, ExHHV, ExLHV values of date palm branches.....</i>	<i>77</i>
<i>Figure 3-7 Pyrolysis profiles of biomass samples at 10 °C/min, 20 °C/min, and 50 °C/min heating rates.....</i>	<i>81</i>
<i>Figure 3-8 DTG curves of biomass samples at 10 °C/min, 20 °C/min, and 50 °C/min heating rates.....</i>	<i>82</i>
<i>Figure 4-1 Elemental analysis of date palm and wastewater derived microalgae char at 400, 500 and 600°C.....</i>	<i>97</i>

<i>Figure 4-2 Van Krevelen diagram of biomass and char. The dotted line separates the half-life of char in years [18].....</i>	<i>98</i>
<i>Figure 4-3 Line fit plots and R2 values of H/C ratio and Mass yield, and O/C and N/C ratios.....</i>	<i>99</i>
<i>Figure 4-4 FTIR of (a) date palm and (b) microalgae char produced at 400, 500 and 600 °C.....</i>	<i>100</i>
<i>Figure 4-5 Nitrogen species found on the surface of the char through XPS analysis.....</i>	<i>102</i>
<i>Figure 4-6 Combustion characteristics of date palm and wastewater derived microalgae biomass and their respective chars produced at different temperatures. The dotted line shows the DTG curves of the respective samples.....</i>	<i>104</i>
<i>Figure 4-7 Statistical analysis of the ignition temperature and burnout temperature (a) mass stabilization method and (b) conversion method.....</i>	<i>106</i>
<i>Figure 4-8 Pyrolysis curves of the biomass and char. The dotted lines shows the DTG curves of the respective samples.....</i>	<i>108</i>
<i>Figure 4-9 Effect of N/C, O/C atomic ratios and chlorine on the energy recovery of the char.....</i>	<i>110</i>
<i>Figure 5-1 Van Krevelen diagram of O/C and H/C atomic ratios. The dotted line at 0.6 and 0.2 O/C ratio separating the range of half-life of char produced [53].....</i>	<i>126</i>
<i>Figure 5-2 Regression analysis of H/C, (O+N)/C, O/C and N/C atomic ratios and Ash correlation with N/C, H/C and yield with the coefficient of determination and p values.....</i>	<i>127</i>
<i>Figure 5-3 FTIR of char (a) and feedstock (b) (WWM = wastewater derived microalgae, DB = date palm biomass).....</i>	<i>128</i>
<i>Figure 5-4 TGA and DTG curves of biomass and chars produced at 400, 500 and 600 °C in air atmosphere.....</i>	<i>131</i>
<i>Figure 5-5 Regression analysis of ignition temperature and burnout temperature of SSP and TSP chars.....</i>	<i>133</i>
<i>Figure 5-6 Kinetic illustrations of chars subjected to combustion.....</i>	<i>135</i>
<i>Figure 5-7 Thermal analysis of co-pyrolysed char in nitrogen atmosphere.....</i>	<i>136</i>
<i>Figure 5-8 Statistical analysis of the mass yield and energy yield of the char.....</i>	<i>138</i>

List of Tables

<i>Table 2-1 Hardwood and softwood composition. (Adapted from references [11],[10],[12])</i>	7
<i>Table 2-2 General characteristics of looping combustion and gasification systems (BCLC, BCLG, BCCLP, BCaLC, BCaLG, and SE-BCaLG represents biomass based chemical looping combustion, biomass based chemical looping gasification, biomass based co-production chemical looping process, biomass based calcium looping combustion, biomass based calcium looping gasification and sorption enhanced BCaLG respectively). (Adapted from reference [16], published by Royal Society of Chemistry)</i>	9
<i>Table 2-3 Carbon capture and conversion efficiencies of different metal ferrites at 850°C. (Adapted from reference [18] with permission from Elsevier)</i>	10
<i>Table 2-4 Pollutants removal from the gas through different post-combustion technologies</i>	14
<i>Table 2-5 Approximate yields of the products obtained by thermochemical conversion of biomass. (Adapted from reference [68] with permission from Elsevier)</i>	21
<i>Table 2-6 Catalytic upgrading of the bio-oil through zeolite cracking. (Adapted from reference [96] with permission from Elsevier)</i>	25
<i>Table 2-7 gaseous products produced during the fast pyrolysis of hemicellulose. (Adapted from reference [111] with permission from Elsevier)</i>	29
<i>Table 2-8 Permissible limits for the pollutants in syngas according to the applications. (Adapted from reference [118] with permission from Elsevier)</i>	36
<i>Table 3-1 Correlations used for calculating the theoretical higher heating value (HHV)</i>	67
<i>Table 3-2 Correlations used to determine the exergy of date palm biomass</i>	68
<i>Table 3-3 Elemental composition of biomass samples (C = Carbon, H = Hydrogen, N = Nitrogen, S = Sulphur, O* = Oxygen (*calculated by difference))</i>	71
<i>Table 3-4 Permissible limits for trace elements in biomass defined in Standard ISO 17225</i>	74
<i>Table 3-5 Correlations against their errors and R² values (AEE = average experimental error, ABE = Average bias error)</i>	78
<i>Table 4-1 Char characteristics produced from date palm biomass and wastewater derived microalgae</i>	96
<i>Table 4-2 Combustion parameters of biomass and their respective chars (1 = [37], 2 = [57])</i>	105
<i>Table 4-3 Energy yield and economic value of the char</i>	109
<i>Table 5-1 Yield, surface area, ash and energy values of the char (CS = Single step, CT = Two step, & 4, 5 and 6 represents 400, 500 and 600 °C respectively)</i>	124
<i>Table 5-2 Ultimate analysis of the char and feedstock (as received basis)</i>	125

<i>Table 5-3 Elemental composition on the surface of the char samples analysed by XPS.</i>	<i>130</i>
<i>Table 5-4 Co-combustion of date palm biomass and wastewater derived microalgae and their co-pyrolysed char</i>	<i>133</i>
<i>Table 5-5 Energy yield and price variation according to the different treatment temperatures</i>	<i>137</i>

List of Abbreviations

HHV	Higher heating value
LHV	Lower heating value
DB	Date palm biomass
WMA	Wastewater derived microalgae
AB	Algae char
MSW	Municipal solid waste
CLC	Chemical looping combustion
BCLC	Biomass based chemical looping combustion
BCLG	Biomass based chemical looping gasification
BCCLP	Biomass based co-production chemical looping process
BCaLC	Biomass based calcium looping combustion
BCaLG	Biomass based calcium looping gasification
SE-BCaLG	Sorption enhanced BCaLG
GHG	Greenhouse gases
L	Leaf ribs
SB	Small part of a branch attached to the ribs
MB	Middle part of the branch
LB	Large part of the branch attached to the trunk
FAO	Food and Agriculture Organization
M	Moisture
VM	Volatile matter
AEE	Average experimental error
ABE	Average bias error
XRF	X-ray fluorescence
XRD	X-ray diffraction
ICP-MS	Inductively coupled plasma mass spectrometry
FTIR	Fourier transform infrared
TGA	Thermogravimetric analysis
DSC	Differential scanning calorimetry
DTG	Derivative thermogravimetric
HTT	Highest treatment temperature
XPS	X-ray photoelectron spectroscopy
EV	Economic aspect
UP	Unit price
PR	Production rate
BPJ	Char price per megajoule
SSP	Single stage combined pyrolysis
TSP	Two stage combined pyrolysis

Chapter 1

Background

The use of biomass in different forms have been the part of the evolution, however, energy potential of the materials have gained significant importance in today's world. Innovative solutions and techniques are being introduced through variety of the research to determine the ideal output from the available resources. Several techniques from combustion of the waste into boilers to conversion of waste into biofuels and bio-based products have been the paramount of current research [1–3]. The use of biomass and organic waste into boilers although considers net zero carbon emissions, however, the uptake of different elements throughout the life span creates notable problems from environmental and technical point of view. The problems related to slagging and fouling, and several emissions is described in detail in the following chapter.

Further use of organic waste from a range of sources are being recommended through pyrolysis and gasification in thermochemical conversion technologies besides hydrothermal processing technologies. Each of the technology is also explained in detail in the following chapter with their major products output, upgradation pathways and current research trends. The use of third generation feedstock is being reported heavily in the research due to their rapid production and multi-functional characteristics [4]. However, the use of third generation feedstock needs the attention in respect of ultimate product performance [5]. Wastewater derived biomass (microalgae) considers the most useful instrument which after the treatment can be utilised in bio-refineries [6,7].

Date palm biomass is being produced in millions of tonnes worldwide and thus generates huge amount of waste [8]. The conversion of the waste into stable carbon materials can contribute to the carbon storage and act as a resource for several further applications [9]. The use of microalgae through pyrolysis produced variety of results. Tang et al. [10] reported the co-pyrolysis of microalgae with plastic and found the improvement in oil quality with high aliphatic hydrocarbon content. In another study by Chen et al. [11] lignocellulosic biomass improved the oil quality when pyrolysed with microalgae and transforms the nitrogen compounds to gas and solid phase.

References

- [1] M. Inman, Cooking up fuel, *Nat. Clim. Chang.* 2 (2012) 218–220. doi:10.1038/nclimate1466.
- [2] H. Wang, Q. Yao, C. Wang, B. Fan, Y. Xiong, Y. Chen, Q. Sun, C. Jin, Z. Ma, New Insight on Promoted thermostability of poplar wood modified by MnFe₂O₄ nanoparticles through the pyrolysis behaviors and kinetic study, *Sci. Rep.* 7 (2017) 1–12. doi:10.1038/s41598-017-01597-4.
- [3] D. Woolf, J. Lehmann, D.R. Lee, Optimal bioenergy power generation for climate change mitigation with or without carbon sequestration, *Nat. Commun.* 7 (2016) 1–11. doi:10.1038/ncomms13160.
- [4] Z. Yakhini, Y. Linzon, A. Golberg, E. Vitkin, R. Jiang, A. Chudnovsky, Thermochemical hydrolysis of macroalgae *Ulva* for biorefinery: Taguchi robust design method, *Sci. Rep.* 6 (2016) 1–14. doi:10.1038/srep27761.
- [5] J. Lee, E.E. Kwon, Y.-K. Park, Recent advances in the catalytic pyrolysis of microalgae, *Catal. Today.* 5 (2019) 188–193. doi:10.1016/j.cattod.2019.03.010.
- [6] D.L. Cheng, H.H. Ngo, W.S. Guo, S.W. Chang, D.D. Nguyen, S.M. Kumar, Microalgae biomass from swine wastewater and its conversion to bioenergy, *Bioresour. Technol.* 275 (2019) 109–122. doi:10.1016/j.biortech.2018.12.019.
- [7] A. Bhatnagar, E. Daneshvar, M.J. Zarrinmehr, O. Farhadian, M. Kornaros, E. Koutra, Sequential cultivation of microalgae in raw and recycled dairy wastewater: Microalgal growth, wastewater treatment and biochemical composition, *Bioresour. Technol.* 273 (2018) 556–564. doi:10.1016/j.biortech.2018.11.059.
- [8] H.H. Sait, A. Hussain, A.A. Salema, F.N. Ani, Pyrolysis and combustion kinetics of date palm biomass using thermogravimetric analysis, *Bioresour. Technol.* 118 (2012) 382–389. doi:10.1016/j.biortech.2012.04.081.
- [9] D. Woolf, J.E. Amonette, F.A. Street-Perrott, J. Lehmann, S. Joseph, Sustainable biochar to mitigate global climate change, *Nat. Commun.* 1 (2010) 1–9. doi:10.1038/ncomms1053.
- [10] Z. Tang, W. Chen, Y. Chen, H. Yang, H. Chen, Co-pyrolysis of microalgae and plastic: Characteristics and interaction effects, *Bioresour. Technol.* 274 (2019) 145–152. doi:10.1016/j.biortech.2018.11.083.
- [11] W. Chen, Y. Chen, H. Yang, M. Xia, K. Li, X. Chen, H. Chen, Co-pyrolysis of lignocellulosic biomass and microalgae: Products characteristics and interaction effect, *Bioresour. Technol.* 245 (2017) 860–868. doi:10.1016/j.biortech.2017.09.022.

Chapter 2

Literature review¹

This chapter provides an overview of the biomass utilisation through different technologies such as combustion, pyrolysis and gasification. From the conventional use of biomass in the form of heating to the modern day use of biomass in the form of electricity generation and biofuel production, biomass has always been part of the evolution of mankind. Modern day use of biomass is gradually becoming more complex, and engineering played an important role in defining different directions. Efficient use of biomass with the desired output and minimising the drawbacks are the core of the research, and marginal focus is being held on developing new techniques. The variety of composition and uptake of different elements throughout the lifespan of biomass produces a variation of results. In general, it can be seen that the optimisation was observed either in the form of chemical looping combustion to prevent greenhouse gas emission or in the upgrading of bio-oil to produce biofuels. The significant factor is the reaction conditions, which define the ultimate product yield and the products' performance in different applications. Moreover, the development of new systems is desired in the present scenario due to the limited possibility of further improvement in the current systems.

¹ This chapter is extracted from the published study “A. Akhtar, V. Krepl, T. Ivanova, A Combined Overview of Combustion, Pyrolysis, and Gasification of Biomass, *Energy & Fuels*. 32 (2018) 7294–7318. doi:10.1021/acs.energyfuels.8b01678.” with permission from American Chemical Society.

This literature review was thoroughly conducted by the first author and first author is responsible for deriving literature data, analysing, processing and publishing in article format.

2.1 Introduction

Sustainability consideration in modern projects is an essential criterion in the developed world and getting recognition day by day in the developing world as well. It is not only the need of the hour from an environmental point of view but also economically suitable for handling large projects on a commercial scale. “Sustainability of any product can be defined by its level of carbon footprint and reduction of this footprint can be achieved by a change of built-in or external characteristics which can also lead to a change of its configuration” [1]. One of the paramount of sustainability is reducing the reliability of fossil fuels for energy generation and chemical extraction on a daily basis. There have been many routes being researched to focus on the alternative sources of energy which reduces not only environmental pollution but also available recurrently. These sources also called renewable sources of energy and fuels. Solar, wind, and biomass are one of the few emerging sources in this scenario where the availability throughout the world and potential to cope with the environmental pollution makes them the most studied areas so far in this category.

Although the importance of each of the energy source cannot be denied, however, biomass contains a significant value. This can be due to its highly versatile composition, availability and conversion into many useful products depending on the technology and conversion pathway. Biomass has a notable advantage in terms of its ability to produce different chemicals that can be modified according to employed route for processing of the biomass that is absent in other sources of energy. Biomass can be utilised through combustion [2], thermochemical [3,4] and biochemical [5] treatment technologies producing energy, biofuels and biochemicals accordingly. *Figure 2-1* explains the different treatment technologies pathway to obtain desired products. Although all the processing techniques contain some form of drawbacks in their end products, however, researchers proposed different measures and procedures to improve the properties. For instance, using the reduced pressurised distillation to improve the heating values and reduce the corrosivity of the bio-oil produced through pyrolysis [6] and changing the fatty ester composition through different ways in biodiesel production from vegetable oil and animal fats [7]. Each of the processes has been reported extensively in the last decade, and breakthroughs have been observed, moving from first generation biofuel to fourth generation biofuels. The production of fuels and chemicals through the waste source to the energy-specific crops and genetically modified crops has reached its peak, and the next pathways must be explored to improve the efficiency of these processes. Multiple process integration of biofuel and energy production with cost optimisation must be the focus of future studies to employ

these processes on the industrial scale [8]. This chapter focuses on the recent advances on biomass-based renewable energy and fuel perspective from each of the processing technologies including combustion, pyrolysis and gasification and provides an overall background in this area.

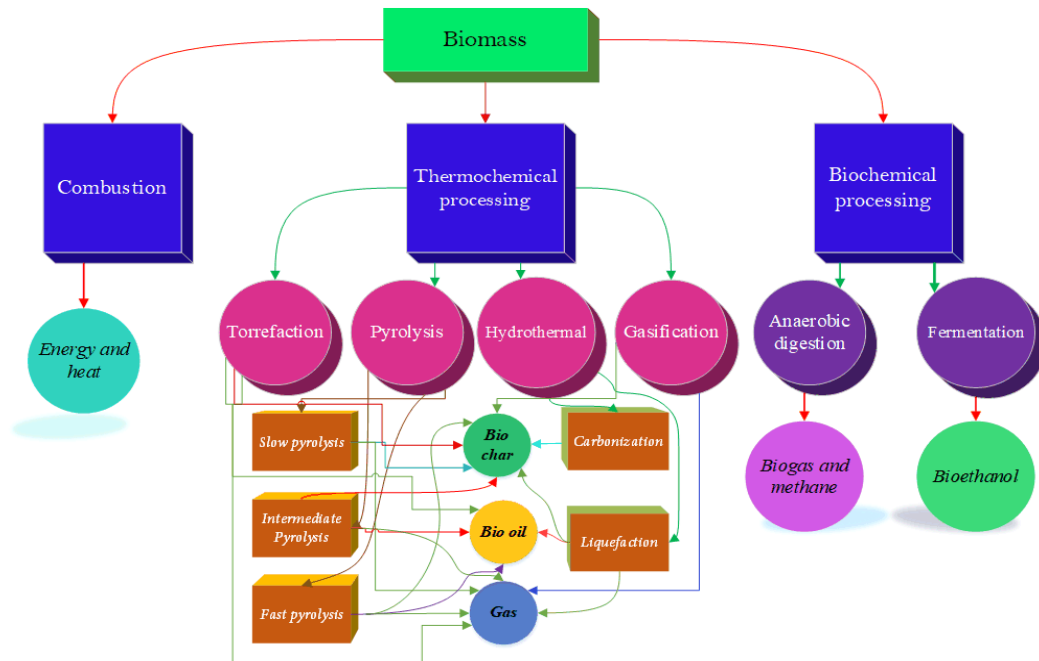


Figure 2-1 Biomass processing technologies and respective products obtained through each of the technologies

2.2 Combustion

2.2.1 Biomass components

Biomass primarily consists of three main components (i) cellulose (ii) hemicellulose and (iii) lignin and three minor components (iv) proteins (v) sugars and aliphatic acids and (vi) fats. They have different combustion behaviours and degradation pattern and releases energy according to the type of the biomass and its composition. Cellulose is a glucose monomer attached through straight link chains in β crystalline form (unchained polymer). Hemicellulose, on the other hand, contains sugar monomers which are amorphous and is a branched polymer. Lignin holds phenylpropane units with biopolymers [9] and works as a glue to hold the fibres of the cellulose. This ability gives the lignin a very prominent place in the field of biochemicals and exhibits versatility. The chemical structure of cellulose, hemicellulose and structural units found in lignin can be seen in *Figure 2-2*. All the components of the biomass contain different reaction behaviour upon degradation into different chemicals which makes it arduous material to deal with, however, this ability holds an advantage in terms of segregation. Conversion of

cellulose into other valuable products through degradation considered to be a demanding job as compared to the rest of the composition [9]. The variation of each of the component in hardwood and softwood biomass is given in *Table 2-1*. It can be seen that the significant difference lies in lignin concentration of both types of biomass where softwood contains higher lignin content than hardwood. Flax and hemp contain a significantly higher concentration of cellulose and a subsequently lower concentration of lignin. Low lignin content fibres prolong the burning which leads to incomplete combustion and lower heat evolved [10], hence not suitable for energy and heat production. Lignin content also significantly affect the activation energy of particular biomass. They might be suitable in construction applications so-called composites or fibre reinforced concrete as heat resistant materials.

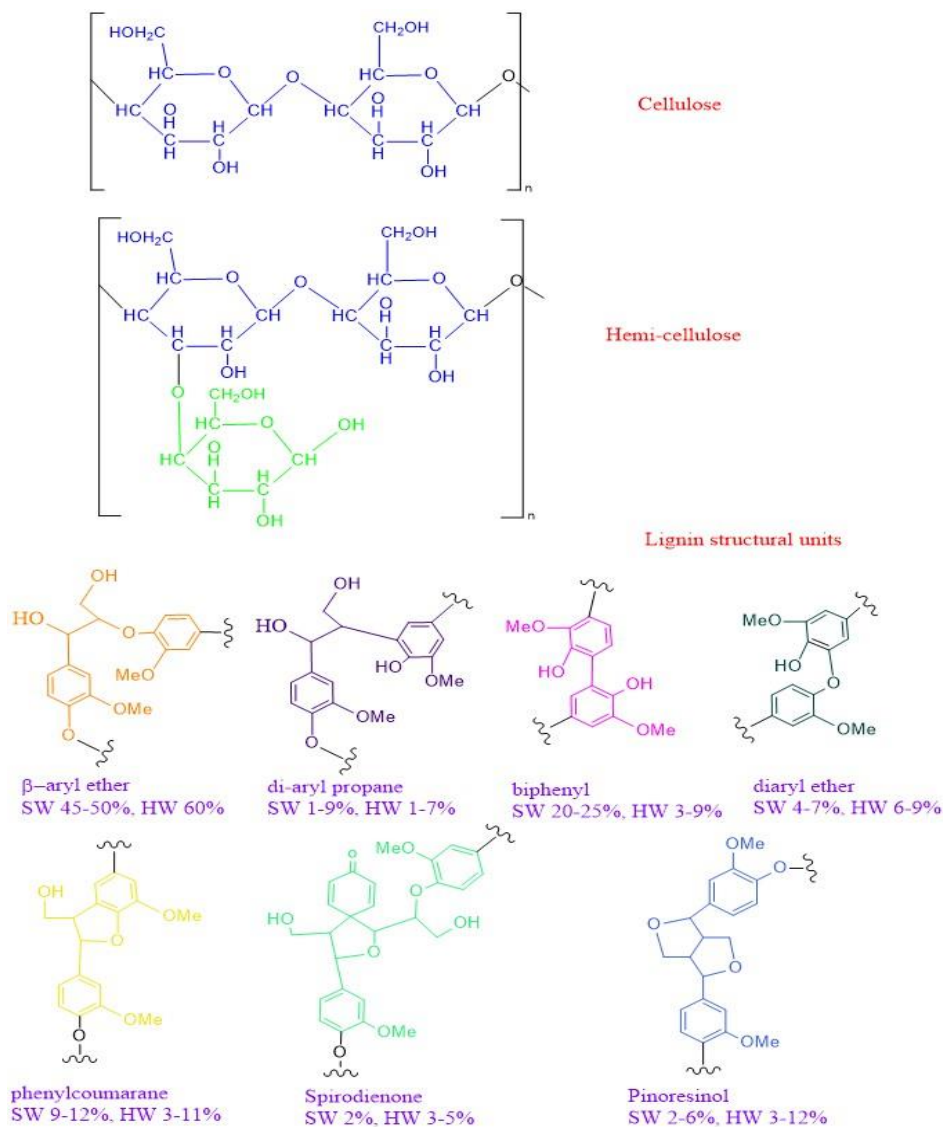


Figure 2-2 Chemical structure of cellulose, hemicellulose and structural units [149] found in lignin (SW = soft wood, HW = hard wood). (With permission from Royal Society of Chemistry)

Table 2-1 Hardwood and softwood composition. (Adapted from references [11],[10],[12])

Composition (%)	Hardwood	Soft Wood	Flax	Hemp	Sugarcane	Bamboo	Pine	Blue gum
Cellulose	40-50	40-50	80	74.1	51.8	54.6	39.9	41.0
Hemicellulose	25-35	25-30	13	7.6	27.6	11.4	24.2	19.4
Lignin	20-25	25-35	2	2.2	10.7	21.7	27.4	28.1

2.2.2 CO₂ emissions

Biomass, a renewable source of energy, produces net zero CO₂ emission upon their combustion into boilers and reactors for energy and heat production. However, there are other techniques such as pyrolysis and gasification which converts the available carbon in biomass into useful products rather than gaseous emissions. Co-firing of the biomass with coal can reduce the greenhouse gases emission significantly while maintaining a consistent supply of renewable feedstock [13]. Carbon capture and storage integration into the combustion plant can significantly enhance the environmental potential, however, the energy consumption is the main barrier in this scenario with the decrease in efficiency. Lopez et al. [14] reported the techno-economic analysis of the coal-biomass co-combustion for up-scale power plants. It was found that 300 MW power plant with 40-50% biomass co-combustion showed promising solution than the lower capacity plants, whereas, a noticeable increase in the cost of energy was observed with the biomass increment. Extra funding was recommended to maintain the financial viability of the plant in Spain scenario. Chemical looping combustion (CLC) technology have a potential in this area in which CO₂ removal from the other gas components is not required. The absence of specific equipment required for CO₂ removal makes this process cost and energy efficient. This concept is reported by Richter and Knoche [15] where metal oxide can be used to support the combustion process rather than direct contact of fuel with oxygen.

2.2.2.1 CO₂ remediation through chemical looping combustion (CLC)

Zhao et al. [16] reviewed comprehensively on biomass-based chemical looping processes and categorised the types of chemical looping technologies according to the desired output product. For instance (a) generation of heat and electricity (b) generation of gaseous fuels (c) co-generation of gas and energy. Table 2-2 shows the general characteristics of the biomass-based chemical looping in a different scenario with relevant input and output for both of the designed chambers. Metal is used in the air reactor or regenerator which upon heating transform into metal oxides to carry the oxygen in the fuel reactor or combustor. This metal oxide later

reduced due to the consumption of oxygen during biomass combustion and returns to the air reactor and the cycle continues. *Figure 2-3* shows the major factors affecting the CO₂ capture efficiency including char gasification, the solid residence time in fuel reactor and CS efficiency in chemical looping combustion. Adanez-Rubio et al. [17] reported the use of a mixture of copper and manganese oxides in chemical looping combustion (CLC) with different types of biomass. It was found that oxygen concentration had a negligible effect on the CO₂ capture efficiency. A higher CO₂ capture with efficient combustion was reported. In another recent study by Wang et al. [18] showed the use of different metal ferrite (Cu, Ni and Co) effect in the carbon capture and conversion efficiency. Ni-based ferrite was found to present lower performance as compared to Cu and Co-based ferrites after multiple cycles in a fluidised bed reactor (*Table 2-3*).

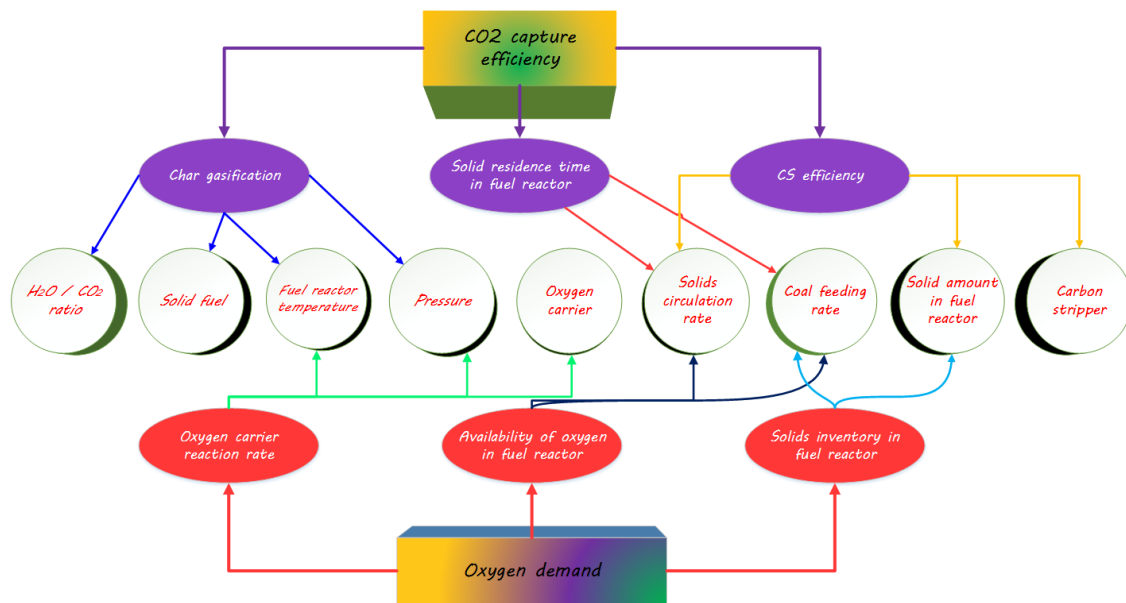


Figure 2-3 Major factors affecting the CO₂ capture and oxygen demand in chemical looping combustion. (Adapted from reference 140 with permission from Elsevier)

Zhang et al. [19] reported the use of chemical looping combustion for partial oxidation of fuel which can lead to syngas production. Among the four carriers, CaFe₂O₄ and Ca₂Fe₂O₅ were found to be optimal for the production of partial oxidation of solid fuels. However, the study conducted on charcoal that may show limitation with the respected carriers on employing the raw biomass due to different minerals present according to its source. There is a number of other studies as well which showed syngas production through chemical looping gasification technology and showed positive results [20,21]. Luo et al. [22] reported the use of iron-based carriers and found that pure Fe₂O₃ lacks the stability as compared to synthetic Fe₂O₃/MgAl₂O₄ and iron ore with temperature limit less than 950 °C using methane as a fuel.

Table 2-2 General characteristics of looping combustion and gasification systems (BCLC, BCLG, BCCLP, BCaLC, BCaLG, and SE-BCaLG represents biomass based chemical looping combustion, biomass based chemical looping gasification, biomass based co-production chemical looping process, biomass based calcium looping combustion, biomass based calcium looping gasification and sorption enhanced BCaLG respectively). (Adapted from reference [16], published by Royal Society of Chemistry)

	Air reactor / Regenerator				Fuel reactor / combustor				O ₂ /CO ₂ carrier			Gasifier			
	Temp range °C	ΔH	Input	Output	Temp. range °C	ΔH	Input	Output	Oxidised	Reduce d		Temp. range °C	ΔH	Input	Output
BCLC	600 - 1200	<0	Air	Depleted Air	600 - 1000	>0	Biomass, H ₂ O/CO ₂	Ash, CO ₂ rich gas	Me _x O _y /heat	Me _x O _{y-1}	O ₂				
BCLG	600 - 1200	<0	Air	Depleted Air	600 - 1000	>0	Biomass, H ₂ O/CO ₂	Ash, Syn gas	Me _x O _y /heat	Me _x O _{y-1}	O ₂				
BCCLP	600 - 1200	<0	Air	Depleted Air	600 - 1000	>0	Biomass, H ₂ O/CO ₂	Ash, CO ₂ rich gas	Me _x O _y /heat	Me _x O _{y-1}	O ₂	600-900	<0	H ₂ O	H ₂
BCaLC	850 - 900	>0	H ₂ O/CO ₂ /O ₂	CO ₂ rich gas	600-700	<0	Biomass, Air	Ash, Depleted air	CaO /heat	CaCO ₃	CO ₂				
BCaLG	850 - 900	>0	H ₂ O/CO ₂ /O ₂	CO ₂ rich gas	600-700	<0	Biomass, H ₂ O	Ash, H ₂ rich gas	CaO /heat	CaCO ₃	CO ₂				
SE-BCaLG			O ₂	CO ₂ rich gas			Biomass, H ₂ O	Ash, H ₂ rich gas	NiO+Ca O	Ni+Ca CO ₃	O ₂ + CO ₂				

The detailed overview of chemical looping combustion technology for solid, liquid and gaseous fuels other than the biomass and according to the different oxygen carriers can be referred further at Nandy et al. [23]. CLC is also found to be economically compatible among the CO₂ capture technologies for fire heaters and boilers [24]. Oxygen carrier recovery from the ashes needs to be considered in future biomass studies and lifetime of oxygen carrier with possible declining in their efficiency on long term scale needs to be investigated.

Table 2-3 Carbon capture and conversion efficiencies of different metal ferrites at 850°C. (Adapted from reference [18] with permission from Elsevier)

Cycle	Carbon conversion (%)			Carbon capture efficiency (%)		
	<i>CuFe₂O₄</i>	<i>NiFe₂O₄</i>	<i>CoFe₂O₄</i>	<i>CuFe₂O₄</i>	<i>NiFe₂O₄</i>	<i>CoFe₂O₄</i>
1 st	95.66	93.53	94.65	95.48	94.04	94.19
2 nd	95.51	91.84	93.78	94.98	92.59	94.07
3 rd	95.46	88.53	93.89	93.65	89.98	93.48
4 th	94.88	86.38	93.21	93.76	87.15	93.40
5 th	94.90	83.85	93.47	93.81	86.30	93.51

2.2.2.2 Co-combustion with other fuels

Co-combustion of biomass and other fuels is also one of the focus of the recent studies which brings the variety of the outcomes depending on the source of biomass and operating conditions. Gu et al. [25] showed that co-combustion of biomass and coal in the presence of iron ore decreases carbon conversion efficiency with the increase in temperature due to inadequate oxygen transport capacity. However, the carbon capture efficiency was enhanced with the temperature increment in the fuel reactor. Luo et al. [26] in another study, reported the co-combustion of coal and biomass in the presence of CuO carrier. It was found that biomass helped to raise the efficiency of coal conversion and also increases in the presence of high alkali and alkaline earth metals in biomass. The potential slagging and fouling needs to be considered while utilising the biomass in co-combustion technology. Co-combustion in the presence of additives may contribute towards a decrease in slagging effect [25,26]. At another instant, it was reported that sewage sludge and coal co-combustion in the presence of hematite (Fe₂O₃) oxygen carrier have the potential to increase the carbonaceous gas conversion efficiency and carbon capture efficiency. The agglomeration was also not occurred even though coal in this study contained high alkali and alkaline earth metals due to high melting points of the sodium compounds [27]. It is possible to combine the woody biomass with sewage sludge

to minimise the slagging and fouling potential in the reactor. However, sludge requires higher temperature and time in reference to the woody biomass for complete combustion including volatiles and char.

2.2.3 NO_x emissions

Even though CO₂ emission is one of the main contributors to environmental pollution and considered as a benchmark for the so-called green system, however, other pollutants are affecting and harming the environment equivalent to CO₂. NO_x emissions are one of the most prominent emission pollutant emits during combustion. This highly depends on the biomass composition which is also one of the main elements that exist in the biomass after carbon, hydrogen and Oxygen. NO_x emission mechanism is divided into two parts, first through the oxidation of the atmospheric nitrogen during biomass combustion and second is oxidation of fuel containing nitrogen [28].

2.2.3.1 NO_x treatment

The NO_x emissions can be controlled through three ways via pre-combustion, during combustion or post-combustion processes. Although pre-combustion primarily emphasise the selective feedstock for biomass burning to reduce the relevant emissions, however, the blending of the biomass with other fuels [29,30] is also one of the solutions where not only GHG emissions but also the post-combustion problems like an agglomeration of ash is reduced. Wang et al. [31] reported that the optimum ratio of biomass in the co-firing scenario is 0.4 to reduce the NO_x emissions, whereas, further increment did not influence the NO_x emissions and combustion efficiency. In another study, it was reported that biomass alone burning produced higher NO emissions than coal and biomass/coal combustion. This could be due to higher nitrogen concentration of concerned biomass (rice husk and wood) and volatile contents than the coal. Oxygen staging in co-firing scenario helped in further reduction of the NO emissions [32].

Combustion technologies are extensively studied to reduce the NO_x emission during the burning process, for instance, selective non-catalytic reduction [33,34], Air staging or two-stage combustion [35,36], and decoupling combustion[37,38]. Hongfang et al. [37] reported the use of decoupling combustion for high nitrogen biomass and encouraged the use of decoupling technique above 600°C. It was also recommended to increase the burning rate of biomass while maintaining the adequate char content in the reactor for efficient removal of NO_x emissions. Li et al. [39] reported the use of iron oxide as a catalyst with lignite biomass

char to reduce the NO in flue gas and found that iron oxide increased the removal efficiency. Temperature also played an essential role in this study where 300 °C showed the highest denitrification. Liu et al. [40] and Khodaei et al. [41] reported the encouraging outcomes regarding reductions in the NO_x emissions up to 40% through air staging technique, however, both of the studies showed an increment in CO emissions. The complete combustion was prohibited, and particulate emission was increased in some instances. Thus, it is recommended to use the air staging technique coupled with other techniques to enhance the reductions of NO_x and other GHG emissions. The oxygen concentration in the combustion chamber also affects the NO_x emission significantly where the lower excess oxygen can potentially decrease the NO and N₂O emissions [30].

2.2.3.2 Catalytic remediation

Chen et al. [42] presented the effect of a catalyst on the emission of NO_x during the combustion of microalgae and oil shale/microalgae. NO_x emissions showed variable behaviour in which oil shale addition decreases the emissions at early stage whereas emissions increase with the time. In another study, the comparative evaluation of the three different types of algae biomass (Enteromorpha, Sargassum and Chlorella) on the NO_x emissions was reported. NO_x emissions in this particular case were not affected by the nitrogen concentration of biomass. The conversion ratio of the S and N in relevant biomass algae also showed similar patterns as of the emissions [43]. At several occasions, emission of pollutants from biomass (NO_x, PM) is higher than coal-based energy production through combustion [44–46] which raises serious concerns in this scenario where proper treatment technologies are the must consider prior to utilising the biomass for energy generation or heat production

2.2.3.3 Post-combustion treatment

Post-combustion techniques involve the treatment of flue gas at the end of the exhaust system and contribute towards the GHG emission control. The broad categories in this area are wet and dry treatment technologies which serve the purpose of removal of particulate matter, acidic gases and heavy metals from the gas. As the name depicts, dry methods involve the cleaning of gas through dry technologies, for instance, passing of the flue gas through filters or electrically charged medium which in turn captures the pollutants. *Figure 2-4* shows three different types of electrostatic precipitators uses for the classification of fly ash during the biomass burning in fluidised bed boilers. Wet methods use the universal water solubility principle and remove the pollutants from the gas through different equipment called scrubbers and mop fans. Schematic diagram of moving bed absorber utilising copper oxide as a sorbent

for the removal of NO_x can be seen in *Figure 2-5*. *Table 2-4* shows different studies conducted to remove pollutants from flue gas either during real biomass combustion or model flue gas.

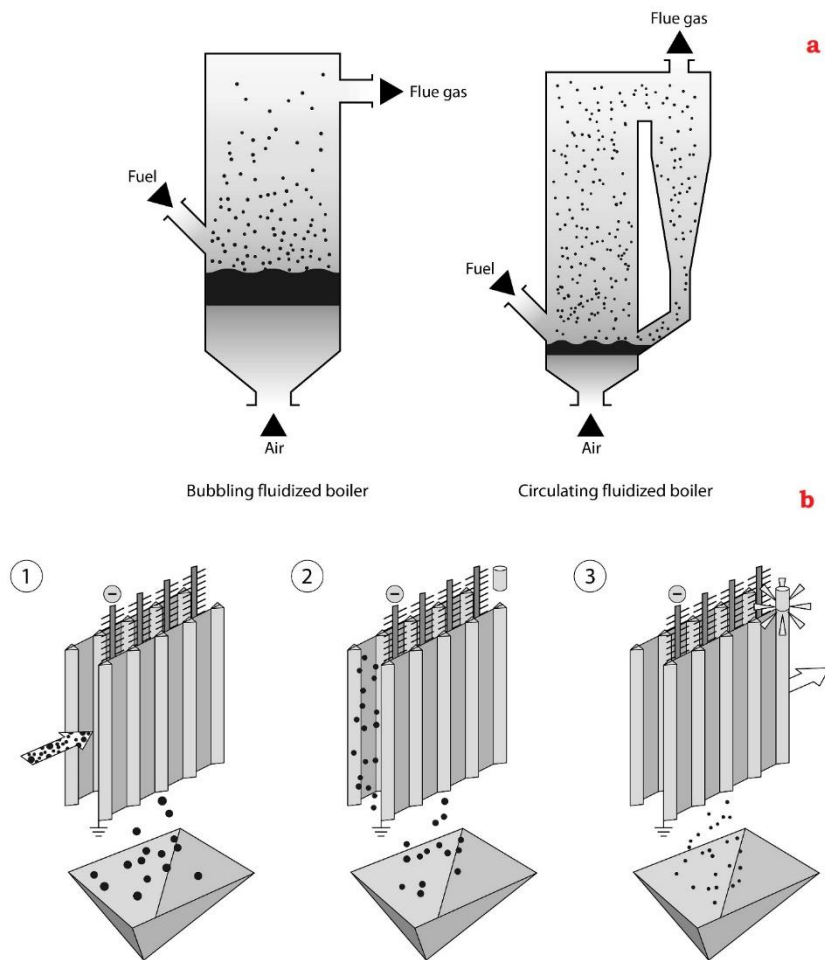


Figure 2-4 Three types of electrostatic precipitators (b) with fluidized boilers classifying the fly ash according to its composition. (Reprinted from reference [150] with permission from Elsevier)

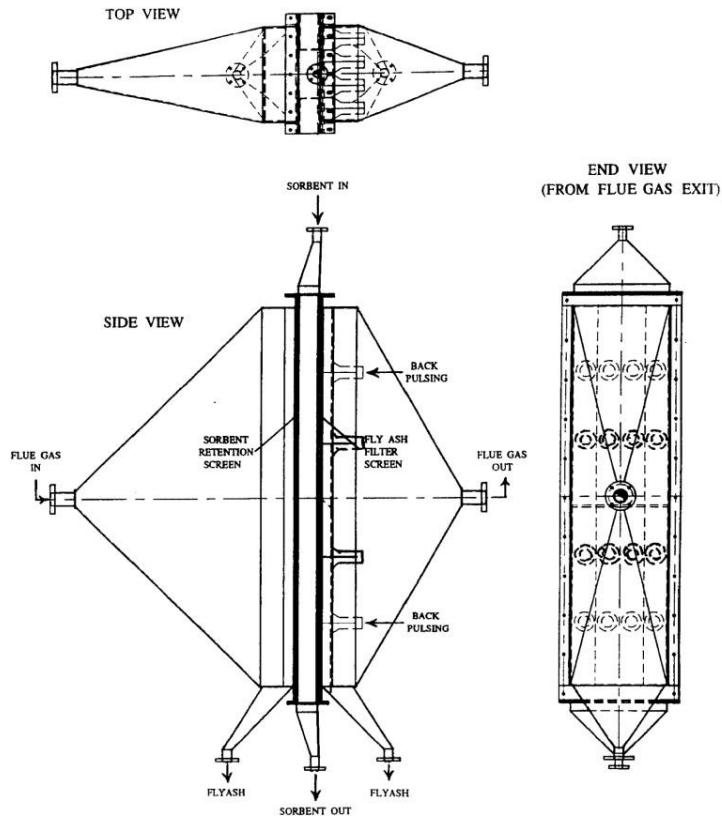


Figure 2-5 Schematic diagram of moving bed absorber. (Reprinted from reference141 with permission from Elsevier)

Table 2-4 Pollutants removal from the gas through different post-combustion technologies

Technology	Type of gas	Efficiency	Combustion chamber	Feedstock	Pollutant	References
Electrostatic precipitator	Flue gas and biogas	~ 98% for flue gas and ~ 75% for biogas	Boiler (50kW) and gasifier (100 kW)	Wood pellets	Particulate matter	[47]
Wet scrubber system with chlorine dioxide	Flue gas	>97% for SO ₂ removal and >80% for NO _x		Artificial flue gas produced	NO _x SO ₂	[48]
Condenser	Flue gas	~ 57% for PM _{2.5} and 43% for PM ₁₀	Industrial Boiler	Coal	Fine particles	[49]
Spray scrubber with 30%	Flue gas	~ 90% CO ₂ removal	Pilot plant CASPAR	Artificial flue gas produced	CO ₂	[50]

Technology	Type of gas	Efficiency	Combustion chamber	Feedstock	Pollutant	References
Mono-ethanolamine						
Moving bed absorber with copper oxide sorbent	Flue gas	~85% fly ash ~ 90 SO ₂ and NO _x removal	Life cycle test system	Coal	SO ₂ NO _x	[51]

2.2.4 Biomass ashes

Besides producing the greenhouse gases in the atmosphere, biomass is also responsible for the production of ashes in the combustion chamber which contains different minerals, trace and heavy metals. There are two main types of ashes produced during biomass combustion (i) fly ash obtained through the flue gas cleaning. (ii) Bottom ashes left after the combustion of biomass. The composition of ashes depends on the biomass uptake of the respective elements during its lifetime and its inherent composition. The ash composition although have the potential to affect the environment; however, the significant problem occurs in the chamber reacting the different elements together to produce the silicates, sulphates and chlorides etc.

2.2.4.1 Slagging and fouling

The alkalis present in the biomass reacts with other minerals and produce intermediate components. These components react further to create slagging and fouling in the reactor which reduces the productivity of the plant and creates problems in the input of the feedstock, ash congestion and energy transfer. These problems also cost economically where the operational cost and energy is required to remove the ashes and respective clogging. *Figure 2-6* shows the forming ash elements exist in various biomass fuels according to its weight. As it can be seen that potassium, silicon and calcium are the major contributors in this area. *Figure 2-7* shows the potassium, sulphur and chlorine transport during the biomass combustion in the form of particles. KCl and K₂SO₄ can be found in the form of coarse particles known as PM₁₀ and in the form of aerosols. In a detailed study presented by Bogush et al. [52], reported different types of biomass ashes generated throughout the UK with the goal of comprehensive characterisation. Most of the ashes produced from the combustion of meat, poultry litter and bone meal tend to be alkaline with a high concentration of P (phosphorus), K (potassium), and Ca (calcium). The high concentration of P and K allows the use of this end-product in agricultural fields. Vassilev et al. [53] presented a comprehensive review on ash elements

present in different types of biomass (532 varieties) and classified the biomass accordingly (Figure 2-8).

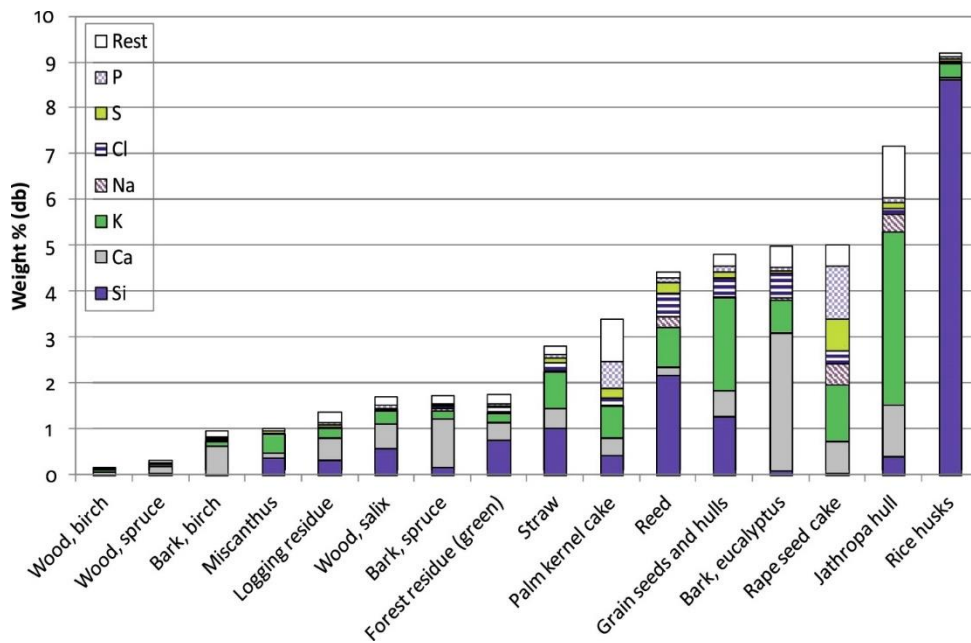


Figure 2-6 Elements contributing towards ash production in biomass during combustion. (Reprinted from reference [151] with permission from Elsevier) (db = dry basis)

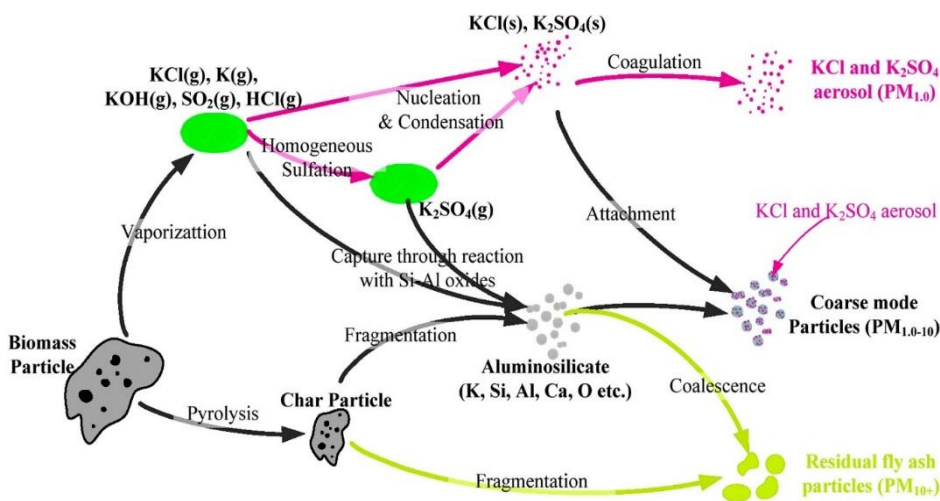


Figure 2-7 Transport pathway of potassium, chlorine and sulphur from biomass to fine particles during combustion of biomass. (Reprinted from reference [142] with permission from Elsevier)

1. WWB - Wood and woody biomass
 - 1.1. Stems
 - 1.2. Barks
 - 1.3. Branches
 - 1.4. Pruning
 - 1.5. Leaves
 - 1.6. Others
 2. HAB - Herbaceous and agricultural biomass
 - 2.1. Grasses
 - 2.2. Straws
 - 2.3. Stalks
 - 2.4. Shells
 - 2.5. Husks
 - 2.6. Pits
 - 2.7. Fruits
 - 2.8. Residues
 3. AB - Aquatic biomass
 4. AHB - Animal and human biomass wastes
 5. CB - Contaminated biomass and industrial biomass wastes (semi-biomass)
 6. BM - Biomass mixtures
 7. OB - Other biomass
- AVB - All varieties of biomass
 NB - Natural biomass
 P - Peat
 L - Lignite
 S - Sub-bituminous coal
 B - Bituminous coal

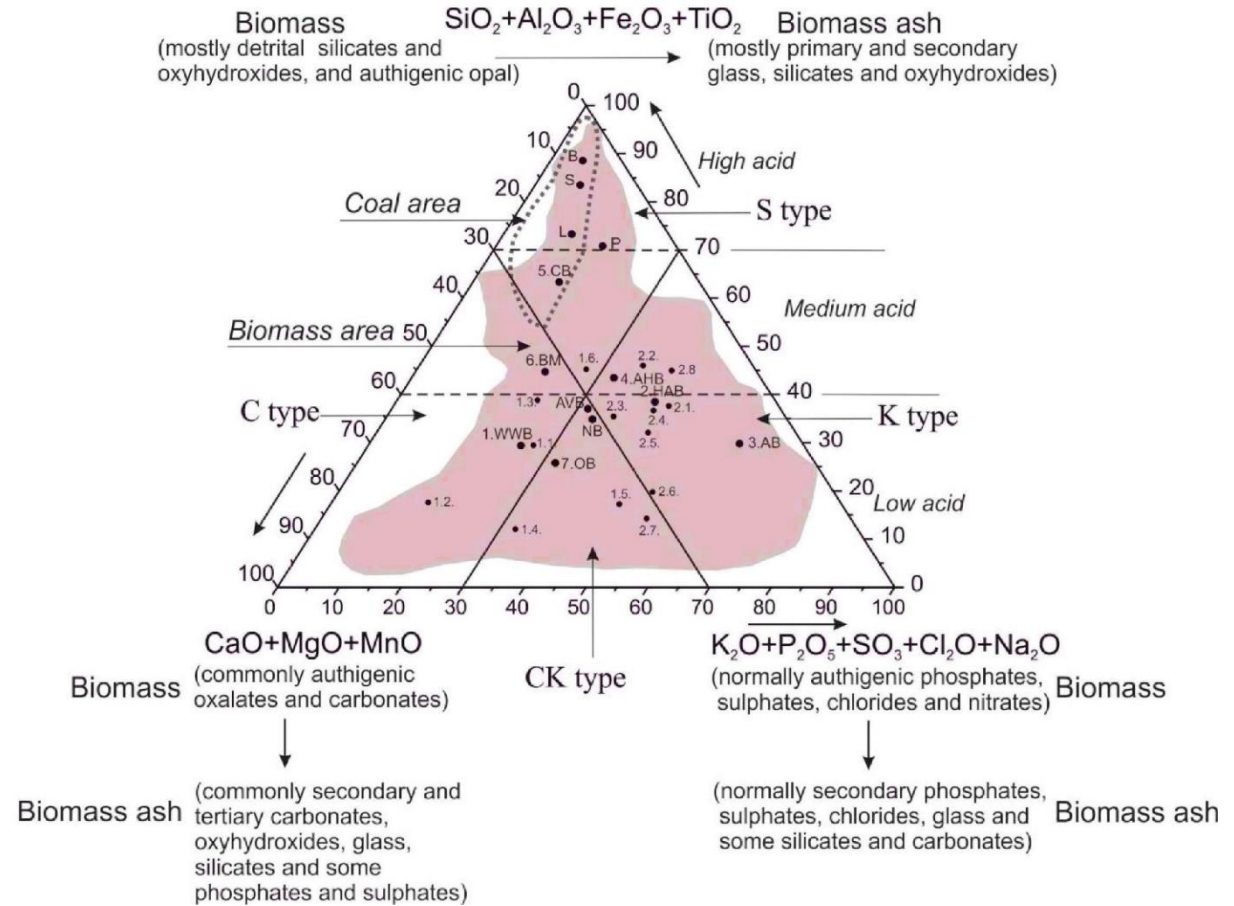


Figure 2-8 Classification of ash produced from biomass combustion according to its chemical composition. (Reprinted from reference [46] with permission from Elsevier)

2.2.4.2 Factors affecting the slagging and fouling

Although there are many factors which influence the creation of slagging and fouling through biomass combustion including peak temperature, heating rate and biomass feed rate. However, to calculate the effect of biomass slagging potential is understood by the relations developed for coal combustion. These relations are generally not suitable for accurate prediction. Garcia et al. [54] presented a comprehensive study to evaluate the established relationships and indices to calculate the biomass slagging capacity, and there was no direct relationship found among the current indices for biomass fuels. Hence it was recommended to obtain real-time data for biomass combustion scenarios and reevaluate the effect of these indices and establish relationships as per their diversity of the composition and combustion behaviour.

Weber et al. [55] reported the high temperature (950-1200 °C) effect on ash deposition to minimise the effect of alkali salts on ash condensation. Ash deposition and sticking efficiency increased at 1170 °C (1.2-2.4%) (0.4) as compared to 970 °C (0.2-0.5%) (0.03-0.09) respectively. This also agrees with the results presented by Yang et al. [56] in which increase in sticking efficiency was observed with the increase in furnace temperature. The deposition time also plays an important role that increases the deposition due to thermophoresis phenomenon and local temperature variation. Kleinhans et al. [57] explained the deposition of ash according to its size and contents. Particle viscosity and kinetic energy are the main parameters explaining the sticking behaviour of ash particles. Alumino-silicate particles containing small size stick together due to low kinetic energy, whereas, large particles rich in iron mainly effected by low viscosity values. At another instant, the fluidised temperature was shown as a critical factor due to silicate melt induced slagging. The higher the fluidised temperature, reduces the high-temperature silicate melt induced slagging [58]. In a separate study, Niu et al. [59] presented an alkali-based slagging mechanism in boilers (*Figure 2-9*). Slagging was defined by chlorine and sulphur ratio ($Cl + K_2O + Na_2O/SiO_2 + Al_2O_3$) and ($S_{volatile} + K_2O + Na_2O/SiO_2 + Al_2O_3$) respectively. Slagging was predominant with chlorine and sulphur ratio higher than 2.4 and 1.9 respectively. Increasing chlorine and sulphur ratio expands the growth of potassium chloride (KCl) and Aphthitalite which ultimately causes the intensification of the slagging process.

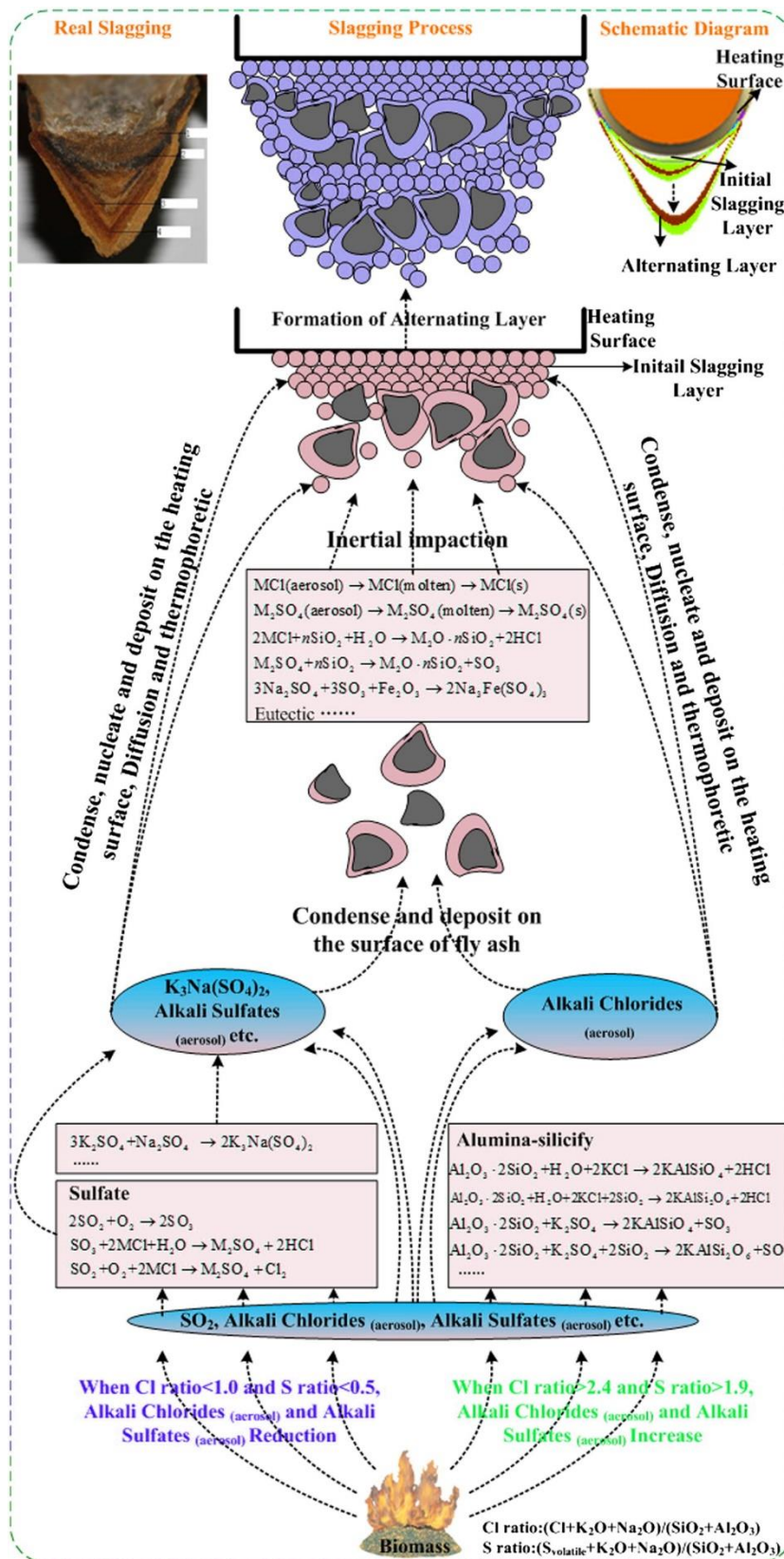


Figure 2-9 Slagging mechanism due to alkali during combustion of biomass. (Reprinted from reference [59] with permission from Elsevier)

2.2.4.3 Biomass ash applications

As the ash production is inevitable during biomass combustion as a by-product, it has found its way in many applications, For instance as a binder replacement in cementitious composites [60], biogas purification by the removal of hydrogen sulphide [61] and sewage sludge treatment [62]. Recently Ribeiro et al. [63] reported the use of industrial fly ash and domestic ash used for soil fertility and plant growth. Domestic ash was found to be effective in transferring of the macronutrients such as K, P and Ca to the soil. However, the increase in plant growth was not observed. Cruz-Paredes et al. [64] compared the phosphorus fertiliser application with biomass ashes in barley crop and pointed out that biomass ashes, not a significant factor in altering the yield of the crop. Hence, it can be used as a substitute for phosphorus fertiliser. A long-term study in this scenario is recommended to see the cyclic effect of ashes on overall production behaviour. In another study by Zhang et al. [65] the replacement of potassium fertiliser with ash tablets (6mm × 2mm) to (15mm × 5mm) was studied for slow availability of nutrients to the plants. The reported methodology reduced the potassium release rate as compared to powder ash to 1/60th. However, it is still higher than conventional potassium fertiliser. The bigger size of tablets (210mm × 70mm) and a smaller diffusion coefficient is recommended to use the biomass ash as a fertiliser.

2.3 Pyrolysis

Thermochemical processing addresses the critical challenges faced by the combustion system as mentioned in the previous section. This processing technique reduces CO₂ emissions, properly utilises the biomass and divert the end-products yield according to the desired outcome. There are three subgroups in this processing technique i) Torrefaction ii) Pyrolysis iii) gasification. There is a newly emerging area in this scenario, the hydrothermal processing, which also contains three subcategories a) hydrothermal carbonisation b) hydrothermal liquefaction (c) Hydrothermal gasification. All the processing of biomass in this category involves the controlled heating in a limited or oxygen-free environment where biomass is primarily converted into three components i) gas ii) liquid and iii) solids. *Table 2-5* shows a typical distribution of these products through each of the processes. The controlled conditions, type of fuels and their product's use are discussed in detail in the subsequent section.

Pyrolysis is a process of heating the organic materials in the absence or limited supply of oxygen at elevated temperature (<700 °C) [66]. It contains mainly three subcategories a) slow pyrolysis b) Intermediate pyrolysis c) fast pyrolysis. Intermediate pyrolysis contains features

of both slow and fast pyrolysis in which major product is liquid (50%) and rest of them are solid (25%) and gas (25%) [67]. Cellulose, hemicellulose and lignin converts to tar, non-condensable vapour and char during pyrolysis at 150 – 350 °C, 275 – 350 °C, 250 – 500 °C respectively.

Table 2-5 Approximate yields of the products obtained by thermochemical conversion of biomass. (Adapted from reference [68] with permission from Elsevier)

Technology	Product distribution (wt. %)		
	Solid (char)	Liquid (bio-oil)	gas
Slow pyrolysis	35	30	35
Fast Pyrolysis	10	70	20
Gasification	10	5	85

2.3.1 Slow pyrolysis

Slow pyrolysis is the heating of the biomass/organic material in the absence or limited supply of oxygen with a slow heating rate and predominantly produces a solid product called biochar or simply *char*. This obtained char product contains different properties according to the type of feedstock and can be used for different applications. Most of the organic waste derived from different sources including but not limited to wood waste [69], farm and agricultural waste [70], municipal solid waste (MSW) [71] and industrial waste [72] can be utilised to process the waste and produce char for further use in different applications. Char produced from lignocellulosic biomass, and agro-industrial waste is found to be more suitable for solid fuel production [73] due to retention in energy density, however, poultry litter char is suitable for soil amendment. Zhang et al. [74] have done a comprehensive study on char production from four different types of biomass (pine, peanut shell, sugar cane and oak) and categorised the char into three categories depending on the elemental composition (*Figure 2-10*). Char produced from peanut shell contains several elements suitable for plants and soil fertility, whereas sugarcane char can be a source of potassium and phosphorus.

The other significant factor affecting the char yield and properties is the reaction conditions in the reactor. For instance, increasing peak temperature and increasing residence time leads to less yield and modifies the properties according to the char produced at relatively fewer peak temperatures. The peak temperature is the temperature at which the pyrolysis reaction terminates, and products start to cool down. Overall, the higher temperature leads to the higher

carbon content, thermally stable char [75], micropore volume and higher surface area [76]. The increasing temperature of the pyrolysis also reduces the nutrients utilised by plants, for instance, phosphorus (P), potassium (K) and nitrogen (N) [73], hence not recommended for improving soil fertility. The residence time of the feedstock in the reactor also contributed towards change in properties, however, the significant effect of residence time observed at the low temperature (350 °C) pyrolysis rather than relatively high temperature (>600°C) pyrolysis.

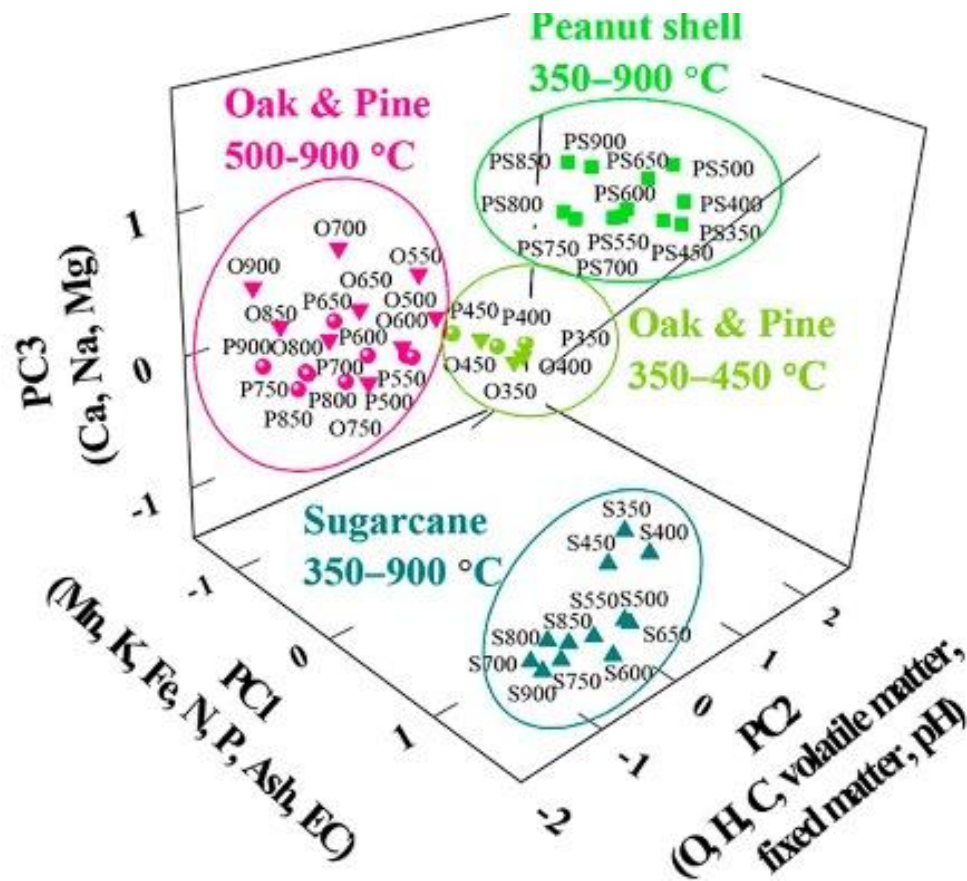


Figure 2-10 Categorization of char according to the feedstock type. (Reprinted from reference [74] with permission from Elsevier)

2.3.1.1 Activation and applications of char

Char properties can be changed post-pyrolysis through different techniques called as physical and chemical activation. This process removes the volatiles and improves the surface area which is valuable in various applications. In a recent study by Bardestani et al. [77] compared

the steam activation and mild air oxidation and found that surface area increased 20 times through the steam activation process, however functional groups decreased. Mild air oxidation, on the other hand, increased the functional groups from 44 to 104.6 $\mu\text{mol m}^{-2}$. Genuino et al. [78] also reported an increase in surface area (+64 %) and adsorptive properties after thermal and chemical activation of MSW derived char. More than 99 % of dye removal was achieved with activated char in the presence of concentration up to 25 mg L^{-1} . Wang et al. [79] reported the increase in adsorption properties for acid red 18 dye with the use of nitrogen-doped activated carbon prepared through ammonium chloride and ammonium acetate in the presence of microwaves.

Char use in heavy metals removal has been reported on several occasions [80–82] and found to contain a significant effect on adsorption properties after the activation. Ahmad et al. [83] recently reported the effect of potassium-rich char on the removal of heavy metals (Cu, Cd and Pb) in aqueous solution avoiding the separate activation. Banana peels and cauliflower leaves were used to produce the char. Banana peels char was found to enhance the sorption capacity than cauliflower char due to electrostatic attraction being the main driver in sorption capacity. At another instant, Rice straw char produced at 600 °C was investigated for the adsorption of Cu and Zn in a single and binary metal system. Biochar was highly active in adsorbing respective metal in the beginning, however, after four hours reaches equilibrium. Char was found to be highly sorbent in the presence of single metal and reduces the efficiency in the presence of both metals. Adsorption of Zn was affected the most in the binary metal system [84].

Char from different materials is also observed to be effective sorbent of NH_4 [85]. Char use in other applications is being recognised with heavy metal removal and soil improvement and amendment. For instance, char use in wood-polypropylene composites is comprehensively reported by Das et al. [86,87] and positive results obtained for mechanical and fire resistance properties. Similarly, char use in concrete applications improved the strength of concrete [88,89]. It is expected that with the passage of time, char use in different applications will further add value and will continue to embark its potential with several varying properties. Although char is one of the highly stable carbon materials with years of carbon storage potential, nonetheless, the use of char as fuel is limited and alternative technology of receiving liquid based fuel product in pyrolysis category is fast pyrolysis.

2.3.2 Fast pyrolysis

Fast pyrolysis yields a high amount of liquid product called bio-oil at high heating rates which sometimes spans from few milliseconds to seconds. The obtained resultant product thus contain several properties and has the potential to use in fuel and chemical based applications. The significant parameter in this scenario is the heating rate which determines the total product output and properties. Bio-oil produced through this process contains many challenges including high viscosity, low heating value and water fractions. There are two routes considered after the production of bio-oil, either convert it into biofuel through upgrading (cracking [90] mechanism, steam reforming [91] and hydrodeoxygenation [92]) or convert it into suitable chemicals which can further be processed to use in different applications. *Figure 2-11* shows a different process method generally used to upgrade bio-oil into useful products.

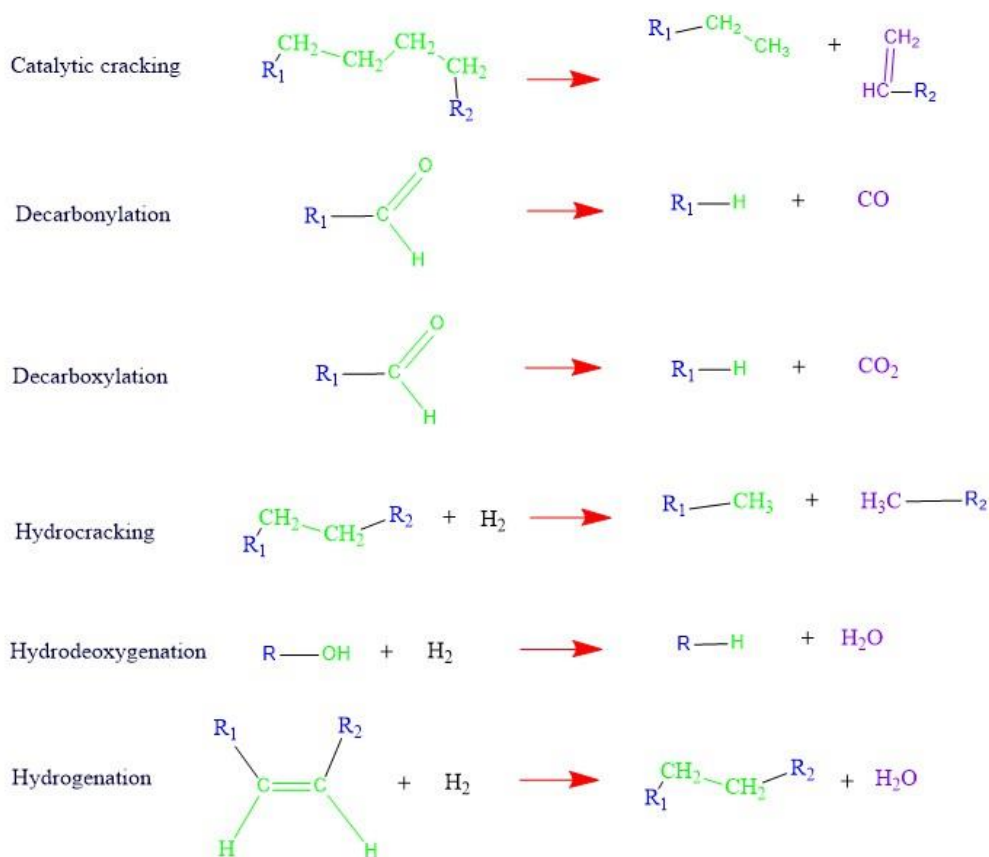


Figure 2-11 Bio-oil upgrading process in a nutshell. (Adapted from reference [96] with permission from Elsevier)

2.3.2.1 Bio-oil upgradation

2.3.2.1.1 Catalytic cracking

Hew et al. [93] have done catalytic cracking of bio-oil produced from empty fruit bunch and reported 400 °C, 15 min and 30 grams of the catalyst as optimum parameters for the conversion of bio-oil to gasoline. The conversion rate was remarkably more than 90%. *Table 2-6* shows a different zeolite cracking catalyst utilisation for the upgrading of the bio-oil and its yield potential. As can be seen, the yield is less than 30% in all cases. Combined catalytic cracking is one of the recent interests of today's research in which bio-oil is combined with different hydrocarbon-rich materials to produce more effective products. For instance, Recently, Ma et al. [94] reported the upgrading of the mixture of bio-oil and kitchen waste oil with the use of catalyst HZSM-5. Kitchen waste oil acted as a hydrogen supplier who helped in the formation of hydrocarbons from oxygenated unsaturated compounds. *Figure 2-12* shows the conversion chain of different reactions occur during the combined upgradation of kitchen waste oil and bio-oil produced from sawdust at 550 °C. In another study, bio-oil was mixed with ethanol and performed co-cracking over the Ni-ZSM-5/MCM-41 catalyst. The significant drop in acid content (0.1 wt. %) was achieved and converted acids to ketones [95].

Table 2-6 Catalytic upgrading of the bio-oil through zeolite cracking. (Adapted from reference [96] with permission from Elsevier)

Catalyst	Setup	Feed	Time (hours)	Pressure (bar)	Temperature (°C)	Oil yield (wt. %)
GaHZSM-5	Continuous	Bio-oil	0.32	1	380	18
H-mordenite	Continuous	Bio-oil	0.56	1	330	17
H-Y	Continuous	Bio-oil	0.28	1	330	28
HZSM-5	Continuous	Bio-oil	0.32	1	380	24
HZSM-5	Continuous	Bio-oil	0.91	1	500	12
MgAPO-36	Continuous	Bio-oil	0.28	1	370	16
SAPO-11	Continuous	Bio-oil	0.28	1	370	20
SAPO-5	Continuous	Bio-oil	0.28	1	370	22
ZnHZSM-5	Continuous	Bio-oil	0.32	1	380	19

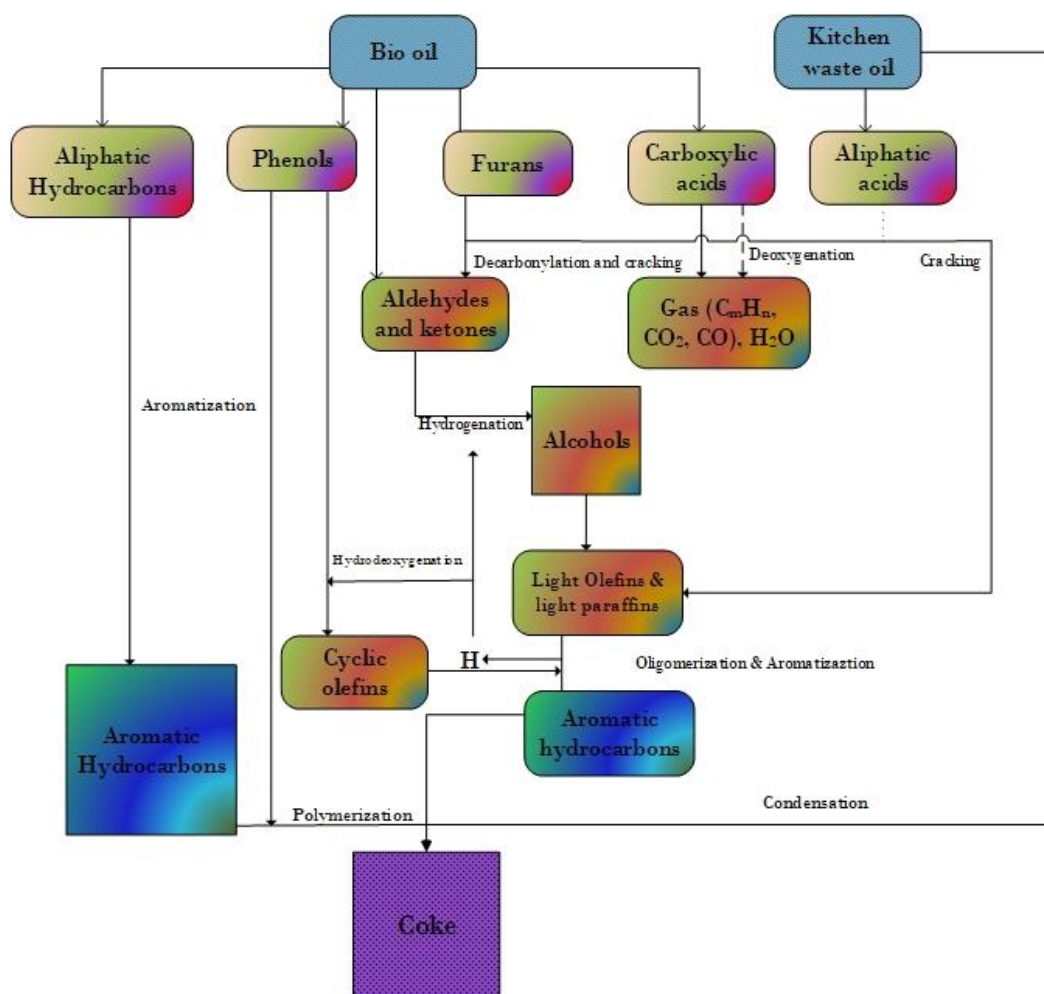


Figure 2-12 Bio-oil and kitchen waste oil upgrading pathway over HZSM-5 catalyst. (Reprinted from reference [94] with permission from Elsevier)

2.3.2.1.2 Catalytic steam reforming

Catalytic steam reforming helps to produce useful gaseous products (H_2 , CO etc) from bio-oil or pyrolysis oil and helps in the elimination of carbon-rich phases. There is a number of studies done on the steam reforming process and optimisation of hydrogen yield [97,98]. Nabgan et al. [99] presented a comprehensive review article recently on the subject matter. Quan et al. [100] conducted the steam reforming of bio-oil through the Fe/olivine catalyst which helped in the conversion of the phenolic-rich oil to the light gas phases such as CO, H_2 and CH_4 . The optimum conditions reported are 800 °C with weight hourly space velocity 0.5 and steam to carbon ratio 2 to achieve carbon conversion efficiency 97%.

Bimbela et al. [101] obtained the highest H₂ production with Ce impregnation onto conventional Ni-Mg-Al catalyst. Ce impregnation at 0.5% produced the highest yield of H₂ as compared to Ni/Mg-Al catalyst and provided stable H₂ production. At another instant, approximately 80% hydrogen production achieved and 97 % carbon conversion attained at 850 °C and steam to carbon ratio 5:1. Most of the carbon removal can be achieved through combustion in the air flow at 600 °C [102]. Char is found to be an effective catalyst in steam reforming process and sufficiently high yield of hydrogen approximately 89 % obtained at 900 °C, steam to a bio-oil model compound ratio of 3 and weight hourly space velocity equal to 1. This high efficiency was obtained due to alkali and alkaline earth metals present in char which influenced the water adsorption and facilitated the formation of reactive hydroxyl groups [103].

2.3.2.1.3 Catalytic hydrodeoxygenation

Bio-oil tend to contain a high amount of oxygen content which results in less energy yield as compared to conventional fuels. Hydrodeoxygenation is the process of oxygen removal in bio-oil and produces energy-rich products which can be called as a bio-fuel. This product has the potential to be incorporated with conventional fuels. Although significant advances have been reported recently, nevertheless, further research is required to improve the quality of biofuels further. Cheng et al. [104] have done in-situ hydrodeoxygenation of pine sawdust bio-oil over Pd/C catalyst. This is a relatively new technique in which hydrogen is not provided through an external source, despite the water present in the bio-oil was used to produce hydrogen. The optimum temperature was reported to be 250 °C yielding heating value of oil 30 MJ/kg with high hydrocarbon content 24%.

This technique was earlier reported by Cheng et al. [105] in which Zinc hydrolysis used despite external hydrogen supply. However, higher treatment temperature (<400 °C) were selected and increasing temperature resulted in improved hydrocarbon content (38-69%) and heating values (33 MJ/kg). Similarly, Mosallanejad et al. [106] presented another approach of in-situ upgrading of bio-oil through hydrodeoxygenation with the use of pulsed corona discharge (plasma reactor). The hydrogen was produced through methyl decomposition rather than the separate addition of hydrogen. This study was done on model compound 4methylanisole rather than bio-oil derived from biomass, hence further detailed study is required on original bio-oil and evaluates the detailed effect on hydrogen production.

2.3.2.1.4 Catalytic hydrocracking

Hydrocracking is the process of converting hydrocarbons containing high boiling temperature to low boiling temperature hydrocarbons. This also includes the use of catalyst during the reaction which can help to reduce the bio-oil into simpler compounds. A study by Lee et al. [107] was reported for selective hydrocracking done on tetralin model compound in the presence of different catalysts (Ni/H beta catalyst with Ni contents from 1-10%, Ni-Sn/H beta and CoMo-S/H beta) to record the benzene, toluene and xylene production. The yield order is as follows Ni-Sn/H beta > CoMo-S/H beta > Ni/H beta. In another recent study, Upare et al. [108] showed that synthesised catalyst (cobalt promoted Mo/ β with different metallic loadings (0.5-1.5)) promoted hydrocracking of model compound tetralin and bio-oil. The highest yield of benzene, toluene and xylene was produced from Co/Mo β catalyst at 0.5 impregnations in both cases, however, the studied compounds produced in less yield in bio-oil (55%) than model compound tetralin (63%). This also shows the possible variation in the results while conducting the experiments with bio-oil rather than model compounds.

2.3.2.2 Cellulose, hemicellulose and lignin degradation during pyrolysis

Cellulose, hemicellulose and lignin, the basic constituent of the biomass, is responsible for the complex chemical reactions upon heating and converting into mixed crude oil during fast pyrolysis. These three components can be identified according to their degradation pattern in the pyrolysis. Hemi-cellulose, cellulose and lignin degradation occur at (220-315 °C), (315-400 °C) and >400 °C respectively [109]. Hemicellulose degradation causes the production of CO₂, formic acid and tar. The other products obtained during degradation are xylose, acetol, CO and 2-furaldehyde [110]. Gaseous products yield obtained during hemicellulose pyrolysis are given in *Table 2-7*. It can be seen that CO₂ is found to be the highest production gas followed by CO and H₂ and among the organic compounds acetic acid produced at highest concentration followed by 1,4-anhydro-D-xylopyranose and furfural. High amount of CO₂ production resulted from decarboxylation of -acetyl groups linked to the xylan chain. Acetic acid and 1,4-anhydro-D-xylopyranose reduced with the increment of temperature and furfural concentration increased with the increment of the peak temperature [111]. Hemi-cellulose degradation into bio-oil, gas and char is shown in *Figure 2-13*.

Table 2-7 Gaseous products produced during the fast pyrolysis of hemicellulose. (Adapted from reference [111] with permission from Elsevier)

Compounds (wt. %)	425 °C	475 °C	510 °C	570 °C	625 °C	690 °C
CO ₂	25.01	24.54	25.61	25.78	24.79	22.87
CO	5.35	5.23	6.02	6.93	9.24	13.33
H ₂	1.08	1.60	2.35	2.49	3.29	3.34
Acetic acid	4.44	4.40	3.82	3.20	-	2.45
1,4-anhydro-D-xylopyranose	3.84	3.43	2.85	2.01	-	0.69
Furfural	1.94	2.30	2.40	2.86	-	3.16
Methanol	0.81	1.01	1.11	1.13	-	1.14
Acetone	0.69	0.77	0.84	1.00	-	1.06

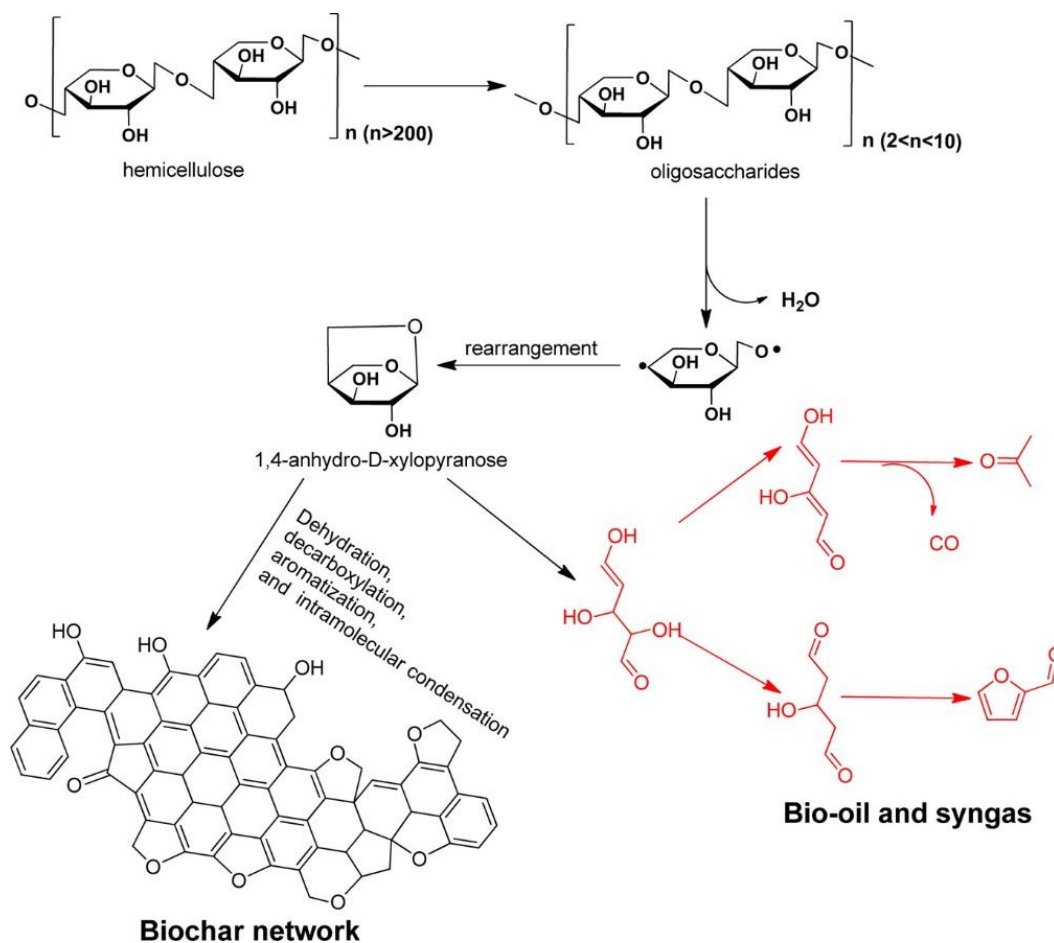


Figure 2-13 Hemicellulose degradation under pyrolysis into bio-oil, gas and char. (Reprinted from reference [152])

Cellulose exists anywhere between 40 to 90 % depending on the type of biomass. Cellulose pyrolysis divided into three phases, development of active cellulose or anhydrocellulose, depolymerisation and char production process. The phenomenon of active cellulose occurs before 300 °C due to dehydration, depolymerisation between 300-390 °C and char production effected from 380 up until 800 °C. Depolymerisation is the step which causes the highest production of volatile compounds [112]. *Figure 2-14* showed the degradation of cellulose to different volatile compounds obtained during fast pyrolysis. Several types of linkages exist in lignin between carbon to carbon, ether and ester, for instance, β -O-4, β - β , β -5, 4-O-5, α -O-4, 5-5. *Figure 2-15* shows a β -O-4 type linkages model compound during the pyrolysis and degradation into sub-compounds upon thermal treatment. Lignin pyrolysis divides into two temperature categories. Initially, alkyl chain conversion and breaking of some of the linkages occur up to 400 °C, and later type H phenols concentration increased in bio-oil and type S phenol concentration decreased with the increment in temperature up to 800 °C [112]. As compared to cellulose and hemicellulose where gas, tar and char are the main products of the pyrolysis, lignin produces gas, char, phenols and lignin derivatives which can later be distilled into different fractions [113]. *Figure 2-16* presents the lignin conversion into chemicals during fast pyrolysis from 400 to 700 °C in a simple equation form.

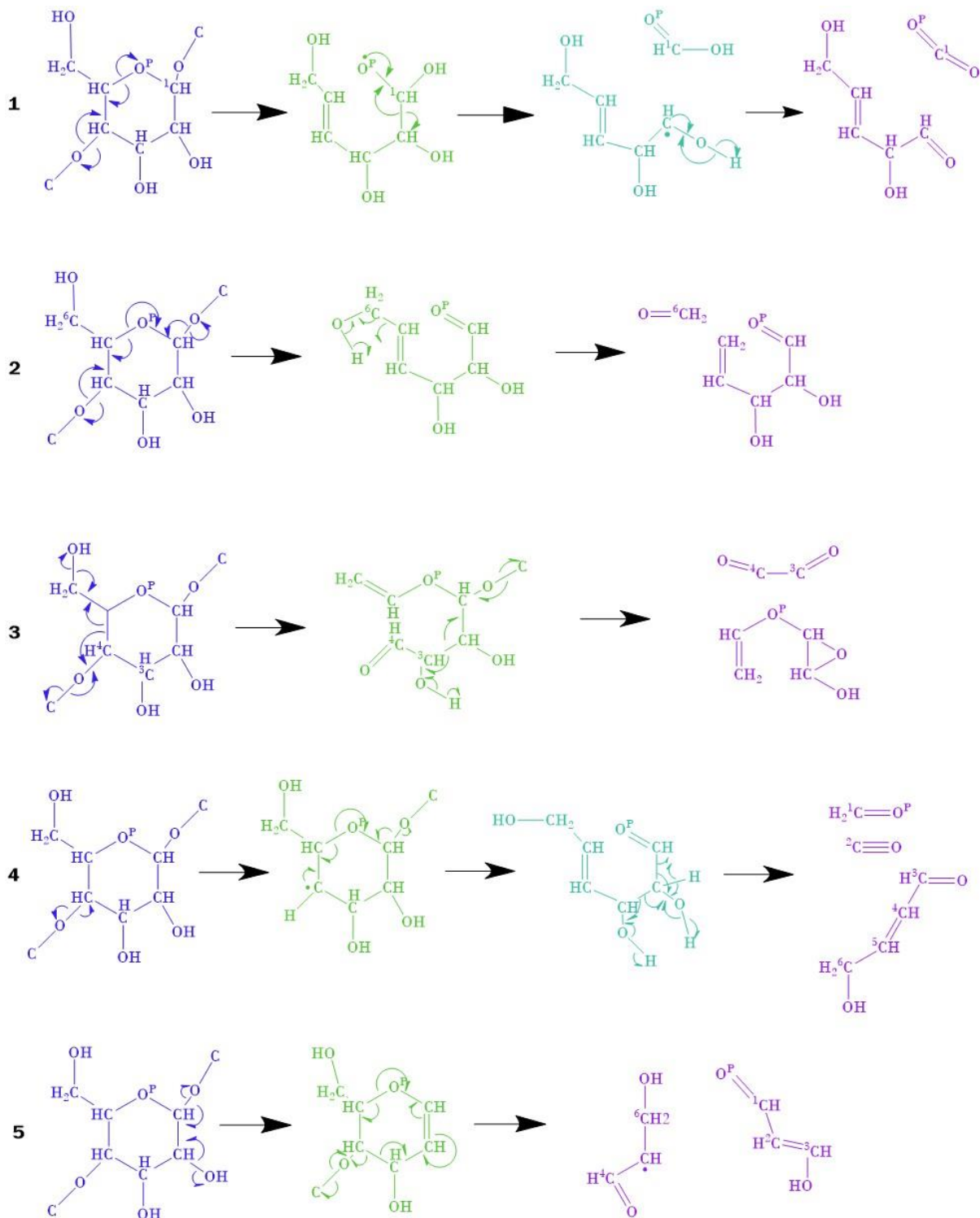


Figure 2-14 Pyrolysis of cellulose to volatiles. Four possible pathways from Glycosidic cleavage to the formation of (1) formic acid, CO_2 and 2,5 dihydroxy-3-pentanal (2) formaldehyde and 2,3 hydroxy-4-pentanal (3) glyoxal and 3-(vinylloxy)-2-oxiranol (4) formaldehyde, carbon monoxide and 4-hydroxy-2-butenal (5) malondialdehyde and a radical intermediate. (Adapted from reference [153] with permission from Royal Society of Chemistry)

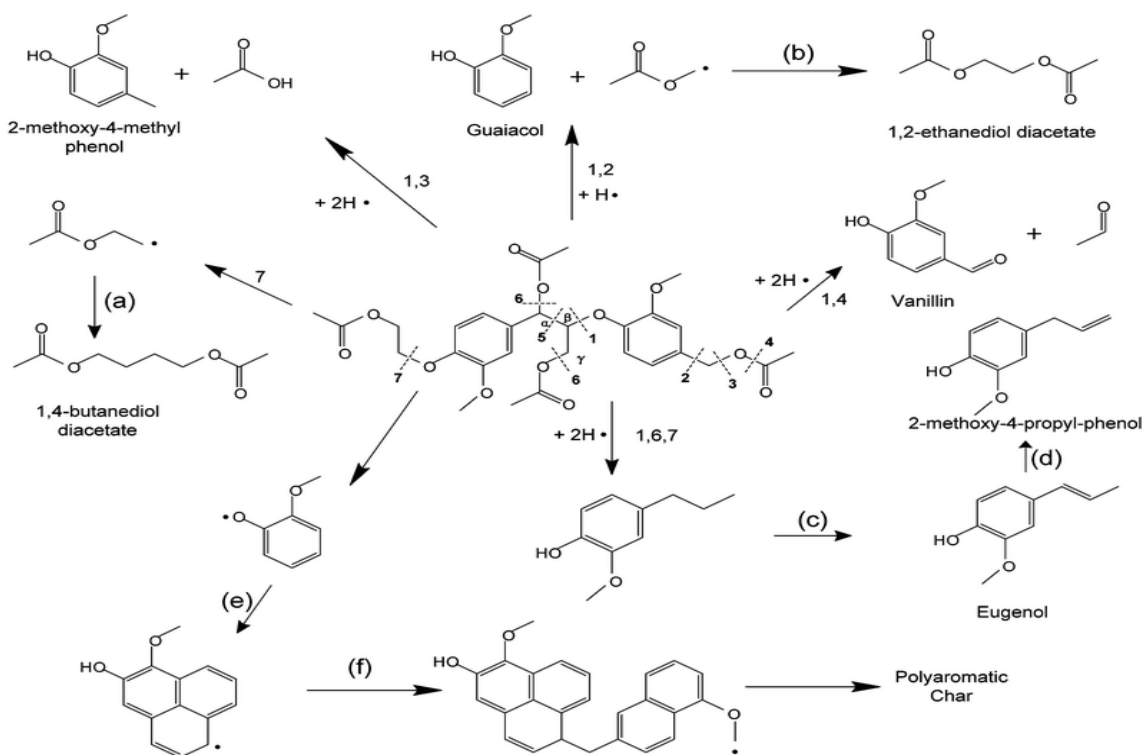


Figure 2-15 Pyrolysis mechanism explained for β -O-4 type lignin model compound. (Reprinted from reference [154] with permission from Royal Society of Chemistry)

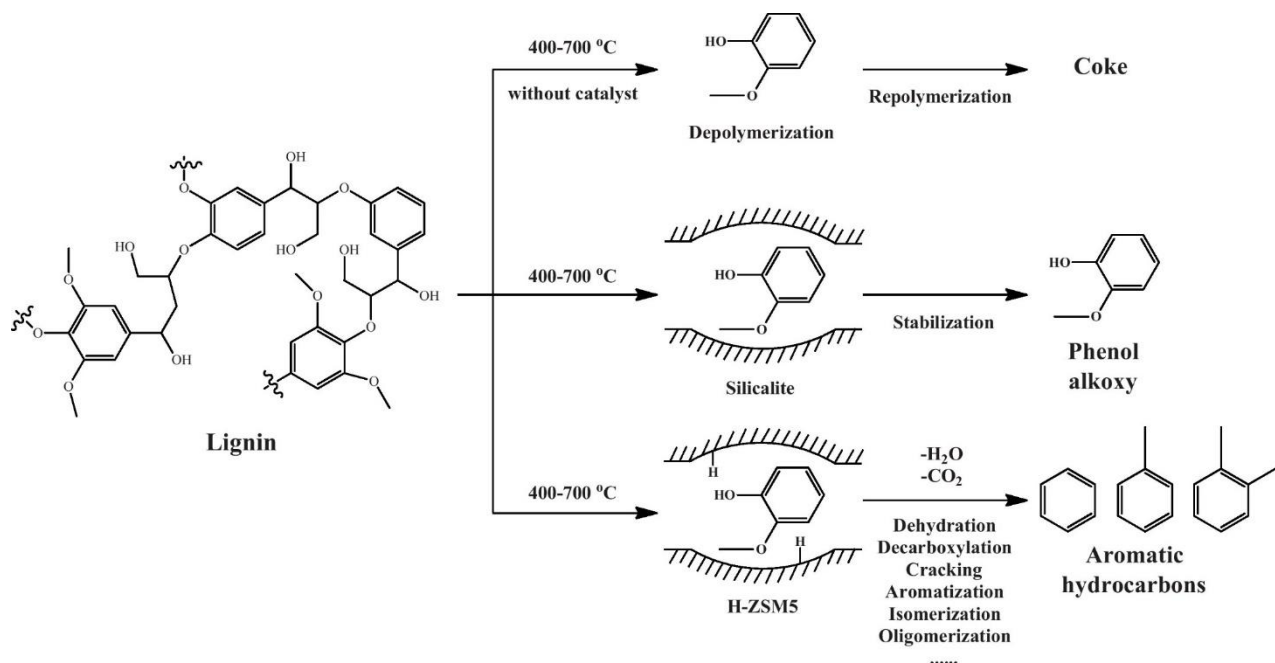


Figure 2-16 Catalytic and non-catalytic process for lignin conversion during fast pyrolysis (Reprinted from reference [155] with permission from Elsevier)

2.4 Gasification

Gasification treatment of the biomass is well studied and implemented commercially as compared to pyrolysis due to the obtained product is easily accessible and require less post-recovery work. The major product is syngas which can be used in electricity generators or in boilers to produce energy and use as a chemical feedstock. The gasification process consists of four main stages (i) oxidation (ii) drying (iii) pyrolysis and (iv) reduction [114]. From the drying of the biomass through pyrolysis, oxidation and reduction of tar, biomass goes through several physical and chemical changes which lead to producing CO, CO₂, H₂ and other gases. These products further processed leading to the production of different types of fuel including methanol, Fischer Tropsch processing to produce biofuels, pure hydrogen production as a fuel, methane production. These products contribute not only towards renewable fuels but also helps to cope with other fossil fuels related to use in chemicals production. Different types of gasifiers are used in the gasification process from conventional updraft or downdraft gasifiers to modern gasifiers like plasma. *Figure 2-17* is showing a schematic diagram of different types of gasifiers with their advantages and disadvantages.

Gasification like other processing techniques also influenced by the reaction conditions including peak temperature, residence time and heating rate. Similarly, the atmosphere inside the reaction chamber also affects the resultant properties of syngas and char. Tang et al. [115] reported the effect of N₂ and CO₂ inert atmosphere on char properties from MSW and found that surface area and porosity is significantly affected by the change in atmosphere. CO₂ improved the properties of the char as compared to N₂ until 700 °C, however, porosity in CO₂ atmosphere degraded due to gasification. In another study by Tang et al. [116] showed that CO₂ act as inert atmosphere under 600 °C, whereas it shifts to reaction atmosphere above 600 °C which leads to the higher production of syngas facilitating the gasification process. Mainly CO₂ is being employed to improve the char properties and enhance the gasification process rather than using it as inert gas for biomass. Recently Azuara et al. [117] reported that CO₂ atmosphere instead of N₂ reduced the CO₂ emission, whereas, CO production increased comparatively.

Reactor Configuration	Advantages	Disadvantages	Representative Diagram
Updraft Fixed Bed	<ul style="list-style-type: none"> High ash content tolerance High moisture content feedstocks are acceptable Less sensitive to feedstock size and quantity Low exit gas temperature 	<ul style="list-style-type: none"> Large amount of tar accumulation Gas cleanup needed for engine operation 	
Downdraft Fixed Bed	<ul style="list-style-type: none"> Low tar accumulation Relatively little gas cleanup is needed 	<ul style="list-style-type: none"> Only dense feedstocks are acceptable Low energy efficiency Product gas leaves reactor at high temperature High ash accumulation High exit draft temperature 	
Bubbling Fluidized Bed	<ul style="list-style-type: none"> Excellent heat transfer High degree of mixing Easy ash removal system Less sensitive to feedstock variations Can handle large quantity, low quality feedstock High reaction rates, low residence time Low investment needed for scale up 	<ul style="list-style-type: none"> Complex operation due to inclusion of fluidizing agent High tar and dust content in produced gas Formation of eutectics at high temperature Require higher gas flow velocities than fixed bed gasifiers 	
Circulating Fluidized Bed	<ul style="list-style-type: none"> Same as bubbling fluidized bed gasifier Particle recycling 	<ul style="list-style-type: none"> Same as bubbling fluidized bed gasifier Requires a high velocity of the gasification agent Operation more difficult than fixed bed reactors 	
Entrained Flow	<ul style="list-style-type: none"> High degree of feedstock flexibility Short residence time Uniform reaction temperature throughout reactor Low degree of tar in produced gas Ash easily removed as slag 	<ul style="list-style-type: none"> High amount of oxidizing agent required High level of heat in produced gas High capital cost due to high reaction parameters 	
Plasma	<ul style="list-style-type: none"> Can treat all hazardous and non-hazardous wastes Ash easily removed as slag Safe means to destroy hazardous waste Little to no ash content present in resulting gas 	<ul style="list-style-type: none"> Large initial economic investment and operating costs Economics still remain uncertain Frequent maintenance required Little or negative net energy production 	

Figure 2-17 Biomass gasifiers traditionally used with their pros and cons. (Adapted from reference [156] with permission from Elsevier)

2.4.1 Advances in syngas treatment

Syngas which is the combination of H_2 and CO_2 required cleaning due to different pollutants (sulphur, nitrogen, tars and particulate matter) exists depending on the type of feedstock and operating conditions. The permissible limits for the pollutants in syngas concerning the application is given in *Table 2-8*. Woolcock et al. [118] presented a comprehensive article on the syngas cleaning technologies and divided the technologies into three categories hot gas cleaning ($>300\text{ }^\circ\text{C}$), warm gas cleaning and cold gas cleaning ($\leq 100\text{ }^\circ\text{C}$). Shi et al. [119] proposed a new methodology through simulations to remove organic contaminants from syngas by introducing oxygen on the principle of thermodynamic equilibrium. The resultant syngas contains a high amount of desired product ($H_2 + CO_2$) approximately 72% in the preheating category. Pre-heating decreased oxygen, fuel and steam consumption. However, a real biomass-based syngas needs to be tested for a thorough evaluation of the proposed work. Recently, Chen et al. [120] developed an improved device (moving granular bed filter) to remove particulate matter from the syngas in a cold test and found to remove the particulate matter up to 87 % for particle size ranging from 0.1 to $0.5\text{ }\mu\text{m}$ with an inlet dust concentration 15000 ppmw. Schematic diagram of the filter is shown in *Figure 2-18*. However, the filter is less effective for the particle size greater than $0.5\text{ }\mu\text{m}$.

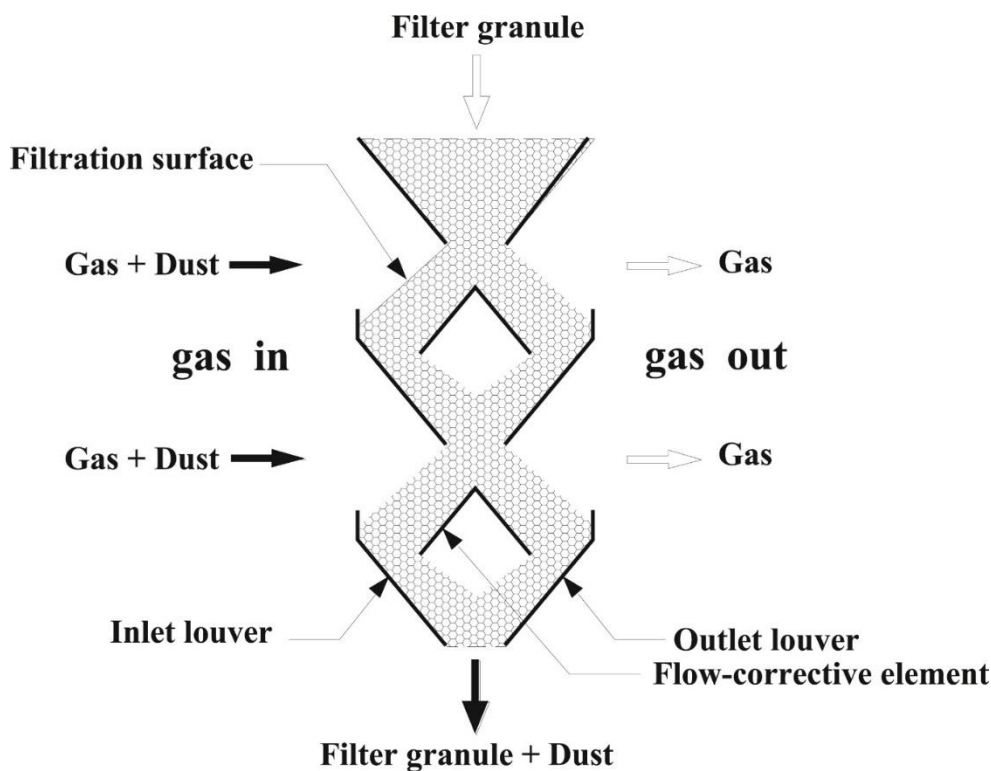


Figure 2-18 Moving granular bed filter for syngas cleaning. (Reprinted from reference [120] with permission from Elsevier)

Table 2-8 Permissible limits for the pollutants in syngas according to the applications. (Adapted from reference [118] with permission from Elsevier)

Contaminant	Applications			
	IC engine	Gas turbine	Methanol synthesis	FT synthesis
Nitrogen (NH₃, HCN)		< 50 µL/L	< 0.1 mg/m ³	< 0.02 µL/L
Alkali		< 0.024 µL/L		< 0.01 µL/L
Inhibitory compounds				< 0.01 µL/L
Class 2-heter atoms, BTX				< 1 µL/L
Tars (condensable)	< 100 mg/m ³		< 0.1 mg/m ³	
Particulate (Soot, dust, char, ash)	< 50 mg/m ³ (PM10)	< 30 mg/m ³ (PM5)	< 0.02 mg/m ³	
Sulphur (H₂S, COS)		< 20 µL/L	< 1 mg/m ³	< 0.01 µL/L
Halides (primarily HCl)		1 µL/L	< 0.1 mg/m ³	< 0.01 µL/L

Filippis et al. [121] successfully reduced the tar and particulate matter (PM) in syngas through the addition of a second fixed bed reactor containing Al₂O₃ spheres. The secondary reactor reduced the tar and PM approximately 60% and 84% respectively. After wet scrubbing, the tar and PM reduced to a great extent containing less than 12 and 7% respectively. On the other hand, Diego et al. [122] reported a high tar removal efficiency through catalytic filter candles in a dual fluidised bed gasifier for biomass gasification. The tar conversion was reported up to 80% with tar removal efficiency up to 95% at 850 °C in the filter enclosing catalytic layer integrated with activated alumina foam tube.

Akay et al. [123] reported that sulphonated polyHIPE polymers (s-PHP) positively influenced the tar removal from the syngas in the range of 80-95% and dew point depression reduced from 90 °C to 70 °C. Authors encouraged the use of tar loaded s-PHP into the soil to enhance crop productivity. In another recent study, lime was also found to be effective in reducing tar concentration during gasification. Tar yield was found to be decreased approximately eight times than the non-lime (silica sand) study in fluidised bed reactor. Tar dew point was also

noted to be decreased to 71 °C from 124 °C [124]. Peng et al. [125] reported that co-gasification of coal/biomass helps improve the tar removal in the presence of carbonates (K_2CO_3 , $KHCO_3$ and $NaHCO_3$) as catalysts with pure oxygen and steam. The highest yield is obtained through K_2CO_3 catalyst.

Plasma has gained considerable attention recently towards syngas treatment to remove impurities. Hrabovsky et al. [126] treated syngas produced from different feedstock (wood pellets, crashed waste polyethylene, fine sawdust, and pulverised lignite) with steam plasma at a very low flow rate (18 g/min) for 1 kg/min flow rate of the treated material. High H_2 and CO concentration were achieved with a low amount of impurities were produced. The composition of the gas was recorded nearly similar to predicted by the thermodynamic equilibrium calculations. Wnukowski et al. [127] recently also observed an increase in H_2 and CO concentration upon treatment with microwave plasma considering benzene as a tar model compound, however, the mechanism described by the authors suggested that methane presence reduced the conversion efficiency up to 60% due to reforming of benzene. Authors also suggested using oxygen as a gasifying agent to improve the H_2 concentration in gas and reduce the nitrogen. In another study, a hybrid plasma and catalytic conversion of toluene as a model tar compound were tested by Liu et al. [128] and found that the catalytic effect increased the conversion efficiency with plasma. The highest conversion efficiency recorded was 52% in the presence of 20 wt. % Ni/Al_2O_3 catalyst in dielectric barrier discharge plasma reactor. The mechanism of toluene conversion as a model tar compound during gasification can be seen in Figure 2-19.

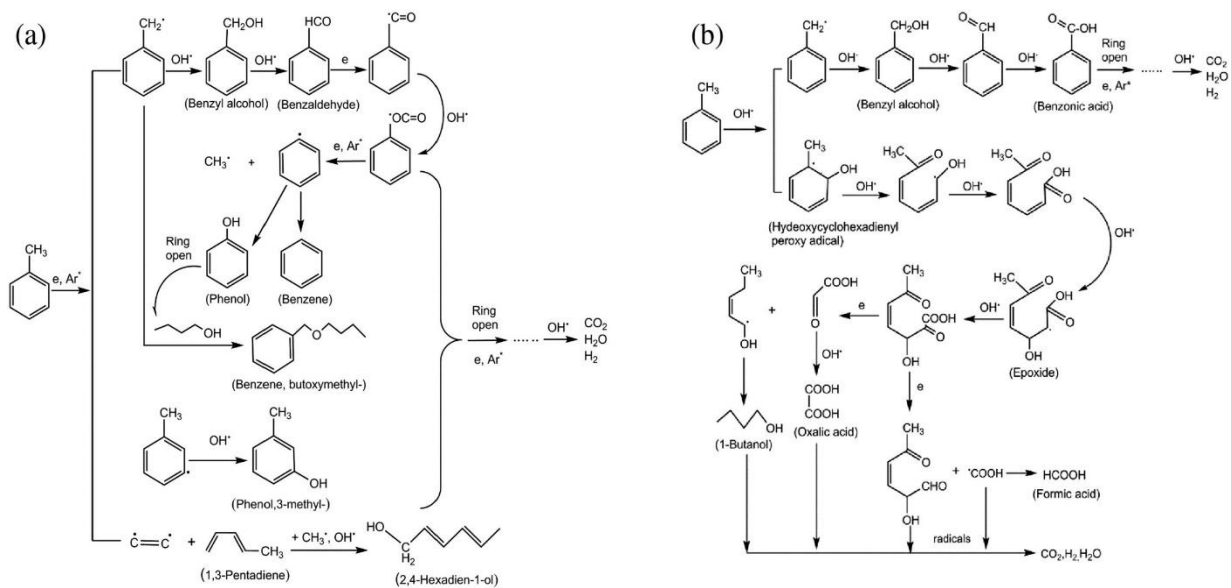


Figure 2-19 Gasification mechanism of toluene as a model tar compound in dielectric barrier discharge plasma reactor (a) energetic electrons and excited Ar (b) OH radicals. (Reprinted from reference [128] with permission from Elsevier)

Furthermore, chemical looping is also finding its way in the treatment of biofuels besides combustion. More et al. [129] presented a new approach converting the methane in the syngas to produce H₂ gas catalytically. Methane cracked over Ni catalyst (carbon carrier) which is later regenerated by oxidising the carbon via CO₂, hence reducing the chances for CO production.

2.4.2 Advances in syngas applications

Zhang et al. [130] recently presented the influence on combustion properties (adiabatic flame temperature, laminar flame speed) with the variation in syngas composition. When the combustion chamber is under adiabatic conditions, creates adiabatic flame temperature. With the peak in adiabatic flame temperature, equivalence ratio approaches to one. The adiabatic flame temperature was found to be less affected by the variation in syngas, however, flame speed is significantly affected by fuel variation. Hydrogen variation at lean combustion effects the flame speed approximately 80%, whereas, methane had negligible effect. Jia et al. [131] on the other hand, presented a pathway to improve the quality of syngas produced from woodchip gasification. Char was impregnated with potassium salts (KCl, KOH, K₂CO₃ and CH₃COOK), however maximum hydrogen yield (197.2 g/kg) was obtained with 6 wt. % KOH solution. The high temperature increased the syngas production, whereas, led to lower hydrogen yield. Oxygen helped to convert the char and adjust the H₂/CO ratio to enhance the quality of syngas.

Gupta et al. [132] developed a hybrid solar-thermal power generation with the use of syngas combustion as an alternating heat source. The system contained a maximum fuel thermal input of 34 kW and a turndown ratio of 1.67. The optimum reported equivalence ratios were 4 and 5 with quick start-up, stable operation and low heat loss approximately 20-27%. Rajbongshi et al. [133] presented a PV-biomass-diesel hybrid energy system for rural electrification, and cost analysis was done for 19 kW peak load with the demand of 178 kWh/day. The cost was found to be US\$ 0.145/kWh for the off-grid system, however, the energy price reduced to US\$ 0.064/kWh. Kohsri et al. [134] recently proposed a hybrid syngas/PV system for a continuous supply of electricity using battery power system. The specific fuel consumption of syngas was found to be at 3.14 Nm³/kWh with an efficiency of biopower system around 16.9% and overall efficiency at 34.3%. The operating plant contained 12.28 kW solar panels, 33.7 kW of syngas genset, 13.8 kW of the bidirectional converter and 60.9 kWh of battery capacity.

Zhao et al. [135] synthesised a novel catalyst from Cu-Mn mixed oxides through calcination and Co-catalyst CaO-ZrO₂ to convert syngas into methyl formate. Methyl formate was formed

due to nucleophilic addition-elimination reaction mechanism, and carbonylation of methanol and CO. Liquid petroleum gas (LPG) synthesis was achieved from syngas by synthesising the CZ@H- β -P catalyst by preparing the zeolite through hydrothermal technique and later coated on Cu/ZnO core with ludox [136]. Moreover, the catalyst promoted the intermediate reactions like the conversion of methanol through dehydrogenation to dimethyl ether which participated in the generation of LPG. CO conversion and hydrocarbons selectivity were recorded at 61.8% and 64.2% respectively.

Syngas combustion was improved in internal combustion engines through methane enrichment which resulted in quick and smooth combustion behaviour than syngas and compressed natural gas alone [137]. This also improved the thermal brake efficiency (30.2%) and brake specific fuel consumption (21.3%) and reduced the CO emissions. Indrawan et al. [138] reported the use of syngas in spark ignition engine with a capacity of 10 kW after modification to observe the parameters like air to fuel ratio and feeding the syngas directly from the reactor. 5 kW power was produced with specific fuel consumption of 1.9 kg/kWh and net electrical efficiency of 21.3%. CO, CO₂, SO₂ and NO_x emissions were produced at a lower concentration than using the natural gas based engine. However, the fuel consumption was higher and produced output was lower than the natural gas burned engine. Syngas and biogas co-combustion in internal combustion engines was studied by Kan et al. [139] to understand the combined behaviour. Syngas fuelled engine performed better than biogas fuelled and hydrogen concentration effected positively on the indicated thermal efficiency of syngas utilisation in IC engines, however, it reverses when ignition advance is relatively higher. The combined combustion of both gases led to the reduction of knocking and the NO_x emissions. Al-Attab et al. [140] proposed a new technique to remove the step for external compression of syngas by injecting the air-syngas mixture directly in the micro gas turbine's compressor. This proposed technique was tested by developing pressurised cyclone combustor with a micro gas turbine. Stable syngas combustion was achieved for air-fuel ratio 3.3-4.1 and NO_x and CO emissions were noted below 250 ppm and 15 ppm respectively. Total energy pathway of the studied system is shown in *Figure 2-20*.

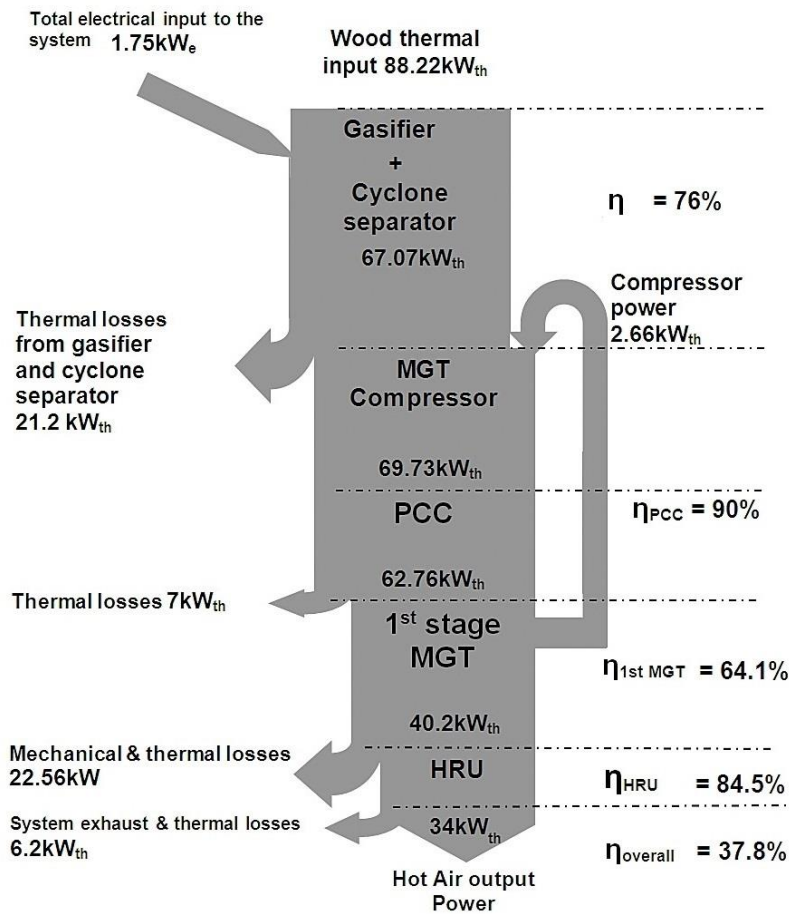
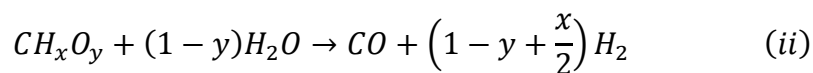
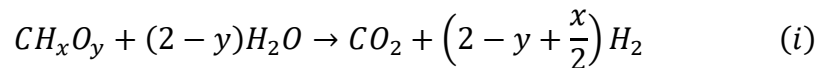


Figure 2-20 Energy distribution during the syngas production in a micro gas turbine. (Adapted from reference [131] with permission from Elsevier)

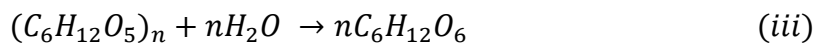
Additionally, Pardo-Planas et al. [141] simulated the hybrid gasification and fermentation process for ethanol production from syngas. The potential of 36.5 million gallons of anhydrous ethanol production was observed through the utilisation of 1200 tons of switchgrass. Syngas fermentation can yield approximately 97 gallons of ethanol per dry ton of biomass. Schematic diagram of the process is shown in Figure 2-21. Recently Sun et al. [142] produced ethanol from the syngas with the help of char fermentation media from four different sources (switchgrass, forage sorghum, red cedar and poultry litter). Red cedar and poultry litter derived char enhanced ethanol production significantly up to 16% and 59% respectively than yeast extract medium. This was due to the inorganic elements present in char which was released during fermentation and reduced the acid stress on anaerobic bacteria, leading to the enhanced ethanol production.

2.4.3 Supercritical water gasification (SWG)

Supercritical water gasification is also a biomass conversion technique which uses the high pressure (around 20-30 MPa) as a helping parameter with relatively low temperature (around 600 °) than conventional gasification (800-1000 °C). The other significant advantage is the use of wet biomass, as the reaction occurs in the presence of water, thus requires no drying of biomass. Supercritical water gasification of biomass is explained in the schematic diagram in *Figure 2-22* and by the following equations (*i – x*) reported by Reddy et al. [143].



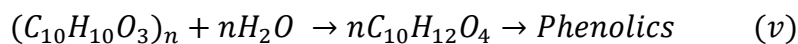
Cellulose hydrolysis



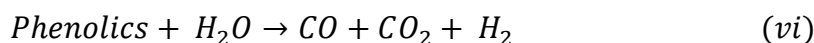
Glucose reforming reaction



Hydrolysis of lignin



Steam reforming reaction



Water-gas shift reaction



Methanation reaction of CO



Methanation reaction of CO₂



Hydrogenation reaction



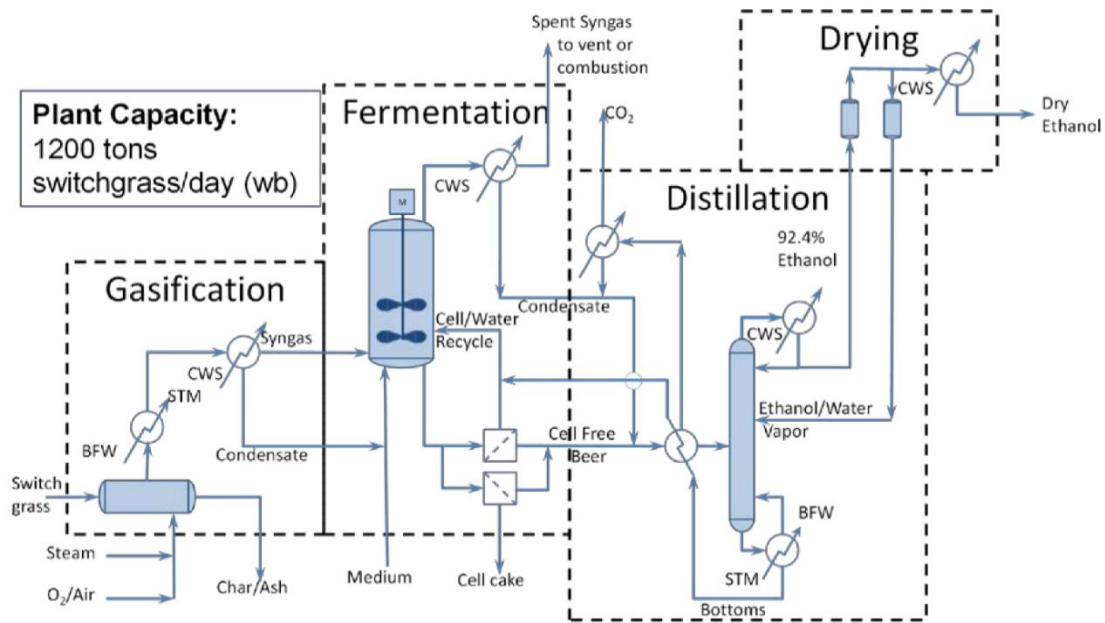


Figure 2-21 Schematic diagram of the hybrid gasification and fermentation system. (Adapted from reference [141] with permission from Elsevier)

Kang et al. [144] conducted the supercritical water gasification for waste biomass and concluded the significant parameters affecting the hydrogen production in the decreasing order as follows, temperature > catalyst loading > catalyst type > biomass type. The temperature around 650 °C and at 100% catalyst loading produced the highest hydrogen. Nanda et al. [145] produced a higher gas yield with nickel impregnated biomass gasification than non-catalytic biomass gasification. The optimum recommended conditions were 500 °C, biomass to water ratio 1:10 and 23-25 MPa with 45 min residence time. The authors did not report the study at more than 500 °C, however, the increasing temperature seems to be more beneficial for higher hydrogen production. Figure 2-23 shows a mechanism of glucose conversion during supercritical water gasification treatment. Amrullah et al. [146] recently conducted the SWG of sewage sludge in a continuous reactor in order to convert the organic phosphorus present in sewage sludge to inorganic phosphorus. The inorganic phosphorus was obtained at a short residence time of 10s in a reactor. This conversion of organic phosphorus to inorganic phosphorus required activation energy around 19.1 kJ/mol and remaining inorganic phosphorus was further converted at 18.7 kJ/mol.

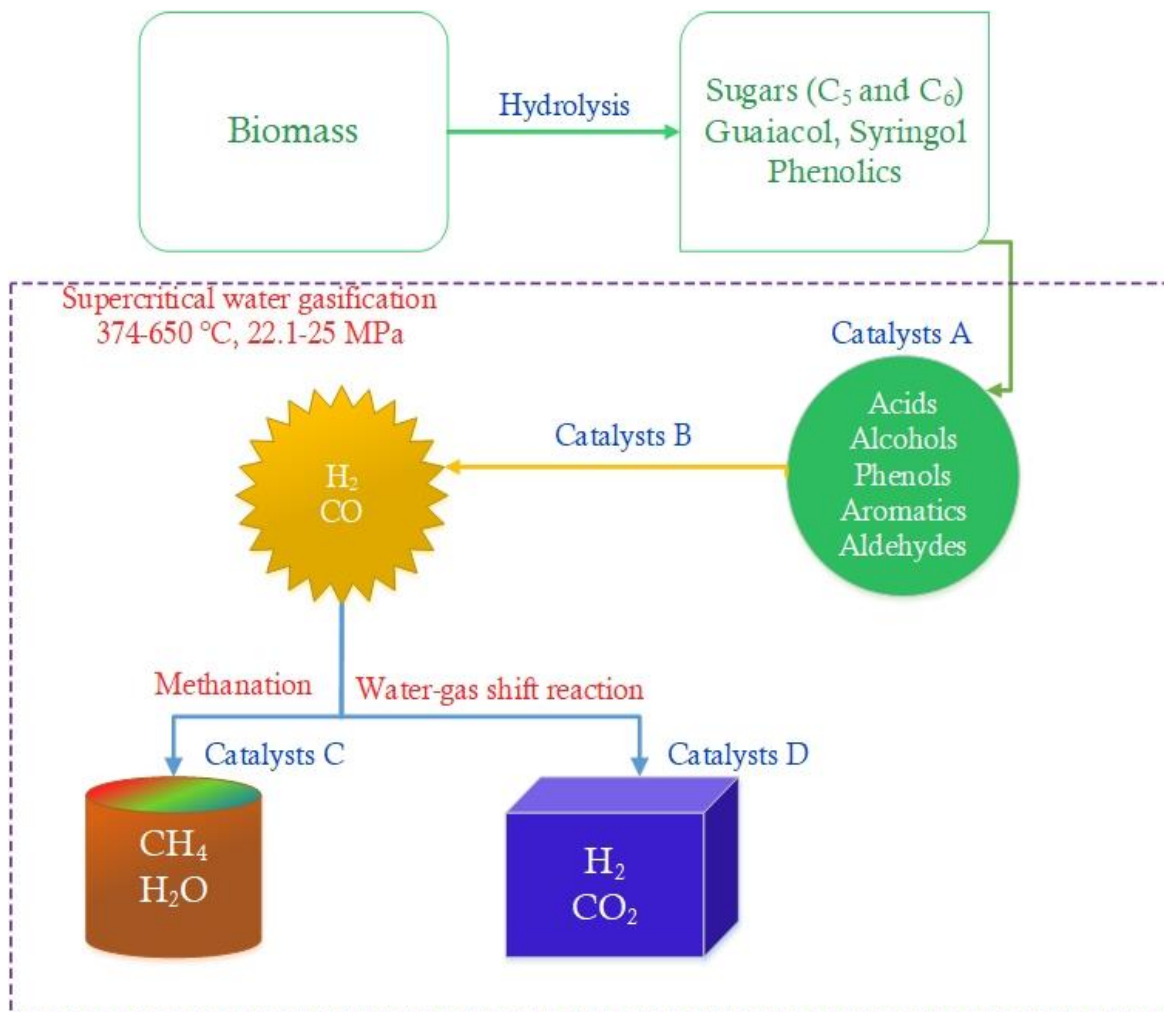


Figure 2-22 Biomass gasification under supercritical conditions. Catalysts A, B, C, and D represents (Ni, Ru, Rh, Pt, Pd, Ni/Al₂O₃, Ni/C, Ru/Al₂O₃, Ru/TiO₂), (Ni, Ru, Pt and activated carbon), (Ni, Rh, Ru, Pt and activated carbon) and (Ni, Ru, NaOH, KOH) respectively. (Reprinted from reference [143] with permission from Elsevier)

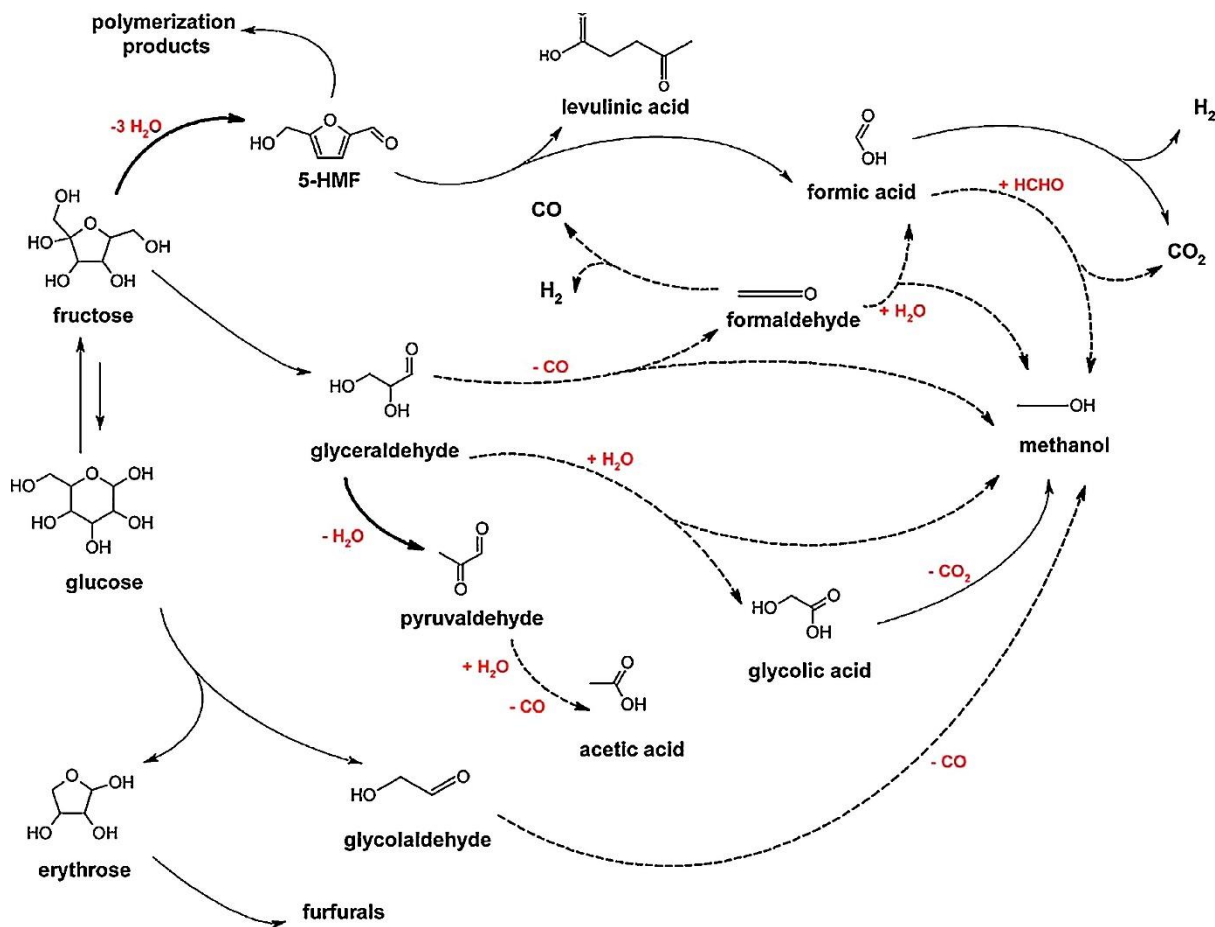


Figure 2-23 Supercritical water gasification of glucose at 400 °C. (Reprinted from reference [157] with permission from Elsevier)

Even though SWG contains several advantages towards biofuel technology, however, there are many disadvantages which need to be explored further, for instance, impurities formation, economically inefficient, clogging and energy inefficient. These critical factors diminish the positive aspects of the process. Although recently some of the studies [147,148] reported positive results in order to reduce this barrier, however, an extensive study on a range of feedstock is required to optimise the efficient working parameters.

2.5 Conclusive remarks

Biomass is a versatile feedstock and contains several merits based on the technology to utilise, however, combining the biomass with coal or another kind of wastes; for instance, plastic can be beneficial. The types of emissions and impurities produced during thermal use contributed significantly to the product's effectiveness. The optimised parameters for each of the technology give some sort of way out to reduce the drawbacks associated with energy efficiency and unwanted by-products. Chemical looping combustion contains significant advantages in reducing greenhouse gasses and improving cost efficiency.

Moreover, co-combustion with coal or sewage sludge increases the carbon conversion and capture efficiency. Slagging and fouling during biomass combustion needs to be re-evaluated according to the type of biomass in a real-time scenario rather than depending on coal-based indices. Pre-treatment of biomass needs to be considered for Ca, Si and K prior to their use in heating technologies. Biomass ash use as a fertiliser is recommended in the form of large tablets to reduce the potassium release rate.

Pyrolysis products from biomass are widely regarded as beneficial in many applications from wastewater treatment to composites and from simple ethanol production to complex upgraded biofuel production. Pyrolysis products typically need to be treated further for appropriate use either in the form of the upgrading of bio-oil or the activation of the char. The upgradation mechanism needs to be thoroughly studied on bio-oil rather than model compounds which makes it difficult to estimate the potential of the relevant technology. Syngas use has been found in several applications due to its instant use in engines, boilers and electricity generators. Hybrid systems are being researched extensively where the use of syngas with other renewable fuels found positive results, both for on and off-grid supply of energy.

Although extensive research has been done in many areas of biomass utilisation, however, further research is required in a number of areas, for instance, refining and improving the quality of biochemicals and reducing the water production during fast pyrolysis. Multiple routes and integration of different systems together required to prepare one efficient set of systems to use according to the type of the biomass. The development of new technologies is also inevitable due to the limitations in the current systems. Thus, further research will bring closer to the sustainable and environmentally friendly approach of energy and biofuels generation.

2.6 References

- [1] L. Magnier, J. Schoormans, R. Mugge, Judging a product by its cover: Packaging sustainability and perceptions of quality in food products, *Food Qual. Prefer.* 53 (2016) 132–142. doi:10.1016/j.foodqual.2016.06.006.
- [2] M. Rover, R. Smith, R.C. Brown, Enabling biomass combustion and co-firing through the use of Lignocol, *Fuel.* 211 (2018) 312–317. doi:10.1016/j.fuel.2017.09.076.
- [3] M.A. Hossain, J. Jewaratnam, P. Ganesan, Prospect of hydrogen production from oil palm biomass by thermochemical process – A review, *Int. J. Hydrogen Energy.* 41 (2016) 16637–16655. doi:10.1016/j.ijhydene.2016.07.104.
- [4] W.H. Chen, B.J. Lin, M.Y. Huang, J.S. Chang, Thermochemical conversion of microalgal biomass into biofuels: A review, *Bioresour. Technol.* 184 (2014) 314–327. doi:10.1016/j.biortech.2014.11.050.
- [5] H. Chen, L. Wang, Sugar Strategies for Biomass Biochemical Conversion, in: *Technol. Biochem. Convers. Biomass*, Elsevier, 2017: pp. 137–164. doi:10.1016/B978-0-12-802417-1.00006-5.
- [6] J.L. Zheng, Q. Wei, Improving the quality of fast pyrolysis bio-oil by reduced pressure distillation, *Biomass and Bioenergy.* 35 (2011) 1804–1810. doi:10.1016/j.biombioe.2011.01.006.
- [7] G. Knothe, Improving biodiesel fuel properties by modifying fatty ester composition, *Energy Environ. Sci.* 2 (2009) 759. doi:10.1039/b903941d.
- [8] S. de Jong, R. Hoefnagels, E. Wetterlund, K. Pettersson, A. Faaij, M. Junginger, Cost optimization of biofuel production – The impact of scale, integration, transport and supply chain configurations, *Appl. Energy.* 195 (2017) 1055–1070. doi:10.1016/j.apenergy.2017.03.109.
- [9] C.-H. Zhou, X. Xia, C.-X. Lin, D.-S. Tong, J. Beltramini, Catalytic conversion of lignocellulosic biomass to fine chemicals and fuels, *Chem. Soc. Rev.* 40 (2011) 5588. doi:10.1039/c1cs15124j.
- [10] G. Dorez, L. Ferry, R. Sonnier, A. Taguet, J.M. Lopez-Cuesta, Effect of cellulose, hemicellulose and lignin contents on pyrolysis and combustion of natural fibers, *J. Anal. Appl. Pyrolysis.* 107 (2014) 323–331. doi:10.1016/j.jaap.2014.03.017.
- [11] M. k Ghose, Properties of Fuels from Wood Sources, in: J.G. Speight (Ed.), *Biofuels Handb.*, 2011: pp. 304–330. <http://pubs.rsc.org.ezproxy.lib.rmit.edu.au/en/content/chapterpdf/2011/9781849731027-00304?isbn=978-1-84973-026-6&sercode=bk>.
- [12] F. Cerededa-Balic, M. Toledo, V. Vidal, F. Guerrero, L.A. Diaz-Robles, X. Petit-Breuilh, M. Lapuerta, Emission factors for PM 2.5 , CO, CO 2 , NO x , SO 2 and particle size distributions from the combustion of wood species using a new controlled combustion chamber 3CE, *Sci. Total Environ.* 584–585 (2017) 901–910.

doi:10.1016/j.scitotenv.2017.01.136.

- [13] M. Mann, P. Spath, The Net CO₂ Emissions and Energy Balances of Biomass and Coal-Fired Power Systems, Proc. 4th Biomass Conf. (1999) 2–7.
- [14] R. López, M. Menéndez, C. Fernández, A. Bernardo-Sánchez, The effects of scale-up and coal-biomass blending on supercritical coal oxy-combustion power plants, Energy. (2018). doi:10.1016/j.energy.2018.01.179.
- [15] H.J. Richter, K.F. Knoche, Reversibility of Combustion Processes, in: Effic. Costing, AMERICAN CHEMICAL SOCIETY, 1983: pp. 3–71. doi:doi:10.1021/bk-1983-0235.ch003.
- [16] X. Zhao, H. Zhou, V.S. Sikarwar, M. Zhao, A.-H.A. Park, P.S. Fennell, L. Shen, L.-S. Fan, Biomass-based chemical looping technologies: the good, the bad and the future, Energy Environ. Sci. 10 (2017) 1885–1910. doi:10.1039/C6EE03718F.
- [17] I. Adánez-Rubio, A. Pérez-Astray, T. Mendiara, M.T. Izquierdo, A. Abad, P. Gayán, L.F. de Diego, F. García-Labiano, J. Adánez, Chemical looping combustion of biomass: CLOU experiments with a Cu-Mn mixed oxide, Fuel Process. Technol. 172 (2018) 179–186. doi:10.1016/j.fuproc.2017.12.010.
- [18] X. Wang, Z. Chen, M. Hu, Y. Tian, X. Jin, S. Ma, T. Xu, Z. Hu, S. Liu, D. Guo, B. Xiao, Chemical looping combustion of biomass using metal ferrites as oxygen carriers, Chem. Eng. J. 312 (2017) 252–262. doi:10.1016/j.cej.2016.11.143.
- [19] J. Zhang, T. He, Z. Wang, M. Zhu, K. Zhang, B. Li, J. Wu, The search of proper oxygen carriers for chemical looping partial oxidation of carbon, Appl. Energy. 190 (2017) 1119–1125. doi:10.1016/j.apenergy.2017.01.024.
- [20] L. Chen, L. Yang, F. Liu, H.S. Nikolic, Z. Fan, K. Liu, Evaluation of multi-functional iron-based carrier from bauxite residual for H₂-rich syngas production via chemical-looping gasification, Fuel Process. Technol. 156 (2017) 185–194. doi:10.1016/j.fuproc.2016.10.030.
- [21] S. Bhavsar, G. Vesper, Chemical looping beyond combustion: production of synthesis gas via chemical looping partial oxidation of methane, RSC Adv. 4 (2014) 47254–47267. doi:10.1039/C4RA06437B.
- [22] M. Luo, S. Wang, L. Wang, M. Lv, Reduction kinetics of iron-based oxygen carriers using methane for chemical-looping combustion, J. Power Sources. 270 (2014) 434–440. doi:10.1016/j.jpowsour.2014.07.100.
- [23] A. Nandy, C. Loha, S. Gu, P. Sarkar, M.K. Karmakar, P.K. Chatterjee, Present status and overview of Chemical Looping Combustion technology, Renew. Sustain. Energy Rev. 59 (2016) 597–619. doi:10.1016/j.rser.2016.01.003.
- [24] H.R. Kerr, Capture and Separation Technology Gaps and Priority Research Needs, Carbon Dioxide Capture Storage Deep Geol. Form. 1 (2005) 655–660. doi:10.1016/B978-008044570-0/50124-0.

- [25] H. Gu, L. Shen, J. Xiao, S. Zhang, T. Song, Chemical looping combustion of biomass/coal with natural iron ore as oxygen carrier in a continuous reactor, *Energy and Fuels*. 25 (2011) 446–455. doi:10.1021/ef101318b.
- [26] M. Luo, S. Wang, L. Wang, M. Lv, L. Qian, H. Fu, Experimental investigation of co-combustion of coal and biomass using chemical looping technology, *Fuel Process. Technol.* 110 (2013) 258–267. doi:10.1016/j.fuproc.2013.01.004.
- [27] S. Jiang, L. Shen, X. Niu, H. Ge, H. Gu, Chemical Looping Co-combustion of Sewage Sludge and Zhundong Coal with Natural Hematite as the Oxygen Carrier, *Energy and Fuels*. 30 (2016) 1720–1729. doi:10.1021/acs.energyfuels.5b02283.
- [28] M. Mladenović, M. Paprika, A. Marinković, Denitrification techniques for biomass combustion, *Renew. Sustain. Energy Rev.* 82 (2018) 3350–3364. doi:10.1016/j.rser.2017.10.054.
- [29] G. Pu, W. Wang, R. Peng, W. Zhu, F. Zhao, F. Fu, Y. Long, NO emission of co-combustion coal and biomass blends in an oxygen-enriched atmosphere, *Energy Sources, Part A Recover. Util. Environ. Eff.* 38 (2016) 3497–3503. doi:10.1080/15567036.2016.1169336.
- [30] X. Wang, Q. Ren, W. Li, H. Li, S. Li, Q. Lu, Nitrogenous Gas Emissions from Coal/Biomass Co-combustion under a High Oxygen Concentration in a Circulating Fluidized Bed, *Energy and Fuels*. 31 (2017) 3234–3242. doi:10.1021/acs.energyfuels.6b03141.
- [31] Y. Wang, X. Wang, Z. Hu, Y. Li, S. Deng, B. Niu, H. Tan, NO emissions and combustion efficiency during biomass co-firing and air-staging, *BioResources*. 10 (2015) 3987–3998. doi:10.15376/biores.10.3.3987-3998.
- [32] L. Duan, Y. Duan, C. Zhao, E.J. Anthony, NO emission during co-firing coal and biomass in an oxy-fuel circulating fluidized bed combustor, *Fuel*. 150 (2015) 8–13. doi:10.1016/j.fuel.2015.01.110.
- [33] S.S. Daood, T.S. Yelland, W. Nimmo, Selective non-catalytic reduction – Fe-based additive hybrid technology, *Fuel*. 208 (2017) 353–362. doi:10.1016/j.fuel.2017.07.019.
- [34] J. Hao, W. Yu, P. Lu, Y. Zhang, X. Zhu, The effects of Na/K additives and flyash on NO reduction in a SNCR process, *Chemosphere*. 122 (2015) 213–218. doi:10.1016/j.chemosphere.2014.11.055.
- [35] F. Sher, M.A. Pans, D.T. Afilaka, C. Sun, H. Liu, Experimental investigation of woody and non-woody biomass combustion in a bubbling fluidised bed combustor focusing on gaseous emissions and temperature profiles, *Energy*. 141 (2017) 2069–2080. doi:10.1016/j.energy.2017.11.118.
- [36] N. Hodžić, A. Kazagić, I. Smajević, Influence of multiple air staging and reburning on NO_x emissions during co-firing of low rank brown coal with woody biomass and natural gas, *Appl. Energy*. 168 (2016) 38–47. doi:10.1016/j.apenergy.2016.01.081.

- [37] C. Hongfang, Z. Peitao, W. Yin, X. Guangwen, Y. Kunio, NO Emission Control during the Decoupling Combustion of Industrial Biomass Wastes with a High Nitrogen Content, *Energy & Fuels*. 27 (2013) 3186–3193. doi:10.1021/ef301994q.
- [38] D. Li, G. Shiqiu, S. Wenli, L. Jinghai, X. Guangwen, NO reduction in decoupling combustion of Biomass and biomass-coal blend, *Energy and Fuels*. 23 (2009) 224–228. doi:10.1021/ef800589c.
- [39] X. Li, Z. Dong, J. Dou, J. Yu, A. Tahmasebi, Catalytic reduction of NO using iron oxide impregnated biomass and lignite char for flue gas treatment, *Fuel Process. Technol.* 148 (2016) 91–98. doi:10.1016/j.fuproc.2016.02.030.
- [40] H. Liu, J. Chaney, J. Li, C. Sun, Control of NO_x emissions of a domestic/small-scale biomass pellet boiler by air staging, *Fuel*. 103 (2013) 792–798. doi:10.1016/j.fuel.2012.10.028.
- [41] H. Khodaei, F. Guzzomi, D. Patiño, B. Rashidian, G.H. Yeoh, Air staging strategies in biomass combustion-gaseous and particulate emission reduction potentials, *Fuel Process. Technol.* 157 (2017) 29–41. doi:10.1016/j.fuproc.2016.11.007.
- [42] C. Chen, F. Chen, Z. Cheng, Q.N. Chan, S. Kook, G.H. Yeoh, Emissions characteristics of NO_x and SO₂ in the combustion of microalgae biomass using a tube furnace, *J. Energy Inst.* 90 (2017) 806–812. doi:10.1016/j.joei.2016.06.003.
- [43] B. Zhao, Y. Su, D. Liu, H. Zhang, W. Liu, G. Cui, SO₂/NO_x emissions and ash formation from algae biomass combustion: Process characteristics and mechanisms, *Energy*. 113 (2016) 821–830. doi:10.1016/j.energy.2016.07.107.
- [44] G. Wielgoński, P. Łechtańska, O. Namiecińska, Emission of some pollutants from biomass combustion in comparison to hard coal combustion, *J. Energy Inst.* 90 (2017) 787–796. doi:10.1016/j.joei.2016.06.005.
- [45] Air Quality Expert Group, The Potential Air Quality Impacts from Biomass Combustion, (2017). https://uk-air.defra.gov.uk/assets/documents/reports/cat11/1708081027_170807_AQEG_Biomass_report.pdf.
- [46] T. Nussbaumer, Combustion and Co-combustion of Biomass: Fundamentals, Technologies, and Primary Measures for Emission Reduction, *Energy and Fuels*. 17 (2003) 1510–1521. doi:10.1021/ef030031q.
- [47] R. Poškas, A. Sirvydas, P. Poškas, H. Jouhara, N. Striūgas, N. Pedišius, V. Valinčius, Investigation of warm gas clean-up of biofuel flue and producer gas using electrostatic precipitator, *Energy*. 143 (2018) 943–949. doi:10.1016/j.energy.2017.11.120.
- [48] A.H. Hultén, P. Nilsson, M. Samuelsson, S. Ajdari, F. Normann, K. Andersson, First evaluation of a multicomponent flue gas cleaning concept using chlorine dioxide gas – Experiments on chemistry and process performance, *Fuel*. 210 (2017) 885–891. doi:10.1016/j.fuel.2017.08.116.
- [49] J. Liu, D. Chen, J. Lu, Experiment on fine particle purification by flue gas condensation

- for industrial boilers, *Fuel*. 199 (2017) 684–696. doi:10.1016/j.fuel.2017.03.028.
- [50] S. Zimmermann, M.O. Schmid, B. Klein, G. Scheffknecht, Experimental Studies on Spray Absorption with the Post Combustion CO₂Capture Pilot-Plant CASPAR, *Energy Procedia*. 114 (2017) 1325–1333. doi:10.1016/j.egypro.2017.03.1252.
- [51] H.W. Pennline, J.S. Hoffman, Flue gas cleanup using the Moving-Bed Copper Oxide Process, *Fuel Process. Technol.* 114 (2013) 109–117. doi:10.1016/j.fuproc.2013.03.020.
- [52] A.A. Bogush, J.A. Stegemann, R. Williams, I.G. Wood, Element speciation in UK biomass power plant residues based on composition, mineralogy, microstructure and leaching, *Fuel*. 211 (2018) 712–725. doi:10.1016/j.fuel.2017.09.103.
- [53] S. V. Vassilev, C.G. Vassileva, Y.C. Song, W.Y. Li, J. Feng, Ash contents and ash-forming elements of biomass and their significance for solid biofuel combustion, *Fuel*. 208 (2017) 377–409. doi:10.1016/j.fuel.2017.07.036.
- [54] A. Garcia-Maraver, J. Mata-Sanchez, M. Carpio, J.A. Perez-Jimenez, Critical review of predictive coefficients for biomass ash deposition tendency, *J. Energy Inst.* 90 (2017) 214–228. doi:10.1016/j.joei.2016.02.002.
- [55] R. Weber, Y. Poyraz, A.M. Beckmann, S. Brinker, Combustion of biomass in jet flames, *Proc. Combust. Inst.* 35 (2015) 2749–2758. doi:10.1016/j.proci.2014.06.033.
- [56] X. Yang, D. Ingham, L. Ma, H. Zhou, M. Pourkashanian, Understanding the ash deposition formation in Zhundong lignite combustion through dynamic CFD modelling analysis, *Fuel*. 194 (2017) 533–543. doi:10.1016/j.fuel.2017.01.026.
- [57] U. Kleinhans, C. Wieland, S. Babat, G. Scheffknecht, H. Spliethoff, Ash particle sticking and rebound behavior: A mechanistic explanation and modeling approach, *Proc. Combust. Inst.* 36 (2017) 2341–2350. doi:10.1016/j.proci.2016.05.015.
- [58] Y. Niu, Z. Wang, Y. Zhu, X. Zhang, H. Tan, S. Hui, Experimental evaluation of additives and K₂O-SiO₂-Al₂O₃ diagrams on high-temperature silicate melt-induced slagging during biomass combustion, *Fuel*. 179 (2016) 52–59. doi:10.1016/j.fuel.2016.03.077.
- [59] Y. Niu, Y. Zhu, H. Tan, S. Hui, Z. Jing, W. Xu, Investigations on biomass slagging in utility boiler: Criterion numbers and slagging growth mechanisms, *Fuel Process. Technol.* 128 (2014) 499–508. doi:10.1016/j.fuproc.2014.07.038.
- [60] P. Chaunsali, H. Uvegi, R. Osmundsen, M. Laracy, T. Poinot, J. Ochsendorf, E. Olivetti, Mineralogical and microstructural characterization of biomass ash binder, *Cem. Concr. Compos.* (2018). doi:10.1016/j.cemconcomp.2018.02.011.
- [61] M. Fernández-Delgado Juárez, P. Mostbauer, A. Knapp, W. Müller, S. Tertsch, A. Bockreis, H. Insam, Biogas purification with biomass ash, *Waste Manag.* 71 (2018) 224–232. doi:10.1016/j.wasman.2017.09.043.
- [62] M. Wójcik, F. Stachowicz, A. Masłoń, Sewage sludge conditioning with the application

- of ash from biomass-fired power plant, *E3S Web Conf.* 30 (2018) 3005. doi:10.1051/e3sconf/20183003005.
- [63] J.P. Ribeiro, E.D. Vicente, A.P. Gomes, M.I. Nunes, C. Alves, L.A.C. Tarelho, Effect of industrial and domestic ash from biomass combustion, and spent coffee grounds, on soil fertility and plant growth: experiments at field conditions, *Environ. Sci. Pollut. Res.* 24 (2017) 15270–15277. doi:10.1007/s11356-017-9134-y.
- [64] C. Cruz-Paredes, Á. López-García, G.H. Rubæk, M.F. Hovmand, P. Sørensen, R. Kjølner, Risk assessment of replacing conventional P fertilizers with biomass ash: Residual effects on plant yield, nutrition, cadmium accumulation and mycorrhizal status, *Sci. Total Environ.* 575 (2017) 1168–1176. doi:10.1016/j.scitotenv.2016.09.194.
- [65] Z. Zhang, F. He, Y. Zhang, R. Yu, Y. Li, Z. Zheng, Z. Gao, Experiments and modelling of potassium release behavior from tablet biomass ash for better recycling of ash as eco-friendly fertilizer, *J. Clean. Prod.* 170 (2018) 379–387. doi:10.1016/j.jclepro.2017.09.150.
- [66] J. Lehmann, S. Joseph, Biochar for environmental management: An introduction, *Biochar Environ. Manag. - Sci. Technol.* 1 (2009) 1–12. doi:10.1016/j.forpol.2009.07.001.
- [67] A. V Bridgwater, Pyrolysis of biomass, in: *Biomass Power World Transform. to Eff. Use*, Pan Stanford Publishing Pte. Ltd., Bioenergy Research Group, European Bioenergy Research Institute, Aston University, Birmingham, United Kingdom, 2015: pp. 473–513. <https://www.scopus.com/inward/record.uri?eid=2-s2.0-84946823335&partnerID=40&md5=7c415836bf69974a1bebd7149e9561a3>.
- [68] D. Mohan, A. Sarswat, Y.S. Ok, C.U. Pittman, Organic and inorganic contaminants removal from water with biochar, a renewable, low cost and sustainable adsorbent - A critical review, *Bioresour. Technol.* 160 (2014) 191–202. doi:10.1016/j.biortech.2014.01.120.
- [69] E.N. Yargicoglu, B.Y. Sadasivam, K.R. Reddy, K. Spokas, Physical and chemical characterization of waste wood derived biochars, *Waste Manag.* 36 (2015) 256–268. doi:10.1016/j.wasman.2014.10.029.
- [70] P. Srinivasan, A.K. Sarmah, Characterisation of agricultural waste-derived biochars and their sorption potential for sulfamethoxazole in pasture soil: A spectroscopic investigation, *Sci. Total Environ.* 502 (2015) 471–480. doi:10.1016/j.scitotenv.2014.09.048.
- [71] S. Taherymoosavi, V. Verheyen, P. Munroe, S. Joseph, A. Reynolds, Characterization of organic compounds in biochars derived from municipal solid waste, *Waste Manag.* 67 (2017) 131–142. doi:10.1016/j.wasman.2017.05.052.
- [72] P. Devi, A.K. Saroha, Risk analysis of pyrolyzed biochar made from paper mill effluent treatment plant sludge for bioavailability and eco-toxicity of heavy metals, *Bioresour. Technol.* 162 (2014) 308–315. doi:10.1016/j.biortech.2014.03.093.

- [73] A.T. Tag, G. Duman, S. Ucar, J. Yanik, Effects of feedstock type and pyrolysis temperature on potential applications of biochar, *J. Anal. Appl. Pyrolysis*. 120 (2016) 200–206. doi:10.1016/j.jaap.2016.05.006.
- [74] H. Zhang, C. Chen, E.M. Gray, S.E. Boyd, Effect of feedstock and pyrolysis temperature on properties of biochar governing end use efficacy, *Biomass and Bioenergy*. 105 (2017) 136–146. doi:10.1016/j.biombioe.2017.06.024.
- [75] Y. Sun, B. Gao, Y. Yao, J. Fang, M. Zhang, Y. Zhou, H. Chen, L. Yang, Effects of feedstock type, production method, and pyrolysis temperature on biochar and hydrochar properties, *Chem. Eng. J.* 240 (2014) 574–578. doi:10.1016/j.cej.2013.10.081.
- [76] W. Suliman, J.B. Harsh, N.I. Abu-Lail, A.M. Fortuna, I. Dallmeyer, M. Garcia-Perez, Influence of feedstock source and pyrolysis temperature on biochar bulk and surface properties, *Biomass and Bioenergy*. 84 (2016) 37–48. doi:10.1016/j.biombioe.2015.11.010.
- [77] R. Bardestani, S. Kaliaguine, Steam activation and mild air oxidation of vacuum pyrolysis biochar, *Biomass and Bioenergy*. 108 (2018) 101–112. doi:10.1016/j.biombioe.2017.10.011.
- [78] D.A.D. Genuino, M.D.G. de Luna, S.C. Capareda, Improving the surface properties of municipal solid waste-derived pyrolysis biochar by chemical and thermal activation: Optimization of process parameters and environmental application, *Waste Manag.* 72 (2018) 255–264. doi:10.1016/j.wasman.2017.11.038.
- [79] L. Wang, W. Yan, C. He, H. Wen, Z. Cai, Z. Wang, Z. Chen, W. Liu, Microwave-assisted preparation of nitrogen-doped biochars by ammonium acetate activation for adsorption of acid red 18, *Appl. Surf. Sci.* 433 (2018) 222–231. doi:10.1016/j.apsusc.2017.10.031.
- [80] C. Kalinke, P.R. Oliveira, G.A. Oliveira, A.S. Mangrich, L.H. Marcolino-Junior, M.F. Bergamini, Activated biochar: Preparation, characterization and electroanalytical application in an alternative strategy of nickel determination, *Anal. Chim. Acta*. 983 (2017) 103–111. doi:10.1016/j.aca.2017.06.025.
- [81] S. Wang, Y. Xu, N. Norbu, Z.W.-I.C.S. Earth, U. 2018, Remediation of biochar on heavy metal polluted soils, *IOP Conf. Ser. Earth Environ. Sci.* (2018). doi:10.1088/1755-1315/108/4/042113.
- [82] X. Zhang, H. Wang, L. He, K. Lu, A. Sarmah, J. Li, N.S. Bolan, J. Pei, H. Huang, Using biochar for remediation of soils contaminated with heavy metals and organic pollutants, *Environ. Sci. Pollut. Res.* 20 (2013) 8472–8483. doi:10.1007/s11356-013-1659-0.
- [83] Z. Ahmad, B. Gao, A. Mosa, H. Yu, X. Yin, A. Bashir, H. Ghozeisi, S. Wang, Removal of Cu(II), Cd(II) and Pb(II) ions from aqueous solutions by biochars derived from potassium-rich biomass, *J. Clean. Prod.* 180 (2018) 437–449. doi:10.1016/j.jclepro.2018.01.133.

- [84] J.H. Park, J.J. Wang, S.H. Kim, J.S. Cho, S.W. Kang, R.D. Delaune, K.J. Han, D.C. Seo, Recycling of rice straw through pyrolysis and its adsorption behaviors for Cu and Zn ions in aqueous solution, *Colloids Surfaces A Physicochem. Eng. Asp.* 533 (2017) 330–337. doi:10.1016/j.colsurfa.2017.08.041.
- [85] X. Gai, H. Wang, J. Liu, L. Zhai, S. Liu, T. Ren, H. Liu, Effects of feedstock and pyrolysis temperature on biochar adsorption of ammonium and nitrate, *PLoS One.* 9 (2014) 1–19. doi:10.1371/journal.pone.0113888.
- [86] O. Das, A.K. Sarmah, Z. Zujovic, D. Bhattacharyya, Characterisation of waste derived biochar added biocomposites: Chemical and thermal modifications, *Sci. Total Environ.* 550 (2016) 133–142. doi:10.1016/j.scitotenv.2016.01.062.
- [87] O. Das, N.K. Kim, A.K. Sarmah, D. Bhattacharyya, Development of waste based biochar/wool hybrid biocomposites: Flammability characteristics and mechanical properties, *J. Clean. Prod.* 144 (2017) 79–89. doi:https://doi.org/10.1016/j.jclepro.2016.12.155.
- [88] A. Akhtar, A.K. Sarmah, Novel biochar-concrete composites: Manufacturing, characterization and evaluation of the mechanical properties, *Sci. Total Environ.* 616–617 (2018). doi:10.1016/j.scitotenv.2017.10.319.
- [89] A. Akhtar, A.K. Sarmah, Strength improvement of recycled aggregate concrete through silicon rich char derived from organic waste, *J. Clean. Prod.* 196 (2018) 411–423. doi:10.1016/j.jclepro.2018.06.044.
- [90] D. V. Naik, V. Kumar, B. Prasad, B. Behera, N. Atheya, K.K. Singh, D.K. Adhikari, M.O. Garg, Catalytic cracking of pyrolysis oil oxygenates (aliphatic and aromatic) with vacuum gas oil and their characterization, *Chem. Eng. Res. Des.* 92 (2014) 1579–1590. doi:10.1016/j.cherd.2013.12.005.
- [91] V. Paasikallio, A. Azhari, J. Kihlman, P. Simell, J. Lehtonen, Oxidative steam reforming of pyrolysis oil aqueous fraction with zirconia pre-conversion catalyst, *Int. J. Hydrogen Energy.* 40 (2015) 12088–12096. doi:10.1016/j.ijhydene.2015.07.017.
- [92] K. Routray, K.J. Barnett, G.W. Huber, Hydrodeoxygenation of Pyrolysis Oils, *Energy Technol.* 5 (2017) 80–93. doi:10.1002/ente.201600084.
- [93] K.L. Hew, A.M. Tamidi, S. Yusup, K.T. Lee, M.M. Ahmad, Catalytic cracking of bio-oil to organic liquid product (OLP), *Bioresour. Technol.* 101 (2010) 8855–8858. doi:10.1016/j.biortech.2010.05.036.
- [94] W. Ma, B. Liu, R. Zhang, T. Gu, X. Ji, L. Zhong, G. Chen, L. Ma, Z. Cheng, X. Li, Co-upgrading of raw bio-oil with kitchen waste oil through fluid catalytic cracking (FCC), *Appl. Energy.* 217 (2018) 233–240. doi:10.1016/j.apenergy.2018.02.036.
- [95] W. Ma, B. Liu, X. Ji, X. Li, B. Yan, Z. Cheng, G. Chen, Catalytic co-cracking of distilled bio-oil and ethanol over Ni-ZSM-5/MCM-41 in a fixed-bed, *Biomass and Bioenergy.* 102 (2017) 31–36. doi:10.1016/j.biombioe.2017.04.006.

- [96] P.M. Mortensen, J.D. Grunwaldt, P.A. Jensen, K.G. Knudsen, A.D. Jensen, A review of catalytic upgrading of bio-oil to engine fuels, *Appl. Catal. A Gen.* 407 (2011) 1–19. doi:10.1016/j.apcata.2011.08.046.
- [97] N. Cakiryilmaz, H. Arbag, N. Oktar, G. Dogu, T. Dogu, Effect of W incorporation on the product distribution in steam reforming of bio-oil derived acetic acid over Ni based Zr-SBA-15 catalyst, *Int. J. Hydrogen Energy.* 43 (2018) 3629–3642. doi:10.1016/j.ijhydene.2018.01.034.
- [98] B. Valle, B. Aramburu, M. Olazar, J. Bilbao, A.G. Gayubo, Steam reforming of raw bio-oil over Ni/La₂O₃-AAI₂O₃: Influence of temperature on product yields and catalyst deactivation, *Fuel.* 216 (2018) 463–474. doi:10.1016/j.fuel.2017.11.149.
- [99] W. Nabgan, T.A. Tuan Abdullah, R. Mat, B. Nabgan, Y. Gambo, M. Ibrahim, A. Ahmad, A.A. Jalil, S. Triwahyono, I. Saeh, Renewable hydrogen production from bio-oil derivative via catalytic steam reforming: An overview, *Renew. Sustain. Energy Rev.* 79 (2017) 347–357. doi:10.1016/j.rser.2017.05.069.
- [100] C. Quan, S. Xu, C. Zhou, Steam reforming of bio-oil from coconut shell pyrolysis over Fe/olivine catalyst, *Energy Convers. Manag.* 141 (2017) 40–47. doi:10.1016/j.enconman.2016.04.024.
- [101] F. Bimbela, J. Ábrego, R. Puerta, L. García, J. Arauzo, Catalytic steam reforming of the aqueous fraction of bio-oil using Ni-Ce/Mg-Al catalysts, *Appl. Catal. B Environ.* 209 (2017) 346–357. doi:10.1016/j.apcatb.2017.03.009.
- [102] Y. Mei, C. Wu, R. Liu, Hydrogen production from steam reforming of bio-oil model compound and byproducts elimination, *Int. J. Hydrogen Energy.* 41 (2016) 9145–9152. doi:10.1016/j.ijhydene.2015.12.133.
- [103] Z. Ma, R. Xiao, H. Zhang, Catalytic steam reforming of bio-oil model compounds for hydrogen-rich gas production using bio-char as catalyst, *Int. J. Hydrogen Energy.* 42 (2017) 3579–3585. doi:10.1016/j.ijhydene.2016.11.107.
- [104] S. Cheng, L. Wei, M.R. Alsowij, F. Corbin, J. Julson, E. Boakye, D. Raynie, In situ hydrodeoxygenation upgrading of pine sawdust bio-oil to hydrocarbon biofuel using Pd/C catalyst, *J. Energy Inst.* 91 (2018) 163–171. doi:10.1016/j.joei.2017.01.004.
- [105] S. Cheng, L. Wei, J. Julson, K. Muthukumarappan, P.R. Kharel, Y. Cao, E. Boakye, D. Raynie, Z. Gu, Hydrodeoxygenation upgrading of pine sawdust bio-oil using zinc metal with zero valency, *J. Taiwan Inst. Chem. Eng.* 74 (2017) 146–153. doi:10.1016/j.jtice.2017.02.011.
- [106] A. Mosallanejad, H. Taghvaei, S.M. Mirsoleimani-azizi, A. Mohammadi, M.R. Rahimpour, Plasma upgrading of 4methylanisole: A novel approach for hydrodeoxygenation of bio oil without using a hydrogen source, *Chem. Eng. Res. Des.* 121 (2017) 113–124. doi:10.1016/j.cherd.2017.03.011.
- [107] J. Lee, Y. Choi, J. Shin, J.K. Lee, Selective hydrocracking of tetralin for light aromatic

- hydrocarbons, *Catal. Today*. 265 (2016) 144–153. doi:10.1016/j.cattod.2015.09.046.
- [108] D.P. Upare, S. Park, M.S. Kim, Y.P. Jeon, J. Kim, D. Lee, J. Lee, H. Chang, S. Choi, W. Choi, Y.K. Park, C.W. Lee, Selective hydrocracking of pyrolysis fuel oil into benzene, toluene and xylene over CoMo/beta zeolite catalyst, *J. Ind. Eng. Chem.* 46 (2017) 356–363. doi:10.1016/j.jiec.2016.11.004.
- [109] H. Yang, R. Yan, H. Chen, C. Zheng, D.H. Lee, D.T. Liang, In-depth investigation of biomass pyrolysis based on three major components: Hemicellulose, cellulose and lignin, *Energy and Fuels*. 20 (2006) 388–393. doi:10.1021/ef0580117.
- [110] P.R. Patwardhan, R.C. Brown, B.H. Shanks, Product distribution from the fast pyrolysis of hemicellulose, *ChemSusChem*. 4 (2011) 636–643. doi:10.1002/cssc.201000425.
- [111] D.K. Shen, S. Gu, A. V. Bridgwater, Study on the pyrolytic behaviour of xylan-based hemicellulose using TG-FTIR and Py-GC-FTIR, *J. Anal. Appl. Pyrolysis*. 87 (2010) 199–206. doi:10.1016/j.jaap.2009.12.001.
- [112] F.X. Collard, J. Blin, A review on pyrolysis of biomass constituents: Mechanisms and composition of the products obtained from the conversion of cellulose, hemicelluloses and lignin, *Renew. Sustain. Energy Rev.* 38 (2014) 594–608. doi:10.1016/j.rser.2014.06.013.
- [113] X. Zhou, L.J. Broadbelt, R. Vinu, *Mechanistic Understanding of Thermochemical Conversion of Polymers and Lignocellulosic Biomass*, 1st ed., Elsevier Inc., 2016. doi:10.1016/bs.ache.2016.09.002.
- [114] A. Molino, S. Chianese, D. Musmarra, Biomass gasification technology: The state of the art overview, *J. Energy Chem.* 25 (2016) 10–25. doi:10.1016/j.jechem.2015.11.005.
- [115] Y. Tang, X. Ma, Z. Lai, H. Lin, J. Wu, Char characteristics of municipal solid waste prepared under N₂ and CO₂ atmospheres, *J. Anal. Appl. Pyrolysis*. 101 (2013) 193–198. doi:10.1016/j.jaap.2013.01.010.
- [116] Y.T. Tang, X.Q. Ma, Z.H. Wang, Z. Wu, Q.H. Yu, A study of the thermal degradation of six typical municipal waste components in CO₂ and N₂ atmospheres using TGA-FTIR, *Thermochim. Acta*. 657 (2017) 12–19. doi:10.1016/j.tca.2017.09.009.
- [117] M. Azuara, E. Sáiz, J.A. Manso, F.J. García-Ramos, J.J. Manyà, Study on the effects of using a carbon dioxide atmosphere on the properties of vine shoots-derived biochar, *J. Anal. Appl. Pyrolysis*. 124 (2017) 719–725. doi:10.1016/j.jaap.2016.11.022.
- [118] P.J. Woolcock, R.C. Brown, A review of cleaning technologies for biomass-derived syngas, *Biomass and Bioenergy*. 52 (2013) 54–84. doi:10.1016/j.biombioe.2013.02.036.
- [119] Z. Shi, S. Shen, T. Li, Y. Sun, W. Shan, Y. Bai, Q. Zhang, F. Li, The evaluation of a process for clean syngas based on lump coal pressurized gasification, *Int. J. Hydrogen Energy*. 42 (2017) 7883–7894. doi:10.1016/j.ijhydene.2017.02.078.
- [120] Y.-S. Chen, S.-S. Hsiau, D.-Y. Shu, System efficiency improvement of IGCC with

- syngas clean-up, *Energy*. (2018). doi:10.1016/j.energy.2018.03.109.
- [121] P. De Filippis, M. Scarsella, B. De Caprariis, R. Uccellari, Biomass Gasification Plant and Syngas Clean-up System, *Energy Procedia*. 75 (2015) 240–245. doi:10.1016/j.egypro.2015.07.318.
- [122] L.F. de Diego, F. García-Labiano, P. Gayán, A. Abad, T. Mendiara, J. Adánez, M. Nacken, S. Heidenreich, Tar abatement for clean syngas production during biomass gasification in a dual fluidized bed, *Fuel Process. Technol.* 152 (2016) 116–123. doi:10.1016/j.fuproc.2016.05.042.
- [123] G. Akay, C.A. Jordan, A.H. Mohamed, Syngas cleaning with nano-structured microporous ion exchange polymers in biomass gasification using a novel downdraft gasifier, *J. Energy Chem.* 22 (2013) 426–435. doi:10.1016/S2095-4956(13)60056-X.
- [124] M. Jeremiáš, M. Pohořelý, K. Svoboda, S. Skoblia, Z. Beňo, M. Šyc, CO₂ gasification of biomass: The effect of lime concentration in a fluidised bed, *Appl. Energy*. 217 (2018) 361–368. doi:10.1016/j.apenergy.2018.02.151.
- [125] W.X. Peng, S.B. Ge, A.G. Ebadi, H. Hisoriev, M.J. Esfahani, Syngas production by catalytic co-gasification of coal-biomass blends in a circulating fluidized bed gasifier, *J. Clean. Prod.* 168 (2017) 1513–1517. doi:10.1016/j.jclepro.2017.06.233.
- [126] M. Hrabovsky, M. Hlina, V. Kopecky, A. Maslani, O. Zivny, P. Krenek, A. Serov, O. Hurba, Steam Plasma Treatment of Organic Substances for Hydrogen and Syngas Production, *Plasma Chem. Plasma Process.* 37 (2017) 739–762. doi:10.1007/s11090-016-9783-5.
- [127] M. Wnukowski, P. Jamróz, Microwave plasma treatment of simulated biomass syngas: Interactions between the permanent syngas compounds and their influence on the model tar compound conversion, *Fuel Process. Technol.* 173 (2018) 229–242. doi:10.1016/j.fuproc.2018.01.025.
- [128] S.Y. Liu, D.H. Mei, M.A. Nahil, S. Gadkari, S. Gu, P.T. Williams, X. Tu, Hybrid plasma-catalytic steam reforming of toluene as a biomass tar model compound over Ni/Al₂O₃ catalysts, *Fuel Process. Technol.* 166 (2017) 269–275. doi:10.1016/j.fuproc.2017.06.001.
- [129] A. More, C.J. Hansen, G. Vesper, Production of inherently separated syngas streams via chemical looping methane cracking, *Catal. Today*. 298 (2017) 21–32. doi:10.1016/j.cattod.2017.07.008.
- [130] K. Zhang, X. Jiang, An investigation of fuel variability effect on bio-syngas combustion using uncertainty quantification, *Fuel*. 220 (2018) 283–295. doi:10.1016/j.fuel.2018.02.007.
- [131] S. Jia, S. Ning, H. Ying, Y. Sun, W. Xu, H. Yin, High quality syngas production from catalytic gasification of woodchip char, *Energy Convers. Manag.* 151 (2017) 457–464. doi:10.1016/j.enconman.2017.09.008.

- [132] M. Gupta, S. Pramanik, R. V. Ravikrishna, Development of a syngas-fired catalytic combustion system for hybrid solar-thermal applications, *Appl. Therm. Eng.* 109 (2016) 1023–1030. doi:10.1016/j.applthermaleng.2016.04.150.
- [133] R. Rajbongshi, D. Borgohain, S. Mahapatra, Optimization of PV-biomass-diesel and grid base hybrid energy systems for rural electrification by using HOMER, *Energy*. 126 (2017) 461–474. doi:10.1016/j.energy.2017.03.056.
- [134] S. Kohsri, A. Meechai, C. Prapainainar, P. Narataruksa, P. Hunpinyo, G. Sin, Design and preliminary operation of a hybrid syngas/solar PV/battery power system for off-grid applications: A case study in Thailand, *Chem. Eng. Res. Des.* (2018) 1–16. doi:10.1016/j.cherd.2018.01.003.
- [135] H. Zhao, K. Fang, F. Dong, M. Lin, Y. Sun, Z. Tang, Textual properties of Cu–Mn mixed oxides and application for methyl formate synthesis from syngas, *J. Ind. Eng. Chem.* 54 (2017) 117–125. doi:10.1016/j.jiec.2017.05.024.
- [136] P. Lu, D. Shen, S. Cheng, E. Hondo, L.G. Chizema, C. Wang, X. Gai, C. Lu, R. Yang, The design of a CZ@H- β -P catalyst with core shell structure and its application in LPG synthesis from syngas, *Fuel*. 223 (2018) 157–163. doi:10.1016/j.fuel.2018.02.159.
- [137] F.Y. Hagos, A.R.A. Aziz, S.A. Sulaiman, Methane enrichment of syngas (H₂/CO) in a spark-ignition directinjection engine: Combustion, performance and emissions comparison with syngas and Compressed Natural Gas, *Energy*. 90 (2015) 2006–2015. doi:10.1016/j.energy.2015.07.031.
- [138] N. Indrawan, S. Thapa, P.R. Bhoi, R.L. Huhnke, A. Kumar, Engine power generation and emission performance of syngas generated from low-density biomass, *Energy Convers. Manag.* 148 (2017) 593–603. doi:10.1016/j.enconman.2017.05.066.
- [139] X. Kan, D. Zhou, W. Yang, X. Zhai, C.H. Wang, An investigation on utilization of biogas and syngas produced from biomass waste in premixed spark ignition engine, *Appl. Energy*. 212 (2018) 210–222. doi:10.1016/j.apenergy.2017.12.037.
- [140] K.A. Al-attab, Z.A. Zainal, Micro gas turbine running on naturally aspirated syngas: An experimental investigation, *Renew. Energy*. 119 (2018) 210–216. doi:10.1016/j.renene.2017.12.008.
- [141] O. Pardo-Planas, H.K. Atiyeh, J.R. Phillips, C.P. Aichele, S. Mohammad, Process simulation of ethanol production from biomass gasification and syngas fermentation, *Bioresour. Technol.* 245 (2017) 925–932. doi:10.1016/j.biortech.2017.08.193.
- [142] X. Sun, H.K. Atiyeh, A. Kumar, H. Zhang, Enhanced ethanol production by *Clostridium ragsdalei* from syngas by incorporating biochar in the fermentation medium, *Bioresour. Technol.* 247 (2018) 291–301. doi:10.1016/j.biortech.2017.09.060.
- [143] S.N. Reddy, S. Nanda, A.K. Dalai, J.A. Kozinski, Supercritical water gasification of biomass for hydrogen production, *Int. J. Hydrogen Energy*. 39 (2014) 6912–6926. doi:10.1016/j.ijhydene.2014.02.125.

- [144] K. Kang, R. Azargohar, A.K. Dalai, H. Wang, Hydrogen production from lignin, cellulose and waste biomass via supercritical water gasification: Catalyst activity and process optimization study, *Energy Convers. Manag.* 117 (2016) 528–537. doi:10.1016/j.enconman.2016.03.008.
- [145] S. Nanda, S.N. Reddy, A.K. Dalai, J.A. Kozinski, Subcritical and supercritical water gasification of lignocellulosic biomass impregnated with nickel nanocatalyst for hydrogen production, *Int. J. Hydrogen Energy.* 41 (2016) 4907–4921. doi:10.1016/j.ijhydene.2015.10.060.
- [146] A. Amrullah, Y. Matsumura, Supercritical water gasification of sewage sludge in continuous reactor, *Bioresour. Technol.* 249 (2018) 276–283. doi:10.1016/j.biortech.2017.10.002.
- [147] O. Yakaboylu, I. Albrecht, J. Harinck, K.G. Smit, G.A. Tsalidis, M. Di Marcello, K. Anastasakis, W. de Jong, Supercritical water gasification of biomass in fluidized bed: First results and experiences obtained from TU Delft/Gensos semi-pilot scale setup, *Biomass and Bioenergy.* 111 (2016) 330–342. doi:10.1016/j.biombioe.2016.12.007.
- [148] R. Samiee-Zafarghandi, J. Karimi-Sabet, M.A. Abdoli, A. Karbassi, Supercritical water gasification of microalga *Chlorella* PTCC 6010 for hydrogen production: Box-Behnken optimization and evaluating catalytic effect of MnO₂/SiO₂ and NiO/SiO₂, *Renew. Energy.* 126 (2018) 189–201. doi:10.1016/j.renene.2018.03.043.
- [149] T.D.H. Bugg, M. Ahmad, E.M. Hardiman, R. Rahmanpour, Pathways for degradation of lignin in bacteria and fungi, *Nat. Prod. Rep.* 28 (2011) 1883. doi:10.1039/c1np00042j.
- [150] K. Ohenoja, M. Körkkö, V. Wigren, J. Österbacka, M. Illikainen, Fly ash classification efficiency of electrostatic precipitators in fluidized bed combustion of peat, wood, and forest residues, *J. Environ. Manage.* 206 (2018) 607–614. doi:10.1016/j.jenvman.2017.10.047.
- [151] M. Hupa, O. Karlström, E. Vainio, Biomass combustion technology development - It is all about chemical details, *Proc. Combust. Inst.* 36 (2017) 113–134. doi:10.1016/j.proci.2016.06.152.
- [152] W.J. Liu, H. Jiang, H.Q. Yu, Development of Biochar-Based Functional Materials: Toward a Sustainable Platform Carbon Material, *Chem. Rev.* 115 (2015) 12251–12285. doi:10.1021/acs.chemrev.5b00195.
- [153] M.S. Mettler, S.H. Mushrif, A.D. Paulsen, A.D. Javadekar, D.G. Vlachos, P.J. Dauenhauer, Revealing pyrolysis chemistry for biofuels production: Conversion of cellulose to furans and small oxygenates, *Energy Environ. Sci.* 5 (2012) 5414–5424. doi:10.1039/C1EE02743C.
- [154] S. Chu, A. V. Subrahmanyam, G.W. Huber, The pyrolysis chemistry of a β -O-4 type oligomeric lignin model compound, *Green Chem.* 15 (2013) 125–136. doi:10.1039/C2GC36332A.

- [155] Z. Ma, E. Troussard, J.A. Van Bokhoven, Controlling the selectivity to chemicals from lignin via catalytic fast pyrolysis, *Appl. Catal. A Gen.* 423–424 (2012) 130–136. doi:10.1016/j.apcata.2012.02.027.
- [156] J. Watson, Y. Zhang, B. Si, W.T. Chen, R. de Souza, Gasification of biowaste: A critical review and outlooks, *Renew. Sustain. Energy Rev.* 83 (2018) 1–17. doi:10.1016/j.rser.2017.10.003.
- [157] D. Castello, A. Kruse, L. Fiori, Low temperature supercritical water gasification of biomass constituents: Glucose/phenol mixtures, *Biomass and Bioenergy.* 73 (2015) 84–94. doi:10.1016/j.biombioe.2014.12.010.

Aim of the thesis

Several studies reported the individual behaviour of date palm biomass and microalgae from a range of perspectives. The major focus is the production of improved bio-oil quality through fast pyrolysis with reduced oxygenated and nitrogenous compounds. However, detailed chemical and energy point of view was missing for biochar (bio-carbon) production through slow pyrolysis by each of the feedstock. Thus, the primary objective of this thesis is to process the waste from date palm cultivation and wastewater derived microalgae individually and in the combined form through pyrolysis process. Further, analysis of the products through different techniques is provided to establish the use of these feedstocks in bio-refineries.

Hypothesis

Following scientific hypothesis are the basis of the conducted research:

- Date palm biomass and microalgae can contribute significantly in char yielding bio-refineries.
- Combined processing of the lignocellulosic biomass and microalgae contains the potential to produce char for multiple applications.
- The introduction of multi-stage processing might help to improve char properties and combined behaviour in bio-refineries.

Following major questions are parts of the hypothesis:

How the behaviour of the char from microalgae differs from lignocellulosic biomass in slow pyrolysis technology? How can we improve the properties of char produced through biorefineries for multiple applications?

Research objectives

Following objectives are the part of the research to comprehensively explain the behaviour of both feedstocks upon pyrolysis:

- To characterize the date palm biomass for heavy metals concentration and comparison with the EU standards.
- To determine the effect of treatment temperature and multi-stage processing of feedstocks via pyrolysis on the product's composition and aromaticity.
- Determination of the potential of char from both feedstocks in combustion and energy-based applications through kinetic modelling.
- Economic evaluation of the product on the basis of treatment conditions and its resultant energy potential.

Experimental procedure

The characteristics of the materials and methods utilised in this thesis are explained individually in each chapter and explained in detail with the corresponding references.

Thesis outline

This thesis is divided into two major parts including literature review and research work. Literature review is explained in the second chapter while third, fourth and fifth chapters included the research work. Third chapter defined the basic characteristics of the date palm biomass and heavy metals presence in different parts of the branches. Fourth chapter included the individual pyrolysis of the date palm biomass and wastewater derived microalgae and evaluation of their products. Fifth chapter contained the multi-stage combined pyrolysis process of the date palm and wastewater derived microalgae. Their products evaluation and product performance was reported. Sixth chapter included the summary of the project and further recommendation for future research.

Characterisation of waste from date palm branches²

This chapter is devoted to the detailed analysis of the date palm branches from chemical to thermal perspective. Date palm biomass generates a huge amount of waste throughout the world which can be utilised to produce energy through thermochemical or biochemical conversion technologies. The objective of this study is to present a detailed characterisation of parts of date palm branches (twig) and analyse the trace elements including heavy metals for environmental safety and potential slagging and fouling in a reactor. The biomass was divided into four parts L (leaf ribs), SB (small part of a branch attached to the ribs), MB (middle part of the branch) and LB (large part of a branch attached to the trunk). Different characterisation techniques applied were XRD, TGA, FT-IR, ICP-MS, XRF, HHV and CHNSO analysis. High crystallinity was observed in LB with all the heavy metals present in permissible limits. However, it showed a considerably high moisture holding capability. Conversely, SB was found to be of low moisture holding capability, moderate higher heating values, and contains one heavy metal (As) higher than the permissible limit defined by European Union standards. It can be concluded that LB can be used directly for energy generation after sun drying. The other parts are required to be treated for heavy metals reduction before being used for energy production, keeping in mind the environmental safety.

² This chapter is extracted from the published study “A. Akhtar, T. Ivanova, I. Jiříček, V. Krepl, Detailed characterization of waste from date palm (*Phoenix dactylifera*) branches for energy production: Comparative evaluation of heavy metals concentration, *J. Renew. Sustain. Energy*. 11 (2019) 13102. doi:10.1063/1.5027578.” with permission from American Institute of Physics.

First author is the major contributor of the article and is responsible for data gathering, analysis, writing and publishing in article format.

3.1 Introduction

Biomass is being considered as a large source of energy and finds its way to produce energy, fuels, and chemicals which otherwise are produced through fossil fuels. Biomass is a composition of carbon, hydrogen, and oxygen at varying percentage according to the source of the material and its characteristics [1]. Biomass can convert and accumulate the light energy into chemical energy and upon deterioration release this energy which can be used in different applications [2]. Biomass with little to no processing can be utilised in various technologies, e.g., to produce biogas in digesters, to produce energy in boilers and to produce chemicals and fuels in various reactors in the presence or absence of oxygen. Irrespective of the type of biomass, it is still considered a net zero carbon energy source [3].

Date palm (*Phoenix dactylifera L.*) tree is resilient. Hence it can survive in tough conditions like the Arabian Peninsula. This tree was once found in most Arabian countries, but due to its fruit, it is being harvested in many countries in Asia and America. Saudi Arabia is home to more than 24 million date palm trees across the country which makes it one of the highest producers in the Arab region [4]. According to the Food and Agriculture Organization (FAO) statistics, it is also the third largest producer in the world after Egypt and Iran [5]. Date palm is associated with the generation of the enormous amount of waste which is of no value except combustion. Each tree can produce approximately 40 kg of waste annually [6] which leads to 960 thousand tonnes of waste in one country. Although date palm waste was being used and studied as a building material [7,8] but continually changing living conditions are making it impossible to utilise whole waste.

This waste can be utilised to produce alternative energy or can further be processed to produce valuable chemicals to meet the need of the hour. Briones et al. [9] reported the production of polyol from date seeds through oxypropylation and liquefaction process and obtained high yields in suitable reaction time. It was approved to use the product as a precursor in polyurethane synthesis directly without any treatment. Lattieff [10] employed the date palm fruit waste to produce biogas and found the optimum solid mix ratio of 0.15 where the observed biogas production was highest at both mesophilic and thermophilic conditions 182 L/kgVS and 133 L/kgVS respectively. Abd-Alla and Elsadek El-Enany [11] suggested the use of rotten date fruits to produce acetone, butanol, and ethanol. The use of yeast extract or ammonium nitrate helped increase the production of biochemicals without the use of a costly reducing agent. Moreover, Fang et al. [12] concluded that hydrothermal pre-treatment of date palm biomass

yields high ethanol production up to 96% for leaflets and 80% for rachis under optimum conditions 210 °C and 10 min.

Date palm waste was proposed to use in cogeneration power plant to produce energy and distilled water. It was concluded that up to 535 kWh electricity could be generated per ton of biomass waste with 2.27 million tonnes of distilled water. Nasser et al. [13] carried out a characterisation of different parts of a date palm tree and concluded that date palm stones and coir are most suitable for renewable energy production. The suitability of date palm biomass for different energy recovery applications has been proven through several studies. However, it is clear from the literature that trace elements including heavy metals presence in date palm branches need to be thoroughly investigated considering their potential effect on environmental safety and living beings. Therefore, the main objective of this chapter is to comprehensively investigate the different parts of date palm branches (twigs) through an array of characterisation techniques and recommend the fair use of this biomass in energy generation applications without compromising on environmental safety. To achieve the desired objective, date palm branches were imported in the fresh state from Saudi Arabia to the Czech Republic, and the biomass then characterised through chemical and thermal analysis.

3.2 Materials and Methods

3.2.1 Biomass collection and processing

Biomass (date palm branches) was imported from Saudi Arabia to the Prague Czech Republic in the fresh state. Some of the biomass left to dry at room conditions in the laboratory rather than accelerated sun drying to see the moisture reduction pattern. While the rest of the biomass was processed (cut and ground) in the fresh state (wet condition) to determine its moisture content immediately upon arrival. Branches (twigs) were divided into four main parts i) L (leaf ribs), ii) SB (small part of the branch attached to the ribs) iii) LB (large part of the branch attached to the truck) iv) MB (middle part of the branch between LB and SB). All the samples were prepared according to BS 14780 [14].

The remaining part was left for air drying. The dried biomass was then cut and ground into powder form to achieve a less than 1 mm size. This processed biomass was stored in airtight bags afterwards. All the experiments were performed three times, and the average values were reported in the figures and tables.

3.2.2 Moisture content

Moisture content was measured by weight loss in the oven for all samples according to ISO 18134-2 [15] standard for biofuels. Moisture content was measured at first for wet biomass and then after air-drying the biomass for two months to determine the moisture holding capability at room conditions. Meanwhile, it was not exposed to solar radiations.

3.2.3 Proximate analysis

Proximate analysis was performed for the above mentioned four samples using the following standards ISO18122 [16] and ISO 18123 [17] to determine the ash content and volatile matter respectively. Fixed carbon was calculated by the difference:

$$FC (\%) = 100 - (M(\%) + VM(\%) + Ash(\%)) \dots\dots\dots (3-1)$$

Where FC (%), M (%), VM (%) and Ash (%) are percentages of fixed carbon, moisture, volatile matter and ash content respectively.

$$Total\ solids (\%) = 100 - M (\%) \dots\dots\dots (3-2)$$

3.2.4 Ultimate analysis

The Ultimate analysis was conducted according to standards BS EN 16948 [18] to determine the Carbon, Hydrogen, Nitrogen content and BS EN 16994 [19] to determine the Sulphur content.

$$O(\%) = 100 - (C(\%) + H(\%) + N(\%) + S(\%) + Ash(\%)) \dots\dots\dots (3-3)$$

Where *O* (%), *C* (%), *H* (%), *N* (%), *S* (%), *Ash* (%) are mass percentages of oxygen, carbon, hydrogen, nitrogen, Sulfur and ash content respectively in equation (3-3).

3.2.5 Heating values

Higher heating values (HHV) and lower heating values (LHV) of biomass were determined according to BS 14918 [20]. The instrument/calorimeter used to measure these values is IKA –C6000 oxygen bomb calorimeter. All standards used in this research are specific to solid biofuels (biomass).

3.2.6 Error analysis

An error analysis was conducted to determine the variation in the experimental values of HHV and LHV. Six correlations were selected, from the literature which used a wide variety of biomass to develop these correlations except date palm residues, to calculate HHV. These correlations are given in *Table 3-1* and are based on the ultimate analysis [21,22], proximate analysis [23,24] and the stoichiometric ratio [25].

Stoichiometric ratio simply can be explained as the air/fuel ratio needed to burn a biomass sample completely. In this study, it was measured on the basis of ultimate analysis (*Table 3-3*).

Following equations (3-4) and (3-5) were used to find the error between experimental and theoretical values and to assess the correlations in *Table 3-1* used in estimating HHV:

$$\text{Average Experimental Error (AEE)} = \frac{1}{n} \sum_{i=1}^n \left| \frac{HHV_C - HHV_M}{HHV_M} \right| \times 100 \% \dots\dots\dots (3-4)$$

$$\text{Average Bias Error (ABE)} = \frac{1}{n} \sum_{i=1}^n \frac{HHV_C - HHV_M}{HHV_M} \times 100 \% \dots\dots\dots (3-5)$$

Subscripts C and M in Eq. (3-4) and (3-5) denoted as calculated and measured respectively.

3.2.7 Exergy

Exergy is a salient feature from the point of view of work performance of any system as it shows the system's ability to do work. "Exergy in simple terms shows the highest amount of work obtainable through a reversible process from the thermodynamic system during reaching equilibrium stage as compared to surroundings" [26]. Song et al. [27] suggested equation (3-12) based on Szargut's R.E. model to estimate specific chemical exergy of solid and liquid fuels which utilises basic elemental composition of fuels making this correlation most straightforward among others. Correlations used to determine the exergy of date palm biomass is presented in *Table 3-2*.

3.2.8 X-ray fluorescence (XRF) spectrometry

X-ray fluorescence (XRF) was employed to measure the inorganic composition of biomass samples which plays a key role during combustion and pyrolysis and significantly affect the desired products. Semi-quantitative (estimated) data were obtained with the help of Niton-XL3t Goldd (Geometrically Optimized Large Area Drift Detector) analyser to find out fractions of inorganic constituents present in biomass samples and concluded their effect in energy use applications.

Table 3-1 Correlations used for calculating the theoretical higher heating value (HHV)

Eq. No.	Correlation	Composition used	Reference
(3-6)	$HHV \left(\frac{MJ}{kg} \right) = 0.3491 \times C + 1.1783 \times H + 0.1005 \times S - 0.1034 \times O - 0.015 \times N - 0.0211 \times Ash$	Ultimate Analysis	[21]
(3-7)	$HHV \left(\frac{MJ}{kg} \right) = -1.3675 + 0.3137 \times C + 0.7009 \times H + 0.0318 \times O^+$	Ultimate Analysis	[22]
(3-8)	$HHV \left(\frac{MJ}{kg} \right) = 0.3536 \times FC + 0.1559 \times VM - 0.0078 \times Ash$	Proximate Analysis	[23]
(3-9)	$HHV \left(\frac{MJ}{kg} \right) = \frac{\text{Stoichiometric ratio}}{0.31}$	Stoichiometric ratio	[25]
(3-10)	$HHV \left(\frac{MJ}{kg} \right) = 19.2880 - 0.2135 \times \left(\frac{VM}{FC} \right) + 0.0234 \times \left(\frac{FC}{Ash} \right) - 1.9584 \times \left(\frac{Ash}{VM} \right)$	Proximate Analysis	[24]
(3-11)	$HHV \left(\frac{MJ}{kg} \right) = 20.7999 - 0.3214 \times \left(\frac{VM}{FC} \right) + 0.0051 \times \left(\frac{VM}{FC} \right)^2 - 11.2277 \times \left(\frac{Ash}{VM} \right) + 4.4953 \times \left(\frac{Ash}{VM} \right)^2 - 0.7223 \times \left(\frac{Ash}{VM} \right)^3 + 0.0383 \times \left(\frac{Ash}{VM} \right)^4 + 0.0076 \times \left(\frac{FC}{Ash} \right)$	Proximate Analysis	[24]

Table 3-2 Correlations used to determine the exergy of date palm biomass

Eq. No.	Correlation	Units	Reference
(3-12)	$Ex_s = 363.439 \times C + 1075.633 \times H - 86.308 \times O + 4.147 \times N + 190.798 \times S - 21.1 \times Ash$	$\left(\frac{kJ}{kg}\right)$	[27]
(3-13)	$Ex_{HHV} = 342.50 + 1.04 \times HHV$	$\left(\frac{kJ}{kg}\right)$	[48]
(3-14)	$Ex_{LHV} = 2289.87 + 1.01 \times LHV$	$\left(\frac{kJ}{kg}\right)$	[48]

3.2.9 Inductively coupled plasma mass spectrometry (ICP-MS) analysis

XRF analysis gave the semi-quantitative data regarding the existence of different trace elements in biomass samples. Therefore, it was necessary to accurately determine the percentage of trace elements in biomass samples and compare the values through both techniques. ELAN DRC-e equipment used for this purpose and Perkin-Elmer microwave was used to prepare the samples for analysis. After preliminary digestion of fine powder samples with sulfuric acid and hydrogen peroxide (30%, v/v), digested in a microwave. The transparent digested product then diluted with demineralized water and measurement of the trace elements were carried out using inductively coupled plasma-mass spectrometry (ICP-MS). The data were presented in percentage according to measured elements.

3.2.10 X-ray diffraction (XRD) analysis

Biomass samples were characterised using X-ray diffraction technique for all parts of the branch with emphasis on its crystallinity determination with Bruker D8 instrument. The operating voltage and current were set at 30 kV and 10 mA respectively. Spectra collected on a wide range for 2θ starting from 7° to 80° with a step size of 0.012 at 0.1 S per step. To prepare the homogeneous samples for all parts of the branch, biomass was first dried and cut into small pieces which were later crushed to pass through 1 mm sieve. The biomass was left at ambient condition for 24 hours before the experiment to remove any uncertainty due to cutting and crushing procedure.

3.2.11 Thermogravimetric (TGA) analysis

Thermogravimetric analysis was conducted for the considered biomass samples in the presence of Argon as a purge gas at a flow rate of 1.66 cm³/sec. TG-750 was used for thermal analysis of the biomass samples. To compare the potential results, the single platinum crucible was used, and the weight of the samples was maintained between 7.2-8.3 mg. Balance and temperature of the equipment maintained for 10 minutes before the start of the experiment. The chamber then started heating the samples separately at heating rates of 10 °C/min, 20 °C/min and 50 °C/min for all the samples. Multiple heating rates were employed to understand the decomposition pattern under different pyrolysis conditions.

3.2.12 Attenuated total reflection fourier transform infrared (ATR-FTIR) spectroscopy

Studied biomass was investigated for the functional group composition present in the date palm biomass through Fourier Transform Infra-Red (FTIR) spectroscopy. The biomass was converted to powdered samples and placed on the diamond (ATR-FTIR) and transmittance spectra were collected. The spectra were collected at a scan rate of 64 with a spectral resolution of 4 cm⁻¹ covering a range of 700-4000 cm⁻¹ wavenumbers.

3.3 Results and Discussion

3.3.1 Moisture content

Moisture content is significant in the case of biomass and its use in energy applications. Some types of biomass are little difficult to dry early than others due to their high moisture holding capability and requires energy to dry for immediate use. *Figure 3-1* displays moisture content alteration pattern for different parts of the branch until it reaches a stable position. Wet biomass had more than 50% moisture content calculated on a dry basis in nearly all samples. However, it started to reduce rapidly at room conditions. At the end of the first month of drying, three out of four samples had a moisture content less than 10% whereas LB had approximately 37% exhibiting high moisture holding capability and which could take extra time in a combustion chamber to dry and burn [28]. The second month revealed the sudden change in moisture in LB reducing it to 8.3%. However, other parts demonstrate less than a 2% change in their moisture while sustaining their values consistently. All parts of the branch are found to be feasible to use after the first month of air drying at room conditions except LB which

requires significantly more time of air drying to use economically for combustion or other energy application.

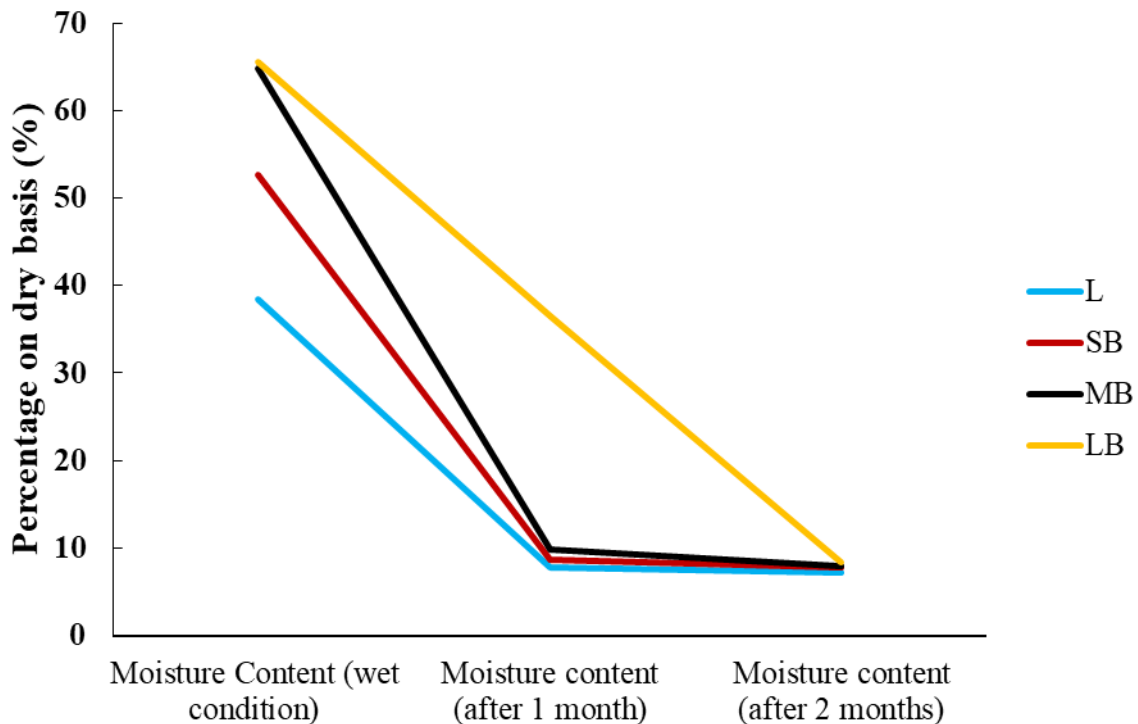


Figure 3-1 Moisture content changing pattern with time (months) in L, SB, MB and LB. L (Leaf ribs), SB (small part of a branch attached to the ribs), MB (middle part of the branch) and LB (large part of a branch attached to the trunk)

3.3.2 Proximate analysis

Proximate analysis is most frequently used the technique to determine biofuel composition and to evaluate its general properties [24]. Figure 3-2 presents the values of total solids, moisture content, volatile matter, fixed carbon and ash content measured on a dry basis determined during the proximate analysis of date palm branches. Volatile matter content in fuel usually gives the information about the reactivity of fuel is describing how easily a fuel can be burned, however, in many cases of biomass, high volatile matter content can also produce many inorganic compounds during combustion [29].

The highest volatile matter was found in MB and lowest in L. Conversely, maximum ash content was found in L which is approximately 2.5 times MB, making L more energy intensive due to more mechanical work required for ash removal and more space required in boilers or combustion chambers. Fixed carbon content showed a small difference in their values with the highest value in L and lowest in LB with the total difference of 2% in their values.

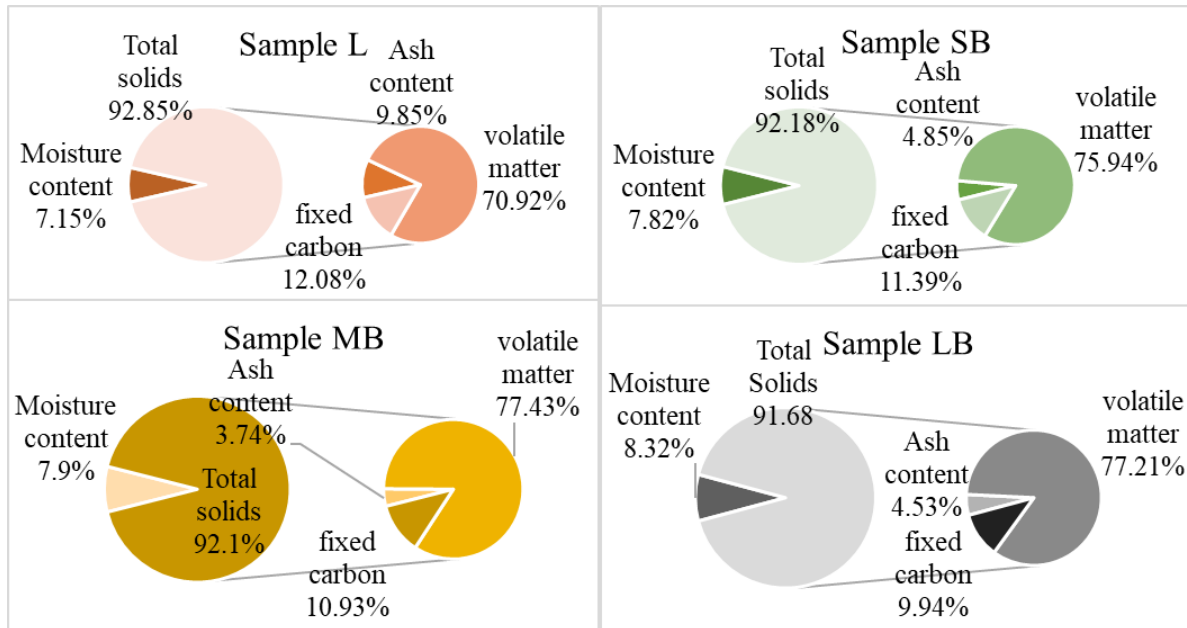


Figure 3-2 Proximate analysis of date palm branches on the dry basis

3.3.3 Ultimate analysis

The results of the elemental composition measured on a dry basis are presented in *Table 3-3*. Chemical evaluation is necessary for energy generation and conversion into different other compounds. Ash content is equivalent to the proximate analysis. Oxygen (O) content is measured through the subtraction method which also contains other inorganic elements with oxygen. Carbon content showed the highest percentage in L and lowest in LB with the difference of more than 2% which translates to heating values.

Table 3-3 Elemental composition of biomass samples (C = Carbon, H = Hydrogen, N = Nitrogen, S = Sulphur, O* = Oxygen (*calculated by difference) and SR = stoichiometric ratio)

Samples	C (%)	H (%)	N (%)	S (%)	O* (%)	Ash (%)	SR (kg/kg)
L	45.22	6.323	0.825	0.1975	37.585	9.85	5.8
SB	44.2	6.301	0.443	0.107	44.1	4.85	5.4
MB	43.72	6.368	0.251	0.086	45.836	3.74	5.3
LB	43.075	6.263	0.22	0.126	45.787	4.53	5.1

3.3.4 X-ray fluorescence spectrometry

X-ray fluorescence (XRF) spectrometry is an important and convenient method to determine inorganic fractions. This method is not only simple but also many researchers find it useful in obtaining excellent results [30–32]. Commercially pre-calibrated XRF Niton XL3t with Gold technology showed relative percentages of inorganic elements including major elements potassium, calcium, chlorine, and silicon (K, Ca, Cl, and Si) and trace elements iron, zinc, chromium, zirconium, cadmium (Fe, Zn, Cr, Zr, and Cd). Even though the data obtained is semi-quantitative, but it depicts some excellent comparison of these elements in biomass samples in *Figure 3-3*. Leaf ribs showed the highest percentage of Si reaching more than 13% whereas other parts showed a significantly lower concentration of approximately 1%. However, as low as 1% Si can be a significant problem during combustion of biomass due to the production of slagging in the form of silicates [30]. Non-woody biomass usually showed more tendency to produce slagging due to the high concentration of Si as compared to woody biomass [33]. SiO₂ concentration may be lowered by using alkaline washing of biomass. This can also help reducing potassium concentration as well [34].

On the other hand, Chlorine concentration is quite low in L as compared to the rest of the samples which causes gaseous emissions of HCl. Chlorine potentially increases the alkali concentration in the vapour phase after combustion [35]. The maximum concentration of Cl found to be in LB exceeding 4%. During combustion, chlorine can cause corrosion and deposit formation in the chamber. Acid washing can help remove a significant amount of alkali material to cope with this problem [34].

Furthermore, Potassium makes salt with different other elements in the form of carbonates and sulphates which found as a significant inorganic element in all parts of the branch with the highest concentration in L exceeding 3%. Aluminum sulphate or sulphur addition can decrease KCl in a gas phase with higher efficiency belongs to aluminum sulphate as compared to sulphur which facilitates the reduction of agglomeration problem [36]. Calcium percentage is highest in SB 3.4% while the lowest in MB 2.7%. Calcium concentration throughout branch showing approximately 3 % depicting little variation in all parts. Calcium existence in approximately every type of biomass makes this essential element of ash in combustion chambers. Calcium usually reacts with silicon and sulphur to make different silicates and sulphates. Pisupati and Bhalla [37] found an interesting relation in pyrolysis process where calcium can help in decreasing of So_x emissions in the form of bio lime.

Moreover, lower calcium content yields more volatile compounds which ultimately reduces NO_x emissions by approximately 15%. Other inorganic elements (Fe, Zn, P, Cr, Zr, and Cd) found in low concentration. The concentration of all other elements found to be less than 0.1%. Zr and Cd showed approximately 0.002% in biomass samples whereas chromium is about 0.01%. James et al. [38] suggested the approach to dividing the fractions of ash to reduce the content of undesirable elements in bottom ash. Similarly, the date palm branches can be divided into parts and process individually before utilisation and can reduce the amount of undesirable elements during combustion or pyrolysis.

3.3.5 ICP-MS analysis

The results obtained from ICP-MS for trace elements is shown in *Figure 3-4* in percentage, to compare the values with XRF. It is clear from the *Figure 3-4* that L contains highest amount of trace elements than all other parts except Ca, Cr and K. The major elements found in leaf ribs is Si (3.6%), K (1.16%) and Ca (1.007%) while others are less than one percent Fe (0.071%), Zn (0.02%), Zr (0.002%), arsenic (As) (0.000372%), Cr (0.000568%) and lead (Pb) (0.000562%). K (1.17%) and Cr (0.0006%) was found highest in LB and Ca (1.07%) was highest in MB. On the other hand, SB contains a minimum percentage of Ca, Cr, Fe, Pb, Zn, and Zr while LB exhibited the lowest concentration of As and Si with zero concentration of Zn and Zr in LB.

Heavy metals emission into the atmosphere exceeding certain limits leads to serious health and environmental concerns. *Table 3-4* presents the limits for four of the trace elements generally found in biomass, and these limits are defined by (ISO-17225-1, 2014; 2, 2014; 3, 2014; 4, 2014; 5, 2014; 6, 2014 and 7, 2014) [38-44] standards. Chromium (Cr) and Lead (Pb) both are within the permissible limits for all the samples. Zinc (Zn) in sample L is double than the described limit in *Table 3-4*. However, SB, MB, and LB contain negligible concentration. Arsenic (As) showed a higher percentage than the allowed limit in L, SB, and MB while slightly less than the acceptable limit in LB. Thus, biomass pre-treatment is essential according to its source before utilising in potential applications particularly in the boilers and combustion chambers where sufficient gas cleaning and control is not available.

In short, L showed a higher percentage of As and Zn whereas Cr and Pb were within permissible limits presented in EN ISO 17225:2014. SB and MB both showed a higher percentage of As in their samples, however, Cr, Pb, and Zn were found to be inadmissible limits. Moreover, LB was found to be within acceptable limits for all of the four elements

making it more favourable to use in energy production application without any significant pre-treatment. Biomass pretreatment is required for arsenic reduction in L, SB, and MB and zinc in L.

Zinc and lead are volatile heavy metals which upon combustion vaporize and convert to fine particles which are usually found in fly ash while others move towards bottom ash and char [46]. Biomass uptake different heavy metals from the soil during its lifetime while some of the biomass is being used particularly for this purpose, for instance, in the phytoremediation process. Liu et al. [47] showed that fast pyrolysis technology could cope with heavy metals contamination of biomass which also resulted in improved heating values. The generated metal-rich char was suggested to use as a fuel for fast pyrolysis process without volatilisation of Cu metal. ICP-MS values showed a substantial difference with XRF values. It is quite evident by comparison of ICP-MS data that elements detection in biomass via XRF technology have considerable limitation and can only be used as an indication.

Table 3-4 Permissible limits for trace elements in biomass defined in Standard ISO 17225

Heavy metals	Unit	Wood pellets		Wood briquettes and chips	Fruit biomass
		Commercial and residential	Industrial use		
As	(mg/kg)	≤1	≤2	≤1	Pellets and Briquettes ≤1
Cr	(mg/kg)	≤10	≤15	≤10	≤50
Pb	(mg/kg)	≤10	≤20	≤10	≤10
Zn	(mg/kg)	≤100	≤200	≤100	≤100

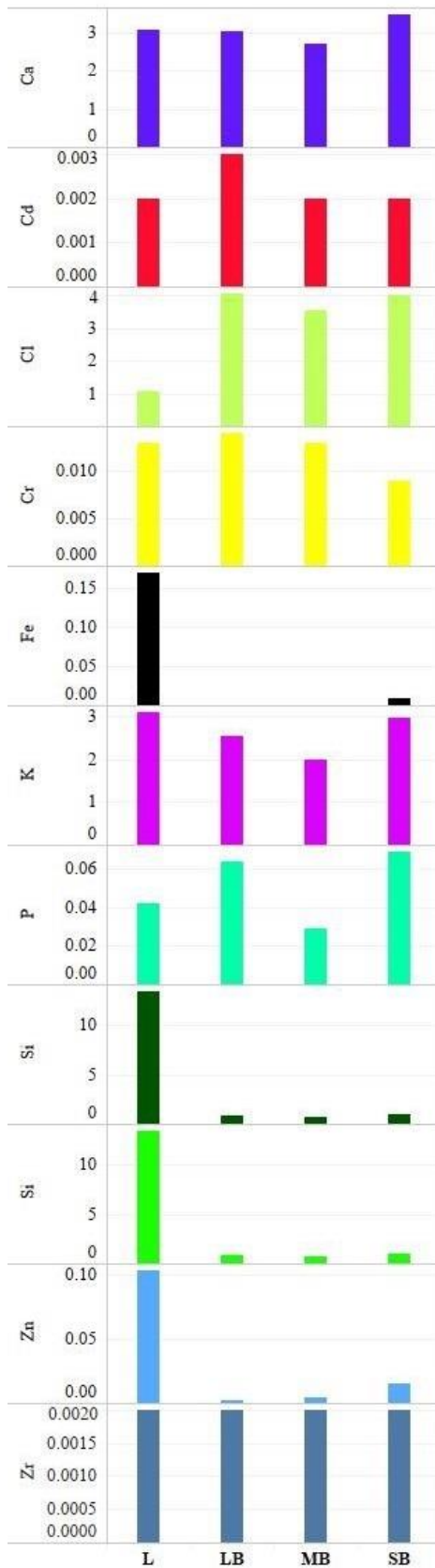


Figure 3-3 Inorganic elements in biomass by XRF analysis in percentage

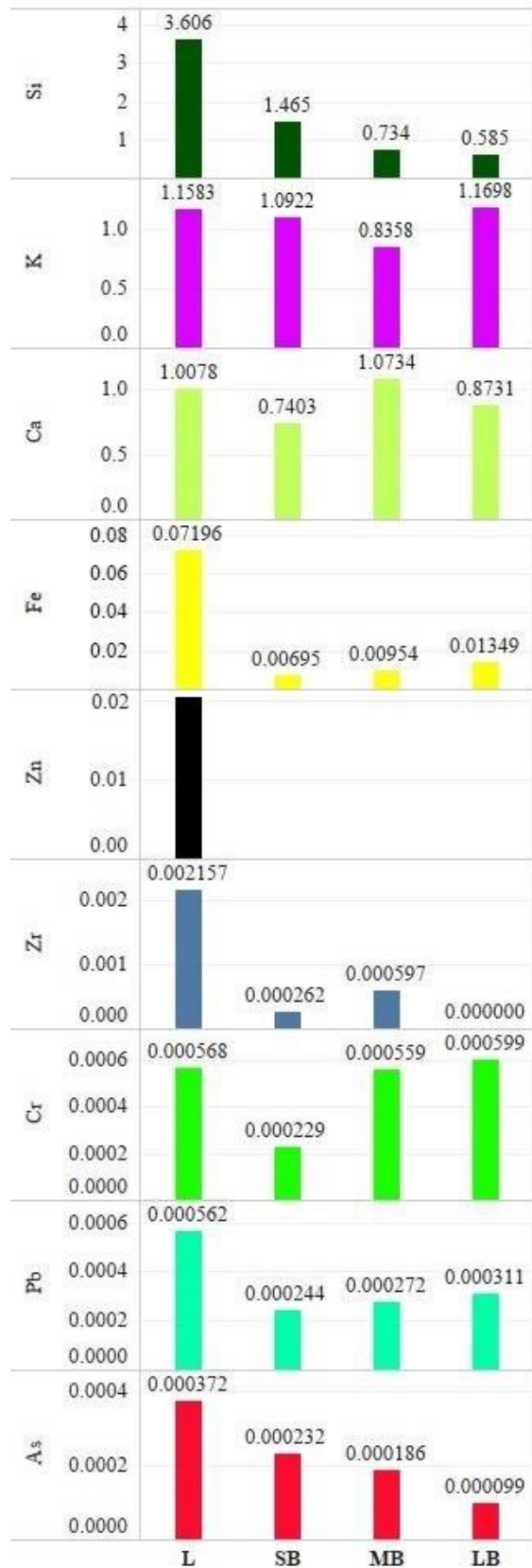


Figure 3-4 ICP-MS analysis of biomass for inorganic elements in percentage

3.3.6 Heating values and Exergy

The heating values of biomass are fundamental in selecting the biomass for energy generation and evaluating its potential for economic viability. *Figure 3-5* shows a trend of HHV, LHV, and Exergy of biomass in four samples. Specific chemical exergy in *Figure 3-5* is calculated using Eq. (3-12). Exergy of organic constituents is nearly equal to specific exergy of fuels due to the negligible value of exergy by inorganic constituents [27]. Highest HHV values were observed in L (18.47 MJ/kg), containing approximately 1.5 MJ/kg and 1.3 MJ/kg higher than LB and MB respectively. Estimation of exergy of biomass samples corresponds to HHV and LHV where highest value existed in L (20.9 MJ/kg) and lowest in LB (19.3 MJ/kg). SB value showed a second maximum energy level with less than 1 (MJ/kg) difference than L.

Zhang et al. [48] exergy correlations were also used to determine exergy values by HHV and LHV to observe the trend of specific chemical exergy and exergy calculated through HHV and LHV. Exergy values showed parallel behaviour with all three correlations in *Figure 3-6*. Although there is no significant difference among the values of Ex_{HHV} , Ex_{LHV} and Ex_s , however, specific chemical Exergy (Ex_s) showed a close pattern to Ex_{LHV} than Ex_{HHV} . The average difference between Ex_{LHV} and Ex_s lies below 0.5 MJ/kg.

$$Ex_{HHV} = 1.1721Ex_s - 3971 \dots \dots \dots (3-15)$$

$$Ex_{LHV} = 1.1318Ex_s - 3008 \dots \dots \dots (3-16)$$

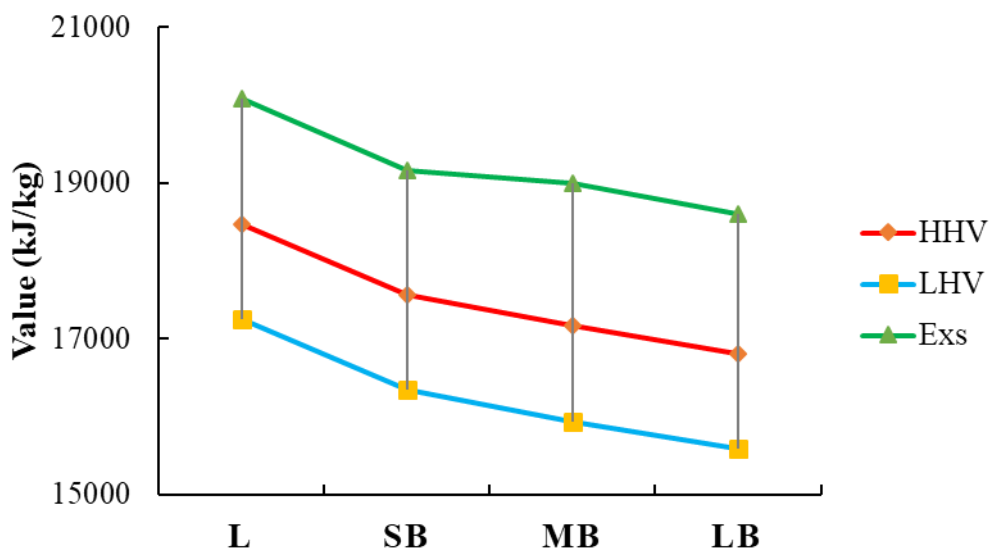


Figure 3-5 Heating values and exergy values of biomass samples

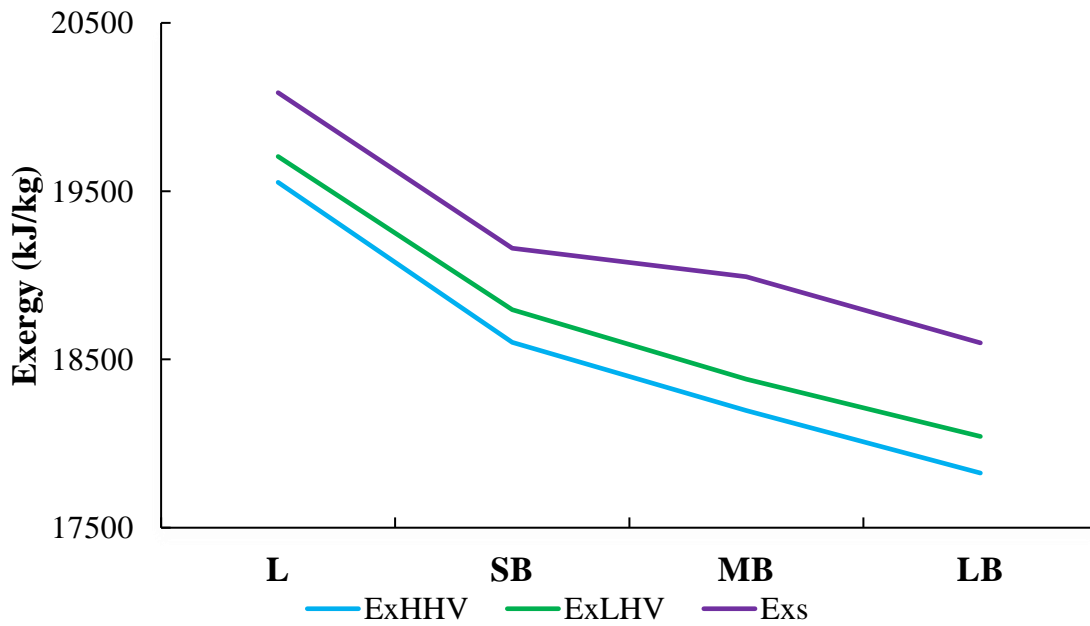


Figure 3-6 Trend of Exs, ExHHV, ExLHV values of date palm branches. (Exs — Specific chemical exergy, ExHHV and ExLHV Exergy on the basis of HHV and LHV)

3.3.7 Error analysis

Average experimental error (AEE), average bias error (ABE) and R^2 values of different correlations for estimating HHV values against measured values of date palm biomass are shown in Table 3-5. It is important to note that among the selected correlations, least AEE, ABE errors are found in Eq. (3-9) considering the stoichiometric ratio is the main parameter for estimation of HHV values with errors less than $\pm 2\%$ and R^2 value of more than 0.98 is showing a straight line correlation between measured and estimated values. While the highest AEE and ABE showed by Eq. (3-8) 10.57% and -10.57% respectively with the lowest R^2 value. Non-Linear correlation proposed by Nhuchhen and Abdul Salam, [24] also showed greater than 5% AEE value with less than 5% ABE with R^2 value 0.51. Overall Eq. (3-6), (3-7), (3-9) and (3-10) showed within $\pm 5\%$ limit for both AEE and ABE whereas Eq. (3-8) and (11) showed higher than $\pm 5\%$ error which is found to be the least suitable correlations for estimating the HHV of date palm biomass. Thus, the most suitable equation to calculate the higher heating value for date palm biomass is equation (3-9) using the stoichiometric ratio as the main tool.

Table 3-5 Correlations against their errors and R^2 values (AEE = average experimental error, ABE = Average bias error)

Eq. No.	Sources	Correlations	AEE (%)	ABE (%)	R^2
3-6	[21]	$HHV = 0.3491 \times C + 1.1783 \times H$ $+ 0.1005 \times S - 0.1034 \times O$ $- 0.015 \times N - 0.0211 \times Ash$	4.14	4.14	0.993
3-7	[22]	$HHV = -1.3675 + 0.3137 \times C + 0.7009 \times H$ $+ 0.0318 \times O^+$	4.50	4.50	0.821
3-8	[23]	$HHV = 0.3536 \times FC + 0.1559 \times VM$ $- 0.0078 \times Ash$	10.5	-10.57	0.328
3-9	[25]	$HHV = \frac{\text{Stoichiometric Ratio}}{0.31}$	1.18	-0.8	0.986
3-10	[24]	$HHV = 19.2880 - 0.2135 \times \left(\frac{VM}{FC}\right)$ $+ 0.0234 \times \left(\frac{FC}{Ash}\right)$ $- 1.9584 \times \left(\frac{Ash}{VM}\right)$	3.22	1.38	0.537
3-11	[24]	$HHV = 20.7999 - 0.3214 \times \left(\frac{VM}{FC}\right)$ $+ 0.0051 \times \left(\frac{VM}{FC}\right)^2$ $- 11.2277 \times \left(\frac{Ash}{VM}\right)$ $+ 4.4953 \times \left(\frac{Ash}{VM}\right)^2$ $- 0.7223 \times \left(\frac{Ash}{VM}\right)^3$ $+ 0.0383 \times \left(\frac{Ash}{VM}\right)^4$ $+ 0.0076 \times \left(\frac{FC}{Ash}\right)$	5.45	3.00	0.51

3.3.8 FTIR analysis

The FTIR spectra of the biomass samples can be referred to in *Appendices A.1*. All four parts showed peaks at similar positions on X-axis wavenumbers (cm^{-1}). Different transmittance was observed explaining the presence of functional groups at different intensities. For instance, broad peaks were observed at 3325 cm^{-1} for all the samples, showing the —OH stretching vibrations. However, MB showed high-intensity peak than other samples. There are wide range of peaks observed from $700\text{--}4000 \text{ cm}^{-1}$ including at 3325 cm^{-1} , 2916 cm^{-1} , 2848 cm^{-1} , 1716 cm^{-1} , 1622 cm^{-1} , 1506 cm^{-1} , 1456 cm^{-1} , 1238 cm^{-1} and 1031 cm^{-1} . The prominent peaks at 2916 and 2848 cm^{-1} signal the presence of alkanes (C—H) and carboxylic acid which also coincides with the peak at 1716 cm^{-1} showing the carbonyl C=O stretching of esters and ketones. This stretching is due to the hemicellulose presence in biomass. The peaks at 1622 and 1506 cm^{-1} indicating the presence of aromatic rings due to benzene C—C ring stretch which is assigned due to lignin existence in the samples. The C—H aliphatic stretching was observed at 1456 cm^{-1} . The high-intensity peaks were observed in the fingerprint region at 1031 cm^{-1} which are due to C—O—C stretch. Moreover, LB and MB showed a sharp peak in this zone than other parts of the branch.

3.3.9 XRD analysis

The XRD spectra for the crystallinity of biomass is shown in *A.2 (Appendices)*, in which SB has shown the higher peaks at 22° followed by MB, LB and L. However, LB exhibited maximum crystallinity (38%) followed by L (36%), SB (35%) and MB (34%) presented in *A.3 (Appendices)*. High crystallinity values may be allocated to difficult decomposition than relative biomass upon thermochemical treatment. It can be seen from XRD spectra that secondary peaks at 16° have different diffraction peaks with LB showing the broader peak while L has a least broad peak. The broad diffraction peak may be attributed to disorder increase between the crystallographic planes [49]. The position of secondary peaks was found to be at 15.84° , 15.88° , 15.76° and 15.64° for LB, MB, SB, and L respectively. Generally the crystallinity of biomass directly related to cellulose content and complex bonding among cellulose, hemicellulose, and lignin, therefore, a more detailed chemical interpretation is generally required to authenticate the XRD results [50]. Although XRD contains some level of uncertainty for biomass interpretation, however, this can give a reasonable comparison among different biomass types.

3.3.10 TGA analysis

Biomass composed of carbohydrate polymers (cellulose and hemicellulose), aromatic polymers (lignin) and some inorganic elements which show different degradation patterns and results in different reactions upon pyrolysis. Polymer compositions in biomass exist in wide percentages according to its source usually in the range of cellulose (40-50%), hemicellulose (25-35%) and lignin (10-40%) [51]. This also results in different decomposition patterns. Cellulose, hemicellulose, and lignin decomposition occur around 240-350 °C, 180-260 °C and 280-500 °C respectively which yields anhydrocellulose and levoglucosan from cellulose, acetic acid and galactoglucomannan from hemicellulose and phenols from lignin pyrolysis [52].

The thermogravimetric analysis (TGA) and derivative thermogravimetric analysis (DTG) curves for date palm biomass pyrolysis according to its divided parts (L, SB, MB, LB) at different heating rates 10 °C/min, 20 °C/min and 50 °C/min are presented in *Figures 3-7 and 3-8*. DTG showed the rate of decomposition of biomass and TGA showed the percentage of weight loss between temperature range (30-800 °C). A comprehensive comparison can be seen for the degradation pattern of all the parts with increasing heating rates. The drying of the biomass occurs around 100 °C for 10 °C/min and 20 °C/min heating rates and 120 °C for 50 °C/min due to rapid heating and less time available to dry the material. The loss of mass at this stage also varies significantly with SB (7.28%), MB (6.83%) and LB (5.81%) showed the least mass loss at 50 °C/min. However, L (4.53%) showed the least mass loss at 20 °C/min during drying of the biomass. The highest mass loss was observed for MB (7.9%) and LB (7.19%) at 20 °C/min while L (6.43%) showed at 50 °C/min and SB (8.65%) at 10 °C/min. At 400 °C, most of the samples lost their weight more than 60% except L at 10 °C/min which lost nearly 56 % of the weight.

As shown in *Figure 3-7*, highest char content was observed at 50 °C/min for SB, MB, and LB while L showed highest char content at 10 °C/min which is the highest in all of the samples at all heating rates. L also exhibited the highest tendency to produce high char content on average than all the samples at all heating rates. Average char content in L and SB during pyrolysis corresponds to the values of proximate analysis given in *Figure 3-2* combining both fixed carbon and ash content. Whereas, MB and LB have considerably higher char content in pyrolysis conditions as compared to proximate values with an increase of 8% and 5% respectively.

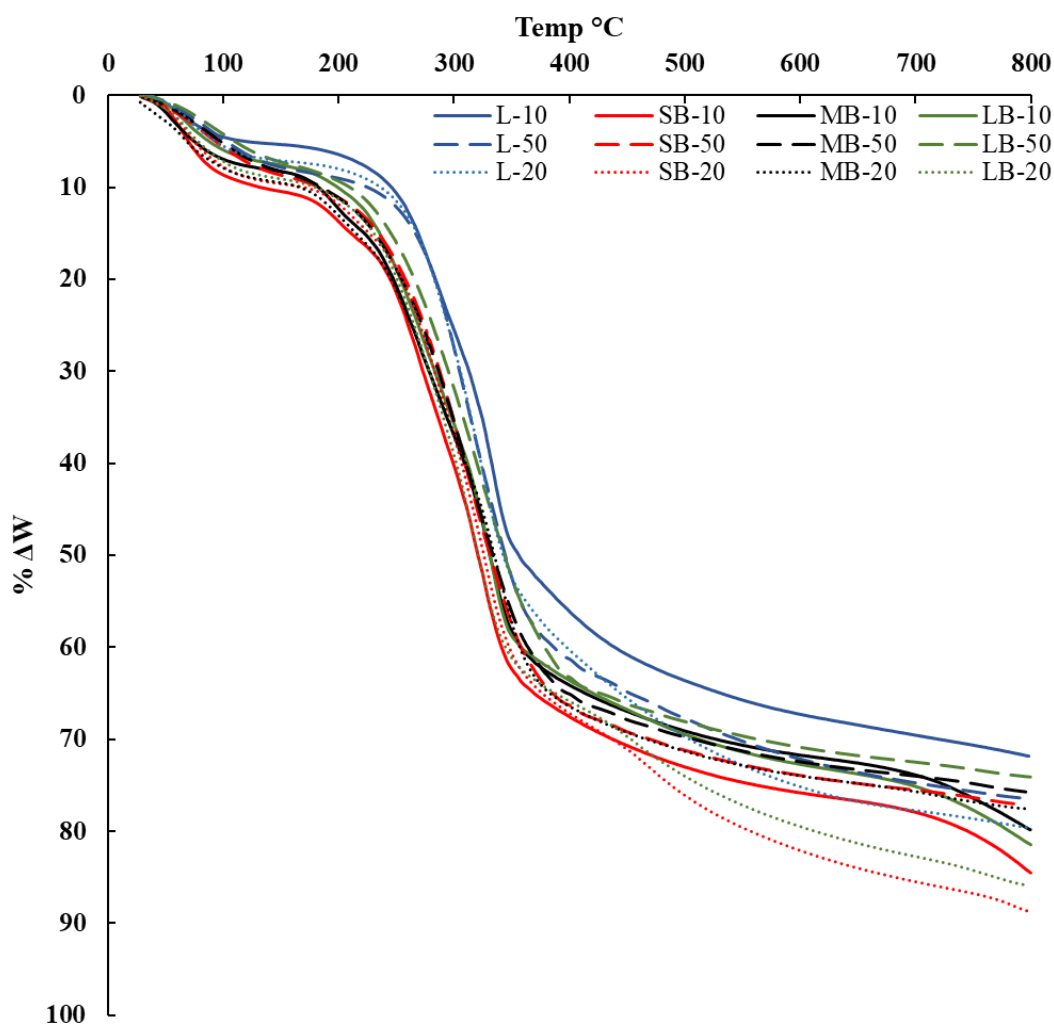


Figure 3-7 Pyrolysis profiles of biomass samples at 10 °C/min, 20 °C/min, and 50 °C/min heating rates

DTG curves in Figure 3-8 provided the extensive data for the rate of devolatilization during the thermal analysis and showed the effect of different heating rates during pyrolysis. 50 °C/min showed single stage decomposition between 200-400 °C for all the samples, however, 20 °C/min and 10 °C/min showed more than one stage of decomposition between 150-400 °C. SB and MB presented three stages of decomposition at 10 °C/min and 20 °C/min and L and LB displayed two stages of decomposition. SB and MB showed the first peak around 200 °C, the second peak around 270 °C during devolatilization and largest peaks between 320-340 °C at 10 °C/min and 20 °C/min heating rate. However, L and LB showed the first peak during devolatilization around 280 °C and second largest peak at 335 °C for 10 °C/min and around 320 °C for 20 °C/min. Biomass at 50 °C/min reached the single largest peaks at slightly less

temperature ranging between 310-325 °C during devolatilization. The secondary devolatilization was highest for both heating rates of 10 °C/min and 20 °C/min.

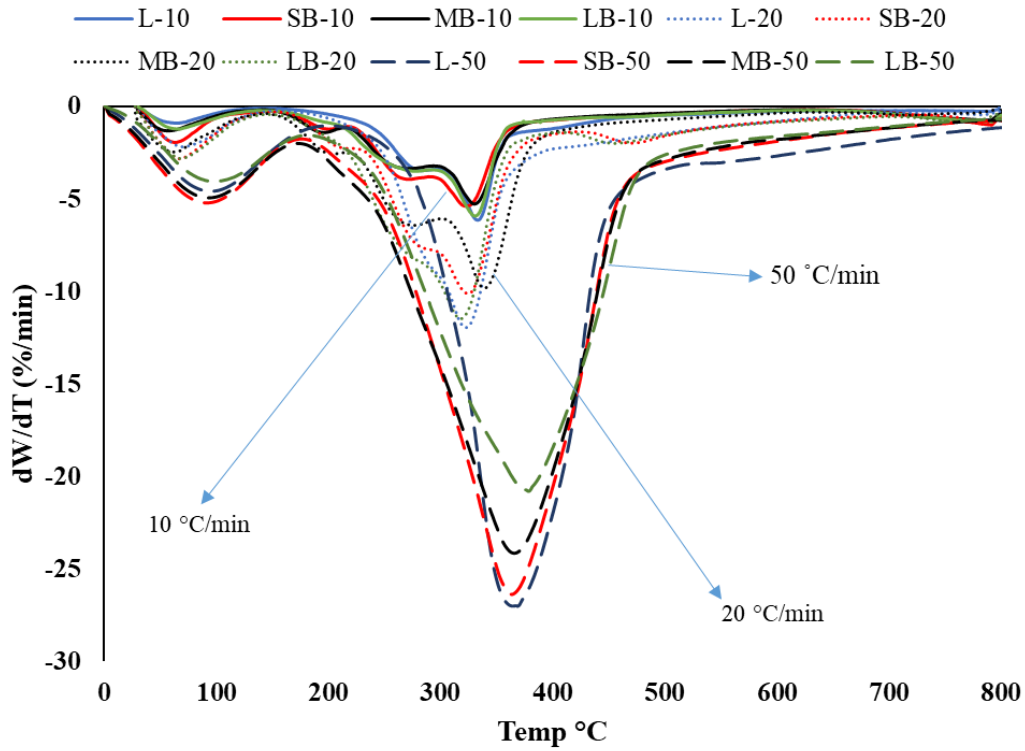


Figure 3-8 DTG curves of biomass samples at 10 °C/min, 20 °C/min, and 50 °C/min heating rates

3.4 Conclusive remarks

The following conclusions can be drawn through detailed characterisation:

- LB holds the ability to retain the moisture content for a longer duration as compared to rest of samples which, however, contains the highest crystallinity followed by L, SB, and MB.
- The highest ash content was exhibited by L which is approximately double the rest of the branch, which also contains the highest HHV values than the rest of the parts.
- Arsenic was found to be higher than the permissible limit in L, SB, and MB and Zinc only in L with no heavy metals above the permissible limit in LB.
- LB can also be used in technologies which require no drying of biomass for instance in hydrothermal treatment technologies.
- The increase in heating rate determines the rapid devolatilization and changes from two-stage devolatilization to single stage devolatilization which also increases char production.

It can be concluded that LB can be used directly for energy generation after sun drying. However, the other parts need to be treated for heavy metals reduction (water and acid washing) or can be pre-treated via torrefaction to produce the biofuel which can later be used with coal for energy generation.

3.5 References

- [1] A. Akhtar, V. Krepl, T. Ivanova, A Combined Overview of Combustion, Pyrolysis, and Gasification of Biomass, *Energy & Fuels*. 32 (2018) 7294–7318. doi:10.1021/acs.energyfuels.8b01678.
- [2] P. McKendry, Energy production from biomass (part 1): overview of biomass, *Bioresour. Technol.* 83 (2002) 37–46. doi:10.1016/S0960-8524(01)00118-3.
- [3] D.F. Dominković, I. Bačeković, B. Čosić, G. Krajačić, T. Pukšec, N. Duić, N. Markovska, Zero carbon energy system of South East Europe in 2050, *Appl. Energy*. 184 (2016) 1517–1528. doi:10.1016/j.apenergy.2016.03.046.
- [4] A. Al-Abbad, M. Al-Jamal, Z. Al-Elaiw, F. Al-Shreed, H. Belaifa, A study on the economic feasibility of date palm cultivation in the Al-Hassa Oasis of Saudi Arabia, *J. Dev. Agric. Econ.* 3 (2011) 463–468. <http://www.academicjournals.org/JDAE>.
- [5] FAO STAT, Food Agric. Organ. United Nations (Statistics Div. (2014). http://faostat3.fao.org/browse/P/*/E (accessed June 1, 2016).
- [6] M. Mallaki, R. Fatehi, Design of a biomass power plant for burning date palm waste to cogenerate electricity and distilled water, *Renew. Energy*. 63 (2014) 286–291. doi:10.1016/j.renene.2013.09.036.
- [7] B. Agoudjil, A. Benchabane, A. Boudenne, L. Ibos, M. Fois, Renewable materials to reduce building heat loss: Characterization of date palm wood, *Energy Build.* 43 (2011) 491–497. doi:10.1016/j.enbuild.2010.10.014.
- [8] R.S. Al-Juruf, F.A. Ahmed, I.A. Alam, H.H. Abdel-Rahman, Development of Heat Insulating Materials Using Date Palm Leaves, *J. Build. Phys.* 11 (1988) 158–164. doi:10.1177/109719638801100304.
- [9] R. Briones, L. Serrano, R. Ben Younes, I. Mondragon, J. Labidi, Polyol production by chemical modification of date seeds, *Ind. Crops Prod.* 34 (2011) 1035–1040. doi:10.1016/j.indcrop.2011.03.012.
- [10] F.A. Lattieff, A study of biogas production from date palm fruit wastes, *J. Clean. Prod.* 139 (2016) 1191–1195. doi:10.1016/j.jclepro.2016.08.139.
- [11] M.H. Abd-Alla, A.-W. Elsadek El-Enany, Production of acetone-butanol-ethanol from spoilage date palm (*Phoenix dactylifera* L.) fruits by mixed culture of *Clostridium acetobutylicum* and *Bacillus subtilis*, *Biomass and Bioenergy*. 42 (2012) 172–178. doi:10.1016/j.biombioe.2012.03.006.
- [12] C. Fang, J.E. Schmidt, I. Cybulska, G.P. Brudecki, C.G. Frankær, M.H. Thomsen, Hydrothermal pretreatment of date palm (*Phoenix dactylifera* L.) leaflets and rachis to

- enhance enzymatic digestibility and bioethanol potential, *Biomed Res. Int.* 2015 (2015). doi:10.1155/2015/216454.
- [13] R. Nasser, M. Salem, S. Hiziroglu, H. Al-Mefarrej, A. Mohareb, M. Alam, I. Aref, Chemical Analysis of Different Parts of Date Palm (*Phoenix dactylifera* L.) Using Ultimate, Proximate and Thermo-Gravimetric Techniques for Energy Production, *Energies*. 9 (2016) 374. doi:10.3390/en9050374.
- [14] EN BS 14780, Solid biofuels — Sample preparation, Br. Stand. Publ. (2011).
- [15] EN ISO 18134-2, Solid biofuels — Determination of moisture content — Oven dry method Part 2 : Total moisture — Simplified method, BSI Stand. Publ. (2015).
- [16] EN ISO 18122, Solid biofuels — Determination of the Ash Content, Br. Stand. Publ. (2015).
- [17] EN ISO 18123, Solid biofuels — Determination of the content of volatile matter, BSI Stand. Publ. (2015).
- [18] BS EN 16948, Solid biofuels — Determination of total content of carbon, hydrogen and nitrogen, BSI Stand. Publ. (2015).
- [19] BS EN 16994, Solid biofuels — Determination of total content of sulfur and chlorine, Br. Stand. Publ. (2015). doi:BS EN 15104:2011.
- [20] EN BS 14918, Solid biofuels — Determination of calorific value, Br. Stand. Publ. (2009).
- [21] S.A. Channiwala, P.P. Parikh, A unified correlation for estimating HHV of solid, liquid and gaseous fuels, *Fuel*. 81 (2002) 1051–1063. doi:10.1016/S0016-2361(01)00131-4.
- [22] C. Sheng, J.L.T. Azevedo, Estimating the higher heating value of biomass fuels from basic analysis data, *Biomass and Bioenergy*. 28 (2005) 499–507. doi:10.1016/j.biombioe.2004.11.008.
- [23] J. Parikh, S. Channiwala, G. Ghosal, A correlation for calculating HHV from proximate analysis of solid fuels, *Fuel*. 84 (2005) 487–494. doi:10.1016/j.fuel.2004.10.010.
- [24] D.R. Nhuchhen, P. Abdul Salam, Estimation of higher heating value of biomass from proximate analysis: A new approach, *Fuel*. 99 (2012) 55–63. doi:10.1016/j.fuel.2012.04.015.
- [25] X. Zhu, R. Venderbosch, A correlation between stoichiometrical ratio of fuel and its higher heating value, *Fuel*. 84 (2005) 1007–1010. doi:10.1016/j.fuel.2004.12.002.
- [26] T. Gundersen, An introduction to the concept of exergy and energy quality, *Nor. Univ. Sci. Technol.* (2011) 1–26. <http://www.ivt.ntnu.no/ept/fag/tep4115/innhold/Exergy>

Light Version 4.pdf.

- [27] G. Song, J. Xiao, H. Zhao, L. Shen, A unified correlation for estimating specific chemical exergy of solid and liquid fuels, *Energy*. 40 (2012) 164–173. doi:10.1016/j.energy.2012.02.016.
- [28] T.M. Runge, C. Zhang, J. Mueller, P. Wipperfurth, *Economic and Environmental Impact of Biomass Types for Bioenergy Power Plants*, 2013.
- [29] B.. Jenkins, L.. Baxter, T.. Miles, T.. Miles, Combustion properties of biomass, *Fuel Process. Technol.* 54 (1998) 17–46. doi:10.1016/S0378-3820(97)00059-3.
- [30] T.J. Morgan, A. George, A.K. Boulamanti, P. Álvarez, I. Adanouj, C. Dean, S. V. Vassilev, D. Baxter, L.K. Andersen, Quantitative X-ray Fluorescence Analysis of Biomass (Switchgrass, Corn Stover, Eucalyptus, Beech, and Pine Wood) with a Typical Commercial Multi-Element Method on a WD-XRF Spectrometer, *Energy & Fuels*. 29 (2015) 1669–1685. doi:10.1021/ef502380x.
- [31] M. Thyrel, *Spectroscopic Characterization of Lignocellulosic Biomass*, 2014. http://pub.epsilon.slu.se/11652/1/thyrel_m_141117.pdf.
- [32] W. Wang, X. Liu, Y. Zheng, Quantitative chemical composition determination and thermal analysis for typical biomass ashes in China, *Asia-Pacific J. Chem. Eng.* 9 (2014) 751–758. doi:10.1002/apj.1821.
- [33] M. Ohman, C. Gilbe, I. Nystrom, H. Hedman, D. Boström, C. Boman, R. Backman, Slag Formation During Combustion of Biomass Fuels with Low Phosphorus Content, 19th Eur. Biomass Conf. Exhib. (2011) 1267–1270. doi:10.5071/19thEUBCE2011-VP2.1.19.
- [34] D.N. Thompson, P.G. Shaw, J.A. Lacey, Post-harvest processing methods for reduction of silica and alkali metals in wheat straw, *Appl. Biochem. Biotechnol.* 105–108 (2003) 205–218. doi:10.1385/ABAB:105:1-3:205.
- [35] T. Lind, J. Hokkinen, J.K. Jokiniemi, S. Saarikoski, R. Hillamo, Electrostatic precipitator collection efficiency and trace element emissions from co-combustion of biomass and recovered fuel in fluidized-bed combustion, *Environ. Sci. Technol.* 37 (2003) 2842–2846. doi:10.1021/es026314z.
- [36] K.O. Davidsson, L.E. Åmand, B.M. Steenari, a. L. Elled, D. Eskilsson, B. Leckner, Countermeasures against alkali-related problems during combustion of biomass in a circulating fluidized bed boiler, *Chem. Eng. Sci.* 63 (2008) 5314–5329. doi:10.1016/j.ces.2008.07.012.
- [37] S. V Pisupati, S. Bhalla, Influence of calcium content of biomass-based materials on simultaneous NO_x and SO₂ reduction., *Environ. Sci. Technol.* 42 (2008) 2509–14.

doi:10.1021/es0719430.

- [38] A.K. James, S.S. Helle, R.W. Thring, G.S. Sarohia, P.M. Rutherford, Characterization of Inorganic Elements in Woody Biomass Bottom Ash from a Fixed-bed Combustion System, a Downdraft Gasifier and a Wood Pellet Burner by Fractionation, *Energy Environ. Res.* 4 (2014) 85–94. doi:10.5539/eer.v4n1p85.
- [39] ISO-17225-1, Solid biofuels - Fuel specifications and classes- Part 1: general requirements, 2014.
- [40] ISO-17225-2, Solid biofuels -- Fuel specifications and classes -- Part 2: Graded wood pellets, 2014.
- [41] ISO-17225-3, Solid biofuels -- Fuel specifications and classes -- Part 3 Graded wood briquettes, 2014.
- [42] ISO-17225-4, Solid biofuels -- Fuel specifications and classes -- Part 4: Graded wood chips, 2014.
- [43] ISO-17225-5, Solid biofuels -- Fuel specifications and classes -- Part 5: Graded firewood, 2014.
- [44] ISO-17225-6, Solid biofuels -- Fuel specifications and classes -- Part 6: Graded non-woody pellets, 2014.
- [45] ISO-17225-7, Solid biofuels -- Fuel specifications and classes -- Part 7: Graded non-woody briquettes, 2014.
- [46] A. Nzihou, B. Stanmore, The fate of heavy metals during combustion and gasification of contaminated biomass-A brief review, *J. Hazard. Mater.* 256–257 (2013) 56–66. doi:10.1016/j.jhazmat.2013.02.050.
- [47] W.J. Liu, K. Tian, H. Jiang, X.S. Zhang, H.S. Ding, H.Q. Yu, Selectively improving the bio-oil quality by catalytic fast pyrolysis of heavy-metal-polluted biomass: Take copper (Cu) as an example, *Environ. Sci. Technol.* 46 (2012) 7849–7856. doi:10.1021/es204681y.
- [48] Y. Zhang, X. Gao, B. Li, H. Zhang, B. Qi, Y. Wu, An expeditious methodology for estimating the exergy of woody biomass by means of heating values, *Fuel.* 159 (2015) 712–719. doi:10.1016/j.fuel.2015.06.102.
- [49] X. Yuan, Y. Duan, L. He, S. Singh, B. Simmons, G. Cheng, Characterization of white poplar and eucalyptus after ionic liquid pretreatment as a function of biomass loading using X-ray diffraction and small angle neutron scattering, *Bioresour. Technol.* 232 (2017) 113–118. doi:10.1016/j.biortech.2017.02.014.
- [50] S. Naik, V. V. Goud, P.K. Rout, K. Jacobson, A.K. Dalai, Characterization of Canadian

biomass for alternative renewable biofuel, *Renew. Energy*. 35 (2010) 1624–1631. doi:10.1016/j.renene.2009.08.033.

- [51] W. Jin, K. Singh, J. Zondlo, Pyrolysis Kinetics of Physical Components of Wood and Wood-Polymers Using Isoconversion Method, *Agriculture*. 3 (2013) 12–32. doi:10.3390/agriculture3010012.
- [52] D. Mohan, C.U. Pittman, P.H. Steele, Pyrolysis of wood/biomass for bio-oil: A critical review, *Energy and Fuels*. 20 (2006) 848–889. doi:10.1021/ef0502397.

Slow pyrolysis of date palm and high rate algal pond biomass³

The processing of waste through pyrolysis technology is gaining momentum worldwide and is considered to be a green technology to reduce CO₂ emissions. This chapter is devoted to analysing the lignocellulosic biomass (date palm), and wastewater derived microalgae and the carbon-rich char produced between temperature range (400-600 °C) from these biomass types. The properties of microalgae char showed significant variation with date palm char exhibited high heating values (24-28 MJ/kg), low ash content (11-16%) and high energy yield (48-42%). Algal biomass char showed considerably high nitrogen content (6-7%) as compared to date palm char (<1%), lower stability, and more significant influence on the price with respect to treatment temperature. Quaternary, pyrrolic, and pyridinic nitrogen species were found on the surface of the microalgae char, whereas no nitrogen species detected on date palm char due to low nitrogen content. The activation energy was also noted to be high for algal char during pyrolysis and combustion process. It can be concluded that date palm char is suitable for energy applications, whereas, algal char can be used for soil amendment, wastewater treatment and applications requiring nitrogen doped char.

³ This chapter is extracted from the accepted article “Akhtar, A., Jiříček, I., Ivanova, T., Mehrabadi, A., Krepl, V., 2019. Carbon conversion and stabilisation of date palm and high rate algal pond (microalgae) biomass through slow pyrolysis. *Int. J. Energy Res.* <https://doi.org/10.1002/er.4565>” with permission from John Wiley & Sons, Ltd.

First author is the major contributor of the article and is responsible for data gathering, analysis, writing and publishing in article format.

4.1 Introduction

Waste production and utilisation are being considered as a circular economy throughout the world where waste produced from different sources are desired to go through the 3R process (reduce, reuse and recycle). Although all the efforts on a government and private sector are being made at the forefront of the green economy throughout the European Union. However, advance research is being conducted to investigate materials which are not only useful to cope with the demand for desired raw material but also can contribute to other applications. Waste from lignocellulosic biomass is considered to one of the products in this area derived from different industries including agricultural farms, dairy farms and forestry residues. Another heavily studied area in this scenario is the use of microalgae in wastewater treatment processes which are not only growing rapidly but also provide a raw material which can later be utilised in energy plants or for biochemical production.

Microalgae in wastewater treatment plants are an interesting option which utilises solar energy for photosynthesis and produces biomass rapidly [1]. The pollutant removal can be efficiently completed in wastewater without expensive treatment technologies. The number of pollutants can be removed such as nutrients, pathogens and heavy metals through the uptake of the nutrients, raising pH and dissolved oxygen and acting as an effective biosorbent respectively [2]. Phong Vo et al. [3] presented a comprehensive overview of the pollutant removal through microalgae photobioreactors. Flat plate photobioreactors contain the potential to produce the highest biomass yield than the rest of them, and a wide range of contaminants could be treated including heavy metals and pharmaceutical and personal care products.

The biomass production through high rate algal ponds can be utilised through several technologies to produce biogas [4], bio-oil [5] and biochar (char) [6,7]. The production of bio-oil is usually accomplished through the hydrothermal liquefaction [8], and fast pyrolysis [9]. Similarly, biochar production requires hydrothermal carbonisation [10] and slow pyrolysis [11]. The utilisation of microalgae often requires pre-treatment to acquire the desired product with high efficiency. The treatment of microalgae can easily be divided into mechanical and non-mechanical methods such as ultrasonication, microwave, through acid and alkali treatment and osmotic shocks [12,13] etc. Cell wall rupture is the main concern during pre-treatment and microwave pre-treatment was found to be most effective and economical, however, barriers in the commercial application are still unknown [13].

Pyrolysis is the process to convert the waste into environment-friendly products in the absence of oxygen and heating the biomass at elevated temperature in the range of 300-700 °C [14]. The heating rate determines the yield of bio-oil, char and syngas production. The slow pyrolysis yields the high amount of char which can, in turn, be useful for soil amendment application [15]. Char has found to contain the significant potential for carbon storage and sequestration while adding net negative carbon into the environment. Woolf et al. [16] estimated the sequestration of carbon up to 130 Gigatons throughout a century. The primary use of char in that scenario was soil amendment and crop cultivation. Biochar supports the soil amendment by increasing the stable carbon content [17]. It is likely that char employment in different applications will lead to high carbon sequestration and the availability of raw materials. Char yielding bio-refineries has the potential to significantly contribute to carbon storage in the form of char for hundreds of years [18].

Bio-refineries can act as the next generation of energy generation hubs while producing by-products which can be utilised in a range of applications. The generation of employment and added economic value could further add the positive aspect [19]. The working bio-refineries by lignocellulosic biomass are presently accounts to 40 across Europe [20]. The location of the biorefineries and supply of the feedstock is one of the prominent factors that can be crucial for determining the net carbon emissions. Other factors such as the utilisation of type of waste which does not affect the animal feed and other applications must be considered. This will bring the pressure significantly on the growth of third-generation feedstock that can further be converted into useful products [21].

Char can be produced from lignocellulosic biomass waste generated from different sources including agricultural waste [22], garden waste [23] and forest waste [24]. Date palm is one of the examples in this scenario which generates millions of tonnes of waste annually. This waste can be converted to char through pyrolysis and can act as a carbon sequestration potential. Several studies recently have shown an optimistic trend of char production from date palm waste, for instance, Ahmad et al. [25] showed that silica composited char produced at 400 °C had the carbon sequestration potential up to 95% and observed an increment in recalcitrant potential due to lower thermal degradability. At another instant, recalcitrant carbon increased with the increase in pyrolysis temperature. Higher temperature leads to the increasing potential of carbon sequestration [26]. Hadoun et al. [27] reported the high surface area for date stem derived char 1455 m²/g produced at 550 °C through phosphoric acid activation.

Char produced from organic waste can be used in several applications such as wastewater treatment processes [28]. Hence the char derived from wastewater algae can also later be used for the treatment of wastewater. Char contains the possibility to use in other applications such as indirect carbon fuel cells [29], char recycled aggregate concrete [30], and as a bio-modifier in asphalt [31]. The versatility of the properties according to the feedstock and treatment conditions makes the char a suitable material and found recognition in several applications. Microalgae biomass produced from high rate algal ponds contains the significant edge having the ability to replenish feedstock rapidly for biorefineries while providing valuable by-products [6].

Microalgal char also found positive results in different applications. Placido et al. [32] reported the production of carbon dots from microalgal char which acts as a heavy metals ion sensor. The detection limit for Pb^{2+} , Cu^{2+} , and Ni^{2+} was in the range of 0.01-0.1 μM . The mechanism described is reversible and purely collisional with some fluorophores less accessible than others. Similarly, char derived from *Chlorella sp.* exhibited high adsorption capacity for p-nitrophenols than powdered activated carbon. The adsorption capacity was nearly 140% higher than activated carbon showing its potential in water treatment processes [28]. At another instant, the microalgal char immobilised complex was used from *Chlorella sp.* for the adsorption of Cd (II) heavy metal. Char immobilised complex (biomass to char ratio 2:3) found to contain superior adsorption capacity at 217.41 mg/g than the individual use of microalgae (169.9 mg/g) and char (95.8 mg/g) [33].

Char properties derived from organic waste can be altered either through operating conditions during pyrolysis or post-processing techniques such as physical and chemical activation. Char properties vary heavily with the peak treatment temperature, for instance, carbon content, surface area, morphology and stability [34]. The required application of a resultant product defines the optimum treatment conditions. There is a significant number of studies proving the use of microalgae for bio-oil and biodiesel production, however, little attention is being paid towards sole char yielding bio-refineries. The main objective of the study is to provide a guideline towards the utilisation of these different types of biomass in bio-refineries at a single point via different treatment temperatures. The overall scenario, in this case, is presented first time from chemical to thermal perspectives, their nitrogen-containing species, functional groups presence and their ability to incorporate in coal co-combustion boilers in case of co-generation application. The relative assessment of these both biomass types brings the aspect

of a detailed comparison of lignocellulosic and microalgal biomass for char production and subsequent product characteristics.

4.2 Experimental section

4.2.1 Biomass feedstock

Date palm from lignocellulosic biomass and wastewater derived microalgae from third generation feedstock were chosen to determine their individual effects in bio-refineries incorporation designed for slow pyrolysis technology. Date palm biomass (branches) (DB) and wastewater derived microalgae (WMA) was first dried and cut into small size (≤ 5 mm) prior to pyrolysis in a fixed bed reactor. Wastewater derived microalgae contained a mixture of species investigated through microscope including *Mucidosphaerium pulchellum*, *Coleastrum sp.*, *Diatom sp.* and *Actinustrum sp.* [6]. The feedstock was characterised through elemental analysis (CHNSO), Energy yield, Fourier Transform Infrared Spectroscopy, and thermogravimetric analysis. The description of each of the techniques can be seen below. Further comprehensive biomass properties can also be referred at Abbas et al. [6] and Akhtar et al. [35].

4.2.2 Char preparation

Each of the feedstock was pyrolysed at different highest treatment temperatures (HTT) including 400, 500 and 600 °C at a residence time of 20 minutes and a heating rate of 15 °C/min in nitrogen atmosphere. To ensure the continuity of the results, only one analysis of the feedstock was pyrolysed at a particular HTT per day to leave enough time for a reactor to cool down before starting another experiment. The weight of the samples was 10 grams for each testing. After the desired residence time, the reactor cooled down to room temperature, and the char yield was calculated on the basis of biomass weight.

4.2.3 Char characterisation

The obtained char was characterised through elemental analysis (CHNSO) using Elementar Vario EL Cube instrument. The obtained elemental composition later used to draw Van Krevelen diagram to understand the aromaticity and degradation pattern of char. Van Krevelen diagram was prepared using H/C and O/C atomic ratios to determine the aromaticity, degradation and half-life of the char samples concerning its feedstock. BET surface area was measured using the Coulter SA 3100 instrument. This instrument works on the principle of nitrogen adsorption at a temperature of 77 K. The degassing of the samples were done at 150 °C for 240 minutes under high vacuum. The energy content of the samples was measured using

the instrument (Adiabatic Isoperibolic Calorimeter, IKA®-Werke, Staufen, Germany Model C5000). Theoretical higher heating value determined from the equation 3-6.

Fourier Transform Infrared Spectroscopy was employed to determine the surface functional groups of the char and the feedstock. The spectra were collected between 400 cm⁻¹ to 4000 cm⁻¹ range and spectral resolution of 4 cm⁻¹. X-ray photoelectron spectroscopy (XPS) of the char samples were conducted by ESCA Probe P instrument for determining the atomic weight of each of the elements and nitrogen species on the surface of the char. Thermogravimetric – differential scanning calorimetric analysis (TGA-DSC) was conducted for char samples in air and nitrogen atmosphere with the help of simultaneous DSC-TGA analyser (SDT Q 600, TA Instruments, USA). Before conducting the experiment, char samples were processed to small size passing through the sieve of 125 µm. Samples weight were kept constant at 5 mg during each testing session. After adding samples into a heating chamber at room temperature, the chamber started heating at 10 °C/min. Air and Nitrogen atmospheres were utilised at 100 ml/min flow rate to understand the combustion and pyrolysis effect for the considered samples. Combustion of the organic matter described through TGA according to their devolatilization patterns such as ignition temperature (T_i), maximum weight loss rate temperature (T_{max}) and burnout temperature (T_b). Intersection method and conversion method was used to determine the ignition temperature and burnout temperature respectively as recommended by Lu et al. [36]. However, the burnout temperature according to the mass stabilisation method was also determined as explained by Muthuraman et al. [37] to compare the values between the two methods.

4.2.4 Kinetics modelling

Kinetics of the biomass can be described by the Arrhenius kinetic model through the following equations:

$$k(T) = Ae^{(-\frac{E}{RT})} \dots\dots\dots (4-1)$$

$$\frac{d\alpha}{dt} = Ae^{(-\frac{E}{RT})} (1 - \alpha)^n \dots\dots\dots (4-2)$$

$$\alpha = \frac{\omega_{\phi} - \omega}{\omega_{\phi} - \omega_f} \dots\dots\dots (4-3)$$

R is the gas constant (8.34 Jk⁻¹mol⁻¹), T is the absolute temperature (K), and E is the activation energy (kJmol⁻¹), n is the order of reaction, A is the pre-exponential factor (s⁻¹), and α is the conversion rate.

After rearranging and integration method (Coats – Redfern method) applied, the equation changed into the following form:

$$\ln\left[-\frac{\ln(1-\alpha)}{T^2}\right] = \ln\frac{AR}{\beta E} - \frac{E}{RT} \dots\dots\dots(4-4)$$

β is the heating rate ($^{\circ}\text{Cmin}^{-1}$ or Kmin^{-1})

E is calculated from the slope of the above equation for the overall thermal process.

4.2.5 Economic analysis

Energy economics defines the economic aspect of char gain of energy with the input cost. There is a limited number of studies calculating the economic aspect of the process to produce char [38]. The economic aspect (EV) of the char could be presented by the following equations (4-5 — 4-6):

$$EV = UP \times PR \dots\dots\dots (4-5)$$

$$UP = BPJ \times HHV \dots\dots\dots (4-6)$$

UP and PR is the unit price and production rate of the char, respectively. BPJ and HHV is the char price per megajoule and a higher heating value of the char respectively.

The price of the char could also be calculated from the correlation (4-7) from the economic model presented by [39].

$$UP (\text{\$kg}^{-1}) = 0.002528 \times 16.2 + 0.02678571 \times T \dots\dots\dots (4-7)$$

Where T is HTT in $^{\circ}\text{C}$.

First, the method based on production rate employed to estimate the cost of biochar production. As the char has the potential to be used with coal; hence, a coal-based parameter was used to determine the value of the studied chars regarding its heating value. Then both calculated prices compared with coal to conclude its feasibility.

4.3 Results and Discussion

4.3.1 Char characteristics

The yield of the char was determined through the original mass balance. The highest yield of the char was obtained at 400°C , and the consistent decrease was observed with the increase of HTT (*Table 4-1*). The major decrease was noted to be between 400 and 500°C in which (date

palm char) DB and (Algal char) AB samples showed 6.52% and 11.09% decrease than the rest of the samples. The decrease in yield was minimal between 500 and 600 °C with less than a 2% decrease. Overall, the highest yield was obtained by AB samples. The surface area of the samples showed contrast trend in which DB samples showed a decreasing trend whereas AB samples showed an increasing behaviour. DB-4 showed the highest surface area 2.044 m²/g and lower ash content 11.2% which agrees with the results obtained by Jouiad et al. [40]. They showed 1.99 m²/g at 400 °C. The change in the surface area with the HTT is not significant in DB samples, however, AB samples showed a noticeable increase from 0.45 to 2.55 m²/g at 400 °C and 600 °C respectively. The applications where the high surface area is one of the major requirements such as adsorption [15,41], AB biomass with high HTT is recommended.

Table 4-1 Char characteristics produced from date palm biomass and wastewater derived microalgae

Samples	Mass yield (%)	HHV (MJ/kg)	BET Surface area (m²/g)	Ash (%)	HHV_T (MJ/kg)
DB-4	35.27	24.61	2.044	11.2	23.69
DB-5	28.75	25.75	1.505	12.7	22.82
DB-6	27.17	28.16	1.405	16.5	23.57
AB-4	43.56	23.78	0.454	26.6	17.97
AB-5	32.46	18.74	1.320	34.4	13.58
AB-6	31.38	15.51	2.554	36.5	12.45

HHV_T Theoretical higher heating value

HHV Measured higher heating value

4.3.2 Ultimate analysis

Elemental analysis of the char shows the increase of carbon content in DB samples with the increase of HTT, and in contrast, AB samples found to decrease the carbon content (*Figure 4-1*). Hence, it is showing relatively different elemental composition and characteristics. Carbon sequestration potential is optimum at low temperature in case of microalgae biomass conversion [7]. Similarly, nitrogen and hydrogen showed considerable differences for both feedstock types. Nitrogen concentration in AB char was noticeably high in the range of 6-7% in all samples. The nitrogen and sulphur concentration decreased with an increase in HTT. DB

samples contained a relatively minor concentration of nitrogen and sulphur as compared to AB samples, showing less than 1% in all of the samples.

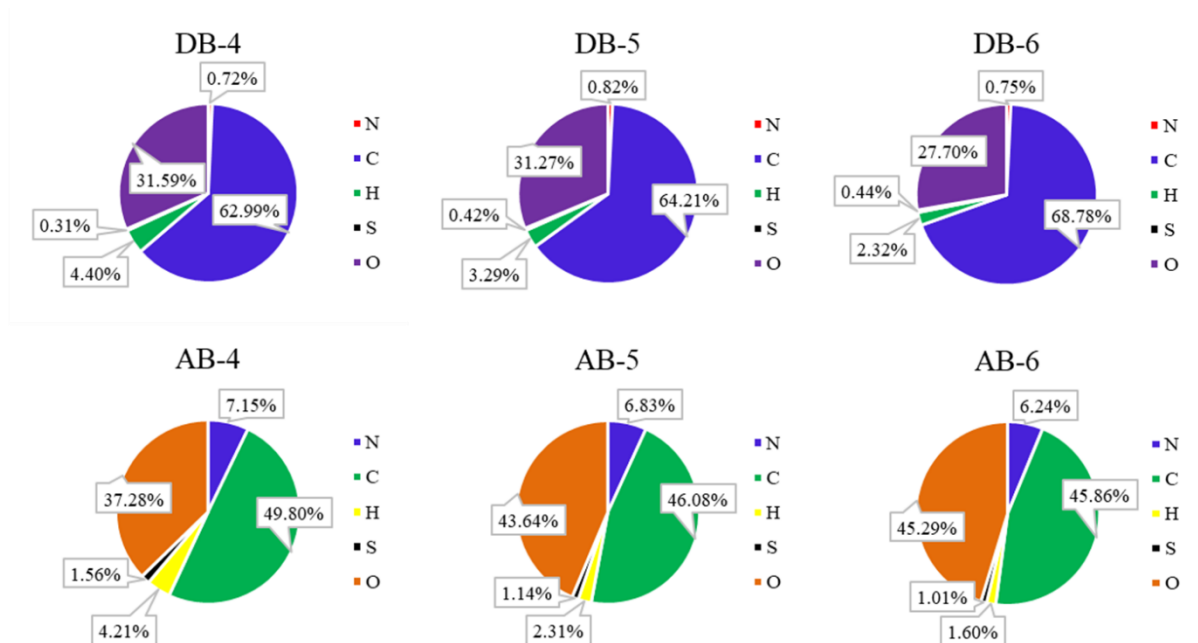


Figure 4-1 Elemental analysis of date palm and wastewater derived microalgae char at 400, 500 and 600 °C

4.3.3 Van Krevelen diagram

Van Krevelen diagram has shown the trends of the char towards the aromaticity and degradation pattern. It is interesting to note that microalgae char increases the O/C ratio with the increase in HTT showing opposite behaviour than lignocellulosic char [42]. The lower ratios of H/C and O/C represents the removal of volatile matter, increase in aromaticity and graphite-like structural arrangement of aromatic rings [43–45]. DB samples showed a consistent decrease of H/C and O/C ratios with the HTT and 600 °C showed the lowest H/C for both feedstock types (Figure 4-2). The major difference lies in the polarity of the char and degradation patterns which might be due to protein and lipids in algae.

4.3.4 Statistical analysis

The Line fit plots of H/C and Mass yield of char is presented in Figure 4-3. The coefficient of determination was moderately high ($R^2 = 0.8$), whereas the R^2 value was closer to 0.9 for polynomial regression analysis. The correlation coefficient between the two variables was also near to 0.9 with p-value 0.016, less than 0.05 showing the significance of the correlation. N/C

and O/C regression analysis also showed similar results, showing a moderately high coefficient of determination ($R^2 = 0.86$) for a linear line fit plot with p-value 0.006 significantly less than 0.05. The power fit line showed slightly higher R^2 value 0.90 and correlation coefficient between N/C and O/C was observed to be 0.93.

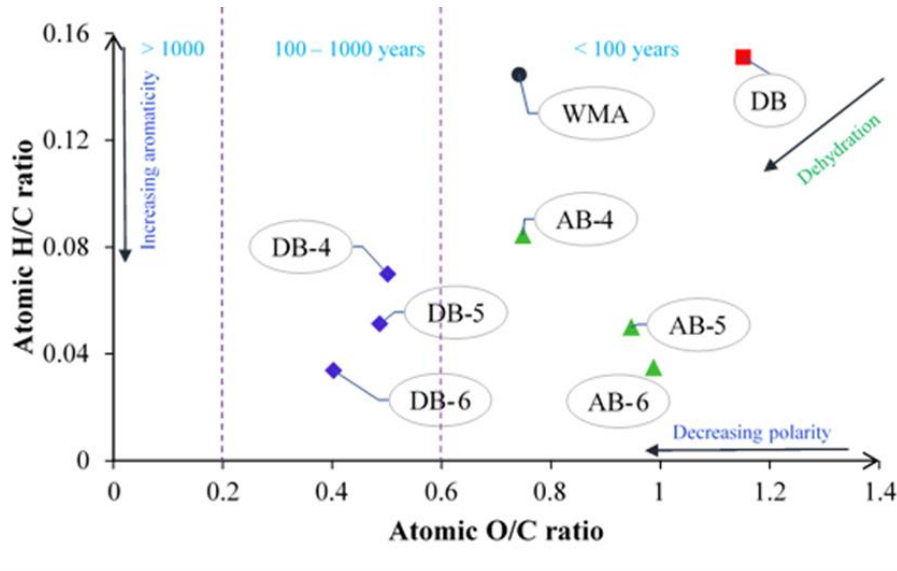


Figure 4-2 Van Krevelen diagram of biomass and char. The dotted line separates the half-life of char in years [18]

4.3.5 Fourier transform infrared spectroscopy

The surface functional groups of individual char were examined by the ATR-FTIR and the spectra obtained can be seen in *Figure 4-4*. Char from both of the feedstock has shown considerably different spectra with peaks of contrast intensities. The effect of HTT can also be visualised easily in which some peaks are sharp when treated at 600 °C which is of lower intensity at a treatment temperature of 400 and 500 °C. Following peaks were observed at 741 cm^{-1} , 871 cm^{-1} , 1039 cm^{-1} , 1402 cm^{-1} , and 1557 cm^{-1} corresponds to aromatic monosubstituted strong C – H bending vibration, alkene strong =C – H bending vibration [46], ethers medium to strong =C – O – C symmetric stretching [47], aromatic ring C = C stretching [47], N – H bending [48] respectively in DB samples. The peaks at 2914 cm^{-1} and 3355 cm^{-1} corresponds to Alkane C – H stretching [49] and alcohol O – H stretching [47] respectively, were visible in DB-4 samples, however, at high treatment temperatures, these peaks disappeared completely.

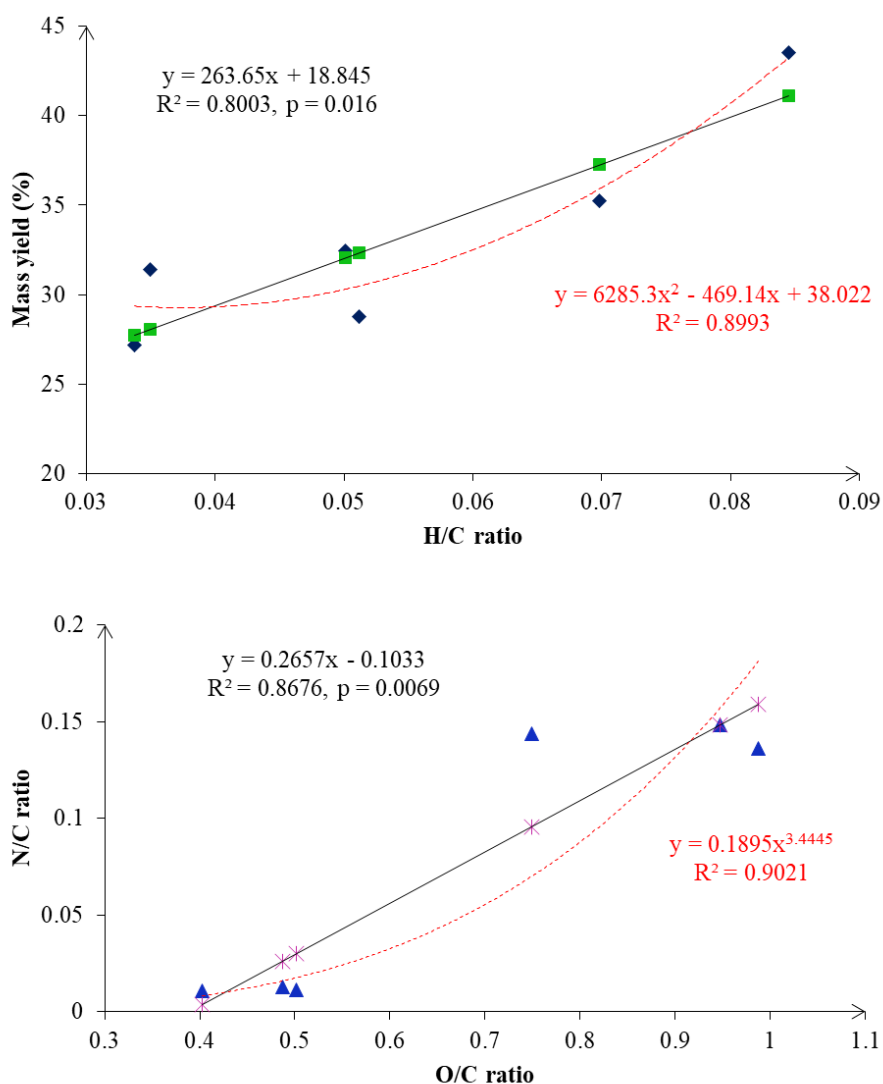


Figure 4-3 Line fit plots and R2 values of H/C ratio and Mass yield, and O/C and N/C ratios

Other peaks also changed their intensities with the treatment temperature such as peak at 871 cm^{-1} in the DB-6 sample is noticeably sharp, however, at lower HTT, this peak is of minor intensity. At another instant, peak at 1402 cm^{-1} and 1559 cm^{-1} was very prominent in DB-6 and DB-4 samples respectively which in other samples are of lower intensity. Similarly, AB char also showed a difference in peak intensities with the change in HTT. The peak at 615 cm^{-1} corresponding to C-N stretch [50] reduced its intensity in AB-6, whereas the peak at 559 cm^{-1} becomes sharp than the rest of the samples. The peak at 1030 cm^{-1} showed the highest intensity in AB samples and change in HTT greatly affected the peak shape. The peak is broad at 400 cm^{-1} and then gradually changes its shape to a sharp peak in AB-6 sample. On the other hand, few peaks disappeared (1372 cm^{-1} , 1430 cm^{-1} , and 2914 cm^{-1}) in AB-6 which can be seen in AB-4 sample. Functional groups define the adsorption of different chemicals and heavy metals

on the char surface, thus, the lower temperature processing can help sustain higher functional groups on char for wastewater treatment and other applications.

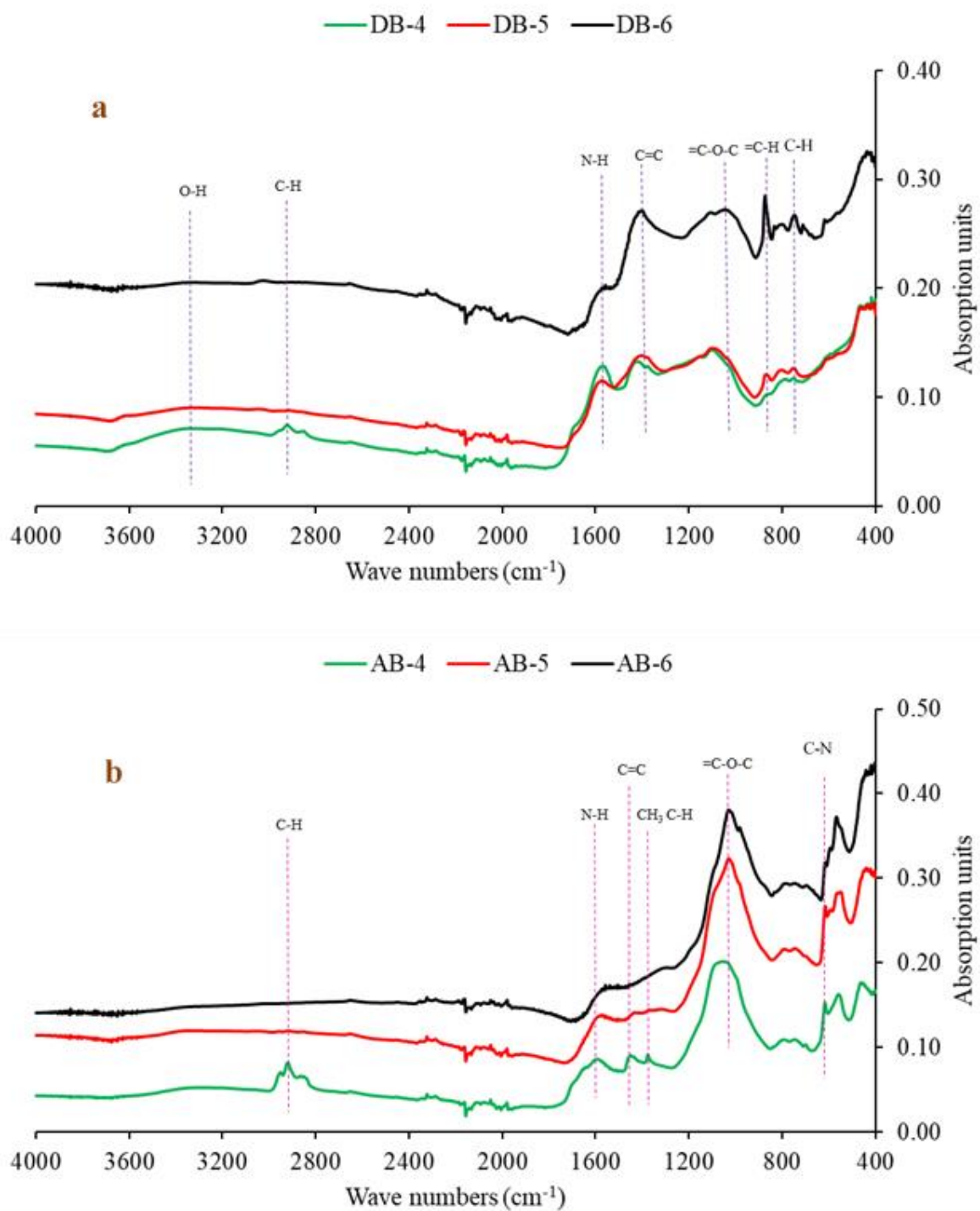
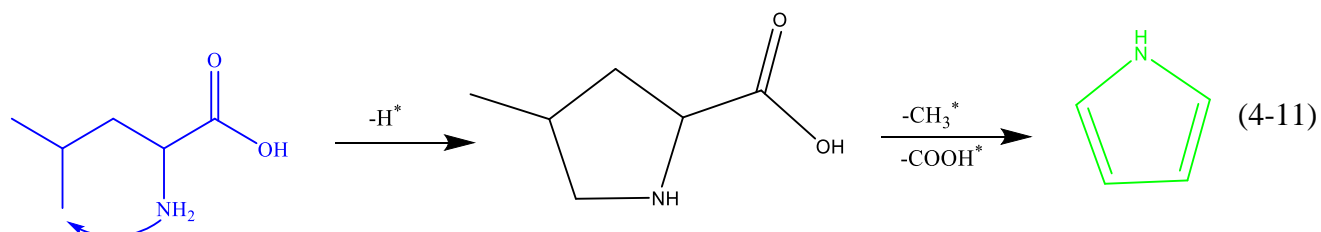
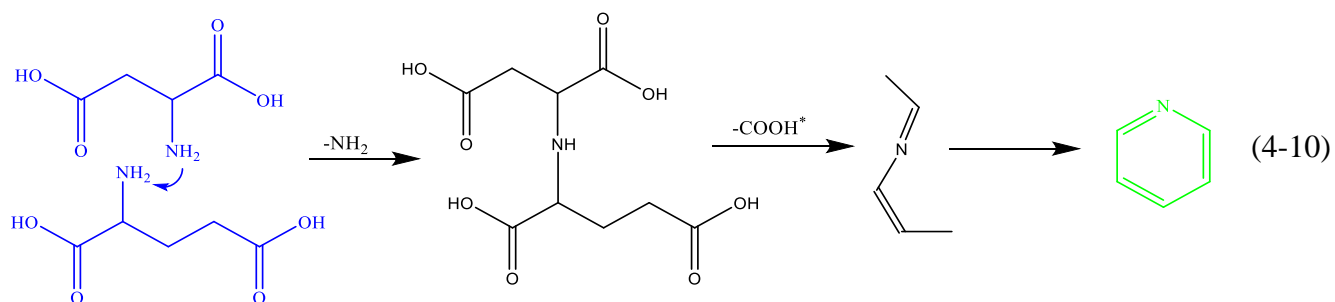
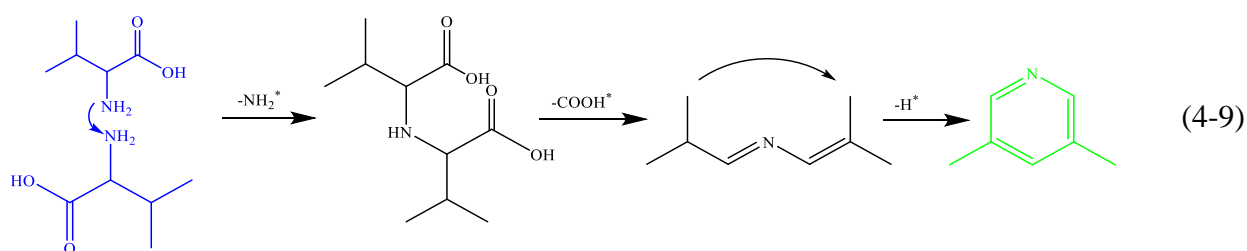
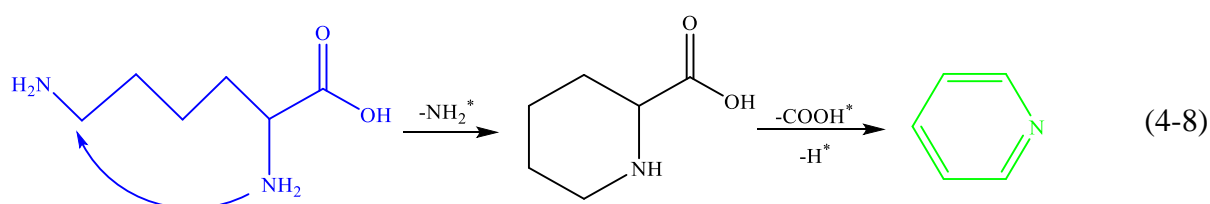


Figure 4-4 FTIR of (a) date palm and (b) microalgae char produced at 400, 500 and 600 °C

4.3.6 X-ray photoelectron spectroscopy

XPS of the char was conducted to determine the surface elemental composition at different HTT produced from both feedstock types. The spectra and surface elemental composition is presented in A.4 & A.5 (Appendices). There could be a clear difference observed in elemental composition with the change in HTT. Nitrogen can only be seen in AB samples and comparatively less oxygen in all of the samples than DB samples. Further analysis of nitrogen species exhibited the presence of pyrrolic, quaternary and pyridinic nitrogen species on the surface of microalgae char (Figure 4-5). Amine-N and Quaternary-N reduced with the increase in treatment temperature.



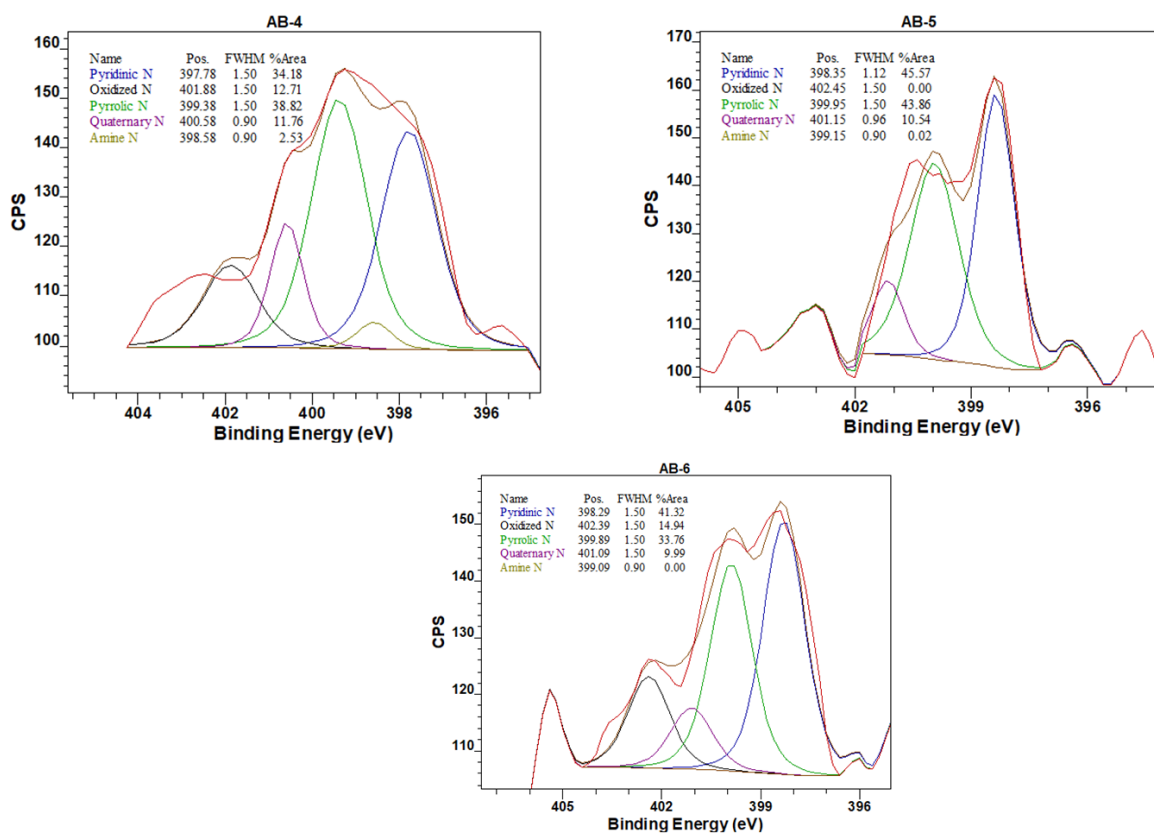
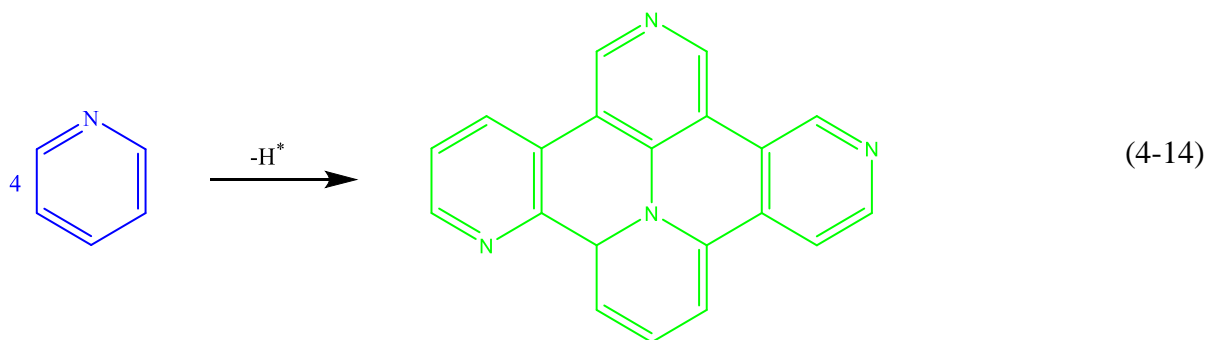
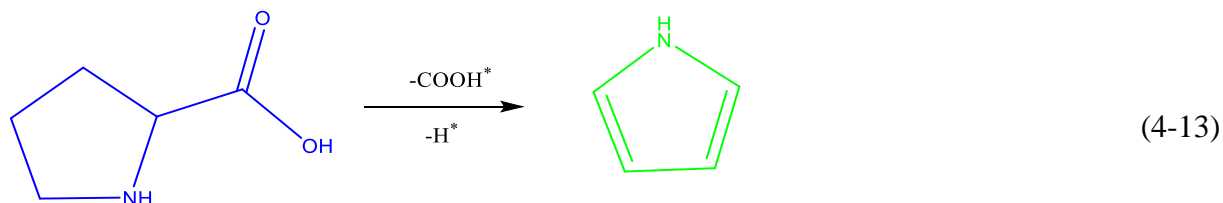
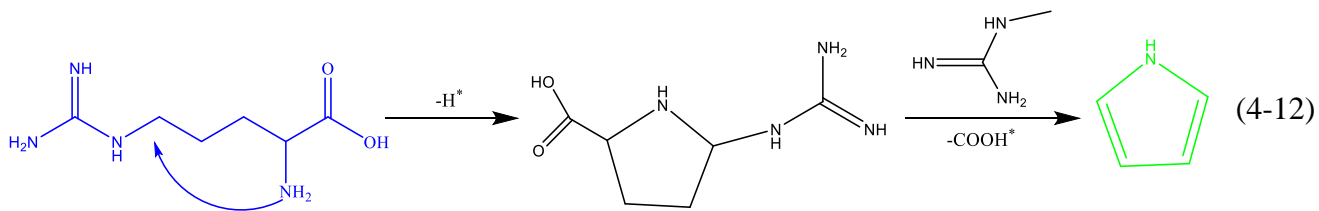


Figure 4-5 Nitrogen species found on the surface of the char through XPS analysis

The reaction pathways of the pyridinic, pyrrolic and quaternary nitrogen species in algae pyrolysis between the temperature range 400 – 600 °C can be presented by the following equations (4-8 — 4-14) [51]. Pyridinic – N and Pyrrolic – N in char are formed through two processes, either direct cyclization of amino acids (proline, arginine, leucine and lysine) [52] or dimerization of amino acids (glutamic acid, aspartic acid and valine) [53].

4.3.7 TGA-DSC analysis

4.3.7.1 Combustion

Thermal analysis of the feedstock and individual char was conducted to present the combustion and pyrolysis behaviour of the samples. First, the TGA-DSC analysis was conducted in an air atmosphere to analyse the combustion pattern of the char (*Figure 4-6*). The degradation of the biomass occurs during different phases of cellulose, hemicellulose and lignin degradation. It can be seen that DB and WMA biomass contained the moisture of approximately 8% and 5% respectively of the total weight of biomass. On the other hand, char contained a relatively low amount of moisture. Overall, biomass lost the high volatile content than their respective chars and produced a lower amount of ash.

DTG curves showed a degradation pattern of both types of feedstock and char, showing the two-stage degradation in all of the samples. Microalgae have shown comparatively very low degradation rate as compared to date palm biomass samples. Both of the biomass showed degradation starting temperature comparatively at a lower range than their chars, depicting the stability of the chars at low-temperature exposure. Char produced at 600 °C showed the highest and single stage degradation occurring mainly around 400 °C. However, the DB-6 showed a sharp peak requiring a low range of temperature for complete degradation whereas AB-6 requires a long range of temperature for complete combustion which agrees with the previous results [54].

Similarly, the ash content of the chars increases with the temperature increase showing the significant change in carbon concentration during pyrolysis of the biomass. Combustion of organic waste mainly derived by the combustion of volatile matter [37] whereas pyrolysed char combustion happens due to the fixed carbon concentration. DSC of the biomass compliments the DTG analysis and have shown similar peaks during the combustion of the biomass and char (*A.6*) (*Appendices*). One peak was observed around 400 °C for DB-6, and AB-6 samples

whereas other samples showed two peaks at a similar temperature corresponding to the DTG curves in DB samples.

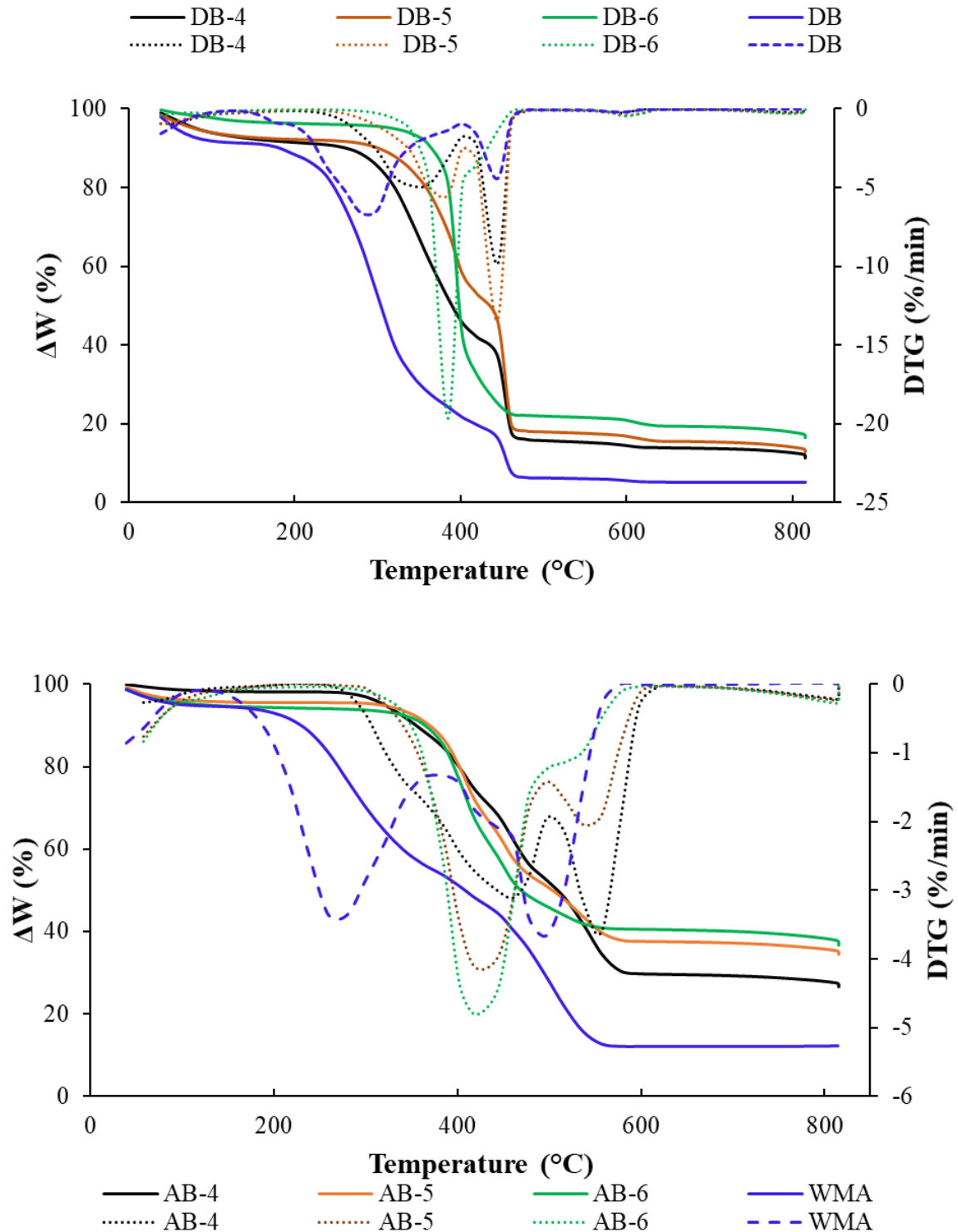


Figure 4-6 Combustion characteristics of date palm and wastewater derived microalgae biomass and their respective chars produced at different temperatures. The dotted line shows the DTG curves of the respective samples.

Combustion parameters of biomass with their respective chars were concluded from the TGA analysis (*Table 4-2*). It can be seen that biomass has shown relatively similar ignition temperatures and substantially increased for pyrolysed char and also increased with the increase of HTT. However, the ignition temperature is relatively less than coal as tested in the literature. Burnout temperature (T_b) was measured through two different approaches. Mass stabilisation method ($T_{b (ms)}$) seems to be closer to the coal burnout temperature mentioned in the literature (*Table 4-2*) than conversion method ($T_{b (cm)}$) for pyrolysed char. Both of the methods were equally suitable for biomass approximation of burnout temperature and resulted in similar values, showing the limitation of utilising these methods only to biomass. However, statistical analysis showed that T_i and $T_{b (cm)}$ have a significantly higher coefficient of determination ($R^2 = 0.89$) as compared to T_i and $T_{b (ms)}$ ($R^2 = 0.184$) for char. This shows that the conversion method seems to be more reliant on determining the ignition temperature of the char with p-value $0.00037 < 0.5$ (*Figure 4-7*).

Table 4-2 Combustion parameters of biomass and their respective chars (1 = [37], 2 = [57])

Samples	T_i (°C)	T_m (°C)	$T_{b (ms)}$ (°C)	$T_{b (cm)}$ (°C)	DTG_m (%/min)	E_a (kJ/mol)	R^2
DB	237	283	557	536	6.58	135.5	0.92
DB-4	298	443	617	757	9.86	123.9	0.87
DB-5	335	443	637	777	13.43	120.6	0.91
DB-6	367	384	637	777	19.64	157.9	0.89
WMA	224	497	557	557	3.66	158.5	0.85
AB-4	352	536	597	797	3.60	171.2	0.90
AB-5	367	404	577	797	4.12	124.3	0.92
AB-6	369	402	557	797	4.82	116.1	0.92
Indian Coal¹	398	452		655	-	-	
Australian Coal¹	416	471		681	-	-	
Indonesian Coal¹	366	418		580	-	-	
Coal A²	466	494		657	-	-	
Coal B²	461	484		692	-	-	
Coal C²	449	460		592	-	-	
Coal D²	385	409		607	-	-	

T_i , T_m , $T_{b (ms)}$, $T_{b (cm)}$, DTG_m and E_a represents the ignition temperature, maximum weight loss rate temperature, burnout temperature (mass stabilisation method), burnout temperature (conversion method), maximum weight loss rate and activation energy.

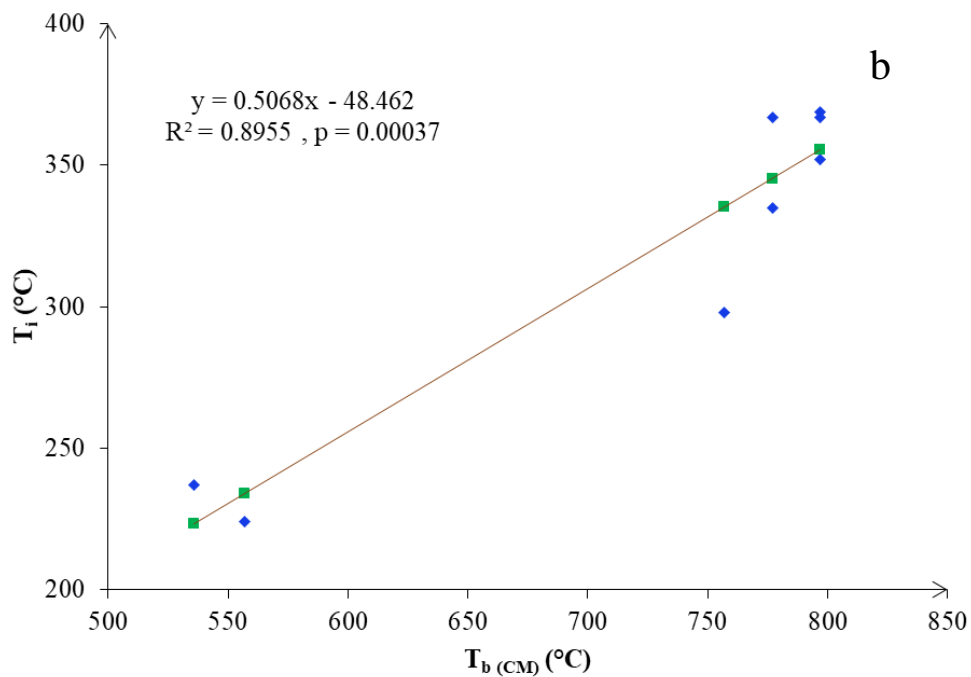
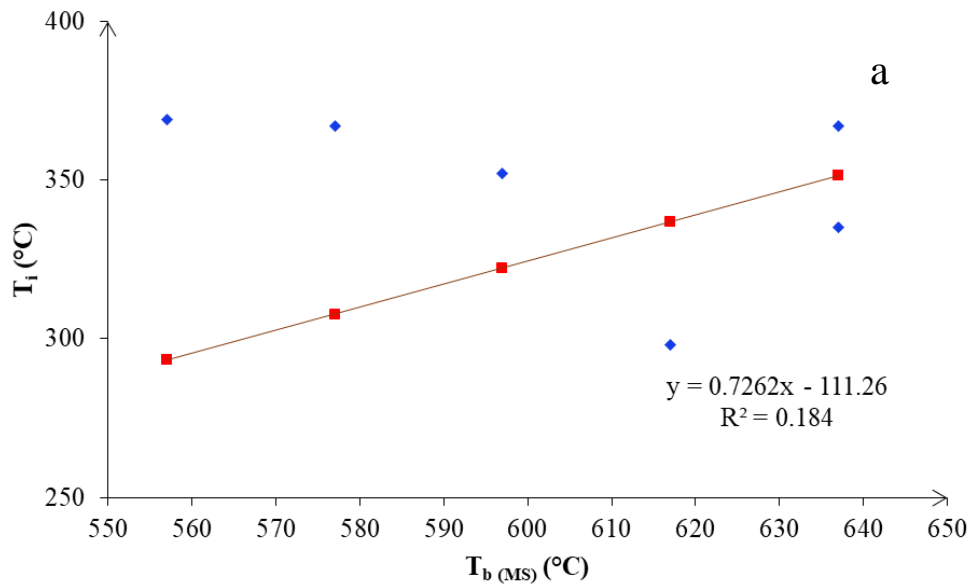


Figure 4-7 Statistical analysis of the ignition temperature and burnout temperature (a) mass stabilization method and (b) conversion method

Kinetics parameters are essential to determine the physical and chemical reaction occurring during the combustion and pyrolysis of the feedstock and chars. The activation energy of the feedstock with their respective chars was calculated to study the possible start of the combustion in each of the samples. The lowest activation energy was exhibited by samples subjected to 500 °C for DB and 600 °C for WMA samples. DB char decreased the activation energy for 400 °C (123 kJ/mol) and 500 °C (120 kJ/mol) as compared to their feedstock,

however, AB chars have found to reduce the activation energy for 500 °C (124 kJ/mol) and 600 °C (116 kJ/mol) (*Table 4-2*). There is a common ground for DB and AB chars in which char produced at 500 °C reduced the activation energy. The degree of conversion shows that chars have a relatively lower temperature range for major degradation during combustion than their biomass (A.7) (*Appendices*).

4.3.7.2 Pyrolysis

Thermal analysis of the biomass and char also conducted in the nitrogen atmosphere, showing the overall degradation patterns up to 1000 °C (*Figure 4-8*). The degradation of the chars has shown substantially lower weight loss as compared to combustion. The consistent decrease in weight loss observed up to 1000 °C than weight stabilisation after 700 °C in the combustion of the samples. Single stage degradation of the samples confirmed during pyrolysis in contrast to two-stage degradation during combustion. Overall mass loss and mass loss rate of DB and AB samples are quite similar to each other. AB-4 and DB-4 samples showed nearly 50% mass loss, and the rest of the samples showed mass loss in the range of 30-40%.

4.3.8 Economic analysis

The economic value of the char was determined by three parameters including HTT, mass yield and heating values (*Table 4-3*). Price determined based on theoretical heating values, and measured heating values show a decreasing trend with the increase in treatment temperature regardless of their heating values. Heating values of DB char are increasing with the HTT whereas decreases with the increase in HTT. This is apparent in both theoretical and measured heating values. This might be due to yield contains the higher influence on determining the price of the product than their heating values and microalgae tend to have higher mass yields than date palm biomass. Hence, lower heating values do not increase the price of char.

Price variation was also calculated based on treatment temperature (HTT) parameter and found that price was lowest at 500 °C treatment temperature for both biomass types. DB samples showed relatively lower prices than AB samples. This can be concluded that treatment temperature and feedstock types are the major influencers in determining the price of the char than their heating values. Energy yield also showed a similar trend in which DB char showed the high energy yield and AB char showed the low energy yield.

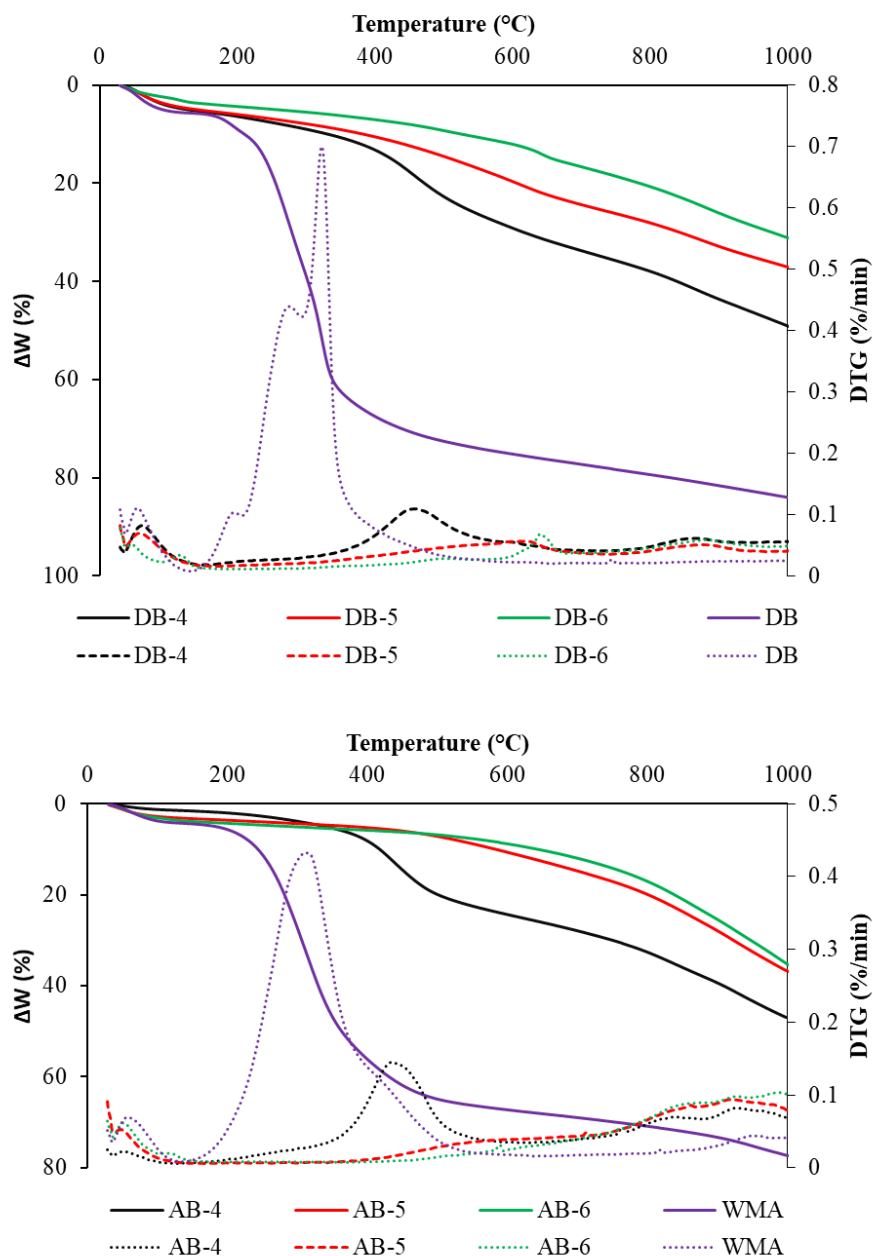


Figure 4-8 Pyrolysis curves of the biomass and char, Dotted lines shows the DTG curves of the respective samples

Treatment temperature 400 °C showed the optimum energy yield for both types of biomass, resulting in approximately 48.22% and 46.76% for DB-4 and AB-4 samples respectively. AB-5 and AB-6 samples reduced the energy yield drastically up to 27 and 21% respectively. The mean value of \$0.02 kg⁻¹ showed substantially less value of forest-based feedstock \$0.092 kg⁻¹ and average price of char \$0.0748 kg⁻¹ for slow pyrolysis according to the developed model [39]. The actual price variation will depend on the end-use of the product in a different scenario. The battery electrode material grade will substantially contain more value and so thus required energy to treat the waste at high temperatures (>1000 °C). The application requiring post-

treatment in terms of activation [55] and magnetic biochar composites [56] production will subsequently raise the price of the char.

Table 4-3 Energy yield and economic value of the char

Samples	Energy Yield (%)	Price (HTT) (\$/kg)	Price (HHV) (\$/kg)	Price (HHV_T) (\$/kg)
DB-4	48.22	0.024	0.022	0.021
DB-5	41.12	0.022	0.018	0.016
DB-6	42.51	0.022	0.019	0.015
AB-4	46.77	0.029	0.026	0.025
AB-5	27.46	0.024	0.015	0.018
AB-6	21.97	0.025	0.012	0.018

The effect of O/C, N/C and chlorine content on the energy recovery was analysed by regression analysis (*Figure 4-9*). The highest coefficient of determination ($R^2 = 0.989$) was found between O/C and energy recovery and lowest between N/C and energy recovery ($R^2 = 0.828$). The p-value of all three variables is less than 0.05 showing the significance of the correlations. All the correlations showed a negative slope, recommending the decrease in energy recovery with the increase in each of the values.

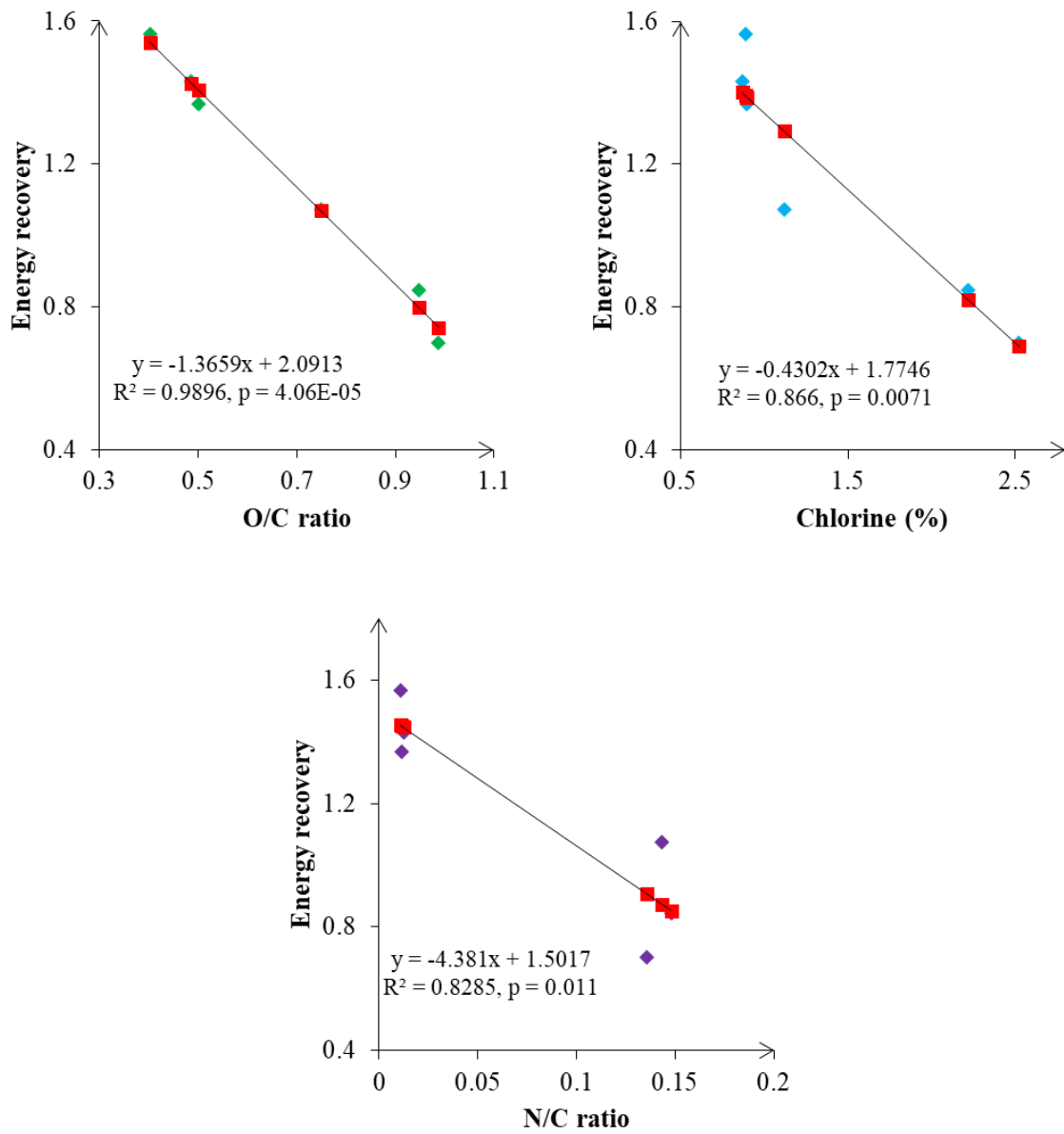


Figure 4-9 Effect of N/C, O/C atomic ratios and chlorine on the energy recovery of the char

4.4 Conclusive remarks

Slow pyrolysis of the date palm branches (DB) and wastewater derived microalgae (WMA) was conducted in the temperature range (HTT) of 400-600 °C. Mass yield decreased, however, ash content increased with the increase in HTT. AB char showed higher mass yield and ash content and reduced the heating values as compared to DB samples. On the other hand, DB chars showed higher stability than AB chars. Combustion of both types of the char samples found to degrade through a two-stage devolatilization process whereas pyrolysis showed one stage devolatilization. DB samples produced at 400 and 500 °C and, AB samples produced at 500 and 600 °C showed lower activation energy during combustion than their feedstock. Amine-N and Quaternary-N species tend to reduce with the increase in treatment temperature in AB samples.

Energy yield and economic costs were found to be lower for AB char than DB samples, particularly at high temperatures. Concisely, we can conclude that AB char holds significantly different properties than DB char. Algal char is recommended for soil amendment, and wastewater treatment and date palm derived char is suitable for energy applications in cogeneration plants. Further research in the area of oxidative pyrolysis and combined pyrolysis of wastewater sludge and microalgae is recommended. The combined processing of both biomass types from similar source might help in the reduction of processing steps and can generate the char of improved quality for multiple applications. Catalytic pyrolysis of microalgae and date palm biomass with an activating agent such as CO₂ might bring properties of high surface area and functional groups enhancement at lower temperature processing.

4.5 References

- [1] N. Abdel-Raouf, A.A. Al-Homaidan, I.B.M. Ibraheem, Microalgae and wastewater treatment, *Saudi J. Biol. Sci.* 19 (2012) 257–275. doi:10.1016/j.sjbs.2012.04.005.
- [2] C. Alcántara, E. Posadas, B. Guieysse, R. Muñoz, Microalgae-based Wastewater Treatment, *Handb. Mar. Microalgae Biotechnol. Adv.* (2015) 439–455. doi:10.1016/B978-0-12-800776-1.00029-7.
- [3] H.N.P. Vo, H.H. Ngo, W. Guo, T.M.H. Nguyen, Y. Liu, Y. Liu, D.D. Nguyen, S.W. Chang, A critical review on designs and applications of microalgae-based photobioreactors for pollutants treatment, *Sci. Total Environ.* 651 (2019) 1549–1568. doi:10.1016/j.scitotenv.2018.09.282.
- [4] R. Gutiérrez, F. Passos, I. Ferrer, E. Uggetti, J. García, Harvesting microalgae from wastewater treatment systems with natural flocculants: Effect on biomass settling and biogas production, *Algal Res.* 9 (2015) 204–211. doi:10.1016/j.algal.2015.03.010.
- [5] A. Mehrabadi, R. Craggs, M.M. Farid, Wastewater treatment high rate algal ponds (WWT HRAP) for low-cost biofuel production, *Bioresour. Technol.* 184 (2015) 202–214. doi:10.1016/j.biortech.2014.11.004.
- [6] A. Mehrabadi, R. Craggs, M.M. Farid, Pyrolysis of wastewater treatment high rate algal pond (WWT HRAP) biomass, *Algal Res.* 24 (2017) 509–519. doi:10.1016/j.algal.2016.08.007.
- [7] K. Chaiwong, T. Kiatsiriroat, N. Vorayos, C. Thararax, Study of bio-oil and bio-char production from algae by slow pyrolysis, *Biomass and Bioenergy.* 56 (2013) 600–606. doi:10.1016/j.biombioe.2013.05.035.
- [8] D. López Barreiro, W. Prins, F. Ronsse, W. Brilman, Hydrothermal liquefaction (HTL) of microalgae for biofuel production: State of the art review and future prospects, *Biomass and Bioenergy.* 53 (2013) 113–127. doi:10.1016/j.biombioe.2012.12.029.
- [9] X. Miao, Q. Wu, C. Yang, Fast pyrolysis of microalgae to produce renewable fuels, *J. Anal. Appl. Pyrolysis.* 71 (2004) 855–863. doi:10.1016/j.jaap.2003.11.004.
- [10] Y. Sun, C. Liu, Y. Zan, G. Miao, H. Wang, L. Kong, Hydrothermal Carbonization of Microalgae (*Chlorococcum* sp.) for Porous Carbons With High Cr(VI) Adsorption Performance, *Appl. Biochem. Biotechnol.* 186 (2018) 414–424. doi:10.1007/s12010-018-2752-0.
- [11] K.L. Yu, P.L. Show, H.C. Ong, T.C. Ling, W.H. Chen, M.A.M. Salleh, Biochar production from microalgae cultivation through pyrolysis as a sustainable carbon sequestration and biorefinery approach, *Clean Technol. Environ. Policy.* 20 (2018) 2047–2055. doi:10.1007/s10098-018-1521-7.

- [12] Y. Hu, M. Gong, S. Feng, C. (Charles) Xu, A. Bassi, A review of recent developments of pre-treatment technologies and hydrothermal liquefaction of microalgae for bio-crude oil production, *Renew. Sustain. Energy Rev.* 101 (2019) 476–492. doi:10.1016/j.rser.2018.11.037.
- [13] C. Onumaegbu, J. Mooney, A. Alaswad, A.G. Olabi, Pre-treatment methods for production of biofuel from microalgae biomass, *Renew. Sustain. Energy Rev.* 93 (2018) 16–26. doi:10.1016/j.rser.2018.04.015.
- [14] G. Bensidhom, A. Ben Hassen-Trabelsi, K. Alper, M. Sghairoun, K. Zaafour, I. Trabelsi, Pyrolysis of Date palm waste in a fixed-bed reactor: Characterization of pyrolytic products, *Bioresour. Technol.* 247 (2018) 363–369. doi:10.1016/j.biortech.2017.09.066.
- [15] A. Akhtar, V. Krepl, T. Ivanova, A Combined Overview of Combustion, Pyrolysis, and Gasification of Biomass, *Energy & Fuels.* 32 (2018) 7294–7318. doi:10.1021/acs.energyfuels.8b01678.
- [16] D. Woolf, J.E. Amonette, F.A. Street-Perrott, J. Lehmann, S. Joseph, Sustainable biochar to mitigate global climate change, *Nat. Commun.* 1 (2010) 1–9. doi:10.1038/ncomms1053.
- [17] B.S. Archanjo, E. Tavakkoli, M.T. Rose, D. Cozzolino, T.J. Rose, S. Morris, J.R. Araujo, B.P. Singh, L. Van Zwieten, L.M. Macdonald, Z. (Han) Weng, A. Cowie, S.W.L. Kimber, S. Joseph, Biochar built soil carbon over a decade by stabilizing rhizodeposits, *Nat. Clim. Chang.* 7 (2017) 371–376. doi:10.1038/nclimate3276.
- [18] K.A. Spokas, Review of the stability of biochar in soils: predictability of O:C molar ratios, *Carbon Manag.* 1 (2010) 289–303. doi:10.4155/cmt.10.32.
- [19] P. Thornley, K. Chong, T. Bridgwater, European biorefineries: Implications for land, trade and employment, *Environ. Sci. Policy.* 37 (2014) 255–265. doi:10.1016/j.envsci.2013.09.004.
- [20] S.S. Hassan, G.A. Williams, A.K. Jaiswal, Lignocellulosic Biorefineries in Europe: Current State and Prospects, *Trends Biotechnol.* 37 (2019) 231–234. doi:10.1016/j.tibtech.2018.07.002.
- [21] S.S. Hassan, G.A. Williams, A.K. Jaiswal, Moving towards the second generation of lignocellulosic biorefineries in the EU: Drivers, challenges, and opportunities, *Renew. Sustain. Energy Rev.* 101 (2019) 590–599. doi:10.1016/j.rser.2018.11.041.
- [22] T.F. Rittl, K. Butterbach-Bahl, C.M. Basile, L.A. Pereira, V. Alms, M. Dannenmann, E.G. Couto, C.E.P. Cerri, Greenhouse gas emissions from soil amended with agricultural residue biochars: Effects of feedstock type, production temperature and soil moisture, *Biomass and Bioenergy.* 117 (2018) 1–9. doi:10.1016/j.biombioe.2018.07.004.

- [23] B. Grycova, A. Prysycz, P. Lestinsky, K. Chamradova, Influence of potassium hydroxide and method of carbonization treatment in garden and corn waste microwave pyrolysis, *Biomass and Bioenergy*. 118 (2018) 40–45. doi:10.1016/j.biombioe.2018.07.022.
- [24] F. Liao, L. Yang, Q. Li, Y.R. Li, L.T. Yang, M. Anas, D.L. Huang, Characteristics and inorganic N holding ability of biochar derived from the pyrolysis of agricultural and forestal residues in the southern China, *J. Anal. Appl. Pyrolysis*. 134 (2018) 544–551. doi:10.1016/j.jaap.2018.08.001.
- [25] M. Ahmad, M. Ahmad, A.R.A. Usman, A.S. Al-Faraj, A. Abduljabbar, Y.S. Ok, M.I. Al-Wabel, Correction to: Date palm waste-derived biochar composites with silica and zeolite: synthesis, characterization and implication for carbon stability and recalcitrant potential, *Environ. Geochem. Health*. (2017) 1. doi:10.1007/s10653-017-0047-y.
- [26] A.R.A. Usman, A. Abduljabbar, M. Vithanage, Y.S. Ok, M. Ahmad, M. Ahmad, J. Elfaki, S.S. Abdulazeem, M.I. Al-Wabel, Biochar production from date palm waste: Charring temperature induced changes in composition and surface chemistry, *J. Anal. Appl. Pyrolysis*. 115 (2015) 392–400. doi:10.1016/j.jaap.2015.08.016.
- [27] H. Hadoun, Z. Sadaoui, N. Souami, D. Sahel, I. Toumert, Characterization of mesoporous carbon prepared from date stems by H₃PO₄ chemical activation, *Appl. Surf. Sci.* 280 (2013) 1–7. doi:10.1016/j.apsusc.2013.04.054.
- [28] H. Zheng, W. Guo, S. Li, Y. Chen, Q. Wu, X. Feng, R. Yin, S.H. Ho, N. Ren, J.S. Chang, Adsorption of p-nitrophenols (PNP) on microalgal biochar: Analysis of high adsorption capacity and mechanism, *Bioresour. Technol.* 244 (2017) 1456–1464. doi:10.1016/j.biortech.2017.05.025.
- [29] N. Jafri, W.Y. Wong, V. Doshi, L.W. Yoon, K.H. Cheah, A review on production and characterization of biochars for application in direct carbon fuel cells, *Process Saf. Environ. Prot.* 118 (2018) 152–166. doi:10.1016/j.psep.2018.06.036.
- [30] A. Akhtar, A.K. Sarmah, Strength improvement of recycled aggregate concrete through silicon rich char derived from organic waste, *J. Clean. Prod.* 196 (2018) 411–423. doi:10.1016/j.jclepro.2018.06.044.
- [31] S. Zhao, B. Huang, X.P. Ye, X. Shu, X. Jia, Utilizing bio-char as a bio-modifier for asphalt cement: A sustainable application of bio-fuel by-product, *Fuel*. 133 (2014) 52–62. doi:10.1016/j.fuel.2014.05.002.
- [32] J. Plácido, S. Bustamante López, K.E. Meissner, D.E. Kelly, S.L. Kelly, Microalgae biochar-derived carbon dots and their application in heavy metal sensing in aqueous systems, *Sci. Total Environ.* (2018) #pagerange#. doi:10.1016/j.scitotenv.2018.11.393.
- [33] Y. Shen, H. Li, W. Zhu, S.H. Ho, W. Yuan, J. Chen, Y. Xie, Microalgal-biochar

- immobilized complex: A novel efficient biosorbent for cadmium removal from aqueous solution, *Bioresour. Technol.* 244 (2017) 1031–1038. doi:10.1016/j.biortech.2017.08.085.
- [34] X. Xiao, B. Chen, Z. Chen, L. Zhu, J.L. Schnoor, Insight into Multiple and Multilevel Structures of Biochars and Their Potential Environmental Applications: A Critical Review, *Environ. Sci. Technol.* 52 (2018) 5027–5047. doi:10.1021/acs.est.7b06487.
- [35] A. Akhtar, T. Ivanova, I. Jiříček, V. Krepl, Detailed characterization of waste from date palm (*Phoenix dactylifera*) branches for energy production: Comparative evaluation of heavy metals concentration, *J. Renew. Sustain. Energy.* 11 (2019) 13102. doi:10.1063/1.5027578.
- [36] J.J. Lu, W.H. Chen, Investigation on the ignition and burnout temperatures of bamboo and sugarcane bagasse by thermogravimetric analysis, *Appl. Energy.* 160 (2015) 49–57. doi:10.1016/j.apenergy.2015.09.026.
- [37] M. Muthuraman, T. Namioka, K. Yoshikawa, Characteristics of co-combustion and kinetic study on hydrothermally treated municipal solid waste with different rank coals: A thermogravimetric analysis, *Appl. Energy.* 87 (2010) 141–148. doi:10.1016/j.apenergy.2009.08.004.
- [38] Z. Yao, S. You, T. Ge, C.H. Wang, Biomass gasification for syngas and biochar co-production: Energy application and economic evaluation, *Appl. Energy.* 209 (2018) 43–55. doi:10.1016/j.apenergy.2017.10.077.
- [39] J. Yoder, S. Galinato, D. Granatstein, M. Garcia-Pérez, Economic tradeoff between biochar and bio-oil production via pyrolysis, *Biomass and Bioenergy.* 35 (2011) 1851–1862. doi:10.1016/j.biombioe.2011.01.026.
- [40] M. Jouiad, N. Al-Nofeli, N. Khalifa, F. Benyettou, L.F. Yousef, Characteristics of slow pyrolysis biochars produced from rhodes grass and fronds of edible date palm, *J. Anal. Appl. Pyrolysis.* 111 (2015) 183–190. doi:10.1016/j.jaap.2014.10.024.
- [41] E.M.C.C. Batista, J. Shultz, T.T.S. Matos, M.R. Fornari, T.M. Ferreira, B. Szpoganicz, R.A. De Freitas, A.S. Mangrich, Effect of surface and porosity of biochar on water holding capacity aiming indirectly at preservation of the Amazon biome, *Sci. Rep.* 8 (2018) 1–9. doi:10.1038/s41598-018-28794-z.
- [42] V. Chiodo, G. Zafarana, S. Maisano, S. Freni, F. Urbani, Pyrolysis of different biomass: Direct comparison among *Posidonia Oceanica*, Lacustrine Alga and White-Pine, *Fuel.* 164 (2016) 220–227. doi:10.1016/j.fuel.2015.09.093.
- [43] K. Jindo, H. Mizumoto, Y. Sawada, M.A. Sanchez-Monedero, T. Sonoki, Physical and chemical characterization of biochars derived from different agricultural residues, *Biogeosciences.* 11 (2014) 6613–6621. doi:10.5194/bg-11-6613-2014.

- [44] K.H. Kim, J.Y. Kim, T.S. Cho, J.W. Choi, Influence of pyrolysis temperature on physicochemical properties of biochar obtained from the fast pyrolysis of pitch pine (*Pinus rigida*), *Bioresour. Technol.* 118 (2012) 158–162. doi:10.1016/j.biortech.2012.04.094.
- [45] M. Uchimiya, L.H. Wartelle, K.T. Klasson, C.A. Fortier, I.M. Lima, Influence of pyrolysis temperature on biochar property and function as a heavy metal sorbent in soil, *J. Agric. Food Chem.* 59 (2011) 2501–2510. doi:10.1021/jf104206c.
- [46] P. Huang, C. Ge, D. Feng, H. Yu, J. Luo, J. Li, P.J. Strong, A.K. Sarmah, N.S. Bolan, H. Wang, Effects of metal ions and pH on ofloxacin sorption to cassava residue-derived biochar, *Sci. Total Environ.* 616–617 (2018) 1384–1391. doi:10.1016/j.scitotenv.2017.10.177.
- [47] P. Rousset, C. Aguiar, N. Labbé, J.M. Commandré, Enhancing the combustible properties of bamboo by torrefaction, *Bioresour. Technol.* 102 (2011) 8225–8231. doi:10.1016/j.biortech.2011.05.093.
- [48] M.M. Phukan, R.S. Chutia, B.K. Konwar, R. Kataki, Microalgae *Chlorella* as a potential bio-energy feedstock, *Appl. Energy.* 88 (2011) 3307–3312. doi:10.1016/j.apenergy.2010.11.026.
- [49] S.W. Park, C.H. Jang, K.R. Baek, J.K. Yang, Torrefaction and low-temperature carbonization of woody biomass: Evaluation of fuel characteristics of the products, *Energy.* 45 (2012) 676–685. doi:10.1016/j.energy.2012.07.024.
- [50] N.R. Dhumal, H.J. Kim, J. Kiefer, Electronic structure and normal vibrations of the 1-ethyl-3-methylimidazolium ethyl sulfate ion pair, *J. Phys. Chem. A.* 115 (2011) 3551–3558. doi:10.1021/jp1122322.
- [51] W. Chen, H. Yang, Y. Chen, M. Xia, X. Chen, H. Chen, Transformation of Nitrogen and Evolution of N-Containing Species during Algae Pyrolysis, *Environ. Sci. Technol.* 51 (2017) 6570–6579. doi:10.1021/acs.est.7b00434.
- [52] O. Debono, A. Villot, Nitrogen products and reaction pathway of nitrogen compounds during the pyrolysis of various organic wastes, *J. Anal. Appl. Pyrolysis.* 114 (2015) 222–234. doi:10.1016/j.jaap.2015.06.002.
- [53] S.S. Choi, J.E. Ko, Dimerization reactions of amino acids by pyrolysis, *J. Anal. Appl. Pyrolysis.* 89 (2010) 74–86. doi:10.1016/j.jaap.2010.05.009.
- [54] Q. Yi, F. Qi, G. Cheng, Y. Zhang, B. Xiao, Z. Hu, S. Liu, H. Cai, S. Xu, Thermogravimetric analysis of co-combustion of biomass and biochar, *J. Therm. Anal. Calorim.* 112 (2013) 1475–1479. doi:10.1007/s10973-012-2744-1.
- [55] F.L. Braghiroli, H. Bouafif, N. Hamza, B. Bouslimi, C.M. Neculita, A. Koubaa, The

- influence of pilot-scale pyro-gasification and activation conditions on porosity development in activated biochars, *Biomass and Bioenergy*. 118 (2018) 105–114. doi:10.1016/j.biombioe.2018.08.016.
- [56] T. Chen, C. Dong, H. Liu, Y. Sun, M. Li, Synthesis of magnetic biochar composites for enhanced uranium(VI) adsorption, *Sci. Total Environ.* 651 (2018) 1020–1028. doi:10.1016/j.scitotenv.2018.09.259.
- [57] B. Feng, R. Yan, C.G. Zheng, Effect of ash components on the ignition and burnout of high ash coals, *Dev. Chem. Eng. Miner. Process.* 7 (1999) 387–395.

Combined multi-stage pyrolysis of date palm biomass and microalgae

This chapter is devoted to present the multi-stage co-pyrolysis of date palm biomass and microalgae and impact on the resultant char properties. The use of waste products in different applications contains prime importance in today's research and industry. Researchers all over the world are working on producing innovative technologies and processes to utilise waste and produce valuable products for different applications. Microalgae-derived char contains low aromaticity and heating values with relatively high nitrogen content than lignocellulosic char. This chapter shows the use of waste from date palm branches and wastewater derived microalgae through co-pyrolysis to produce char of improved properties. Two batches of experiments were conducted (a) single stage pyrolysis and (b) two-stage pyrolysis in the range of highest treatment temperature of 400-600 °C. Single stage pyrolysed char showed, lower aromaticity, higher yield, ash content and heating values of the char than two-stage pyrolysed char. Similarly, ignition temperature and activation energy were higher during combustion by single stage pyrolysed char than two-stage char. Economic analysis also showed slightly higher prices for single stage pyrolysed char. Hence, two-stage pyrolysed char is suitable in the energy applications, whereas low-temperature processing (400-500 °C) will result in optimum properties in terms of yield and heating values.

5.1 Introduction

Organic waste materials are considered as a new energy material in modern research realm and contain the significant value to derive further products for the production of energy in the form of biogas, syngas, biofuels and char [1]. Different kinds of waste are being investigated through pyrolysis from manure [2,3] to agricultural residues [4,5], municipal solid waste [6,7] to industrial waste [8,9]. Although all the waste utilisation techniques are beneficial and provide some sort of riddance from the waste, pyrolysis holds a significant place among all of them. This is due to the versatility of the products obtained through different reaction conditions such as bio-oil and biochar (char). Bio-oil is the result of fast pyrolysis whereas char is the primary product of the slow pyrolysis of lignocellulosic biomass [10]. The peak temperature and types of feedstock also play an important role in describing the yield and properties of the resultant product.

Char is primarily composed of a carbon-rich material with the loss of weight and volatiles which is formed under the absence of oxygen whereas the feedstock is heated slowly to peak temperature [1]. Char is being investigated for soil improvement and amendment and found positive results through several studies [11–13], however, recently reported also in different other applications from the use in wastewater treatment as an effective adsorbent [14,15] to the use in the batteries as a carbon material [16,17]. The possibility of the char to alter the properties according to the required application is responsible for the multidisciplinary applications with significant advantages over the conventional materials. Although several factors are influential in determining the ultimate char properties, most of the applications require either very high treatment temperature ($>700\text{ }^{\circ}\text{C}$) or post-processing through different techniques.

Different renewable lignocellulosic feedstock has been reported in several studies. However, an emerging feedstock which is being considered for char production is microalgae. Microalgae is a unicellular photosynthetic organism which is not visible to the naked eye generally lies in size range of 1-400 μm [18]. Microalgae are a promising feedstock in renewable energy technology which has higher biomass growth than most of the other feedstock and can be used for wastewater treatment [19]. Microalgae use nitrogen and phosphorus hence reducing the concentration of inorganic elements in the wastewater. Microalgae can be used for other purposes in a wastewater treatment facility such as heavy metals removal, or reduction of chemical/biochemical oxygen demand [20] and performs the functions in a relatively short time

[21]. While considering the multiple benefits, microalgae are quite a promising feedstock for the production of char.

There are many studies reported the use of algae for char production and char utilisation for different applications. Bordoloi et al. [22] recently reported the use of algal (*S. dimorphus*) char for the adsorption of cobalt (II) ion from aqueous solution. In another study by Son et al. [23] the use of macroalgal char for heavy metal adsorption is investigated. Magnetic char was prepared from algae for the adsorption of Cd, Cu and Zn with a higher selectivity for the Cu removal. The oxygen-containing functional groups were found to be the primary influencer regarding the heavy metals adsorption. Zheng et al. [24] showed adsorption of p-nitrophenols (PNP) via three types of microalgal (*Chlorella sp.*, *Chlamydomonas sp.*, and *Coelastrum sp.*) derived char. *Chlorella sp.* was found to be more effective adsorbent of PNP for wastewater treatment than other types of char due to high polarity of binding sites with higher O-containing functional groups.

Similarly, char derived from lignocellulosic biomass is also of significant importance while providing material for different applications. Al-Wabel et al. [25] recently reported the use of date palm derived char to enhance the germination of lettuce and increased the shoot length whereas hydrochar inhibited the germination to 20%. Date seed derived char was also found to contain the potential of heavy metal removal in aqueous solution. Cu^{2+} and Ni^{2+} adsorption was observed at 0.421 and 0.333 mmol g^{-1} respectively [26]. At another instant, Usman et al. [27] reported the Cd (II) sorption through the date palm char produced at two different temperatures 300 °C and 700 °C. Char prepared at 700 °C found to contain 1.5 times higher adsorption capacity than produced at 300 °C.

Different feedstocks have reported for co-pyrolysis and showed a variety of results. Huang et al. [28] reported the effect of co-pyrolysis of sewage sludge and rice straw/sawdust on the heavy metals leaching in char. Cu, Zn and Ni contents were reduced in the obtained product, however, the surface area and thermal stability decreased with the sawdust biomass. Meng et al. [29] conducted the co-pyrolysis of rice straw with pig manure and recommended to use in 1:3 ratio at 600 °C to reduce the ammonium acetate extractable and Zn and Cu heavy metals in char.

Co-pyrolysis of microalgae and lignocellulosic biomass have also been reported on several occasions for the production of bio-oil. Chen et al. [30] performed a co-pyrolysis of bamboo and microalgae (*Nannochloropsis sp.*) at 600 °C. It was observed that most of the nitrogen-

containing species transferred to the char in the form of pyrrolic-N and quaternary-N and reduced the nitrogen concentration in bio-oil. Duan et al. [31] reported the co-pyrolysis of waste tyre rubber and microalgae in a temperature range (290-370 °C) in supercritical ethanol. The microalgae facilitated the conversion of tyre rubber at a lower temperature than the pyrolysis of tyre rubber alone. Chen et al. [32] at another instant reported the co-pyrolysis of lignocellulosic biomass and microalgae. Nitrogen species increased in char (>75%) and reduced in gas and bio-oil which resulted in nitrogen-doped char yield. Thus co-pyrolysis of microalgae with other feedstock also showed promising results with the potential to incorporate in biorefineries and produce char of improved properties. Char worked as an adsorbent of nitrogen during the co-pyrolysis of algae with other biomass types during bio-oil production.

Although co-pyrolysis of lignocellulosic biomass and microalgae showed an optimistic trend to improve the properties of bio-oil and gas, further studies are required for exclusive char production. There is no literature explaining the behaviour of date palm biomass and wastewater derived microalgae for the exclusive char production through slow pyrolysis technology. As both feedstocks are waste-derived materials, hence contain a promising aspect of providing feedstock for biorefineries. A two-stage combined pyrolysis process of waste date palm biomass and wastewater derived microalgae was performed. Char properties from co-pyrolysis of both of this feedstock (date palm branches + wastewater derived microalgae) were investigated in detail, and economic analysis of the produced char was conducted.

5.2 Materials and Methods

5.2.1 Pyrolysis experiment

Date palm branches (DB) were first dried, cut and crushed into a small particle size of less than 1 mm. Wastewater derived microalgae (WWM) was collected from a wastewater treatment plant. The derived microalgae contained a number of species including *Actinostrium sp.*, *Coleastrum sp.*, *Diatom sp.*, and *Mucidosphaerium pulchellum*. Co-pyrolysis of the microalgae and date palm biomass was conducted in a fixed bed system. The feedstock was used in a 1:1 ratio and mixed thoroughly before conducting the experiment. The feedstock was put into the sample holder and placed into the reactor before starting the experiment. The initial air in the reactor was vented out by flowing nitrogen gas at 20 cm³/min. When sufficient flow was detected, the chamber started heating to the highest treatment temperature (HTT) (400 °C, 500 °C and 600 °C) with the residence time of 20 minutes. In single stage pyrolysis (SSP), the chamber cooled down to normal temperature after reaching HTT and char is recovered,

whereas; for two-stage pyrolysis (TSP), chamber started reheating after the drop of temperature up to 150 °C. For instance, after reaching the HTT of 400 °C with a residence time of 20 minutes at HTT, the temperature drops up to 250 °C and then later started increasing again to HTT (400 °C) with the residence time of 5 minutes. The reactor cooled down after the completion of the second step. This process was further repeated for 500 °C and 600 °C.

5.2.2 Char characterisation

Char yield was calculated at the end of the experiment through mass change and is presented as a mass yield. BET specific surface area was determined through Coulter SA 3100, working on the principle of N₂ gas phase adsorption at a temperature of 77 K. The samples were degassed at 150 °C under high vacuum for 240 minutes prior to conducting of the experiment. The elemental composition of biomass and char was measured by instrument Elementar Vario EL Cube. To present the variation in values according to co-pyrolysed char, biomass in a 1:1 ratio was mixed and analysed for elemental composition. The energy content of the feedstock and char was determined by Adiabatic Isoperibolic Calorimeter Model C5000, IKA-Werke, Staufen, Germany. Higher heating values of the char were also calculated based on an elemental composition from the equation (5-1) given below:

$$HHV_T = 0.3491 \times C + 1.1783 \times H + 0.1005 \times S - 0.1034 \times O - 0.015 \times N - 0.0211 \times Ash \text{ [33](5-1)}$$

The combustion and pyrolysis behaviour of the char and the feedstock were examined by the simultaneous TGA-DSC analyser (SDT Q600, TA Instruments, USA). Air and nitrogen atmosphere was employed for combustion and pyrolysis at the flow rate of 100 ml/min and Constant heating rate of 10 K/min. All the samples were processed to granular form passing through the sieve of 125 µm. To analyse the feedstock, both of the biomass samples were mixed in a 1:1 ratio prior to conducting the experiment, to describe the co-combustion and co-pyrolysis conditions for feedstock. The combustion parameters such as ignition temperature, maximum weight loss rate temperature and complete burnout temperature were determined through intersection and conversion method [34].

Surface functional groups were investigated by ATR-FTIR spectroscopy. The spectra were collected at a scan rate of 100 with a spectral resolution of 4 cm⁻¹ in the range of 400 cm⁻¹ to 4000 cm⁻¹. The atomic elemental composition and nitrogen containing species on the surface of the char products were observed by x-ray photoelectron spectroscopy (XPS) using the instrument ESCA Probe P.

5.2.3 Energy economics

Energy economics can be described by the output characteristics of the char in terms of its energy recovery (5-2) and yield (5-3) in the process of transition from biomass to char:

$$\text{Energy recovery of char (\%)} = \frac{\text{Heating value of char}}{\text{Heating value of biomass}} \times 100 \dots\dots\dots(5-2)$$

$$\text{Energy yield (\%)} = \frac{\text{Weight}_{\text{char}}}{\text{Weight}_{\text{raw}}} \times \frac{\text{HHV}_{\text{char}}}{\text{HHV}_{\text{raw}}} \times 100 \text{ [35]} \dots\dots\dots(5-3)$$

The direct cost was also calculated to compare the value of the char with coal[34,35]. Following correlations were used from the literature to calculate the economic value (EV) (\$kg⁻¹) of the char:

$$EV = UP \times PR \dots\dots\dots (5-4)$$

$$UP (\$kg^{-1}) = 0.002528 \times 16.2 + 0.02678571 \times T \dots\dots\dots (5-5)$$

UP and PR is the unit price (\$kg⁻¹) and production rate of the char (kg/kg), respectively. T is in °C.

$$UP = BPJ \times HHV \dots\dots\dots (5-6)$$

BPJ and HHV is the char price per megajoule and a higher heating value of the char respectively.

The cost was calculated by HHV and HTT parameters which later compared with coal price due to char's potential to be used with coal for energy production.

5.3 Results and Discussion

5.3.1 Char characteristics

Yield, surface area and heating values of the char are presented in *Table 5-1*. Yield is decreasing while the surface area is increasing with the increase of temperature. The yield and surface area range was observed to be between 30-40% and 1-2 m²/g respectively for all the samples. TSP showed a minor decrease in surface area as well as a decrease in yield than SSP. At higher temperatures, yield difference reduces to less than 1%. Overall, more than 8% decrease in yield observed for HTT 600 °C than 400 °C. Likewise, heating values also decreased with an increase

in temperature. Conversely, the ash content increases with the increase in HTT from 21 to 27% in SSP samples and 20 to 26% in TSP samples.

Ultimate analysis of the feedstock and all the char samples was conducted to determine the C, H, N, S and O contents with H/C, O/C and (O+N)/C atomic ratios (*Table 5-2*). Increasing the treatment temperature increased the carbon content and decreased the hydrogen and nitrogen content in the char. On the contrary, both feedstocks (DB+WWM) in the combined form showed a higher amount of hydrogen and nitrogen and lower carbon content than the chars. This also agrees with other studies which reported the relatively high nitrogen content of microalgae [30,38]. Co-pyrolysis reduced the overall nitrogen concentration in char and TSP slightly reduced the nitrogen and hydrogen content than SSP.

Table 5-1 Yield, surface area, ash and energy values of the char (CS = Single stage, CT = Two stage, & 4, 5 and 6 represents 400, 500 and 600 °C respectively)

Samples	Mass yield (g/kg)	Surface Area (m²/g)	Ash content (%)	HHV_M (MJ/kg)	HHV_T (MJ/kg)
CS-4	400.3	1.013	21.3	24.47	23.36
CS-5	335.1	1.471	24.4	23.62	21.75
CS-6	310.2	2.022	27.4	23.59	22.14
CT-4	384	1.055	20.1	23.20	22.54
CT-5	321.7	1.335	26.2	22.46	22.34
CT-6	302.9	1.967	26	22.82	23.22

HHV_T Theoretical higher heating value

HHV_M Measured higher heating value

Table 5-2 Ultimate analysis of the char and feedstock (as received basis)

Samples	C (%)	H (%)	S (%)	N (%)	O (%)	H/C	O/C	(O+N)/C
DB+WWM	45.67	6.74	0.65	4.21	42.73	0.148	0.94	1.03
CS-4	61.65	4.52	0.49	4.18	29.16	0.07	0.47	0.54
CS-5	62.12	3.14	0.59	3.85	30.29	0.05	0.49	0.55
CS-6	65.27	2.37	0.76	3.68	27.92	0.04	0.43	0.48
CT-4	63.30	3.27	0.60	3.98	28.86	0.05	0.46	0.52
CT-5	64.29	2.71	0.89	3.72	26.79	0.04	0.42	0.50
CT-6	67.86	2.29	0.76	3.56	25.53	0.03	0.38	0.43

5.3.2 Atomic ratios and Van Krevelen diagram

The atomic ratios (H/C and O/C) of the feedstock and chars are presented in the Van Krevelen diagram (*Figure 5-1*) showing the decrease in ratios as the temperature increases. Feedstock tends to show higher H/C and O/C ratios than their respective chars [39]. Lower O/C ratios represent the formation of graphite-like structures through a structural arrangement of aromatic rings [40]. The lower ratios in char depict a reduction in volatile matter content and increase in aromaticity [41]. The H/C ratios were significantly lower than most of the chars reported [41–43] indicating a significant increase in aromaticity. Both of the treatment processes showed a decrease in ratios with the increase in temperature. However, TSP revealed a rather significant decrease in which TSP at 500 °C showed equivalent ratios to the SSP at 600 °C. It is worthwhile to note that O/C ratios reduced comparatively at 600 °C for SSP samples than 400 °C and 500 °C. Chiodo et al. [44] previously reported that algae char tend to show high O/C ratios than lignocellulosic biomass derived char when pyrolysed individually at all HTTs (400, 500 and 600 °C). Hence, a co-pyrolysis is a suitable approach to gain overall lower O/C ratio in the end product, and TSP can further reduce the atomic ratio to increase the aromaticity of the char.

The regression analysis was performed to determine the correlation between atomic ratios H/C, N/C, O/C and (O+N)/C. H/C atomic ratio showed a high coefficient of determination ($R^2 = 0.987$) and a notably low p-value 5.72E-06 (*Figure 5-2*). This shows the significance of the correlation and dependence of both the atomic ratios on each other. H/C also showed a high

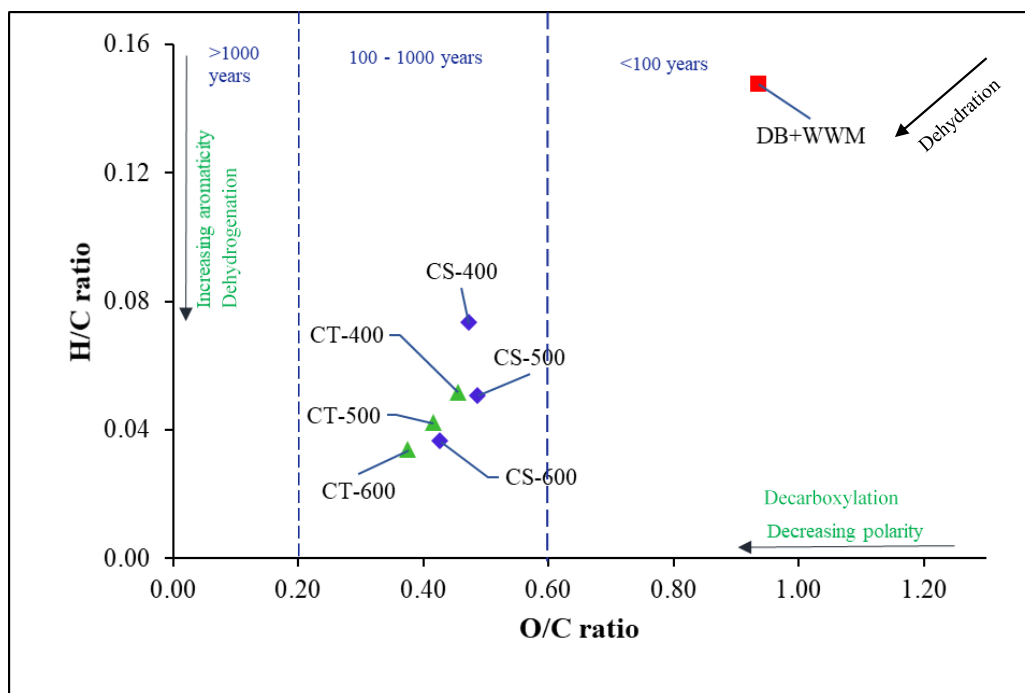


Figure 5-1 Van Krevelen diagram of O/C and H/C atomic ratios. The dotted line at 0.6 and 0.2 O/C ratio separating the range of half-life of char produced [53]

coefficient of determination with (O+N)/C atomic ratio, however relatively lower than N/C with p-value also significantly low $0.00027 < 0.05$. N/C and O/C analysis also resulted in similar R^2 and p-value. Another part of regression analysis carried out to determine the influence of the H/C, N/C and mass yield on the ash production in a co-pyrolysed char. All three parameters showed moderate to the high coefficient of determination with substantially low p-values. However, the trend shows a negative slope such as increasing atomic ratios and yield decreased the ash content of char.

5.3.3 Fourier transform infrared spectroscopy

The presence of functional groups in the char and feedstock was analysed by ATR-FTIR spectroscopy. The changes in the patterns of functional groups due to thermal treatment are quite visible among samples. The spectra of feedstock and char can be seen in Figure 5-3. Different treatment temperatures showed peaks of different intensities. The samples subjected to the two-stage approach also showed significant changes at 500 °C and 600 °C, however, the spectra seems to be similar at 400 °C HTT with similar intensities. WWM feedstock showed peaks at 996 cm^{-1} , 1375 cm^{-1} , 1452 cm^{-1} , 1625 cm^{-1} , 2917 cm^{-1} , 3328 cm^{-1} corresponding to the =C-H bending vibration [45], CH_3 C-H bending vibration [46], C=C stretching [47], N-H bending [48], C-H stretching [47,49], O-H stretching vibration.

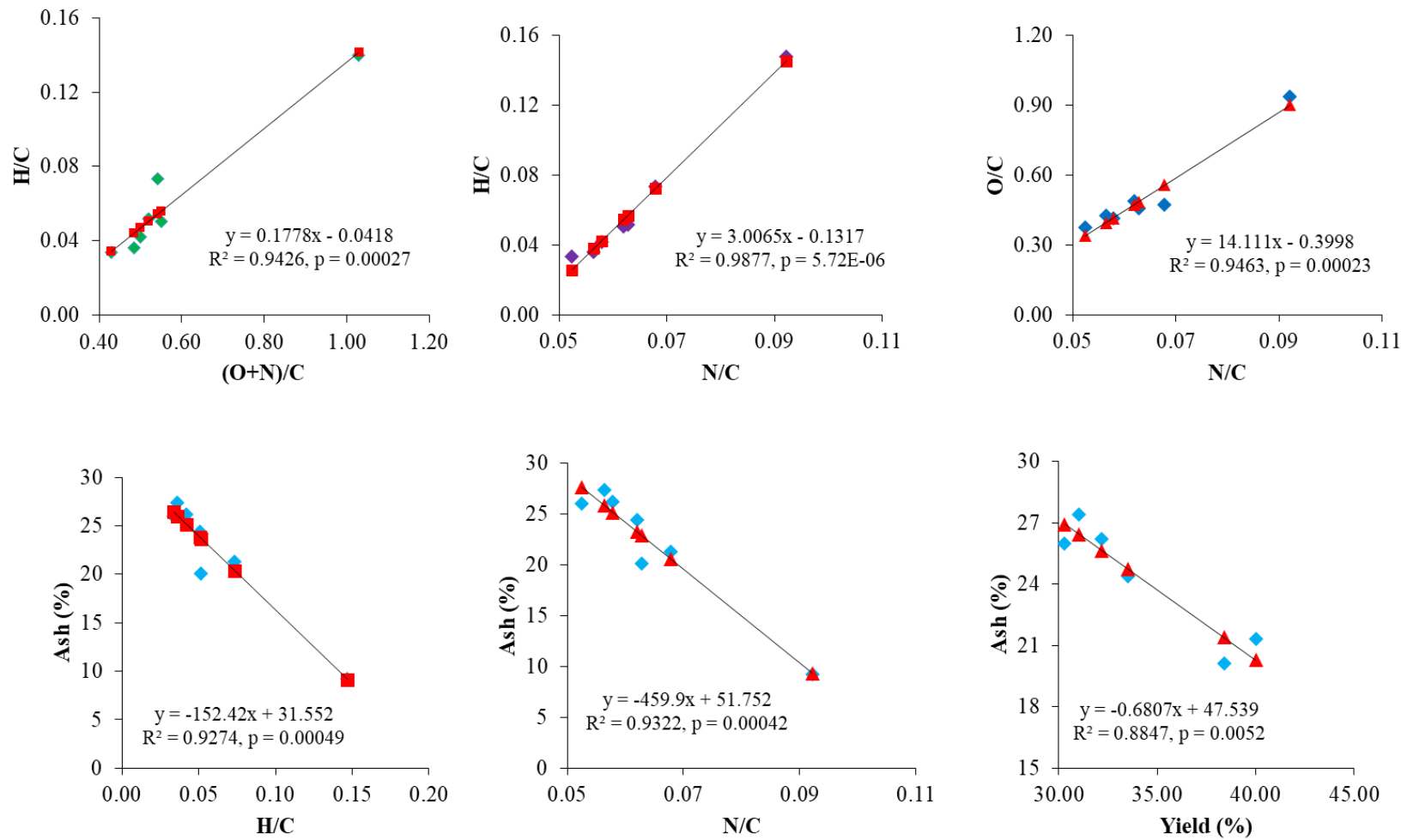


Figure 5-2 Regression analysis of H/C, (O+N)/C, O/C and N/C atomic ratios and Ash correlation with N/C, H/C and yield with the coefficient of determination and p values

DB feedstock, on the other hand, contained relatively higher peaks at 1031 cm^{-1} and 3328 cm^{-1} . DB feedstock showed peaks at 1031 cm^{-1} , 1240 cm^{-1} , 1367 cm^{-1} , 1507 cm^{-1} representing C-O stretching [47], O=C-O-C stretching [47], $\text{CH}(\text{CH}_3)_2$ bending and N-H bending vibration [48] respectively while the rest of the peaks were similar to WWM feedstock. Char clearly showed a different pattern than the feedstock resulting in the appearance of some peaks while few peaks wholly disappeared. For instance, peaks around 860 cm^{-1} and 870 cm^{-1} for =C-H bending vibration [50] did not appear in the char with HTT of $400\text{ }^\circ\text{C}$. However, peaks were started forming at $500\text{ }^\circ\text{C}$ and becomes sharp at $600\text{ }^\circ\text{C}$.

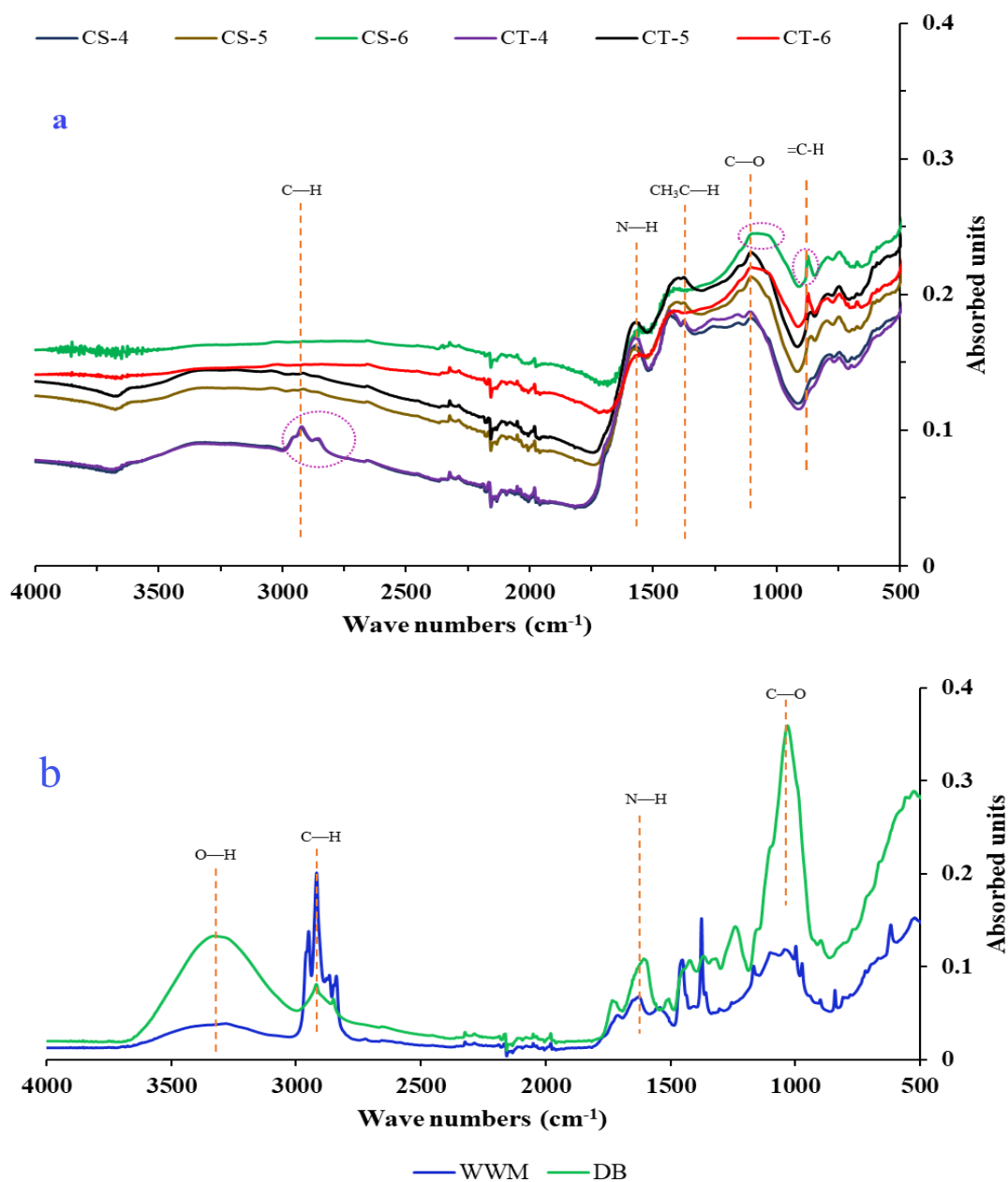


Figure 5-3 FTIR of char (a) and feedstock (b) (WWM = wastewater derived microalgae, DB = date palm biomass)

Similarly, relatively small peaks appeared at 1370 cm^{-1} for CH_3 C-H bending vibration [49] at $400\text{ }^\circ\text{C}$ and $500\text{ }^\circ\text{C}$ whereas disappeared at $600\text{ }^\circ\text{C}$. The peaks around 1100 cm^{-1} representing C-O stretch [49,50] become significantly broad at $600\text{ }^\circ\text{C}$, however, appeared as a minor peak at $400\text{ }^\circ\text{C}$. The N-H bending vibration at 1557 cm^{-1} were also of higher intensity at 400 and $500\text{ }^\circ\text{C}$ rather than $600\text{ }^\circ\text{C}$. The peaks at 2910 cm^{-1} and $3325\text{-}3355\text{ cm}^{-1}$ corresponding to C-H stretching [47] and Alcohol O-H broad stretching vibration [47] respectively, did not appear at $600\text{ }^\circ\text{C}$ which was the most significant peak in DB. The difference between SSP and TSP peaks are quite significant at $600\text{ }^\circ\text{C}$ and reduces as the HTT decreases. It can be seen that peaks at $400\text{ }^\circ\text{C}$ are of quite similar intensity for SSP and TSP with a marginal difference around 1200 cm^{-1} and 1580 cm^{-1} . Peak shift was not significant in any of the samples, however, peaks were of higher intensity at $500\text{ }^\circ\text{C}$ for TSP than SSP and at $600\text{ }^\circ\text{C}$ vice versa.

5.3.4 X-ray photoelectron spectroscopy

The data on the atomic elemental composition of the char samples were observed through XPS technology for C1s, O1s, N1s, Ca2p, Cl2p and K2p (*Table 5-3*). Na1s, Si2s, S2s and P2p of minor percentages were also observed in a few samples. These elements were mostly found in samples subjected to a high treatment temperature and in two-stage pyrolysis. The atomic percentage of carbon is relatively higher at lower HTT whereas it is decreasing with the increasing temperature. Upon subjecting to the two-stage pyrolysis (TSP), the variation in carbon content was not significant. All the samples showed the atomic ratio of 74-77% of carbon on the surface. Oxygen concentration, on the other hand, was found to be highest at $500\text{ }^\circ\text{C}$ in both SSP and TSP treatment processes. Oxygen was found to be increased in TSP samples than SSP, indicating the presence of higher oxygen functional groups. Conversely, N was found to be lowest in TSP samples and Ca showed the maximum concentration at $600\text{ }^\circ\text{C}$ for both treatment processes.

Nitrogen species investigated in char samples subjected to SSP and TSP. It is important to note that these values depict the char surface properties rather than the bulk presence of the nitrogen in the samples. Pyridinic, quaternary and pyrrolic nitrogen species were the highest among all of them in TSP samples whereas, pyridinic and pyrrolic in SSP samples except CS-4 which also showed the presence of quaternary-N (A.8) (*Appendices*). Furthermore, pyridinic – N and pyrrolic – N substantially increased with the decrease of oxidized – N and quaternary – N upon increasing the HTT. Oxidized and quaternary – N was removed altogether when HTT approached $500\text{ }^\circ\text{C}$ in SSP. However, amine – N concentration seems to be highest at HTT 500

°C. A contrast behaviour in nitrogen species was observed in TSP samples, showing quaternary-N was available in all of the samples. Oxidized – N showed similar behaviour and reduced to less than 1% after 500 °C HTT. This can be seen that overall nitrogen concentration decreased with the increase in HTT and the further decrease was observed in TSP samples, causing most of the nitrogen to convert to the gaseous phase. The left out nitrogen was present in the form of pyridinic, pyrrolic, and amine nitrogen species which were also the major nitrogen species in a study presented by Chen et al. [32] at 600 °C. Nitrogen-doped char holds the potential to use in different applications such as reducing the NO_x reduction when co-combusted with coal [51] and superior electrochemical efficiency with potential supercapacitors applications [52].

Table 5-3 Elemental composition on the surface of the char samples analysed by XPS

Samples	C 1s	O 1s	N 1s	Ca2p	Cl2p	K2s	Na1s	Si2s	S2s	P2p
CS-4	82.45	10.82	5.39	1.34	-	-	-	-	-	-
CS-5	75.11	14.48	3.12	1.08	2.52	3.68	-	-	-	-
CS-6	71.51	11.59	2.79	2.15	3.43	3.50	2.06	1.46	1.51	-
CT-4	76.98	13.48	3.87	1.20	2.28	1.29	-	0.89	-	-
CT-5	74.89	14.54	3.84	0.35	1.38	1.09	0.91	1.80	-	1.21
CT-6	77.25	14.43	1.32	2.21	2.27	1.59	0.93	-	-	-

5.3.5 TGA-DSC analysis

5.3.5.1 Combustion

A simultaneous thermogravimetric – differential scanning calorimetric analysis of the biomass and char samples was conducted to determine the weight loss and degradation pattern during combustion and pyrolysis. Co-combustion of feedstock (date palm branches and microalgae) showed a slightly different behaviour than the combustion of co-pyrolysed char (*Figure 5-4*). The moisture contained in the feedstock was more than 6 %, whereas, for the chars, it was in the range of 4-5% of its total weight. Degradation stages noted in DTG curves verified 2 stage devolatilization in which feedstock showed the first peak around 300 °C and a second peak around 490 °C. All the chars, on the other hand, showed the first peak after 400 °C, exhibiting

higher stability than the feedstock. The degradation at first peak gradually increased with the increase of HTT (400 > 500 > 600). SSP relatively showed lower peak than TSP at 400 and 500 °C.

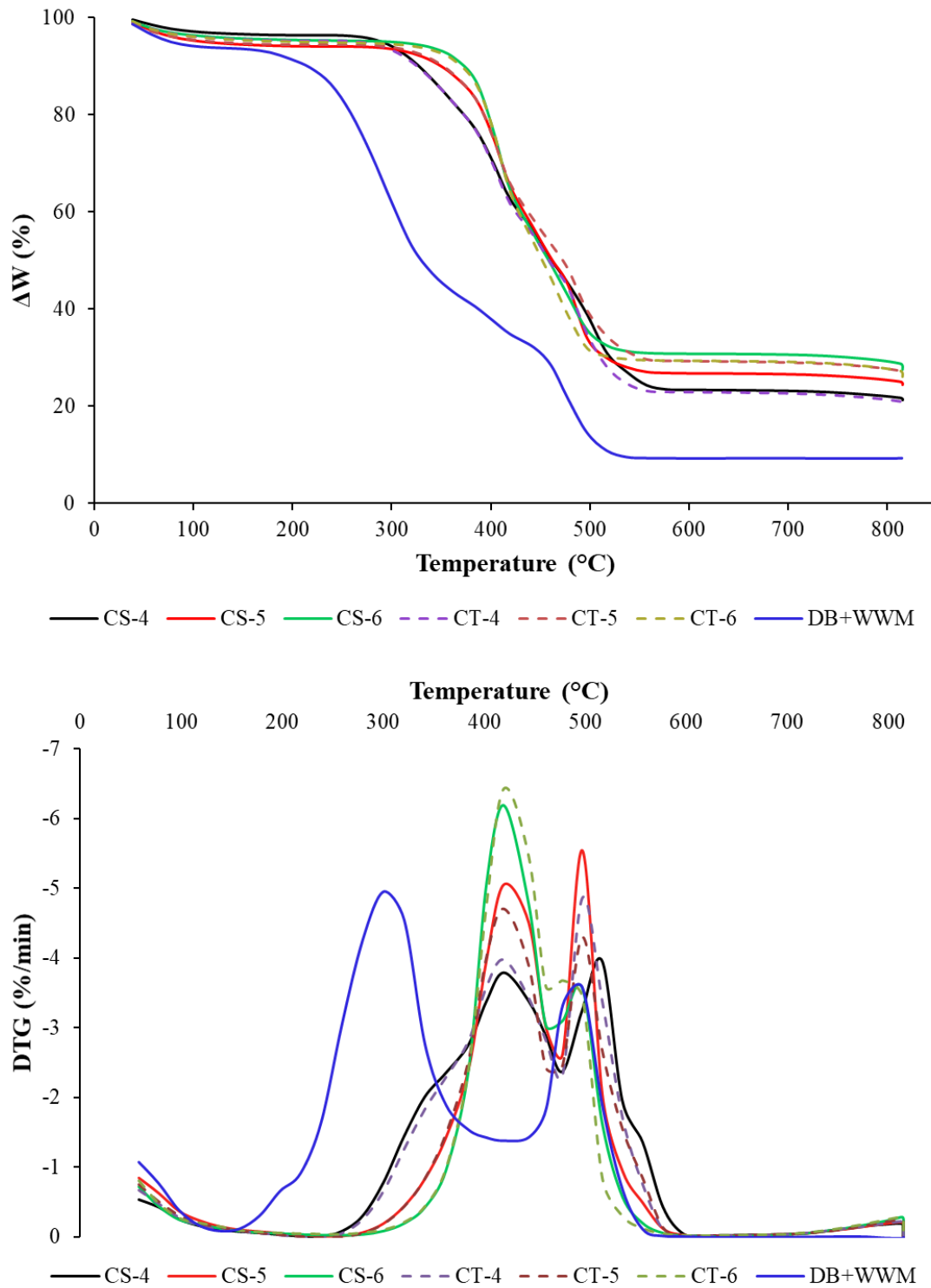


Figure 5-4 TGA and DTG curves of biomass and chars produced at 400, 500 and 600 °C in air atmosphere

The second peak at 600 °C disappears for TSP, however, a small second peak can be seen in the SSP sample. TSP has also shown contrast behaviour than SSP in other samples, CS-4 exhibit reduced second peak and CS-5 the highest peak, whereas, CT-5 showed the lowest second peak. The change in degradation pattern is due to lower fixed carbon content upon reaching the second stage. This might be the reason for disappearing the second peak in CT-6 samples and contributing towards higher first peak than the rest of the samples. Thus, CT-6 might have the potential to fully utilise the char at a lower temperature than its peers. The range for overall combustion of feedstock is 241-557 °C, whereas, this range reduced for CT samples (340-577 °C). DSC curves have shown a comparatively similar trend to DTG for heat flow, however, the change is distinctive for CS-4 and CT-4 samples, showing three peaks with gradually increasing intensity (A.9) (*Appendices*). The first peak reduced its intensity in CT-4 samples than CS-4. Unlike, DTG, feedstock exhibit second highest peak, showing the contributing potential of energy in the second phase despite low degradation.

Combustion parameters have been calculated to view the overall combustion behaviour from starting the ignition towards complete burnout of the samples. It was shown that the char has long burning time and contain the ability to generate energy for the long duration of time than co-combustion of feedstock (*Table 5-4*). This is evident from the measured heating values as well. TSP relatively reduced the ignition temperature of chars than SSP chars. Although, conversion method shows 95% and 88% burnout of the feedstock samples, however, this might not generate a significant amount of energy after second stage degradation majorly after 600 °C. The change in weight loss is less than 1% for biomass and less than 5% for all char samples from 600 to 800 °C. The economic feasibility of char concerning its remaining energy potential after second stage degradation could be explored in future studies and generalise the char and biomass for its energy generation potential. Statistical analysis was also performed between ignition temperature and burnout temperature to determine the significance and correlation coefficient. Burnout temperature have shown a high correlation coefficient ($R^2 = 0.96$) in relation to ignition temperature with p-value $6.5E-05 < 0.5$ (*Figure 5-5*).

Table 5-4 Co-combustion of date palm biomass and wastewater derived microalgae and their co-pyrolysed char

Samples	T _i (°C)	T _{max} (°C)	T _b (°C)	DTG _{max}	E (kJ/mol)	R ²
DB+WWM	241	301	536	-4.95	160.5	0.93
CS-4	343	514	757	-3.96	150.3	0.90
CS-5	362	497	777	-5.55	128.3	0.90
CS-6	367	419	797	-6.19	134.3	0.91
CT-4	339	499	777	-4.87	133.7	0.92
CT-5	351	419	777	-4.71	123.3	0.93
CT-6	353	420	797	-6.42	132	0.90

T_i, T_{max}, T_b, DTG_{max}, and E represents the ignition temperature, maximum weight loss rate temperature, burnout temperature, maximum weight loss rate and activation energy respectively.

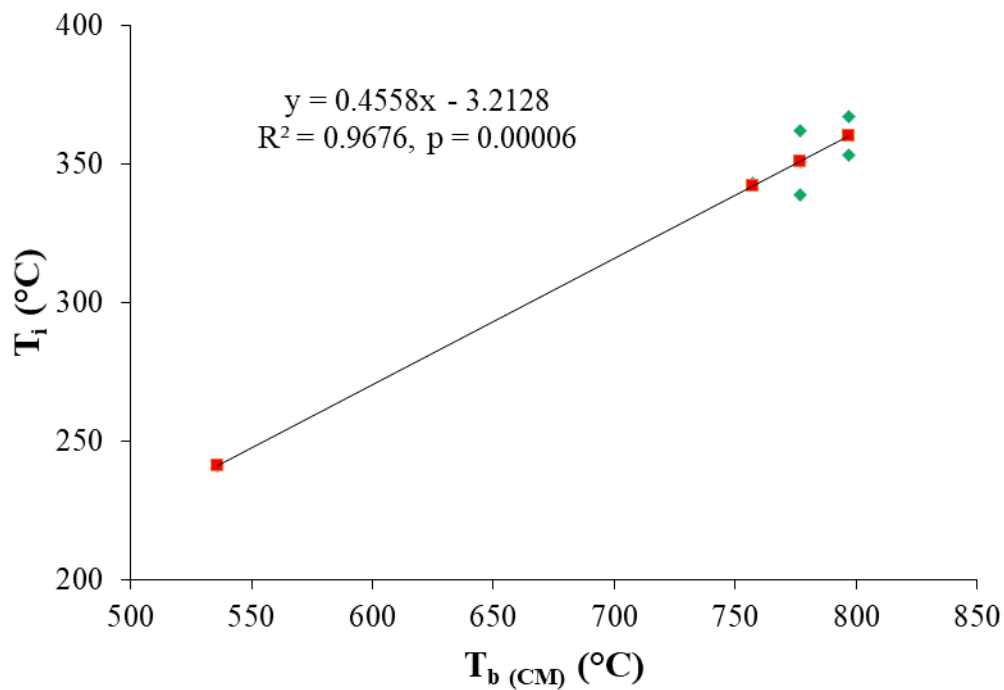


Figure 5-5 Regression analysis of ignition temperature and burnout temperature of SSP and TSP chars

Kinetics

The activation energy of the samples can be calculated through the Arrhenius kinetic model, and it can be determined through the following equations (5-7 — 5-10):

$$k(T) = Ae^{\left(\frac{-E}{RT}\right)} \dots\dots\dots (5-7)$$

$$\frac{d\alpha}{dt} = Ae^{\left(\frac{-E}{RT}\right)} (1 - \alpha)^n \dots\dots\dots(5-8)$$

$$\alpha = \frac{\omega_{\varphi} - \omega}{\omega_{\varphi} - \omega_f} \dots\dots\dots(5-9)$$

E is the activation energy (kJmol⁻¹), R is the gas constant (8.34 Jk⁻¹mol⁻¹), T is the absolute temperature (K), and A is the pre-exponential factor (s⁻¹), n is the order of reaction, and α is the conversion rate.

After rearranging and integration method (Coats – Redfern method) applied, the equation changed into the following form:

$$\ln\left[-\frac{\ln(1-\alpha)}{T^2}\right] = \ln\frac{AR}{\beta E} - \frac{E}{RT} \dots\dots\dots(5-10)$$

β is the heating rate (°Cmin⁻¹ or Kmin⁻¹)

The kinetic illustration is presented in *Figure 5-6*, and activation energy (E) is calculated from the slope of the curves for the overall combustion process and is presented in *Table 5-4*. The lower the activation energy, the lower the energy required to begin the combustion process. It can be seen that all of the chars have shown overall lower activation energy according to the co-combustion of the feedstock. The lowest amount of activation energy was noted by TSP chars, and at 500 °C HTT char have shown relatively less activation energy both for SSP and TSP than the rest of the samples. SSP samples showed the range of activation energy from 128 kJmol⁻¹ to 150 kJmol⁻¹ which is dropped in case of TSP and found in the range of 123 to 133 kJmol⁻¹. CS-5 and CT-5 both samples reduced the activation energy more than 30 kJmol⁻¹ according to the feedstock. Regression analysis showed a high coefficient of correlation in all of the samples, exhibiting R² ≥ 0.90.

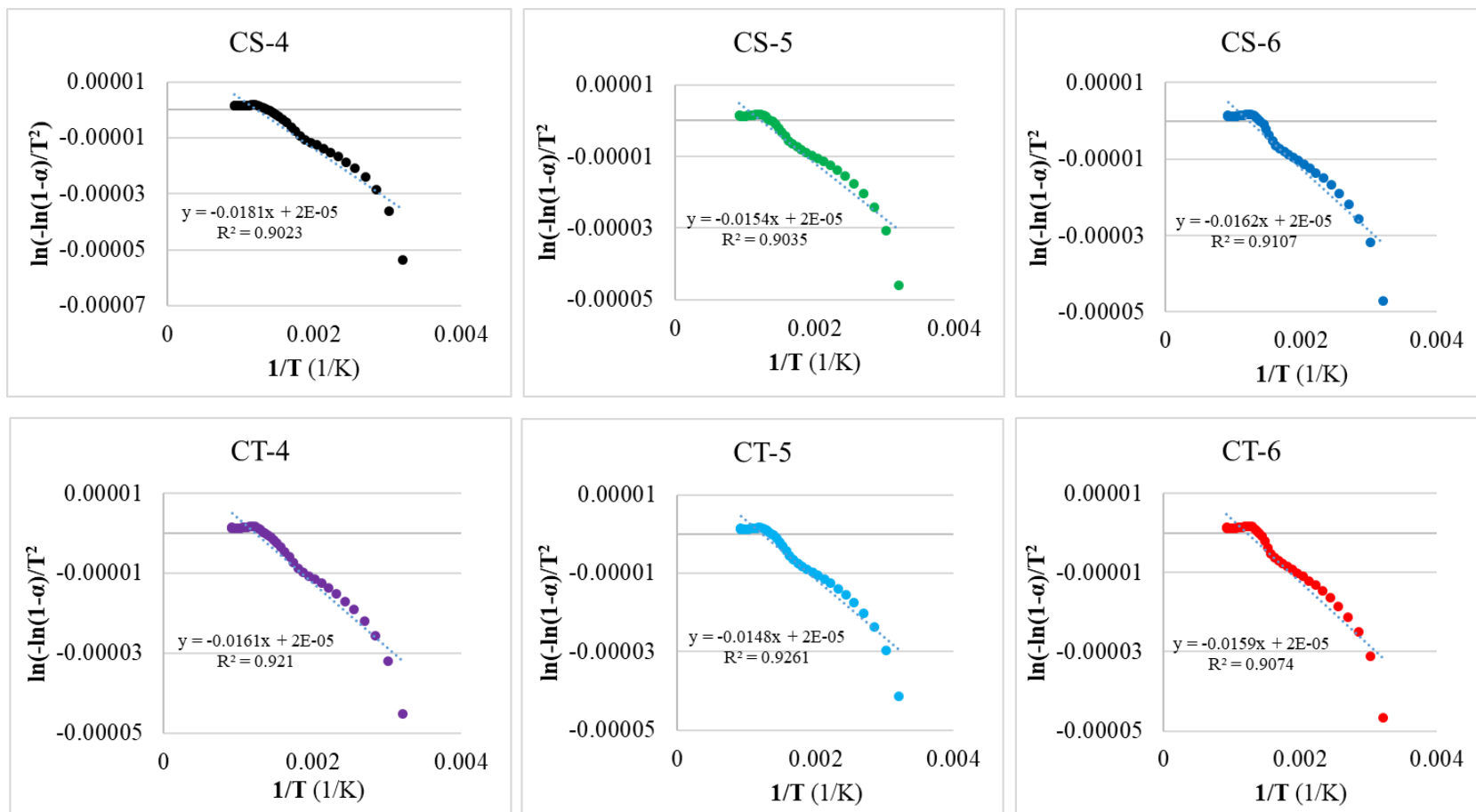


Figure 5-6 Kinetic illustrations of chars subjected to combustion

5.3.5.2 Pyrolysis

A similar set of experiments conducted in a nitrogen environment to illustrate the pyrolysis conditions for the concerned samples (*Figure 5-7*). It can be seen that char has shown single stage degradation with a couple of minor peaks after 800 °C as compared to two-stage combustion. Degradation can be seen as limited with maximum weight loss occurred in samples subjected to 400 °C HTT. The increase in temperature resulted in less degradation with high char content. Although degradation happened in small percentage than combustion, however, it continuous to devolatilize for a longer duration. There is a small degradation noted between 800-1000 °C which resulted in a weight loss of more than 10% in this range in all of the samples of SSP and TSP. TSP samples reduced the weight loss further around 3-4 % at 400 and 600 °C HTT.

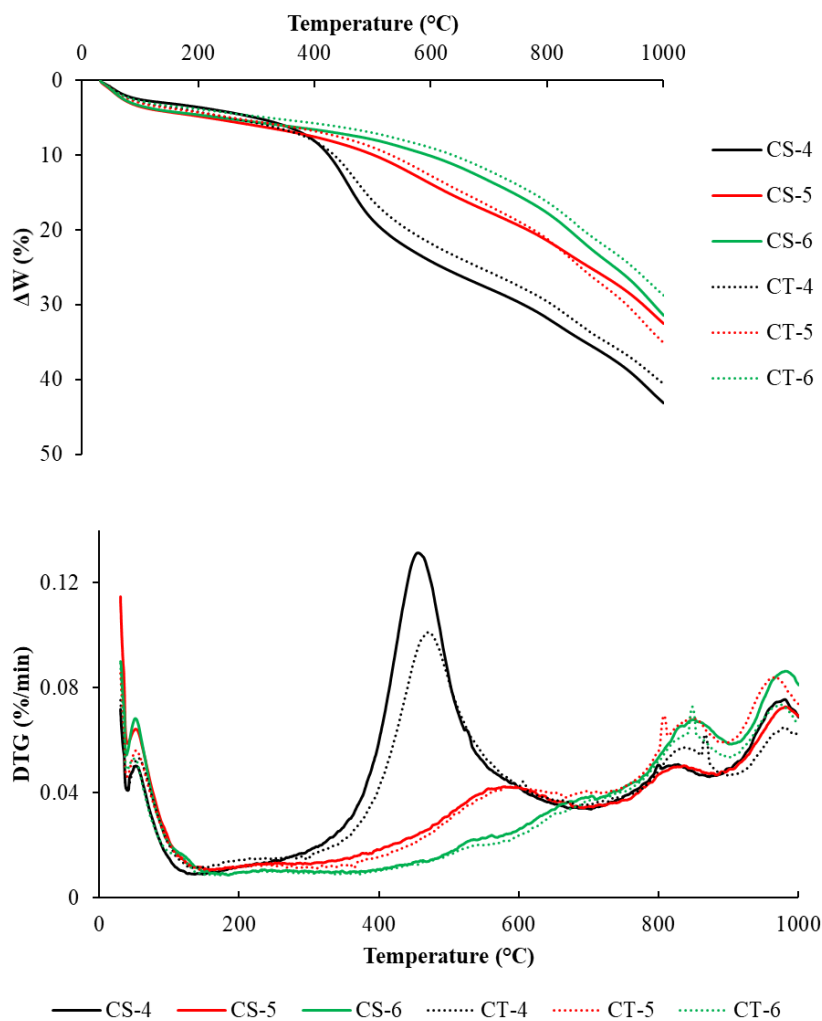


Figure 5-7 Thermal analysis of co-pyrolysed char in nitrogen atmosphere

Weight loss rate curve showed a comprehensive outlook of the samples in which the highest peak shifted for CS-5, CS-6, CT-5 and CT-6 samples from 400-500 °C towards 500-600 °C. Weight loss rate reduced substantially after 500 °C with a sudden decline in a peak in CS-4 and CT-4 samples, whereas, it continues to increase for the rest of the samples. This might be due to the higher char's stability treated at high temperatures as shown in Van Krevelen diagram (Figure 5-1). Combined feedstock also showed single stage degradation, hence, confirming the single stage pyrolysis of the biomass. The smooth curve could be observed after 600 °C, however, weight loss continues to occur up to 10% of the total weight from 600 °C to 1000 °C.

5.3.6 Energy economics

The economic potential of the char based on the yield and treatment temperature shows that char's price decreases as the HTT increases. It is worthwhile to note that the difference may become significant for large-scale production. The overall price range for all of the samples indicates between \$0.024 to 0.027 kg⁻¹ with maximum value for CS-4 char at \$0.027 kg⁻¹ and lowest for CT-5 char at \$0.024 kg⁻¹ (Table 5-5). Overall TSP samples showed a lower price through these variables. The price of the coal per kg is \$0.068 kg⁻¹ for the heating value 26.9 MJkg⁻¹ [36]. Price is markedly lower than coal, however, the heating value is also lower in the range of 22-24 MJkg⁻¹. Therefore, the price evaluation based on heating values of the char was also calculated. Both of the measured and calculated heating values were considered.

Table 5-5 Energy yield and price variation according to the different treatment temperatures

Samples	Energy recovery	Energy yield (%)	Economic value (HTT) (\$/kg)	Economic value (HHV_M) (\$/kg)	Economic value (HHV_T) (\$/kg)
CS-4	1.26	50.38	0.0272	0.025	0.024
CS-5	1.22	40.72	0.0250	0.020	0.018
CS-6	1.21	37.64	0.0253	0.018	0.017
CT-4	1.19	45.83	0.0261	0.023	0.021
CT-5	1.16	37.16	0.0240	0.018	0.018
CT-6	1.17	35.56	0.0247	0.017	0.018

The economic value was found in the range of \$0.017-0.025 kg⁻¹, stating that the decrease in heating values will lower the price of the char. Prices based on the measured heating values showed slightly higher prices than calculated from the theoretical heating values. Prices based on the HHV also showed a similar trend to HTT, in which prices tend to decrease with the increase in treatment temperature. Hence treatment temperature, in this case, is the major driver of the price of the char. Energy yield also reduces with the increase in treatment temperature. The regression analysis of mass yield and energy yield showed a high coefficient of determination ($R^2 = 0.969$) and p-value (0.00035) substantially lower than 0.05 (Figure 5-8). The higher mass yield translates to higher energy yield.

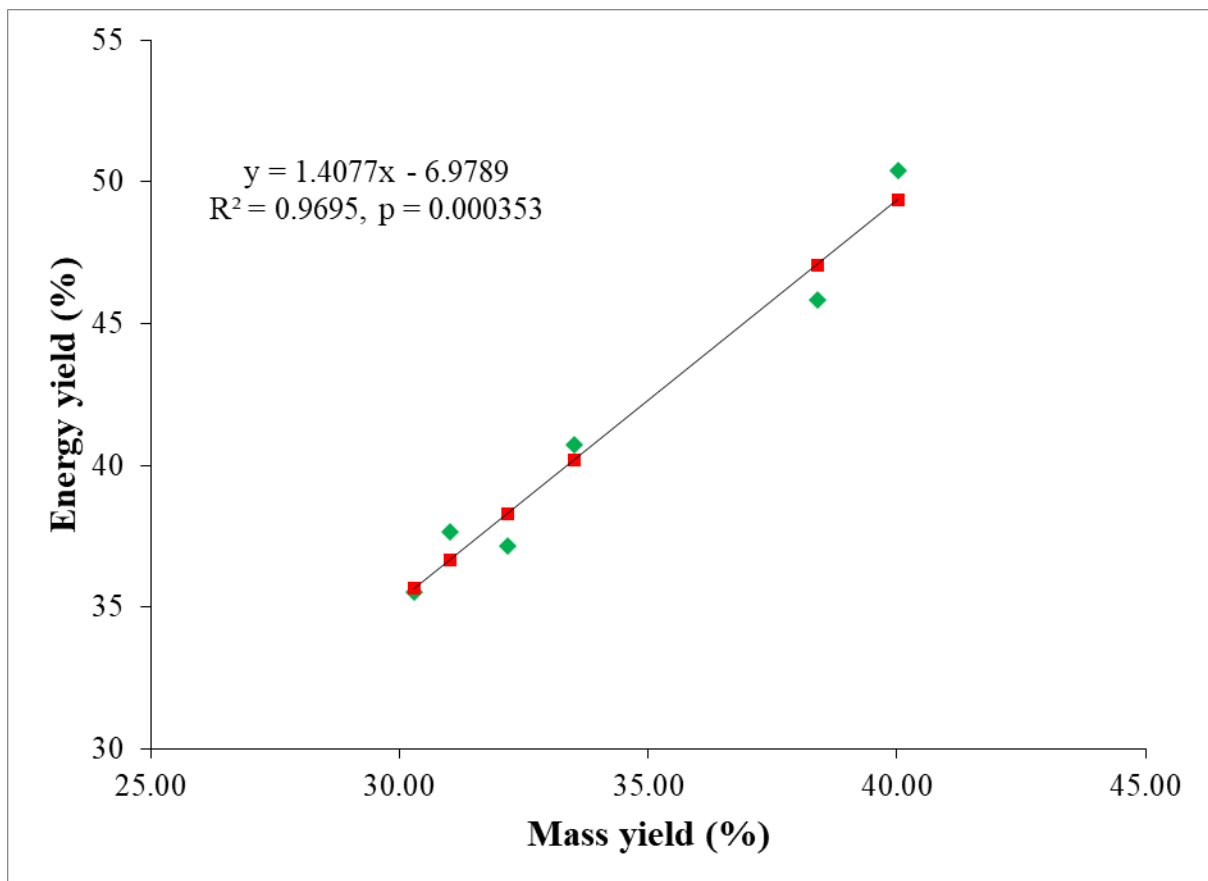


Figure 5-8 Statistical analysis of the mass yield and energy yield of the char

5.4 Conclusive remarks

Co-pyrolysis of date palm branches and wastewater derived microalgae was conducted at 400, 500 and 600 °C for a single stage and two stage pyrolysis. Char aromaticity increased, and mass yield decreased substantially with the increase in treatment temperature in both SSP and TSP from 40% to 30% by weight. Nitrogen concentration was decreased with the increase in temperature, and similar results were found for nitrogen species on the surface of the char. The nitrogen-doped char holds the potential to be used in a range of applications from the reduction of NO_x emissions to supercapacitors.

Combustion of the feedstock and the char samples produced at 400 and 500 °C showed two-stage degradation whereas pyrolysis showed single stage degradation. The optimum treatment temperature for two-stage pyrolysis is 500 °C to gain the lowest activation energy during combustion, moderate heating values and lowest price. Similarly, the activation energy of the subsequent pyrolysis of char samples also decreased than their feedstock. TSP samples at treatment temperatures (≥ 500 °C) showed higher activation energy than SSP samples. The economic analysis showed a decrease in price with the increase in treatment temperature. It can be concluded that co-pyrolysed char from TSP samples contain the superior properties and potential applications in multiple areas such as energy and adsorption.

5.5 References

- [1] A. Akhtar, V. Krepl, T. Ivanova, A Combined Overview of Combustion, Pyrolysis, and Gasification of Biomass, *Energy & Fuels*. 32 (2018) 7294–7318. doi:10.1021/acs.energyfuels.8b01678.
- [2] N. Scarlat, F. Fahl, J.F. Dallemand, F. Monforti, V. Motola, A spatial analysis of biogas potential from manure in Europe, *Renew. Sustain. Energy Rev.* 94 (2018) 915–930. doi:10.1016/j.rser.2018.06.035.
- [3] F. Tasnim, S.A. Iqbal, A.R. Chowdhury, Biogas production from anaerobic co-digestion of cow manure with kitchen waste and Water Hyacinth, *Renew. Energy*. 109 (2017) 434–439. doi:10.1016/j.renene.2017.03.044.
- [4] S. Kamel, H.A. El-Sattar, D. Vera, F. Jurado, Bioenergy potential from agriculture residues for energy generation in Egypt, *Renew. Sustain. Energy Rev.* 94 (2018) 28–37. doi:10.1016/j.rser.2018.05.070.
- [5] F. Valenti, S.M.C. Porto, R. Selvaggi, B. Pecorino, Evaluation of biomethane potential from by-products and agricultural residues co-digestion in southern Italy, *J. Environ. Manage.* 223 (2018) 834–840. doi:10.1016/j.jenvman.2018.06.098.
- [6] C. Gopu, L. Gao, M. Volpe, L. Fiori, J.L. Goldfarb, Valorizing municipal solid waste: Waste to energy and activated carbons for water treatment via pyrolysis, *J. Anal. Appl. Pyrolysis*. 133 (2018) 48–58. doi:10.1016/j.jaap.2018.05.002.
- [7] A.T. Sipra, N. Gao, H. Sarwar, Municipal solid waste (MSW) pyrolysis for bio-fuel production: A review of effects of MSW components and catalysts, *Fuel Process. Technol.* 175 (2018) 131–147. doi:10.1016/j.fuproc.2018.02.012.
- [8] A. Fernandez, A. Saffe, R. Pereyra, G. Mazza, R. Rodriguez, Kinetic study of regional agro-industrial wastes pyrolysis using non-isothermal TGA analysis, *Appl. Therm. Eng.* 106 (2016) 1157–1164. doi:10.1016/j.applthermaleng.2016.06.084.
- [9] R. Kumar Singh, B. Ruj, A. Jana, S. Mondal, B. Jana, A. Kumar Sadhukhan, P. Gupta, Pyrolysis of three different categories of automotive tyre wastes: Product yield analysis and characterization, *J. Anal. Appl. Pyrolysis*. (2018). doi:10.1016/j.jaap.2018.08.011.
- [10] D. Mohan, A. Sarswat, Y.S. Ok, C.U. Pittman, Organic and inorganic contaminants removal from water with biochar, a renewable, low cost and sustainable adsorbent - A critical review, *Bioresour. Technol.* 160 (2014) 191–202. doi:10.1016/j.biortech.2014.01.120.
- [11] Y. Chen, J. Xu, Z. Lv, R. xie, L. Huang, J. Jiang, Impacts of biochar and oyster shells waste on the immobilization of arsenic in highly contaminated soils, *J. Environ. Manage.* 217 (2018) 646–653. doi:10.1016/j.jenvman.2018.04.007.
- [12] S. Li, C. Liang, Z. Shanguan, Effects of apple branch biochar on soil C mineralization and nutrient cycling under two levels of N, *Sci. Total Environ.* 607–608 (2017) 109–119. doi:10.1016/j.scitotenv.2017.06.275.

- [13] M. Wang, Y. Zhu, L. Cheng, B. Anderson, X. Zhao, D. Wang, A. Ding, Review on utilization of biochar for metal-contaminated soil and sediment remediation, *J. Environ. Sci. (China)*. 63 (2017) 156–173. doi:10.1016/j.jes.2017.08.004.
- [14] K.R. Thines, E.C. Abdullah, N.M. Mubarak, M. Ruthiraan, Synthesis of magnetic biochar from agricultural waste biomass to enhancing route for waste water and polymer application: A review, *Renew. Sustain. Energy Rev.* 67 (2017) 257–276. doi:10.1016/j.rser.2016.09.057.
- [15] S. Wongrod, S. Simon, G. Guibaud, P.N.L. Lens, Y. Pechaud, D. Huguenot, E.D. van Hullebusch, Lead sorption by biochar produced from digestates: Consequences of chemical modification and washing, *J. Environ. Manage.* 219 (2018) 277–284. doi:10.1016/j.jenvman.2018.04.108.
- [16] C. del M. Saavedra Rios, V. Simone, L. Simonin, S. Martinet, C. Dupont, Biochars from various biomass types as precursors for hard carbon anodes in sodium-ion batteries, *Biomass and Bioenergy*. 117 (2018) 32–37. doi:10.1016/j.biombioe.2018.07.001.
- [17] I. Izanar, M. Dahbi, M. Kiso, S. Doubaji, S. Komaba, I. Saadoune, Hard carbons issued from date palm as efficient anode materials for sodium-ion batteries, *Carbon N. Y.* 137 (2018) 165–173. doi:10.1016/j.carbon.2018.05.032.
- [18] K.L. Yu, P.L. Show, H.C. Ong, T.C. Ling, J. Chi-Wei Lan, W.H. Chen, J.S. Chang, Microalgae from wastewater treatment to biochar – Feedstock preparation and conversion technologies, *Energy Convers. Manag.* 150 (2017) 1–13. doi:10.1016/j.enconman.2017.07.060.
- [19] N. Abdel-Raouf, A.A. Al-Homaidan, I.B.M. Ibraheem, Microalgae and wastewater treatment, *Saudi J. Biol. Sci.* 19 (2012) 257–275. doi:10.1016/j.sjbs.2012.04.005.
- [20] H.J. Choi, S.M. Lee, Effects of microalgae on the removal of nutrients from wastewater: Various concentrations of *Chlorella vulgaris*, *Environ. Eng. Res.* 17 (2012) 3–8. doi:10.4491/eer.2012.17.S1.S3.
- [21] A. Mehrabadi, R. Craggs, M.M. Farid, Wastewater treatment high rate algal ponds (WWT HRAP) for low-cost biofuel production, *Bioresour. Technol.* 184 (2015) 202–214. doi:10.1016/j.biortech.2014.11.004.
- [22] N. Bordoloi, R. Goswami, M. Kumar, R. Kataki, Biosorption of Co (II) from aqueous solution using algal biochar: Kinetics and isotherm studies, *Bioresour. Technol.* 244 (2017) 1465–1469. doi:10.1016/j.biortech.2017.05.139.
- [23] E.B. Son, K.M. Poo, J.S. Chang, K.J. Chae, Heavy metal removal from aqueous solutions using engineered magnetic biochars derived from waste marine macro-algal biomass, *Sci. Total Environ.* 615 (2018) 161–168. doi:10.1016/j.scitotenv.2017.09.171.
- [24] H. Zheng, W. Guo, S. Li, Y. Chen, Q. Wu, X. Feng, R. Yin, S.H. Ho, N. Ren, J.S. Chang, Adsorption of p-nitrophenols (PNP) on microalgal biochar: Analysis of high adsorption capacity and mechanism, *Bioresour. Technol.* 244 (2017) 1456–1464.

doi:10.1016/j.biortech.2017.05.025.

- [25] M.I. Al-Wabel, M.I. Rafique, M. Ahmad, M. Ahmad, A. Hussain, A.R.A. Usman, Pyrolytic and hydrothermal carbonization of date palm leaflets: Characteristics and ecotoxicological effects on seed germination of lettuce, *Saudi J. Biol. Sci.* (2018). doi:10.1016/j.sjbs.2018.05.017.
- [26] Z. Mahdi, Q.J. Yu, A. El Hanandeh, Investigation of the kinetics and mechanisms of nickel and copper ions adsorption from aqueous solutions by date seed derived biochar, *J. Environ. Chem. Eng.* 6 (2018) 1171–1181. doi:10.1016/j.jece.2018.01.021.
- [27] A. Usman, A. Sallam, M. Zhang, M. Vithanage, M. Ahmad, A. Al-Farraj, Y.S. Ok, A. Abduljabbar, M. Al-Wabel, Sorption Process of Date Palm Biochar for Aqueous Cd (II) Removal: Efficiency and Mechanisms, *Water. Air. Soil Pollut.* 227 (2016). doi:10.1007/s11270-016-3161-z.
- [28] H. jun Huang, T. Yang, F. ying Lai, G. qiang Wu, Co-pyrolysis of sewage sludge and sawdust/rice straw for the production of biochar, *J. Anal. Appl. Pyrolysis.* 125 (2017) 61–68. doi:10.1016/j.jaap.2017.04.018.
- [29] J. Meng, S. Liang, M. Tao, X. Liu, P.C. Brookes, J. Xu, Chemical speciation and risk assessment of Cu and Zn in biochars derived from co-pyrolysis of pig manure with rice straw, *Chemosphere.* 200 (2018) 344–350. doi:10.1016/j.chemosphere.2018.02.138.
- [30] W. Chen, Y. Chen, H. Yang, M. Xia, K. Li, X. Chen, H. Chen, Co-pyrolysis of lignocellulosic biomass and microalgae: Products characteristics and interaction effect, *Bioresour. Technol.* 245 (2017) 860–868. doi:10.1016/j.biortech.2017.09.022.
- [31] P. Duan, B. Jin, Y. Xu, F. Wang, Co-pyrolysis of microalgae and waste rubber tire in supercritical ethanol, *Chem. Eng. J.* 269 (2015) 262–271. doi:10.1016/j.cej.2015.01.108.
- [32] W. Chen, H. Yang, Y. Chen, K. Li, M. Xia, H. Chen, Influence of biochar addition on nitrogen transformation during co-pyrolysis of algae and lignocellulosic biomass, *Environ. Sci. Technol.* 52 (2018) 9514–9521. doi:10.1021/acs.est.8b02485.
- [33] S.A. Channiwala, P.P. Parikh, A unified correlation for estimating HHV of solid, liquid and gaseous fuels, *Fuel.* 81 (2002) 1051–1063. doi:10.1016/S0016-2361(01)00131-4.
- [34] J.J. Lu, W.H. Chen, Investigation on the ignition and burnout temperatures of bamboo and sugarcane bagasse by thermogravimetric analysis, *Appl. Energy.* 160 (2015) 49–57. doi:10.1016/j.apenergy.2015.09.026.
- [35] W.H. Chen, M.Y. Huang, J.S. Chang, C.Y. Chen, W.J. Lee, An energy analysis of torrefaction for upgrading microalga residue as a solid fuel, *Bioresour. Technol.* 185 (2015) 285–293. doi:10.1016/j.biortech.2015.02.095.
- [36] J. Yoder, S. Galinato, D. Granatstein, M. Garcia-Pérez, Economic tradeoff between biochar and bio-oil production via pyrolysis, *Biomass and Bioenergy.* 35 (2011) 1851–1862. doi:10.1016/j.biombioe.2011.01.026.

- [37] Z. Yao, S. You, T. Ge, C.H. Wang, Biomass gasification for syngas and biochar co-production: Energy application and economic evaluation, *Appl. Energy*. 209 (2018) 43–55. doi:10.1016/j.apenergy.2017.10.077.
- [38] W. Chen, K. Li, M. Xia, H. Yang, Y. Chen, X. Chen, Q. Che, H. Chen, Catalytic deoxygenation co-pyrolysis of bamboo wastes and microalgae with biochar catalyst, *Energy*. 157 (2018) 472–482. doi:10.1016/j.energy.2018.05.149.
- [39] L. Leng, H. Huang, H. Li, J. Li, W. Zhou, Biochar stability assessment methods: A review, *Sci. Total Environ*. 647 (2019) 210–222. doi:10.1016/j.scitotenv.2018.07.402.
- [40] K. Jindo, H. Mizumoto, Y. Sawada, M.A. Sanchez-Monedero, T. Sonoki, Physical and chemical characterization of biochars derived from different agricultural residues, *Biogeosciences*. 11 (2014) 6613–6621. doi:10.5194/bg-11-6613-2014.
- [41] K.H. Kim, J.Y. Kim, T.S. Cho, J.W. Choi, Influence of pyrolysis temperature on physicochemical properties of biochar obtained from the fast pyrolysis of pitch pine (*Pinus rigida*), *Bioresour. Technol.* 118 (2012) 158–162. doi:10.1016/j.biortech.2012.04.094.
- [42] M. Uchimiya, L.H. Wartelle, K.T. Klasson, C.A. Fortier, I.M. Lima, Influence of pyrolysis temperature on biochar property and function as a heavy metal sorbent in soil, *J. Agric. Food Chem.* 59 (2011) 2501–2510. doi:10.1021/jf104206c.
- [43] Y. Lee, P.R.B. Eum, C. Ryu, Y.K. Park, J.H. Jung, S. Hyun, Characteristics of biochar produced from slow pyrolysis of *Geodae-Uksae 1*, *Bioresour. Technol.* 130 (2013) 345–350. doi:10.1016/j.biortech.2012.12.012.
- [44] V. Chiodo, G. Zafarana, S. Maisano, S. Freni, F. Urbani, Pyrolysis of different biomass: Direct comparison among *Posidonia Oceanica*, Lacustrine Alga and White-Pine, *Fuel*. 164 (2016) 220–227. doi:10.1016/j.fuel.2015.09.093.
- [45] M. Jouiad, N. Al-Nofeli, N. Khalifa, F. Benyettou, L.F. Yousef, Characteristics of slow pyrolysis biochars produced from rhodes grass and fronds of edible date palm, *J. Anal. Appl. Pyrolysis*. 111 (2015) 183–190. doi:10.1016/j.jaap.2014.10.024.
- [46] L.J. Leng, X.Z. Yuan, H.J. Huang, H. Wang, Z. Bin Wu, L.H. Fu, X. Peng, X.H. Chen, G.M. Zeng, Characterization and application of bio-chars from liquefaction of microalgae, lignocellulosic biomass and sewage sludge, *Fuel Process. Technol.* 129 (2015) 8–14. doi:10.1016/j.fuproc.2014.08.016.
- [47] P. Rousset, C. Aguiar, N. Labbé, J.M. Commandré, Enhancing the combustible properties of bamboo by torrefaction, *Bioresour. Technol.* 102 (2011) 8225–8231. doi:10.1016/j.biortech.2011.05.093.
- [48] M.M. Phukan, R.S. Chutia, B.K. Konwar, R. Katakai, Microalgae *Chlorella* as a potential bio-energy feedstock, *Appl. Energy*. 88 (2011) 3307–3312. doi:10.1016/j.apenergy.2010.11.026.
- [49] S.W. Park, C.H. Jang, K.R. Baek, J.K. Yang, Torrefaction and low-temperature

- carbonization of woody biomass: Evaluation of fuel characteristics of the products, *Energy*. 45 (2012) 676–685. doi:10.1016/j.energy.2012.07.024.
- [50] P. Huang, C. Ge, D. Feng, H. Yu, J. Luo, J. Li, P.J. Strong, A.K. Sarmah, N.S. Bolan, H. Wang, Effects of metal ions and pH on ofloxacin sorption to cassava residue-derived biochar, *Sci. Total Environ.* 616–617 (2018) 1384–1391. doi:10.1016/j.scitotenv.2017.10.177.
- [51] X. Wang, J. Gao, Z. Sun, J. Cheng, L. Xu, Q. Du, Y. Qin, Effect of nitrogen doping on reactivity of coal char in reducing NO, *Can. J. Chem. Eng.* 96 (2018) 873–880. doi:10.1002/cjce.23022.
- [52] M. Demir, S.K. Saraswat, R.B. Gupta, Hierarchical nitrogen-doped porous carbon derived from lecithin for high-performance supercapacitors, *RSC Adv.* 7 (2017) 42430–42442. doi:10.1039/c7ra07984b.
- [53] K.A. Spokas, Review of the stability of biochar in soils: predictability of O:C molar ratios, *Carbon Manag.* 1 (2010) 289–303. doi:10.4155/cmt.10.32.

Comprehensive summary

The use of date palm branches and wastewater derived microalgae through pyrolysis technology was addressed in this dissertation mainly focussing on its chemical and energy perspective. The thesis primarily consisted of four major parts. (I) A detailed overview of the use of biomass through combustion, pyrolysis and gasification technology and the potential and pitfall of each of the technologies with current research trends. (II) Characterising the waste from date palm branches for their potential of energy production and subsequently the presence of heavy metal concentration and comparison according to the European Union standards. (III) Slow pyrolysis of date palm branches and wastewater derived microalgae at varying conditions and comparison of the properties of biochar/biocarbon obtained from the process was presented in detail. Economic values are also presented based on proposed economic models. (IV) An advanced multistage combined pyrolysis process is presented for date palm and wastewater derived microalgae. Their thorough understanding and influence on the resultant product are shown for further derivation.

This study investigated date palm branches in detail to determine the potential of different parts in energy production chambers. The biomass was divided into four parts L (leaf ribs), SB (small part of a branch attached to the ribs), MB (middle part of the branch) and LB (large part of a branch attached to the trunk). It was found that LB part of the branch holds the ability to retain the moisture content for a longer duration as compared to rest of samples which, however, contains the highest crystallinity followed by L, SB, and MB. The highest ash content was exhibited by L which is approximately double the rest of the branch, which also contains the highest HHV (higher heating value) values than the rest of the parts. Arsenic was found to be higher than the permissible limit defined in European Union standards in L, SB, and MB and Zinc only in L part with no heavy metals above the permissible limit in LB part. LB can also be used in technologies which require no drying of biomass for instance in hydrothermal treatment technologies.

The increase in heating rate determines the rapid devolatilization and changes from two-stage devolatilization to single stage devolatilization which also results in an increase in char production. It was concluded that LB part of date palm could be used directly for energy generation after sun drying. However, the other parts need to be treated for heavy metals

reduction (water and acid washing) or can be pre-treated via torrefaction to produce the bio-fuel which can later be used with coal for energy generation.

Further detailed investigation on two waste-based feedstock, date palm biomass and wastewater derived microalgae, was conducted to utilise in potential bio-refineries. The individual and combined pyrolysis behaviour were presented to evaluate their performance for both scenarios. Slow pyrolysis of the date palm branches (DB) and wastewater derived microalgae (WMA) was conducted in the temperature range of 400-600 °C. Mass yield decreased; whereas, ash content increased with the increase in highest treatment temperature (HTT). Algae char (AB) showed higher mass yield and ash content and reduced heating values as compared to date char samples. On the other hand, DB chars showed higher stability than AB chars. Combustion of both types of the char samples found to degrade through a two-stage devolatilization process whereas pyrolysis showed one stage devolatilization.

DB samples at 400 and 500 °C and, AB samples at 500 and 600 °C showed lower activation energy during combustion than their feedstock. Amine-N and Quaternary-N species tend to reduce with the increase in treatment temperature in AB char samples. Energy yield and economic costs were found to be lower for AB char than DB char samples, particularly at high temperatures. Concisely, it was concluded that AB char holds significantly different properties than DB char. Algal char is recommended for soil amendment, and wastewater treatment and date palm derived char is suitable for energy applications in cogeneration plants.

Co-pyrolysis of date palm branches and wastewater derived microalgae was conducted at 400, 500 and 600 °C for a single stage and two stage pyrolysis. Char aromaticity increased, and mass yield decreased substantially with the increase in treatment temperature in both single stage pyrolysis and two stage pyrolysis from 40% to 30% by weight. Nitrogen concentration was decreased with the increase in temperature, which determines its transformation to the gas phase and similar results were found for nitrogen species on the surface of the char. The nitrogen-doped char holds the potential to be used in a range of applications from the reduction of NO_x emissions to supercapacitors.

Combustion of the feedstock and the char samples produced at 400 and 500 °C showed two-stage degradation whereas pyrolysis showed single stage degradation. 500 °C is the optimum treatment temperature for two-stage pyrolysis to gain the lowest activation energy during combustion, moderate heating values and lowest price. Similarly, the activation energy of the subsequent pyrolysis of char samples also decreased than their feedstock. Two-stage pyrolysed

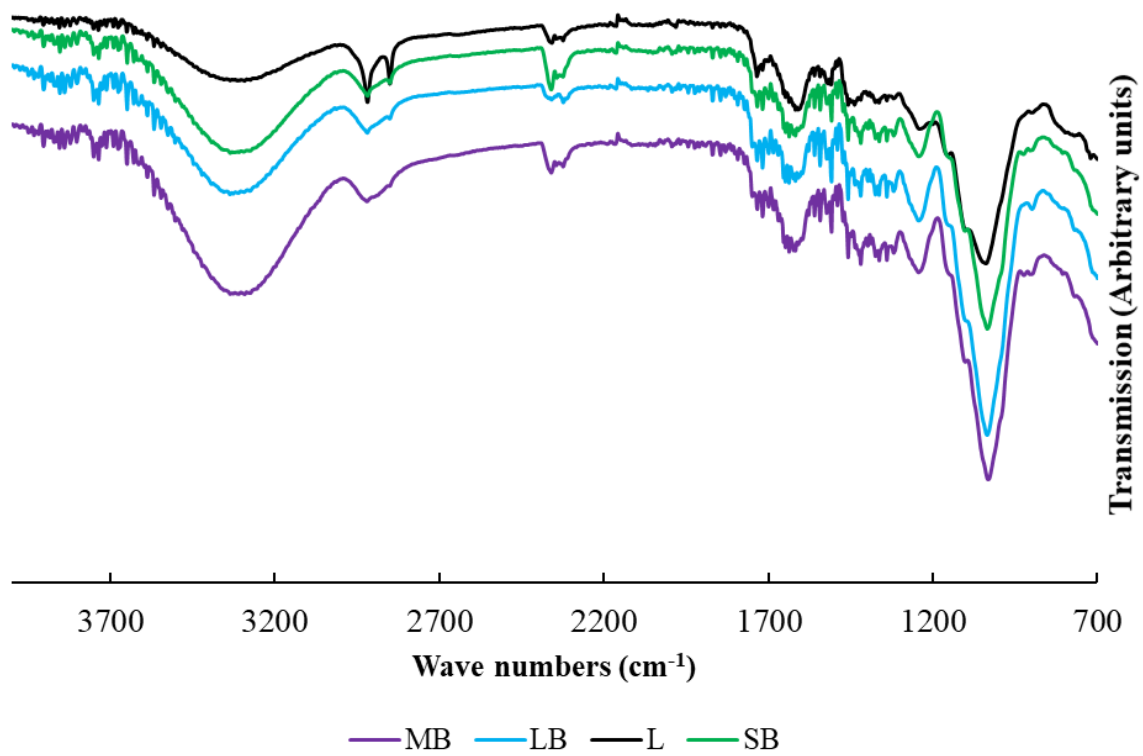
carbon at treatment temperatures (≥ 500 °C) showed higher activation energy than single stage pyrolysed carbon. The economic analysis showed a decrease in price with the increase in treatment temperature due to a decrease in energy content. It can be concluded that co-pyrolysed char from multi-stage pyrolysis process contains the superior properties and potential applications in multiple areas such as energy and adsorption.

Future research recommendation

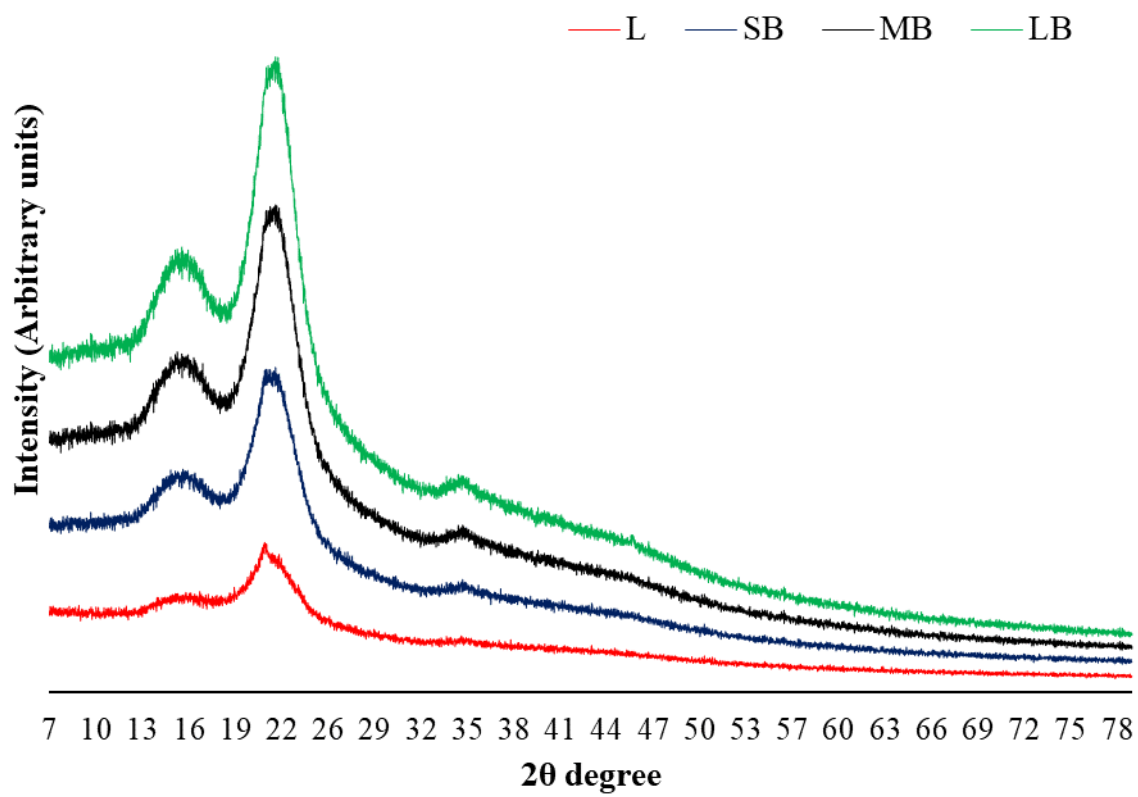
Further research in the area of oxidative and multi-stage combined pyrolysis of wastewater sludge and microalgae is recommended. The combined processing of both biomass types from similar source might help in the reduction of processing steps and can generate the char of improved quality for multiple applications. Catalytic pyrolysis of microalgae and lignocellulosic biomass with an activating agent such as CO₂ might bring properties of high surface area and functional groups enhancement at lower temperature processing.

A further consideration in the area of ternary and quaternary pyrolysis through the use of Taguchi method is desirable to recommend the multiple types of biomass in biorefineries which might result in advanced carbon properties and yield high-value product. The resultant product in this scenario might have the potential to be used in several adsorption and soil amendment applications. In addition, similar feedstock needs to be thoroughly investigated through multiple reactors to observe energy efficiency and variation in product performance according to reactor types. This research direction has the potential to integrate a set of reactors which can further be utilised to enhance high-quality carbon production.

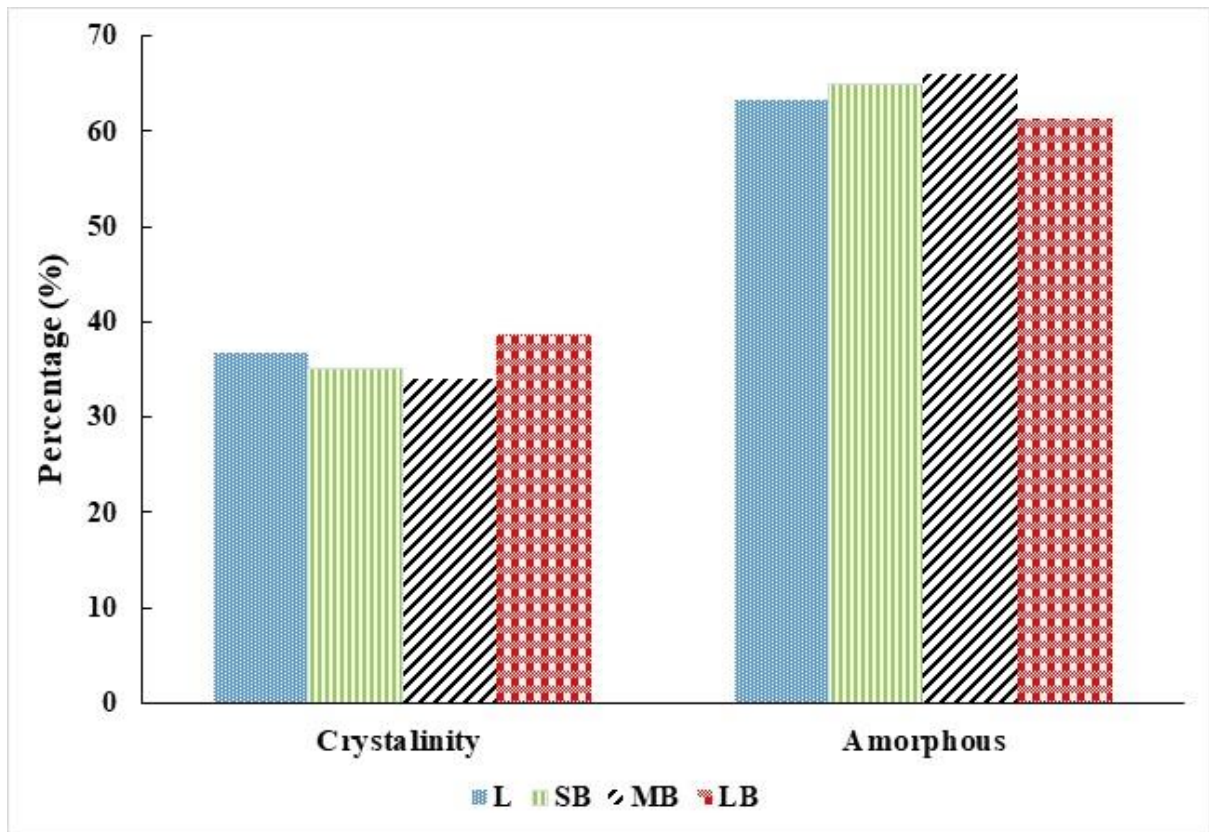
Appendices



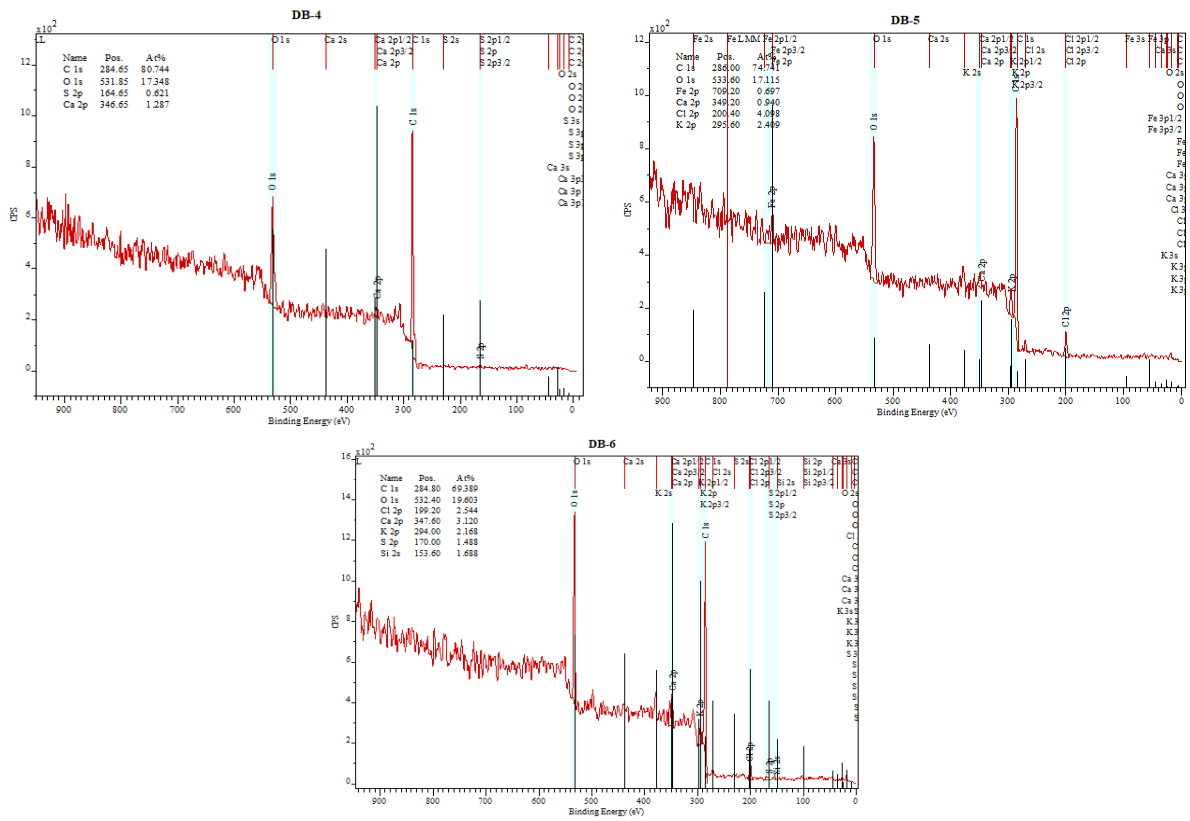
A.1 FT-IR analysis of date palm branch parts (L, SB, MB and LB)



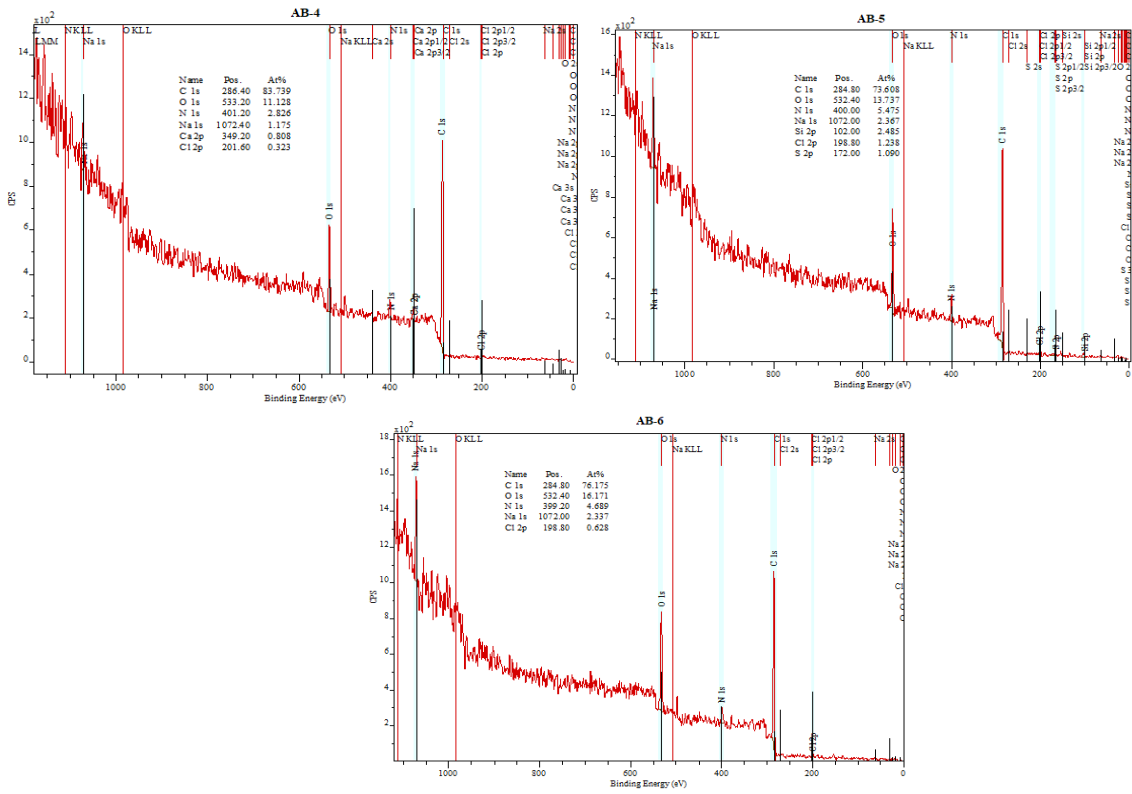
A.2 XRD spectra of biomass samples (L, SB, MB and LB)



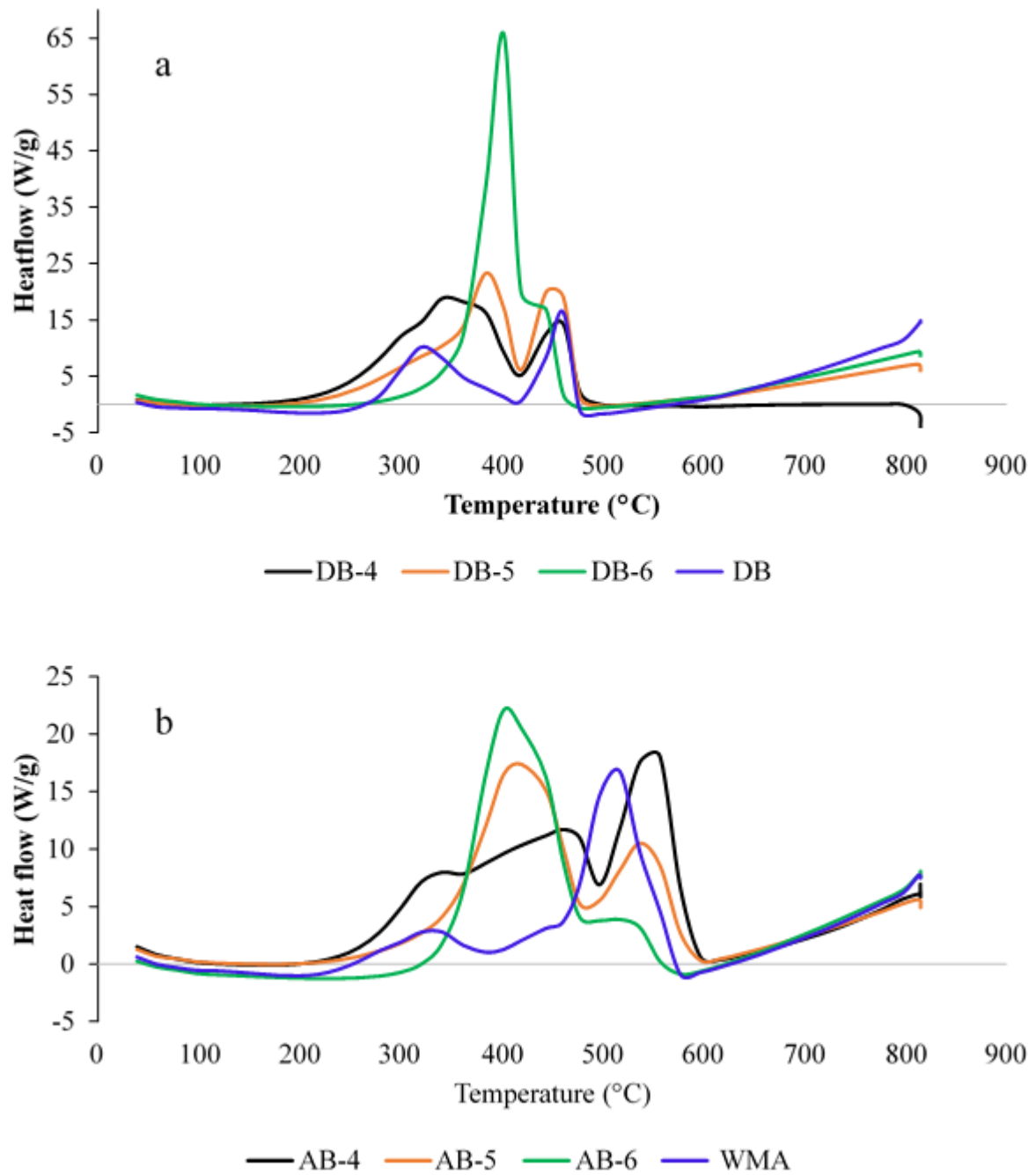
A.3 Crystallinity of parts of date palm branches



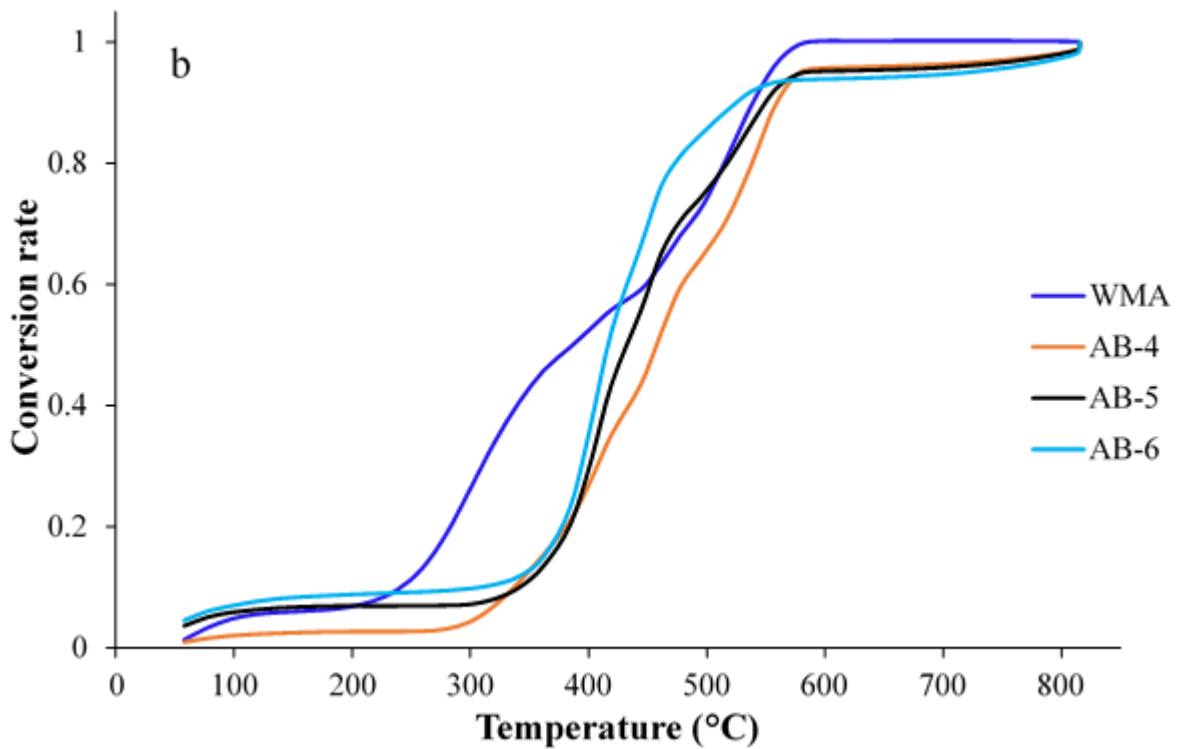
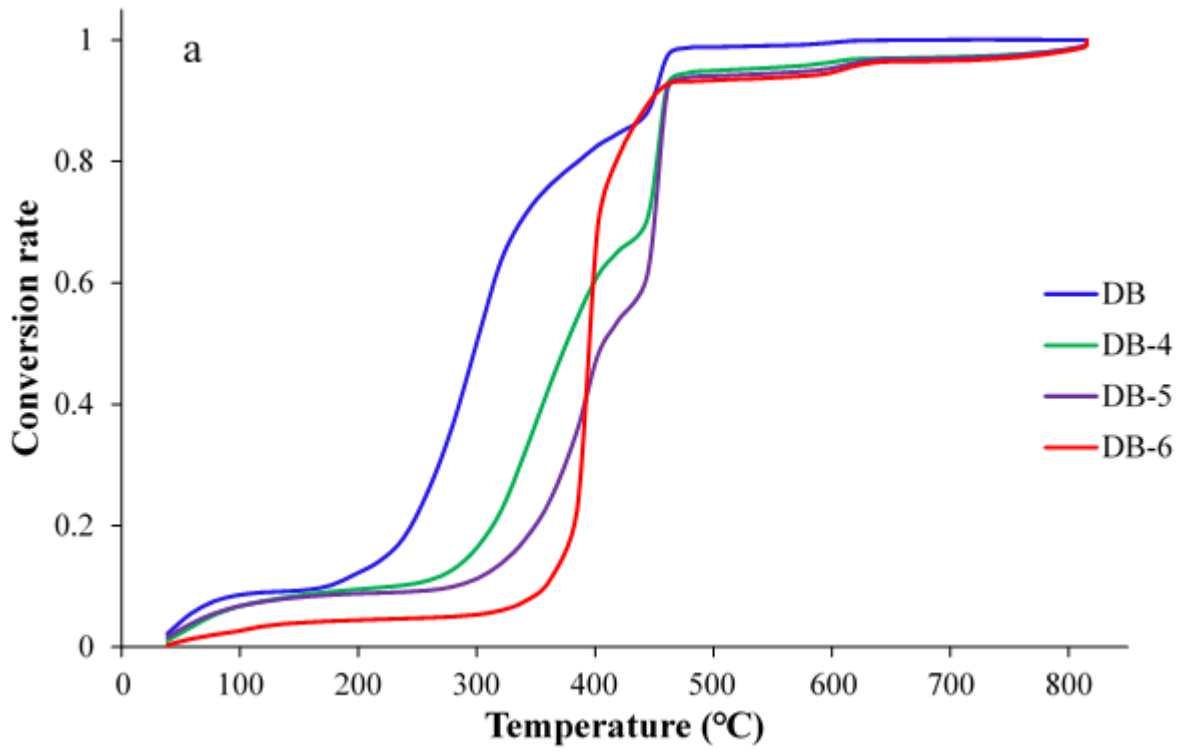
A.4 XPS spectra of date palm char DB-4, DB-5 and DB-6 produced at 400, 500 and 600 °C respectively



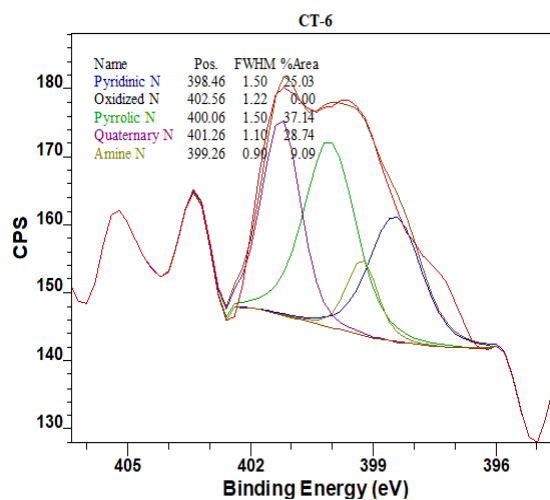
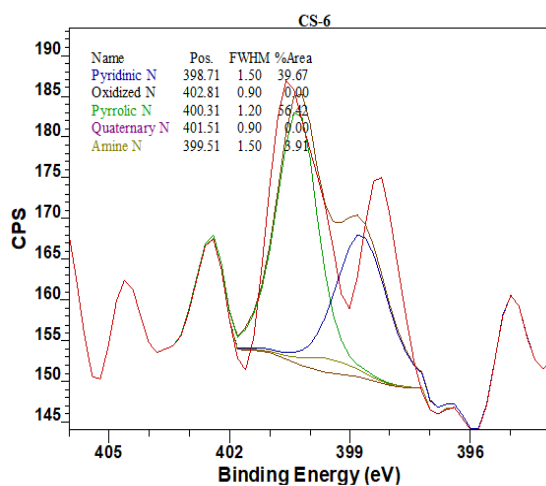
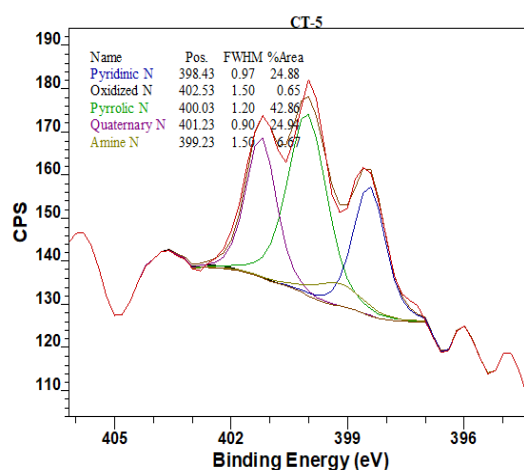
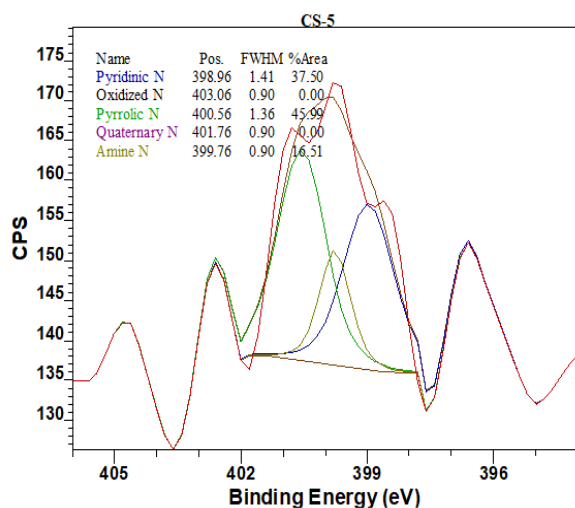
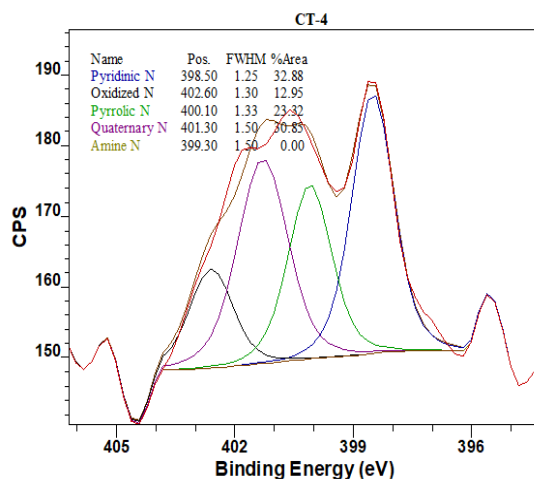
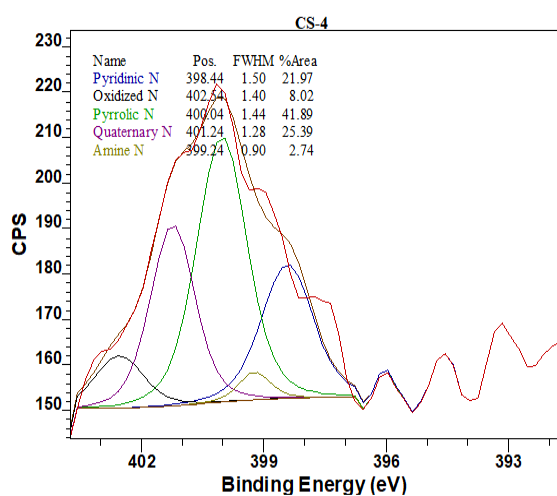
A.5 XPS spectra of wastewater derived microalgae char AB-4, AB-5 and AB-6 produced at 400, 500 and 600 °C respectively



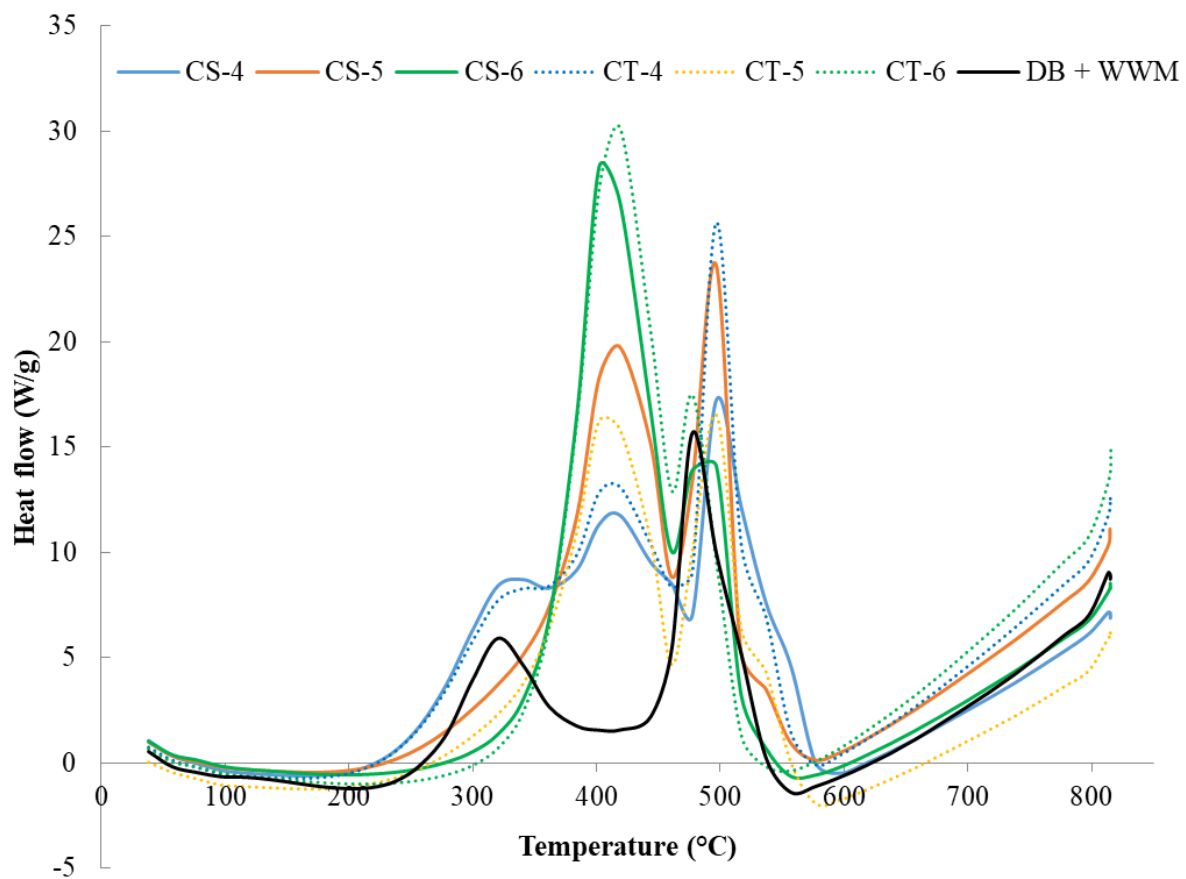
A.6 DSC curves of (a) date palm biomass with its chars and (b) wastewater derived microalgae with their chars



A.7 Degree of conversion of (a) date palm biomass with chars and (b) wastewater derived microalgae with chars



A.8 Nitrogen species distribution on char surfaces analysed by XPS



A.9 DSC curves of combined feedstock and co-pyrolysed char in air atmosphere

Journal publications

Following publications contributed to this dissertation:

1. **Akhtar, A.**, Jiříček, I., Ivanova, T., Mehrabadi, A., Krepl, V., 2019. Carbon conversion and stabilisation of date palm and high rate algal pond (microalgae) biomass through slow pyrolysis. *Int. J. Energy Res.* <https://doi.org/10.1002/er.4565>
2. **Akhtar, A.**, Ivanova, T., Jiříček, I., Krepl, V., 2019. Detailed characterization of waste from date palm (*Phoenix dactylifera*) branches for energy production: Comparative evaluation of heavy metals concentration. *J. Renew. Sustain. Energy* 11, 13102. <https://doi.org/10.1063/1.5027578>
3. **Akhtar, A.**, Krepl, V., Ivanova, T., 2018. A Combined Overview of Combustion, Pyrolysis, and Gasification of Biomass. *Energy & Fuels* 32, 7294–7318. <https://doi.org/10.1021/acs.energyfuels.8b01678>

Article in Review

1. **Akhtar, A.**, Jiříček, I., Krepl, V., Mehrabadi, A., Ivanova, T, A detailed investigation on multi-stage co-pyrolysis of date palm biomass and wastewater derived microalgae: products characterisation, and kinetic modelling.

Conference presentation

Akhtar, A., Ivanova, T., Krepl, V., 2015. Analysis of properties of waste palm tree branches, In: 2nd International Tropical Biodiversity Conservation Conference (TBCC). Prague.